MCEER
EARTHQUAKE ENGINEERING TO EXTREME EVENTS

ISSN 1520-295X

Open Space Damping System Theory and Experimental Validation

by

Erkan Polat and Michael C. Constantinou

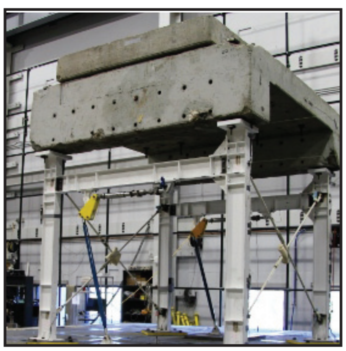

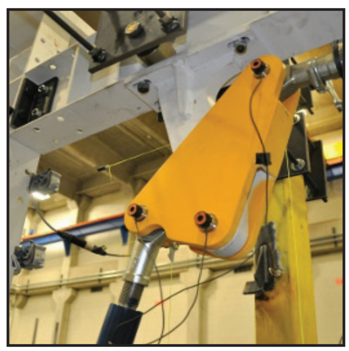

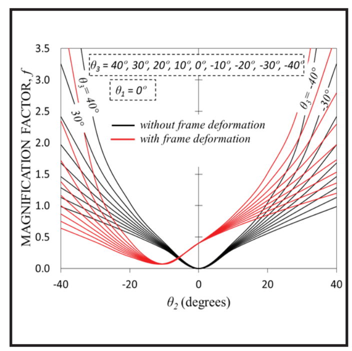

Technical Report MCEER-16-0007

December 13, 2016

This research was conducted at the University at Buffalo, State University of New York, and was supported primarily by MCEER Thrust Area 3: Innovative Technologies.

NOTICE

Open Space Damping System Theory and Experimental Validation

by

Erkan Polat[1] and Michael C. Constantinou[2]

Publication Date: December 13, 2016
Submittal Date: May 9, 2016

Technical Report MCEER-16-0007

MCEER Thrust Area 3: Innovative Technologies

1 PhD Candidate, Department of Civil, Structural and Environmental Engineering, University at Buffalo, State University of New York

2 Samuel P. Capen Professor and SUNY Distinguished Professor, Department of Civil, Structural and Environmental Engineering, University at Buffalo, State University of New York

MCEER
University at Buffalo, State University of New York
212 Ketter Hall, Buffalo, NY 14260
E-mail: *mceer@buffalo.edu*; Website: *http://mceer.buffalo.edu*

Preface

MCEER is a national center of excellence dedicated to the discovery and development of new knowledge, tools and technologies that equip communities to become more disaster resilient in the face of earthquakes and other extreme events. MCEER accomplishes this through a system of multidisciplinary, multi-hazard research, in tandem with complimentary education and outreach initiatives.

Headquartered at the University at Buffalo, The State University of New York, MCEER was originally established by the National Science Foundation in 1986, as the first National Center for Earthquake Engineering Research (NCEER). In 1998, it became known as the Multidisciplinary Center for Earthquake Engineering Research (MCEER), from which the current name, MCEER, evolved.

Comprising a consortium of researchers and industry partners from numerous disciplines and institutions throughout the United States, MCEER's mission has expanded from its original focus on earthquake engineering to one which addresses the technical and socio-economic impacts of a variety of hazards, both natural and man-made, on critical infrastructure, facilities, and society.

The Center derives support from several Federal agencies, including the National Science Foundation, Federal Highway Administration, Department of Energy, Nuclear Regulatory Commission, and the State of New York, foreign governments and private industry.

This report describes the open space damping system that has been developed to preserve open space within the frame of its installation. The report describes the function of the system, presents a theory to predict its behavior and presents computational models to verify the theory. Moreover, the report presents an experimental study of a large scale model with the open space damping system that is used to acquire data for validating the developed analytical and computational models. Comparisons of experimental results in terms of structural drift, floor accelerations and force-displacement loops to results obtained by computational tools demonstrate the validity of the computational models.

“This Page Intentionally Left Blank”

ABSTRACT

Seismic energy dissipation systems are typically installed in buildings within diagonal or chevron bracing to improve the seismic performance by reducing drift, and under certain conditions by reducing acceleration. Alternative installation methods have been developed in which novel mechanisms are utilized to magnify the displacements within the damping system and thus improve performance when drift is small and by doing so may also reduce the cost of damping. Examples are the lever-arm, the toggle-brace, the coupled-truss and the scissor-jack damper systems which have found a limited number of applications. All damping system installation methods visually and physically obstruct an otherwise accessible area within the bay of the frame to which they are installed. This drawback has resulted in the occasional rejection of use of damping systems by architects. This report introduces a novel configuration for damping devices with the main advantage of preserving open space within the frame of installation — hence the name "open space damping system". The report introduces the concept, presents the theory and then presents computational models to verify the theory and to investigate the effects of frame configuration, frame deformations and large deformations on the effectiveness of the system. An experimental study of a large scale model with the open space damping system was conducted and used to acquire data for validating the developed analytical and computational models. Testing consisted of (a) a single portal frame tested under imposed lateral motion, and (b) a single story 32kip model tested on the shake table under seismic excitation. Two different configurations of the open space system (plus a third variant of one of the two) in three different structural system configurations were tested. The tests demonstrate the increase in damping provided by the damping system. Comparisons of experimental results in terms of structural drift, floor accelerations and force-displacement loops to results obtained by computational tools demonstrate the validity of the computational models.

“This Page Intentionally Left Blank”

ACKNOWLEDGEMENTS

The authors acknowledge the financial support by the Turkish Government in terms of a scholarship (stipend and tuition) for graduate studies to the first author. This support is greatly appreciated. Moreover, the authors are grateful to Mr. Douglas P. Taylor and Mr. John Metzger of Taylor Devices, Inc., North Tonawanda, NY for their support of the work in the development of the open space damping system and for many inspiring discussions, and to engineers Sean Frye and Kyle Schmidt of Taylor Devices, Inc. for their work in construction of the steel frame. The cost of the steel model used in the testing was paid by Taylor Devices, Inc.

The authors wish to thank Mr. Mark Pitman, Mr. Scot Weinreber, Mr. Robert Staniszewski, Mr. Lou Moretta and Mr. Jeffrey Cizdziel of the Structural Engineering and Earthquake Simulation Laboratory for their support during the experimental part of the work.

“This Page Intentionally Left Blank”

TABLE OF CONTENTS

LIST OF FIGURES

LIST OF FIGURES CONT'D

LIST OF FIGURES CONT'D

"This Page Intentionally Left Blank"

LIST OF TABLES

"This Page Intentionally Left Blank"

SECTION 1
INTRODUCTION AND THEORY OF OPEN SPACE DAMPING SYSTEM

1.1 General

Typical installation methods for damping systems in buildings result in the occupation of an entire bay of the frame to which they are installed (Soong and Dargush, 1997; Constantinou et al, 1998; Symans et al, 2008; McNamara et al, 2000; Christopoulos and Filiatrault, 2006). Examples are provided in Figure 1-1 where the most used configurations of diagonal, chevron and toggle-brace (Constantinou et al, 1997, 2001) are shown as installed in the Smith Memorial Center Building at Portland State University, Portland, Oregon, the San Francisco Civic Center and the Yerba Buena Tower in San Francisco. The obstruction of space is evident. The scissor-jack-damper configuration (Sigaher and Constantinou, 2003) allows for open space but it requires installation of the system at a large angle of inclination that, in turn, results in large forces in the toggles and higher cost of damping. Figure 1-2 shows an installation of the scissor-jack-damper system at the Olympic Committee Building in Cyprus where open space is provided at the expense of a large angle of inclination.

The installation of damping systems with obstruction of space is often undesirable by owners, architects and engineers. A noted example is the 24-story San Diego Courthouse (Sarkisian et al, 2015) where a damping system was installed only in the transverse direction whereas installation in the longitudinal direction would have compromised the interior layout and was unacceptable to the architect. Also, use of a scissor-jack damping system in the longitudinal direction would have been acceptable but the cost was unacceptable. The situation of the San Diego Courthouse provided the motivation for the work described in this report.

The development of simple and effective configurations of damping systems that preserve open space is thus useful and may extend the application of damping systems in buildings. This report describes a configuration for the installation of damping devices in buildings that preserves open space. The damper is installed parallel to the beams and damping is provided through a mechanism that allows for limited but sufficient magnification of motion. A theory is presented to relate the damper force and displacement to the frame lateral force and drift. This theory is verified by comparison to results obtained by computational models in commercial software.

The effects of the frame connection details and flexibility on the effectiveness of the damping mechanism are investigated. Also, large deformation effects are investigated and found to be insignificant for typical installation configurations. It is concluded that the open space damping system can provide displacement magnification that falls in-between the standard configurations of diagonal and chevron installation but without obstruction of space.

(a) **(b)**

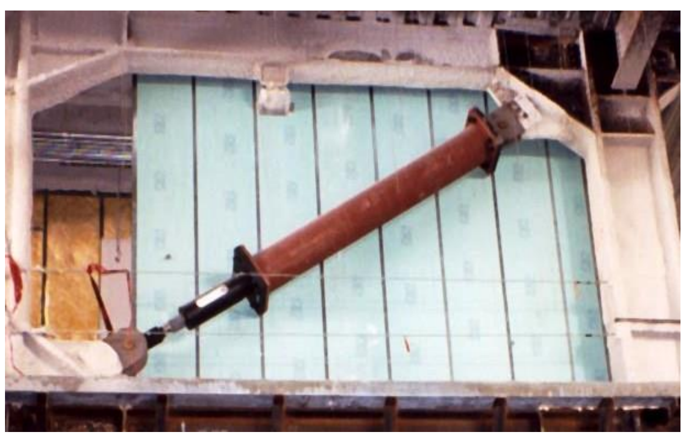

(c)

Figure 1-1 Installation Methods of Damping Systems with Obstruction of Space (Images Courtesy of Taylor Devices, Inc.): (a) Chevron; (b) Reverse Toggle-Brace; (c) Diagonal

Figure 1-2 Installation of Scissor-Jack-Damper System with Open Space and Large Angle of Inclination (image by Michael C. Constantinou)

In addition to the aforementioned diagonal, chevron, toggle-brace and scissor-jack systems, other systems with magnifying effects have been developed and are briefly mentioned below. They include the lever-arm system of Taisei Corporation or DREAMY (Hibino, et al., 1990), the Seesaw energy dissipation system (Kang and Tagawa, 2013), the Eccentric Lever-arm System (Baquero Mosquera, et al, 2016) and the Coupled Truss and Damping Mechanism used in the 57-story Torre Mayor building (Figure 1-3) in Mexico City (Rahimian, 2002).

Figure 1-3 Coupled Truss and Damping Mechanism in Torre Mayor building in Mexico

Consider a simple portal frame with some form of damping system installed. The period under elastic conditions is T and the effective seismic weight is W. The story drift, u, and the damper deformation u_D are related through the magnification factor f (Constantinou et al, 2001):

$$u_D = f \cdot u \quad (1\text{-}1)$$

For installation of dampers on top of chevron bracing, the damper deformation is identical to story drift (when excluding the supporting frame deformations) so that $f=1.0$. For the dampers installed in the diagonal configuration, $f=\cos\theta$ where θ is the angle of inclination of the damper with respect to horizontal axis. The force F_D along the damper axis is similarly related to the lateral force acting on the frame F by:

$$F = f \cdot F_D \quad (1\text{-}2)$$

The damping ratio of a single-story frame with a linear fluid viscous damper assembly in which the damper force is linearly related to the damper velocity ($F_D = C\dot{u}$, where $\dot{u}$ is the damper velocity) is given by the following equation (Constantinou et al, 2001) where g is the acceleration of gravity:

$$\beta = \frac{C \cdot f^2 \cdot g \cdot T}{4 \cdot \pi \cdot W} \quad (1\text{-}3)$$

Equations (1-1) to (1-3) are valid for all types of damper installation configurations, including the open space damping system described in this report. Figure 1-4 illustrates frames with several damper installation configurations and presents expressions for the magnification factor. Note that the expressions for the magnification factor only account for the effects of the lateral frame deformations and do not include vertical motion, frame and bracing deformations and large rotation effects, with the exception of the Coupled Truss and Damping Mechanism for which the vertical motion is important in the effectiveness of the system. Particularly for the seesaw configuration, the magnification factor is markedly affected by the change of length of the cables forming the mechanism. The magnification factor shown in Figure 1-4 for the seesaw configuration applies when the cable deformation is zero and when the cables are tension-only members.

Diagonal

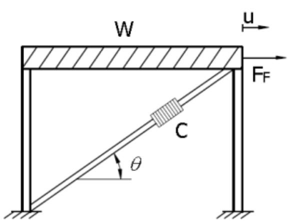

$f = cos\theta$

Chevron

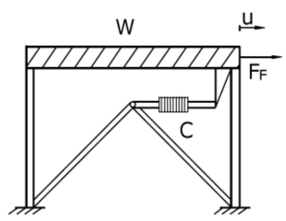

$f = 1.00$

Lower Toggle

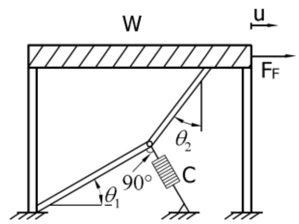

$f = \frac{sin\theta_2}{\cos(\theta_1 + \theta_2)}$

Upper Toggle

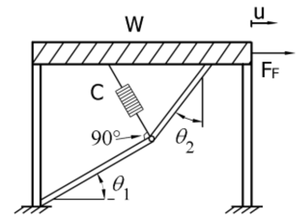

$f = \frac{sin\theta_2}{\cos(\theta_1 + \theta_2)} + sin\theta_2$

Reverse Toggle

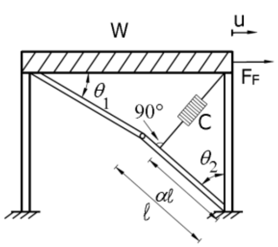

$f = \frac{\alpha sin\theta_1}{\cos(\theta_1 + \theta_2)} - cos\theta_2$

Scissor-Jack

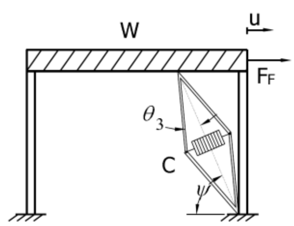

$f = \frac{cos\psi}{tan\theta_3}$

Lever-Arm

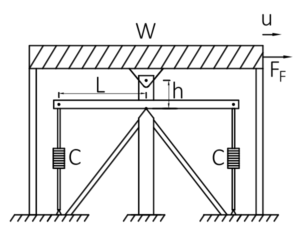

$f = \frac{L}{h}$

Seesaw

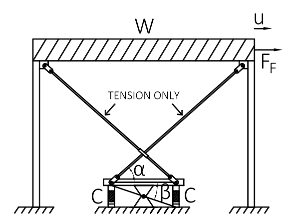

$f = \frac{cos\alpha cos\beta}{\sin(\alpha + \beta)}$

Eccentric Lever-arm System

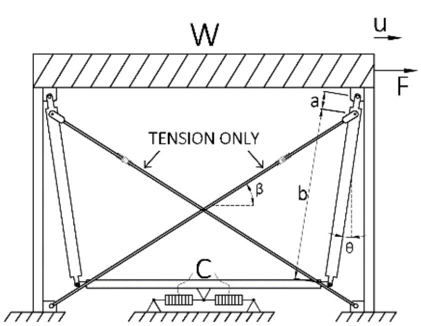

$$f = \frac{a + b}{a}\frac{cos\theta cos\beta}{\cos(\beta + \theta)} - 1$$

Coupled Truss and Damping Mechanism

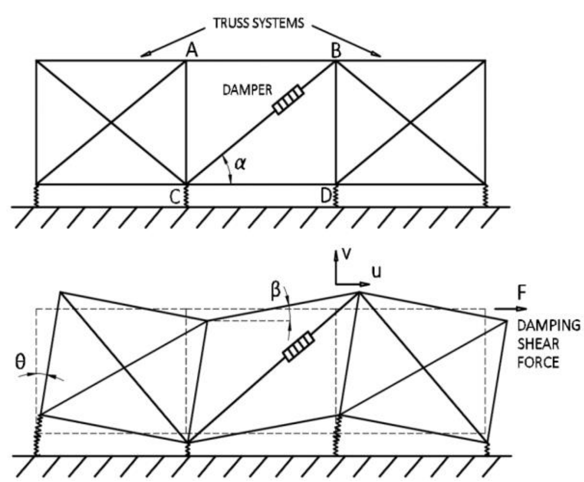

$$u_D = ucosa + vsina$$

$$f = \frac{u_D}{\mathrm{u}}$$

Figure 1-4 Magnification Factors of Various Damper Configurations

The majority of applications of damping systems utilize the diagonal configuration, followed by the chevron brace and with a few applications of the toggle and scissor-jack configurations. The magnification factor for the diagonal configuration is typically in the range of 0.7 to 0.9. It may be also noted that all of the damper configurations illustrated in Figure 1-4 occupy entire frame bays.

1.2 Open Space Damping System

Consider now the open space damping system configurations illustrated in Figure 1-5 for a single story frame. In these configurations, a damper is attached to the beam and the damper piston rod is driven by a brace and an inclined lever mechanism (rocker plate). The brace is inclined and may be connected to the column (Figure 1-5(a)) or to the beam below (Figure 1-5(b))- the difference between the two being the sign of the angle θ_2 (negative in the case of Figure 1-5(a) and positive in the case of Figure 1-5(b). Note that angles are positive in the counterclockwise direction so that angle θ_1 is positive for all cases of Figure 1-5, angle θ_2 is negative in Figure 1-5(a) and Figure 1-5(c) but is positive in Figure 1-5(b) and angle θ_3 is negative in Figure 1-5(a) and Figure 1-5(b) but is positive in Figure 1-5(c). Note that Figure 1-5(c) shows a modification of the mechanism where the rocker plate is reversed so that a larger angle θ_1 can be achieved. The magnification factor is shown in the figure (the derivation will be presented next). As an example, using parameters h/L=2, θ_1=0, θ_2=-25°, θ_3=-20° for the open-space configuration of Figure 1-5(a), which allows for the most open space, the magnification factor is f=0.8. For the configuration of Figure 1-5(b) with θ_1=0, θ_2=25° and θ_3=-20°, the magnification factor is 1.12. Thus for some geometries of the open-space damper configurations, a magnification factor similar to the diagonal and chevron brace configurations is achieved. Greater magnification factors may also be achieved as will be described in the sequel.

1.3 Magnification Factor of the Open Space Damping System

Figure 1-6 illustrates the open space damping system configuration of Figure 1-5(a) within a bay of one story frame in the un-deformed (Figure 1-6(a)) and deformed (Figure 1-6(b)) states, where the kinematics are considered without any due consideration for the frame

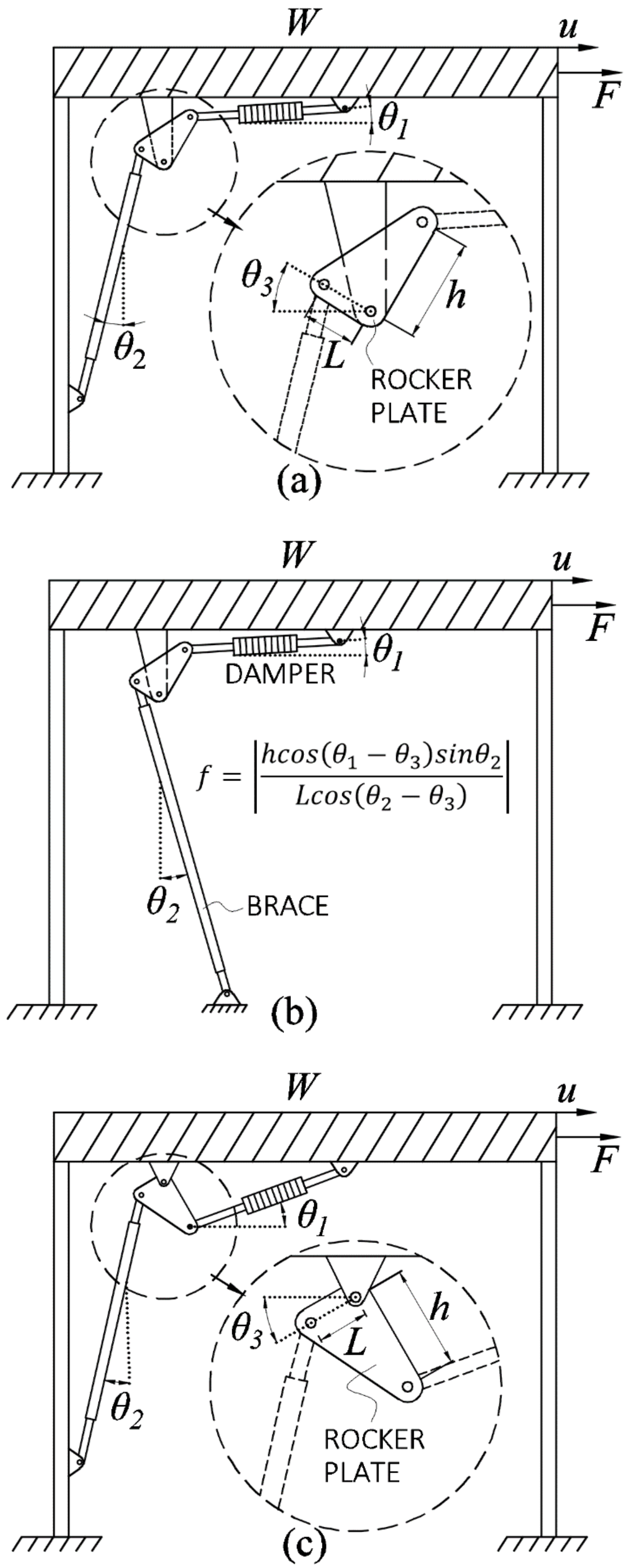

Figure 1-5 Configurations of the open space damping system

deformation, an assumption that will be relaxed in later analysis. The analysis presented next also applies for the configurations of Figure 1-5(b) and Figure 1-5(c), which are distinguished from those of Figure 1-5(a) only by the sign of the three angles as previously discussed. The relationship between the damper displacement (u_D) and story drift (u) is represented by factor f defined as follows:

$$f = \frac{u_D}{u} = \frac{|\overline{B'D'} - \overline{BD}|}{u} \tag{1-4}$$

where $\overline{BD}$ and $\overline{B'D'}$ are the lengths of segments *BD* and *B'D'*, respectively. The displacement of the damper assuming large rotations is given by Equation (1-5). The ± sign in Equation (1-5) is used to distinguish two cases related to the orientation of the rocker plate: when point B is positioned above point A (as in Figure 1-5(a) and Figure 1-5(b)), the sign is positive (+) and when point B is below point A (as in Figure 1-5(c)) the sign is negative (-). The rotation θ (positive θ is in counter-clockwise direction) of the rocker plate at point A is determined by solving Equation (1-6). Details of the derivation of Equations (1-5) and (1-6) are presented in Appendix A. Equations (1-5) and (1-6) reveal a complex nonlinear relation between the damper displacement (u_D) and the drift (u). An explicit closed-formed solution of these equations to relate u_D to u is not possible so a solution can only be obtained by numerical means.

$$u_D = \pm(h\sin(\theta_1 - \theta_3) + \ h\sin(\theta - \theta_1 + \theta_3)) \tag{1-5}$$

$$\begin{aligned}\frac{u^2}{L_{EC}} + \frac{2uL}{L_{EC}}(\cos(\theta_3) - \cos(\theta_3 - \theta)) + 2u\sin(\theta_2) + 2Lsin(\theta - \theta_2 + \theta_3) \\ + 2Lsin(\theta_2 - \theta_3) = 0\end{aligned} \tag{1-6}$$

Significant simplification is achieved by assuming that θ is small so that $sin\theta \sim \theta$ and $cos\theta \sim 1$ and that the drift u is small so that u^2 and $u\theta$ are higher order terms and are ignored. Under these conditions, the displacement of the damper is given by Equation (1-7) and angle θ is given by Equation (1-8). The magnification factor is given by Equation (1-9).

$$u_D = \pm\left(h\theta cos(\theta_1 - \theta_3)\right) \tag{1-7}$$

$$\theta = -\frac{usin\theta_2}{Lcos(\theta_2 - \theta_3)} \tag{1-8}$$

$$f = \left|\frac{hcos(\theta_1 - \theta_3)sin\theta_2}{Lcos(\theta_2 - \theta_3)}\right| \tag{1-9}$$

Equation (1-9) shows that the magnification factor attains very large values as the difference between angles θ_2 and θ_3 approaches 90° (but the 90 degree configuration is useless as it acts as a bracing system). Figure 1-7 present graphs of the magnification factor for a range of values of angles θ_1, θ_2 and θ_3. The graphs demonstrate that magnification factor is slightly dependent on angle θ_1, so that the configuration with $\theta_1=0$ is preferred as it results in the most open space.

1.4 Forces in Members of Open Space Damping System

Forces in the open space damping system are needed for the assessment of the adequacy of the braces and for establishing the relation between the force in the damper and the horizontal component of the damping force that acts on the structure.

The forces that act on the open space damping system and to the frame to which the system is attached are shown in Figure 1-8. Force F that acts on the frame represents the component of the inertia force that is balanced by forces supplied by the damping system. Considering equilibrium in the un-deformed configuration (an assumption consistent with small displacement theory), the force T in the brace is given by:

$$T = \frac{h}{L} F_D \frac{\cos(\theta_3 - \theta_1)}{\cos(\theta_3 - \theta_2)} \tag{1-10}$$

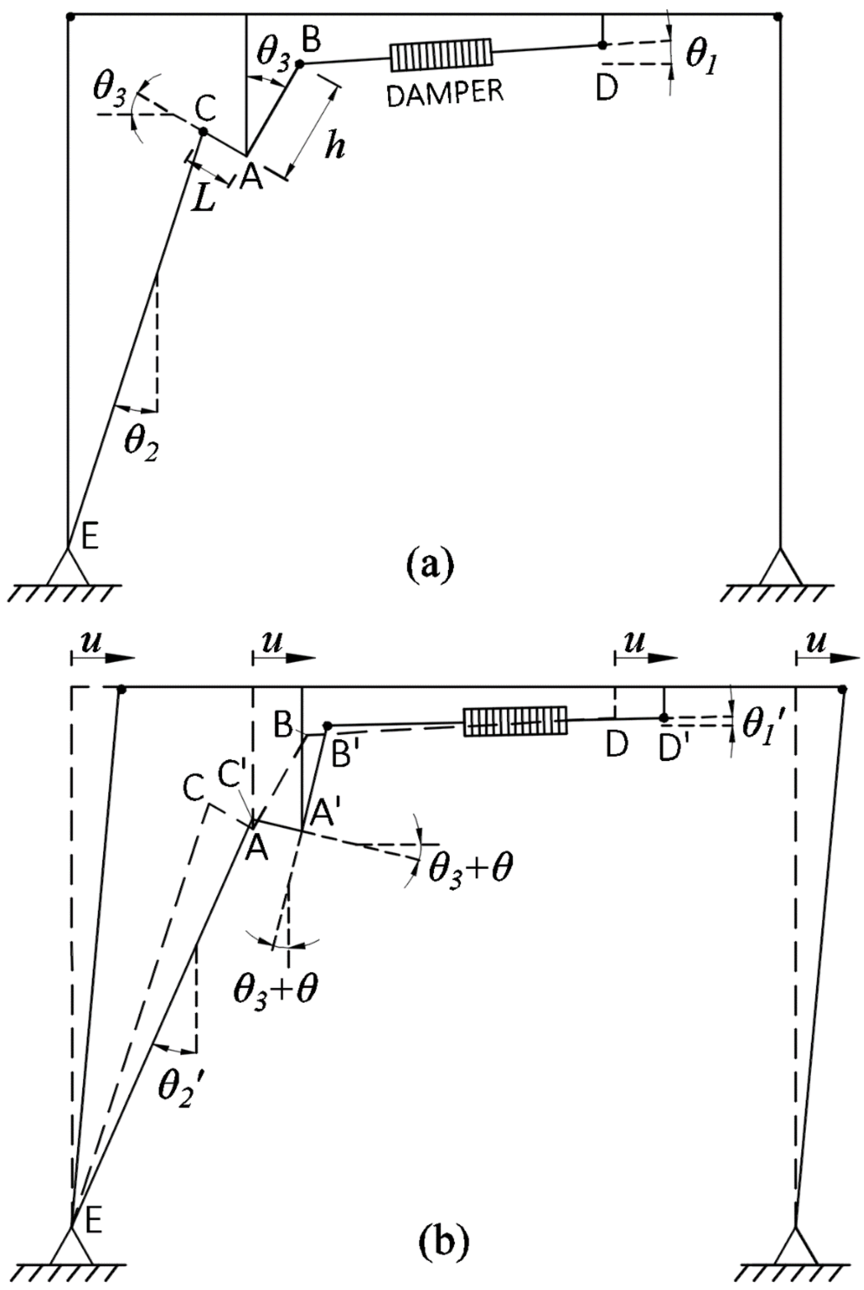

Figure 1-6 Analysis of Motion Open Space Damping System

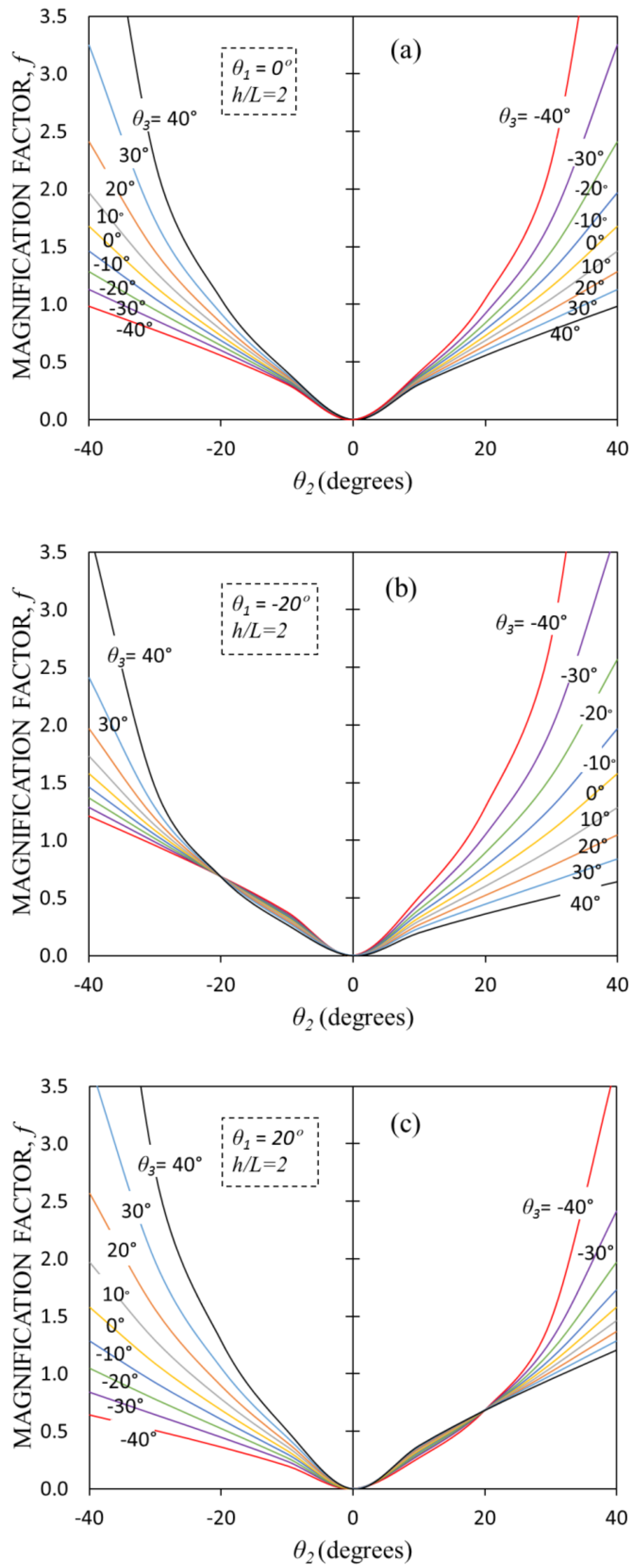

Figure 1-7 Dependency of Magnification Factor on Angles θ_2 and θ_3: (a) θ_1=0°; (b) θ_1=-20°; (c) θ_1=20°

The horizontal component of force T is equal to force F, so that:

$$F = T sin\theta_2 \tag{1-11}$$

The ratio of force F to force F_D is then obtained by use of Equations (1-10) and (1-11) to arrive at Equation (1-12) after use of Equation (1-9) for the magnification factor.

$$\frac{F}{F_D} = f = \frac{u_D}{u} \tag{1-12}$$

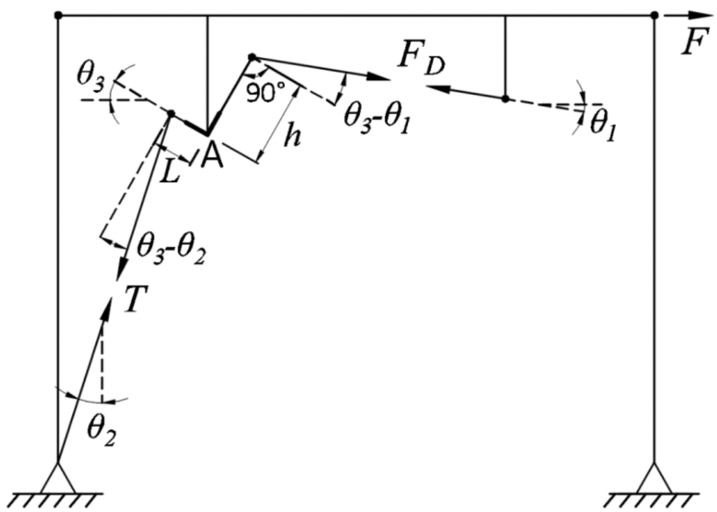

Figure 1-8 Analysis of Forces in Open Space Damping System

1.5 Effect of Beam Deformation

The analysis of the open space damping system movement is revisited taking into consideration the effect of the vertical deflection and rotation of the beam to which the damper is attached. These vertical deformations and rotations are caused by the internal forces in the frame and may include the damper force effects.

Figure 1-9 presents the deformed configuration of a single-story frame, inclusive of vertical and rotational deformations of the beam (note that angle θ_1 in Figure 1-9 is shown negative only for clarity in the illustration). Let v_1 and v_2 denote the vertical deformations and ψ_1

and ψ_2 denote the rotations of points F and G where the damper assembly is connected to the beam. The distance between points F and A is denoted as h_1 and that between points G and D as h_2. Positive vertical displacements are downwards and positive rotations are counterclockwise.

Returning to Equations (1-7) and (1-8) for the case of small rotations, the damper displacement u_D and the rotation of rocker plate θ are given by:

$$u_D = \pm\theta h cos(\theta_1 - \theta_3) + (h_2\psi_2 - h_1\psi_1)cos\theta_1 + (v_1 - v_2)sin\theta_1 \tag{1-13}$$

$$\theta = -\frac{1}{Lcos(\theta_2 - \theta_3)}[(u + h_1\psi_1)sin\theta_2 + v_1 cos\theta_2] \tag{1-14}$$

Again, the positive (+) sign in Equation (1-13) is used when point B is located above point A and the negative (-) sign is used when point B is located below point A. Substituting Equation (1-14) into Equation (1-13) forms:

$$\begin{aligned} u_D = \pm\left(-\frac{hcos(\theta_1 - \theta_3)}{Lcos(\theta_2 - \theta_3)}[(u + h_1\psi_1)sin\theta_2 + v_1 cos\theta_2]\right) \\ + (h_2\psi_2 - h_1\psi_1)cos\theta_1 + (v_1 - v_2)sin\theta_1 \end{aligned} \tag{1-15}$$

The vertical displacements v_1 and v_2 and the rotations ψ_1 and ψ_2 may be further written as functions of the lateral displacement u in the form:

$$v_1 = a_1 u, \qquad v_2 = a_2 u, \qquad \psi_1 = \beta_1 u, \qquad \psi_2 = \beta_2 u \tag{1-16}$$

Coefficients α_1, α_2, β_1 and β_2 are constants independent of the lateral frame deformation and velocity provided that the frame is elastic and the effect of the damper force on the frame deformations is disregarded.

The magnification factor can then be written as:

$$f = \left| \pm\left(-\frac{hcos(\theta_1 - \theta_3)}{Lcos(\theta_2 - \theta_3)}[(1 + \beta_1 h_1)sin\theta_2 + \alpha_1 cos\theta_2]\right) + (h_2\beta_2 - h_1\beta_1)cos\theta_1 + (\alpha_1 - \alpha_2)sin\theta_1 \right| \quad (1\text{-}17)$$

Consider a single story portal frame with pinned supports and with W8x15 steel sections for the columns and a W8x13 section for the beam. Height and bay length are 75.13inch (1908mm) and 100inch (2540mm), respectively. Let points F and G be located at 0.23 and 0.68 of the beam length starting from the left column centerline (this is an actual frame built for testing of the open space damper configuration-see Figure 2-1 in next section). Static analysis of the frame for a rigid beam-to-column connection on the left and a simple beam to-column connection on the right resulted in α_1 = 0.164, β_1 = -0.0046, α_2 = 0.12, β_2 = 0.0047. The analysis was performed with lateral force acting at the beam-to-column connection. Note that the amplitude of the applied force does not affect the values of these parameters. Figure 1-10 compares the magnification factor as determined using the deformed beam configuration (red lines) to that when the frame deformations are neglected (case α_1=β_1=α_2=β_2=0, black lines). The results demonstrate the frame deformation may result in either an increase or a decrease in the magnification factor, depending on the configuration of the system. For example the use of a positive angle θ_2 (configuration of Figure 1-5(b)), results in an increase in the magnification factor whereas a negative angle θ_2 (configuration of Figure 1-5(a)) results in a decrease in the magnification factor. Also, when the portal frame is changed to one with a simple beam-to-column connection on the left and a rigid beam-to-column connection on the right the situation reverses so that a negative value of angle θ_2 (configuration of Figure 1-5(a)) results in an increase in the magnification factor.

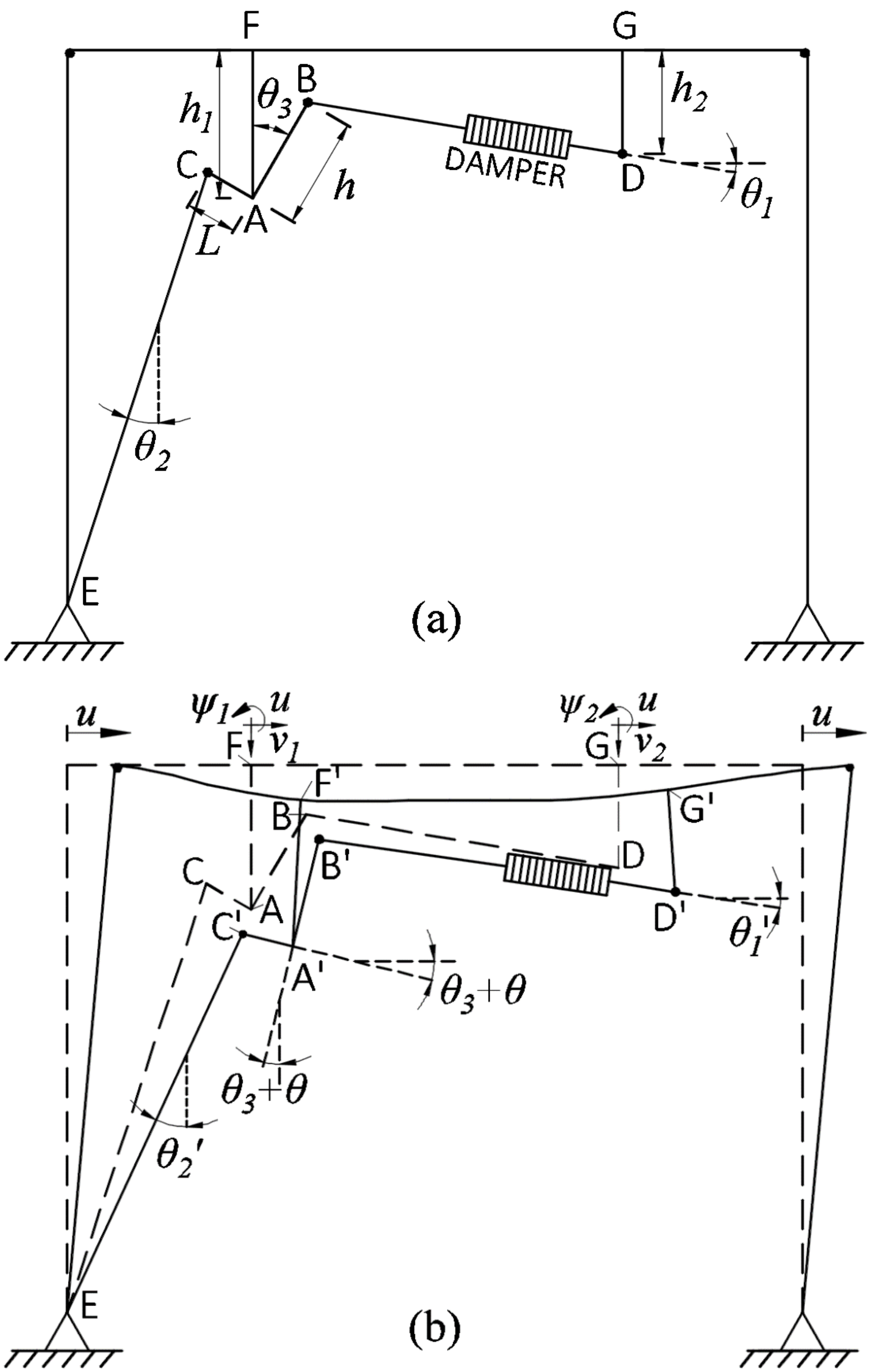

Figure 1-9 Analysis of Motion of Open-Space Damping System Considering Horizontal and Vertical Displacements

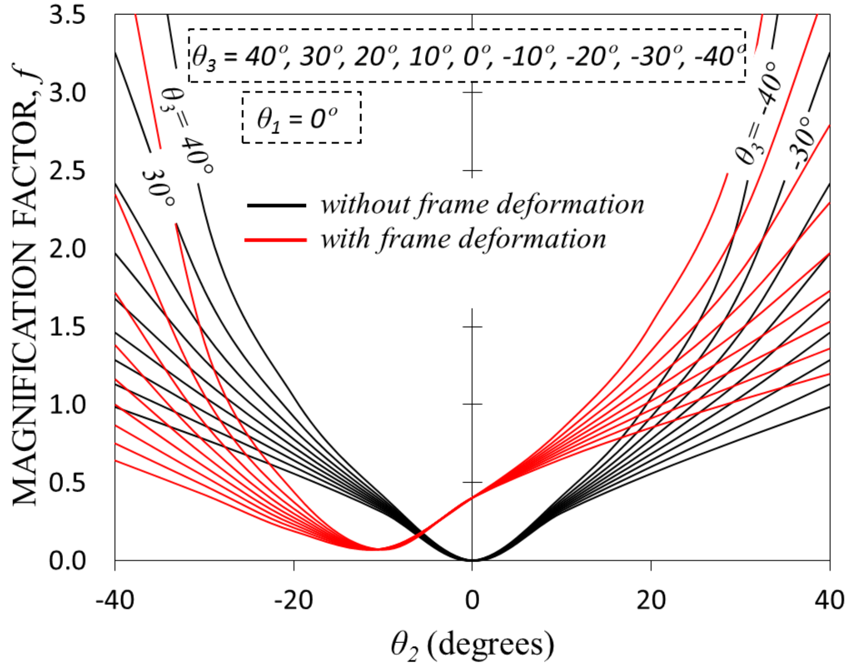

Figure 1-10 Dependency of Magnification Factor on Geometry of Open Space Damping System with and without Effect of Vertical Deformation

SECTION 2
VERIFICATION OF THE THEORY

2.1 Introduction

A verification of the theory is presented based on analysis of sample frames using the computer program SAP2000, v17 (Computer and Structures, 2015) based on the assumption of small deformations (therefore, also small angles of rotation) and elastic behavior (both these assumptions will be relaxed later in this report). The frame has been designed and built as a half-length scale model for testing the open space damping system in individual frames and in a one-story building model on the earthquake simulator (see Section 3 and Figure 3-1).

2.2 Computational Model and Theory Verification

The frame features simple connections to the ground and beam-to-column connections that are simple but can be converted to rigid. For example, Figure 2-1 illustrates a case where the beam-to-column connection on the left is rigid and the beam-to-column connection on the right is simple. The beam is a W8X13 section and the columns are W8X15 sections. The frame features two open space damping system configurations-those of Figure 1-5(a) and 1-5(b), named Model 1 and Model 2, respectively. A third configuration (see Figure 3-1), Model 3, is a modification of Models 1 and 2 in which the damper is connected directly at the column near the beam-to-column connection so that there is reduced effect of the frame deformations on the magnification factor. The braces are solid rods of 2 inch (51mm) diameter. Based on the information presented in Figure 2-1, Model 1 is characterized by parameters $\theta_1=0$, $\theta_2=-17°$ and $\theta_3=-20°$, Model 2 is characterized by parameters $\theta_1=0$, $\theta_2=17°$ and $\theta_3=-20°$ and Model 3 (see Figure 3-1), has the brace configured as that of Model 2 and is characterized by parameters $\theta_1=-2°$ (damper is installed slightly inclined to accommodate the connection details), $\theta_2=17°$ and $\theta_3=-20°$. All three configurations have h= 10 inch (254mm) and L=5 inch (127mm).

The SAP2000 model, illustrated in Figure 2-1, was skeletal with proper offsets for all details of the frame and the damping system but without a damper so that the damper force effects were excluded. The beam-to-column joint on the right was subjected to a prescribed displacement (1inch or 25.4mm) and the change of length of the points of attachment of the damper was calculated. The ratio of this displacement to the imposed joint displacement (1 inch) is the magnification factor. When analysis was conducted with simple beam-to-column connections (frame is a mechanism), there was only rigid body motion so that the result is comparable to the result obtained by Equation (1-9). For the cases where one or two beam-to-column connections are rigid, there are frame deformations and the results are comparable to the results obtained by Equation (1-17). To utilize Equation (1-17), parameters α_1, β_1, α_2 and β_2 were calculated by applying a lateral force on the frame and calculating the displacements of the points of attachments of the damper as previously described. Note that the calculation of parameters α_1, β_1, α_2 and β_2 is performed herein only for verifying Equation (1-17). In practice, if a static analysis of a structure is performed, the magnification factor can be directly obtained without the need of Equation (1-17). Table 2-1 presents values of the magnification factor as determined by the presented theory for small rotations, excluding frame deformation effects (Equation (1-9)) and then including frame deformation effects (Equation (1-17)) for four different frame connection details. The results in Table 2-1 demonstrate the accuracy of Equations (1-9) and (1-17). There is insignificant difference between the theoretical and computational results on the magnification factor.

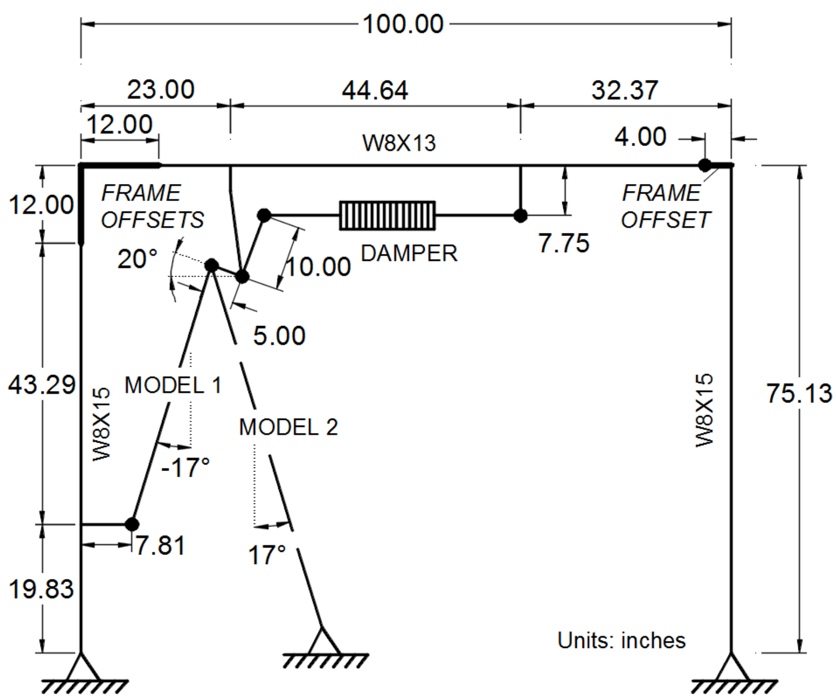

Figure 2-1 Illustration of Computational Model

A further computational analysis was performed in which the model was enhanced with a linear viscous damper having constant 0.36 kip-sec/in (C=63N-sec/mm). The right beam-to-column connection was driven in harmonic cyclic motion of 1Hz frequency and 1 inch (25.4mm) amplitude. The peak damper force acting on the frame is nearly equal to 0.25 of the frame base shear force-that is, is sufficiently large. The magnification factor, calculated as the ratio of the peak damper displacement to the amplitude of the imposed motion, is included in Table 2-1. The value of the magnification factor includes the effects of the damping force on the frame deformations. It may be seen that there is insignificant effect of the damping force on the magnification factor when is calculated with due consideration of the frame deformation effects. That is, consideration of the frame deformation effects is important but the damping force effects are insignificant.

The results of Table 2-1 demonstrate the significance of the frame deformation on the magnification factor. Depending on the frame configuration and the open space damping system configuration, there may be increase or decrease of the magnification factor. Of interest is to note the case of configuration S-S without a damper for which the analyzed structure is a mechanism and one would expect that Equation (1-9) would predict an exact result as there is no deformations of the frame. The results in Table 2-1show some differences, particularly for Model 3, as a result of rigid-body rotations so that the points of connection of the damping system to the beam and columns experience additional motion.

To investigate the effect of increased damping forces on the system behavior another study was conducted by increasing the damper coefficient from C=0.36kip-sec/in to C=0.72kip-sec/in and repeating the analysis for prescribed displacement of 1inch amplitude at 1Hz frequency. Table 2-2 compares the results in the two cases of damping constant. There is insignificant effect on the magnification factor despite the increase in the damper forces. Figures 2-2 and 2-3 present the calculated damper force-damper displacement and frame lateral force and lateral displacement loops in the two models of Table 2-2. Note that the nomenclature used in the figures relates to the cases in the table: e.g. Rigid-Simple implies a rigid beam-to-column connection at the left joint and a simple beam-to-column connection at the right joint of the frame. The maximum values of damper displacement and force, and of the force exerted by the damping system on the frame (zero displacement force intercept) are marked on the loops of Figures 2-2 and 2-3. The effect of the damping system is seen in these figures by the increase in the zero displacement force intercept and the increase in energy dissipated per cycle (area of hysteresis loop) in the frame lateral force-displacement loops.

Table 2-1 Values of magnification factor obtained by theory and by computational analysis

Beam-to-Column Connection	Assumptions	Model	Theory	Computational Analysis
S-S	No frame deformation. No damper (Theory using Eq. 1-9)	1	0.55	0.59
		2	0.69	0.69
		3	0.70	0.82
R-S	With frame deformations. No damper (Theory using Eq. 1-17)	1	0.33	0.35
		2	0.89	0.91
		3	1.03	1.07
S-R	With frame deformations. No damper (Theory using Eq. 1-17)	1	0.62	0.67
		2	0.70	0.68
		3	0.78	0.75
R-R	With frame deformations. No damper (Theory using Eq. 1-17)	1	0.42	0.46
		2	0.83	0.83
		3	0.91	0.91
R-S	With frame deformations. With damper	1	NA	0.35
		2		0.91
		3		1.07
S-R	With frame deformations. With damper	1	NA	0.67
		2		0.68
		3		0.75
R-R	With frame deformations. With damper	1	NA	0.46
		2		0.82
		3		0.91
S: Simple, R: Rigid, R-S: Rigid on left and simple on right, etc.				

Table 2-2 Magnification Factor, Peak Damper Force and Peak Damper Displacements of Model 1 and Model 2 for C=0.36 and 0.72kip-sec/in in 2Hz, 1inch Motion of Frame Top

	Beam-to-Column Connection (Left-Right)	C (kip-sec/in)	Damper Force (kip)	Damper Disp. (in)	Magnification Factor
MODEL 1	Rigid-Simple	0.36	1.59	0.35	0.35
		0.72	3.15	0.35	0.35
	Simple-Rigid	0.36	3.04	0.67	0.67
		0.72	6.02	0.66	0.66
MODEL 2	Rigid-Simple	0.36	4.14	0.91	0.91
		0.72	8.17	0.90	0.90
	Simple-Rigid	0.36	3.07	0.68	0.68
		0.72	6.02	0.67	0.67

2.3 Large Rotation and Inelastic Behavior Effects

The described damping system employs a displacement magnification mechanism that operates by rotating parts. When the angles of rotation change, the magnification mechanism may be affected as indicated in the results of Figure 1-7 for the cases of large values of the magnification factor where it is seen that small changes in geometry result in large changes in the magnification factor. The effect of large rotation is investigated by activating in program SAP2000 the capability for geometric nonlinearities, P-delta and large-displacement/rotation effects. The frame shown in Figure 2-1 in the configurations of Model 1 and Model 2 with rigid connections on the left and simple connections on the right, and Model 3 (see Figure 3-1) with both rigid connections, and without a damper has been analyzed with due consideration of the geometric nonlinearity effects and under elastic frame conditions. Note the analyzed frame has realistic damping system geometry that can produce useful magnification factors.

The calculation of the magnification factor followed the procedure previously described in which the joint on the right was subjected to a prescribed displacement. This process was repeated for several values of the displacement. Figure 2-4 presents the magnification factor calculated as the damper displacement (change of length of points of attachment of the damper) divided by the imposed frame lateral displacement as function of the frame drift ratio (drift divided by height of 75.13 inch (1908mm)) without and with due consideration of geometric nonlinearity effects. Drift ratio values of up to 0.04 are considered. It is evident that geometric nonlinearity effects have insignificant effect for values of the drift ratio up to 0.04. It should be noted that the values of the magnification factor in the three models are 0.91, 0.35 and 0.91, respectively, as calculated by small deformation theory (see Table 2-1). Per Figure 1-7, these values of the magnification factor are rather insensitive to variations in the geometry, which explains the result of the analysis with large deformations/rotation effects. It is evident based on inspection of the results in Figure 1-7 that configurations with large magnification factors (larger than unity) will have more sensitivity to geometric effects. However, these configurations will also be intrusive and will defeat the desire for open space. For the analyzed configurations which are practical, large rotation effects are insignificant.

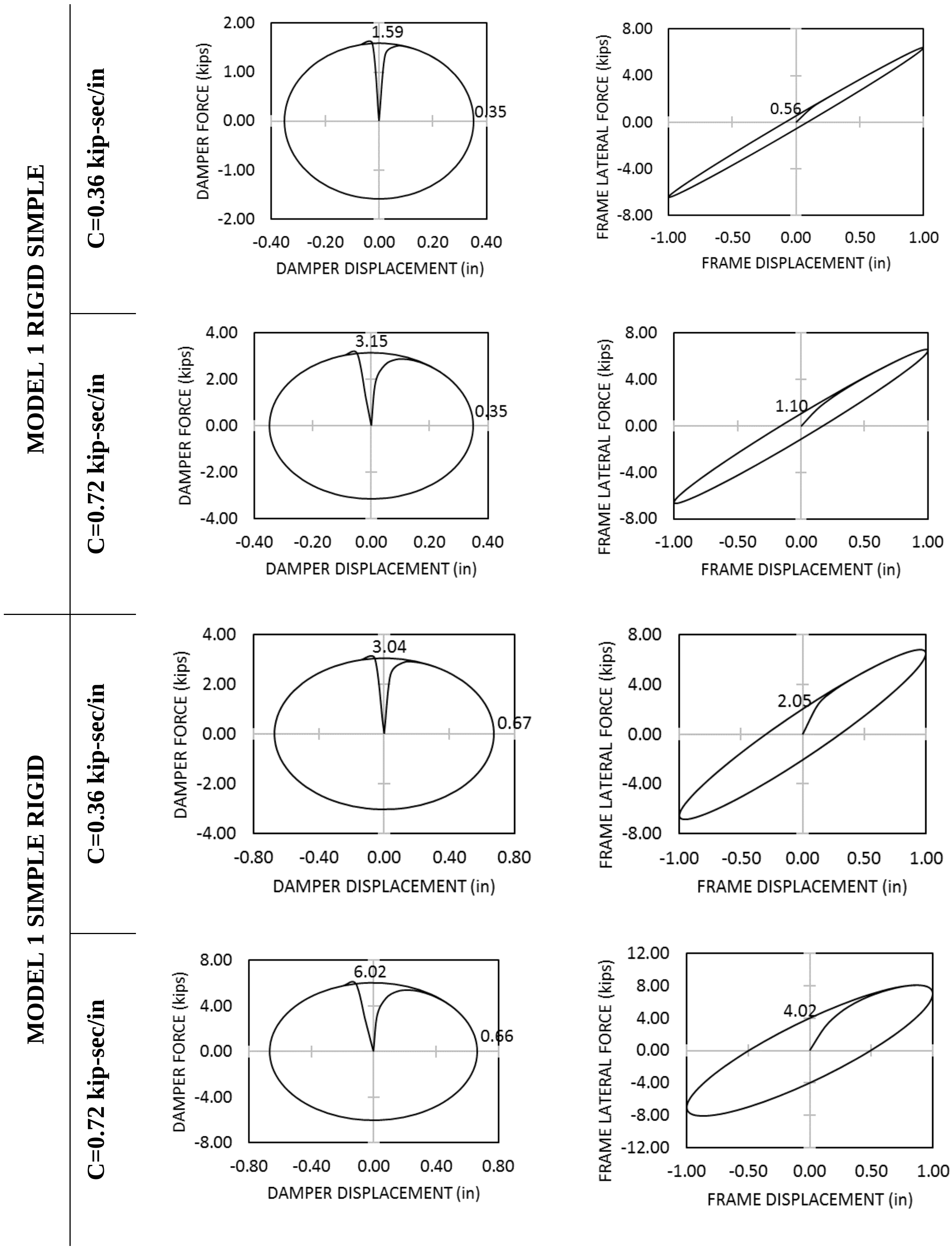

Figure 2-2 Damper force-displacement loops and frame lateral force-displacement loops of Model 1 with C=0.36 and 0.72 kip-sec/in

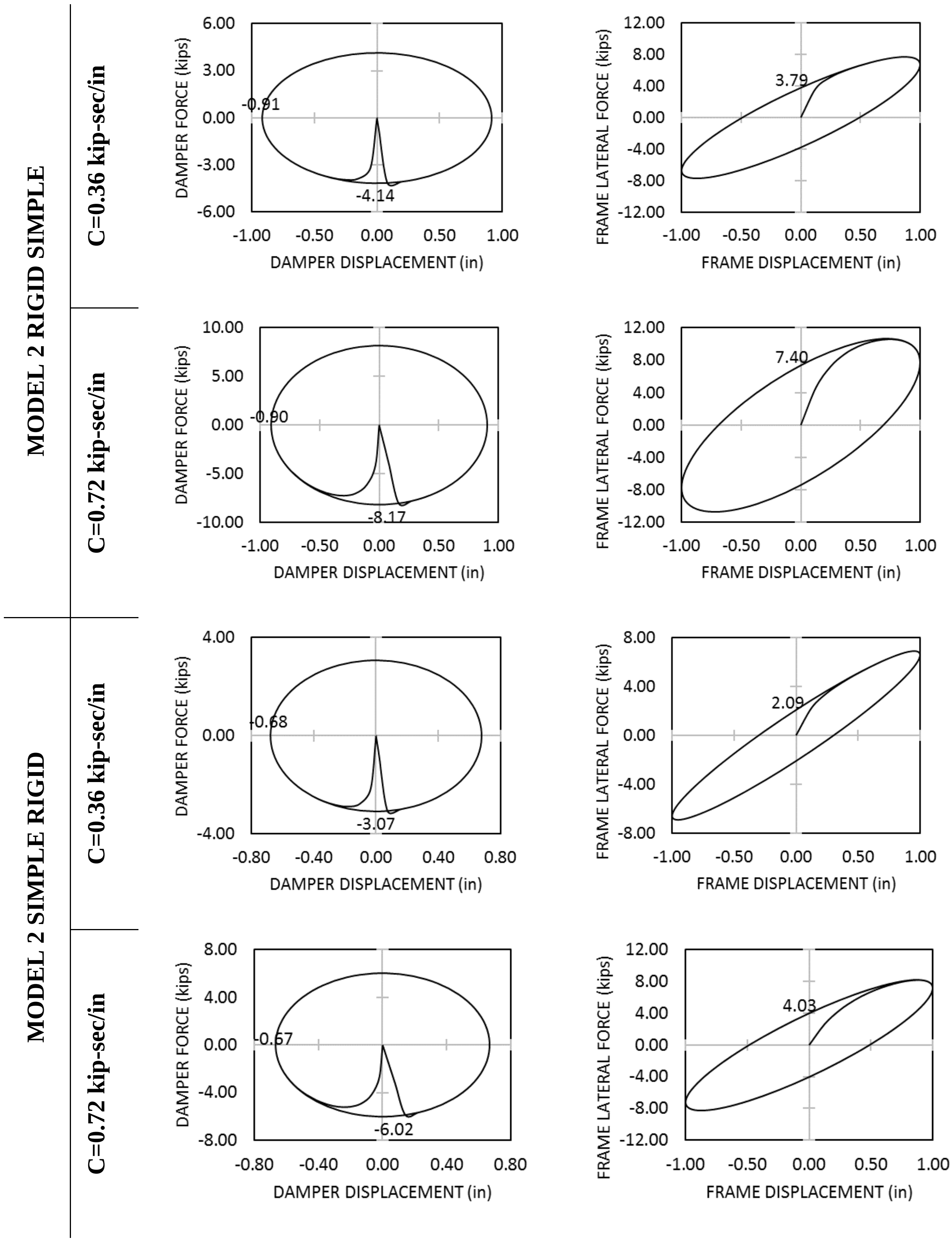

Figure 2-3 Damper force-displacement loops and frame lateral force-displacement loops of Model 2 with C=0.36 and 0.72 kip-sec/in

Damping systems (DS) may be installed in frames that are designed to remain elastic and typically will features simple connections, whereas the seismic force resisting system (SFRS) will be provided by separate frames that typically will undergo inelastic deformations. Also, the DS and SFRS may be integrated into a single configuration in which the two systems have common elements. The commentary to the recent FEMA P-1050 (FEMA, 2015) best illustrates these concepts. In the former system configuration, the DS and SFRS do not share any elements and frame deformation and inelastic effects do not affect the magnification factor. In the latter configuration, the DS and SFRS have common elements and the frame deformation and inelastic action may have effects on the magnification factor. This is investigated by recalculating the magnification factor in the examples of Figure 2-4 by allowing inelastic action and also considering small and large deformation/rotation effects. For the inelastic analysis, plastic hinges were assumed to form at the location of the rigid beam-to-column connections. Analysis was performed using the FEMA 356 plastic hinge feature of program SAP2000 with material yield strength of 345MPa or 50ksi. The results are included in Figure 2-4 where it is seen that the effect of inelastic action on the magnification factor is small and beneficial. The result may be explained by considering that when plastic hinges develop there is less column rotation and deformation effects on the beam to which the rocker plate is attached.

The analysis of the example frames also produced results on member forces that are of interest to discuss as the addition of the damping system changes the load paths and affects, among other things (e.g., see Constantinou et al, 1998), the member axial forces. Concentrating on the case of Model 3 with R-R configuration as having the largest magnification factor (0.91 per Table 2-1), the inclined brace force, the column axial forces and the beam axial force were calculated in the analysis under elastic, small rotations conditions. The analysis included the damper force and the frame was driven in prescribed motion of 1Hz frequency and 1 inch (25.4 mm) amplitude as previously described in connection with the results of Table 2-1. Peak values of damper force, column and beam additional axial force and brace axial force (compression or tension) were as follows: (a) Damper, 2.09kip (9.3kN), (b) Brace, 4.95kip (22.0kN), (c) Column 13.76 kip (61.2kN) and (d) Beam, 14.1kip (62.7kN). Note that the axial beam and column forces are caused by the (portal) frame action during application of the lateral force that has a peak value of 17.2kip (76.4kN). Analysis of the same frame without the damper resulted in peak column axial force of 12.8 kip (56.9kN) and peak beam axial force of 8.4kip (37.4kN). The addition of the damping system results in insignificant additional axial force in the column due to the fact that the peak damping force does not occur at the same time as the peak lateral force (actually the peak damper force occurs at the instant of peak velocity for which the drift is zero in the analyzed harmonic motion) but has an important effect on the axial force in the beam.

It should be noted that the forces calculated above could also be predicted by static analysis and use of theory as follows. The damper force F_D is given by $\omega f C u$ where ω is the frequency of harmonic motion (2π rad/sec for 1Hz), C=0.36kip-sec/in (63N-sec/mm) (the damper constant), f=0.91 (the magnification factor) and u=1 inch (25.4mm) (amplitude of frame motion). The result is 2.07kip (9.2kN) (computational analysis gave 2.09kip (9.3kN)). Use of Equation (14) yields the force in the brace T=4.92kip (21.9kN) (computational analysis gave 4.95kip (22.0kN)) and Equation (15) gives the lateral component of the damping force acting on the frame as F=1.44kip (6.4kN).

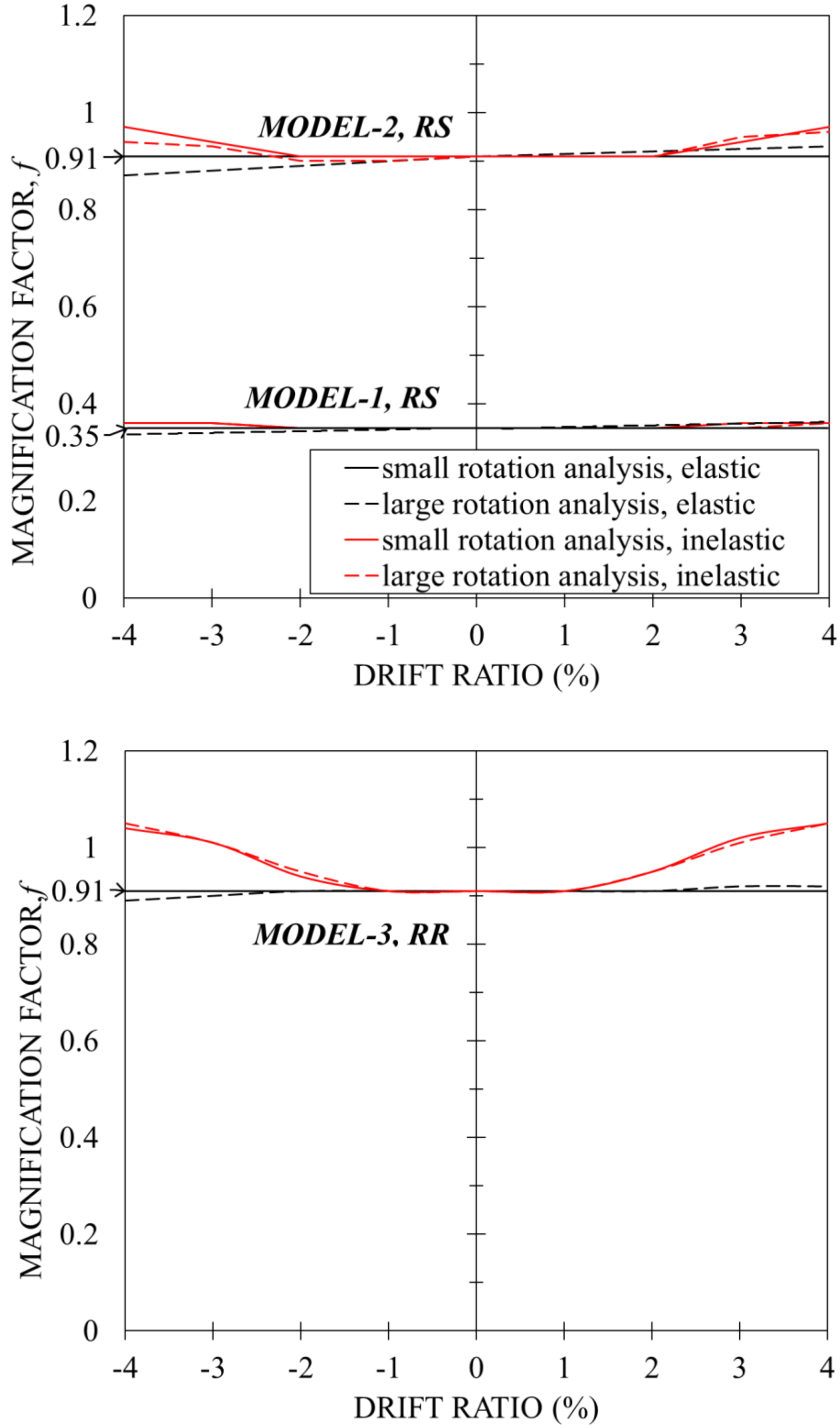

Figure 2-4 Magnification Factor as Function of Drift Ratio without and with Due Consideration of Large Deformation/Rotation Effects

SECTION 3
TESTING OF INDIVIDUAL FRAMES WITH OPEN SPACE DAMPING SYSTEM

3.1 Description of Tested Structure

A half-length length scale steel frame was constructed for the purpose of testing the open space damping system. The model structure consisted of two identical frames of the geometry shown in Figure 3-1. Testing was first conducted with one frame attached to the strong floor and cyclically driven by an actuator. The two configurations of Figures 1-5(a) and 1-5(b) were tested in this way. This testing is described in this section. Section 4 describes earthquake simulator testing in which two frames were used in three different configurations: the two of Figures 1-5(a) and 1-5(b) and a variant of the configuration of Figure 1-5(b).

Figure 3-1 shows the geometry and open space damping system configurations of the tested frames. Three different models are shown (Model 1, Model 2 and Model 3) of which only the first two were used in the individual frame testing, whereas all three models were used in the earthquake simulator testing. Views of the tested frame and details of connections are presented in Figures 3-2 and 3-3. Column base plates were simply connected to a beam, which in turn was connected to the strong floor. All connections of the damping system feature true pins.

Testing was conducted with a hydraulic actuator attached to the column joint on the left side of the frame as seen in Figures 3-2 and 3-3, and harmonic displacement history was imposed with a frequency at 0.05Hz (quasi-static), 1 Hz and 2Hz (dynamic). The amplitude of the motion was either 0.5inch or 1inch. Histories of the frame lateral displacement at the beam-column joint, damper displacement (change of length), damper force and lateral frame force (force measured by the load cell on the actuator) were recorded. Note that the lateral frame force includes the inertia force of the moving parts of the actuator, the beam and part of the columns. The peak value of the inertia force was estimated to be less than 65lbs and was deemed negligible by comparison to the base shear force. Accordingly, no corrections for the inertia effects were made.

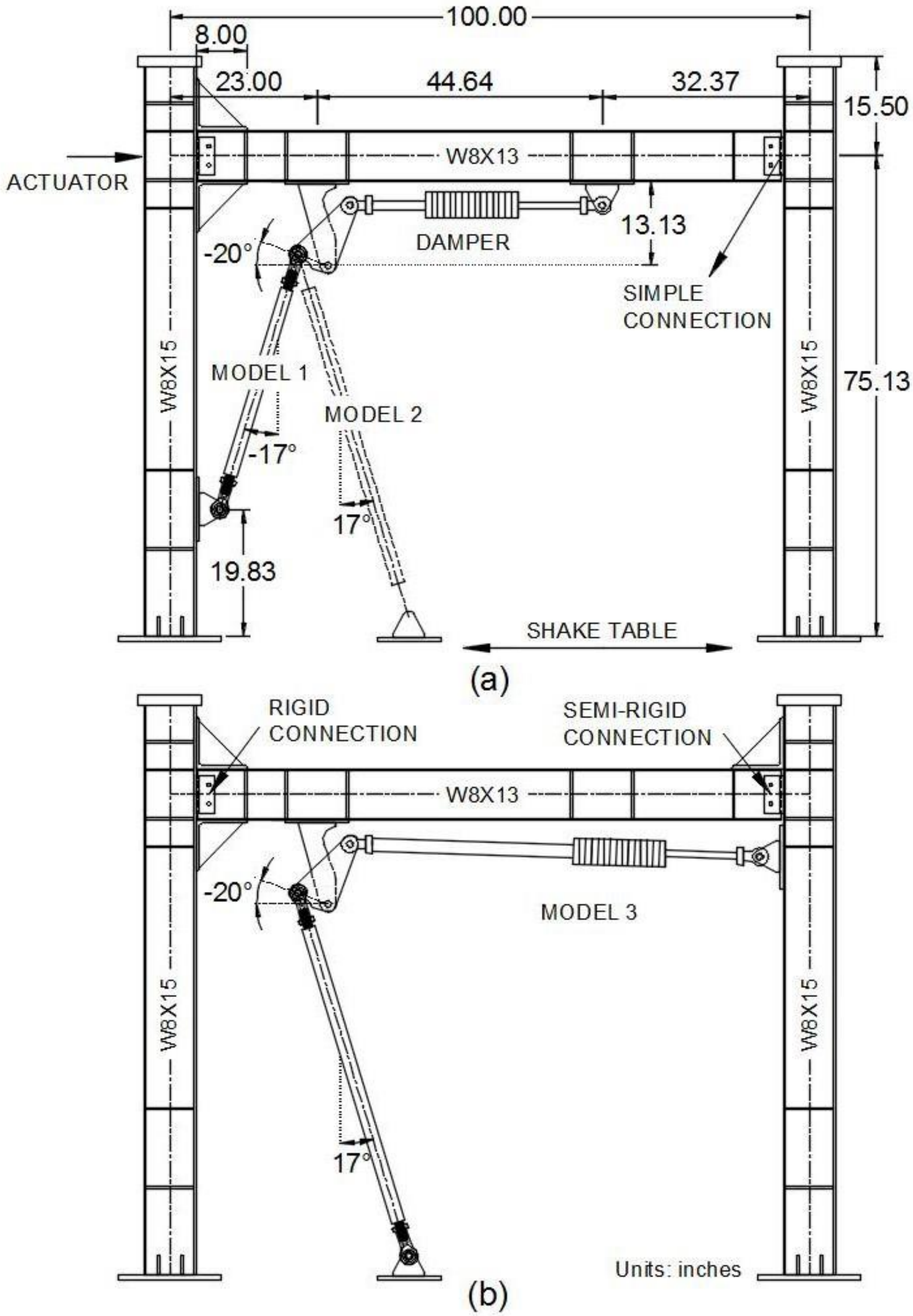

Figure 3-1 Geometry and Open Space Damping System Configurations of Tested Frames: (a) Models 1 and 2 with Rigid-Simple Beam-to-Column Connections; (b) Model 3 with Rigid-Simple Beam-to-Column Connections

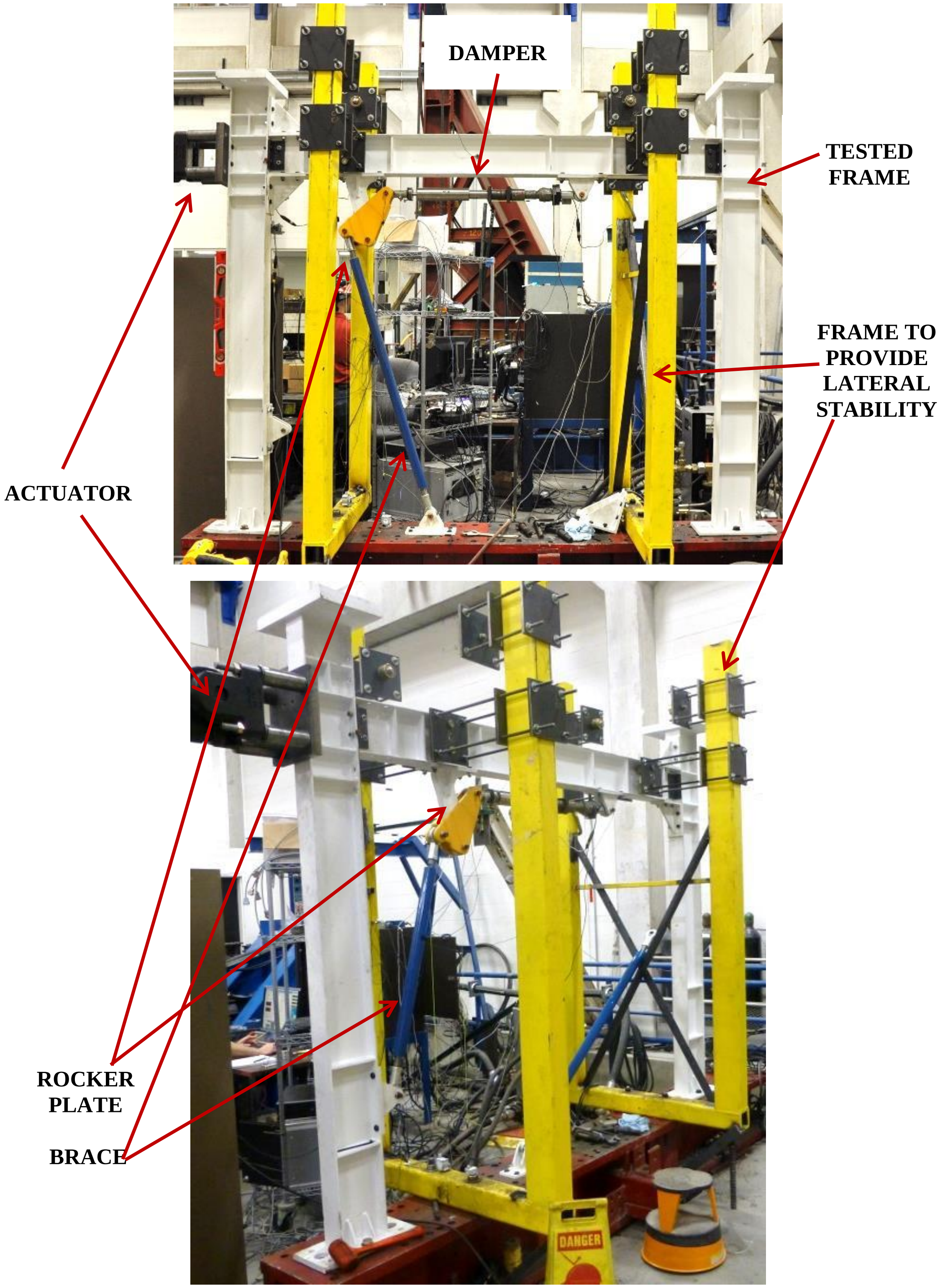

Figure 3-2 Views of Tested Single Frame

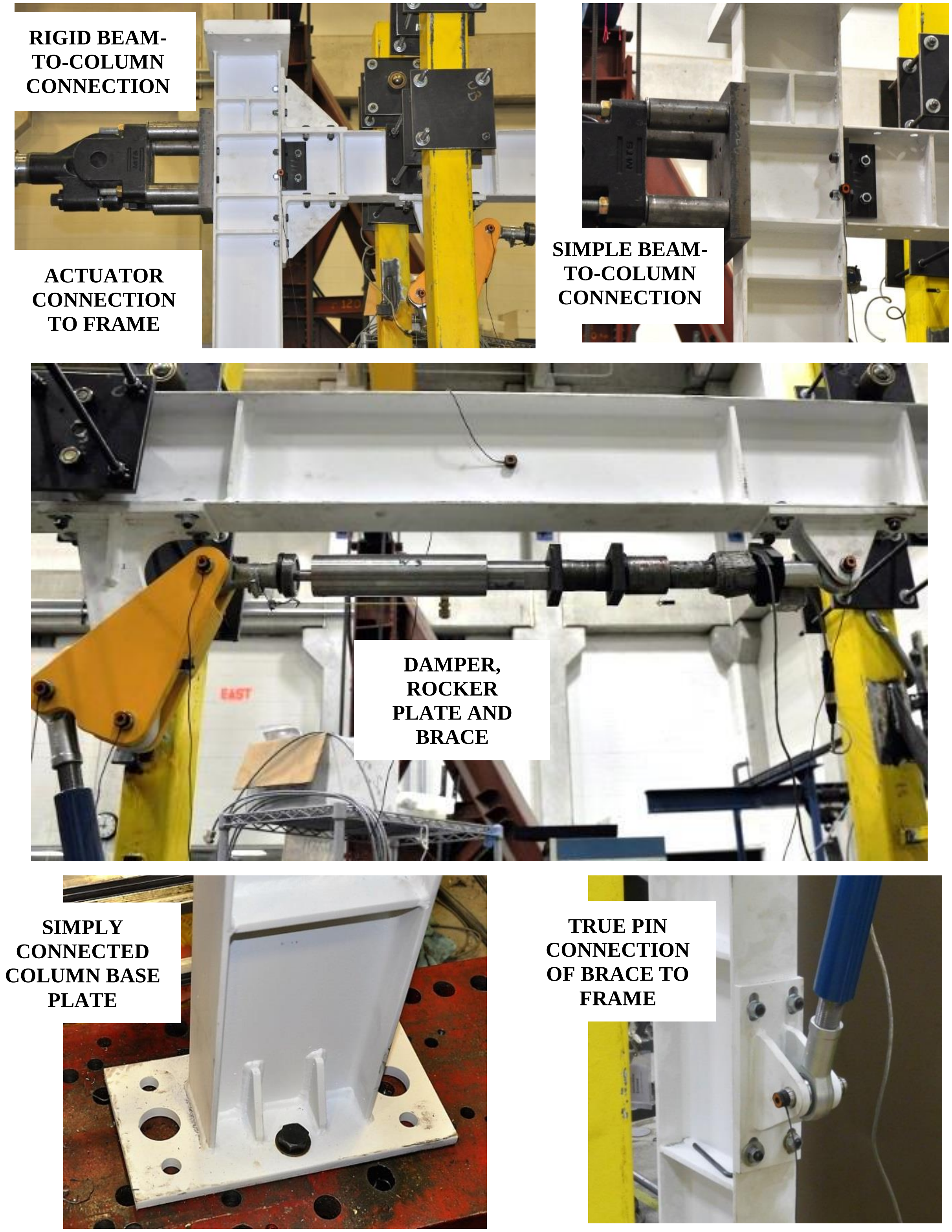

Figure 3-3: Close-up Views of Tested Frame

The tested structure features the following:

1. The beam-to-column connections could be easily converted between simple and rigid by using stiffened angles bolted to the top and bottom flanges of the beam and to the column flange as shown in Figure 3-2 and 3-3. This enabled testing with one rigid and one simple connection per frame (referred to as rigid-simple or simple-rigid configurations), and two rigid connections per frame (rigid-rigid configuration). However, all so-called simple connections exhibited some rotational stiffness and hysteresis, so that in effect all "simple" connections were semi-rigid connections with the degree of fixity dependent on the amount of torque applied to the bolts and relaxation with repeated testing. This complicated the analytical prediction of response for the purposes of comparison to the experimental results.
2. All connections of the open space damping system were built as true pins. Examples are shown in Figure 3-3 for the rocker plate connecting the horizontal damper to the vertically inclined brace and the brace connection to the column.
3. Lateral stability of the single frame was provided by two auxiliary frames as seen in Figure 3-2.
4. Two linear viscous dampers were used in the experiments, each with a damping coefficient C_o=0.36 kip-sec/in. These devices are the same as those used in Sarlis et al. (2013), where results on the testing of the dampers were reported. The dampers were not individually tested prior to conducting the tests reported herein.

3.2 Instrumentation of Tested Frame

Instrumentation of the tested frame consisted of displacement transducers in the form of string potentiometers, load cells and Krypton light-emitting diodes (LED). The Krypton measurement system operates by reading infrared signals from LED and measures absolute displacement, velocity and acceleration. The system was used to acquire motion readings (displacement, velocity and acceleration) of various points on the open space damping system and for backup of the string potentiometers. Figure 3-4 illustrates the instrumentation diagram of the tested frame on the strong-floor and Table 3-1 presents the list of the channels used. The damper load cell was manufactured in-house and was calibrated prior to testing- the error of the reading of the load cell was less than 2-percent. The actuator load cell was calibrated by the manufacturer and had a valid calibration certificate.

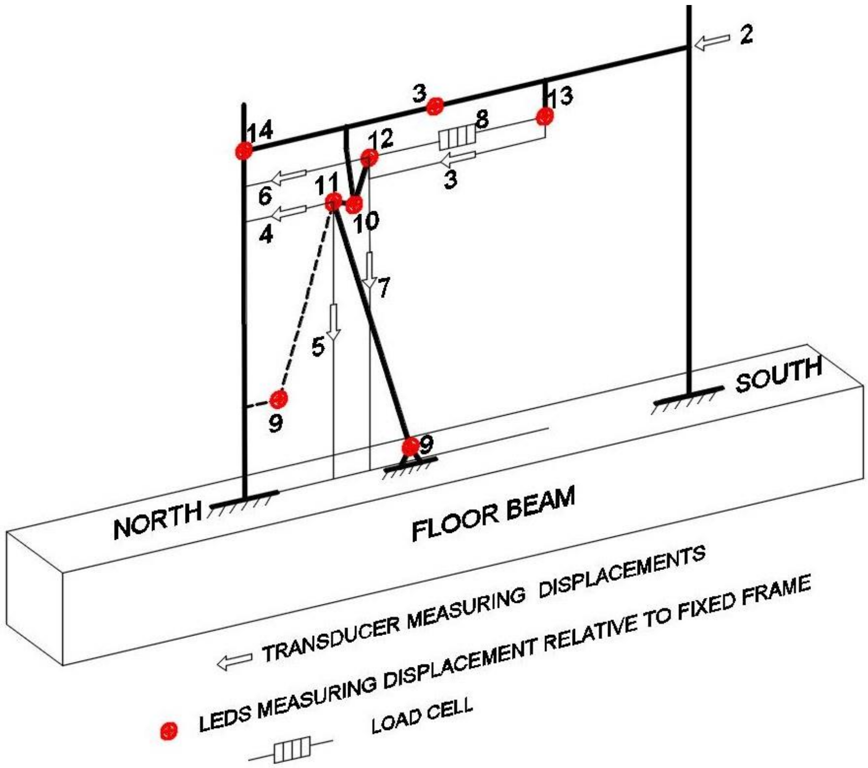

Figure 3-4 Instrumentation Diagram of Tested Frame

Table 3-1 List of Channels Used in Frame Testing

CHANNEL	INSTRUMENT	QUANTITY MEASURED	UNIT
1	/	Time	sec
2	Disp. Transducer	Column Joint Horiz. Displ	in
3	Disp. Transducer	Damper Relative Displ.	in
4	Disp. Transducer	Rocker Plate Horiz. Displ	in
5	Disp. Transducer	Rocker Plate Vert. Displ	in
6	Disp. Transducer	Rocker Plate Horiz. Displ	in
7	Disp. Transducer	Rocker Plate Vert. Displ	in
8	Load Cell	Damper Force	kip
9	LED	Rod Base Pin Dipl.	in
10	LED	Rocker Plate Pivot Displ.	in
11	LED	Rocker Plate Displ.	in
12	LED	Damper Displ.	in
13	LED	Damper Displ.	in
14	LED	Column Joint Horiz. Displ	in
15	Load Cell	Actuator Force	kip

3.3 Results of Testing of Frame

Selected representative results are presented in this section. Appendix B presents a larger collection of results acquired in the testing of individual frames. The results include the following information:

1. Model number, beam-to-column connection type, information on the amplitude and frequency of imposed motion. The model number is 1 or 2 per Figure 3-1(a). The beam-to-column connection is classified as type R-S when the beam-to-column connection on the left is rigid and the one on the right is simple. The beam-to-column connection is classified as type S-R when the beam-to-column connection on the left is simple and the one on the right is rigid.
2. Loop of frame lateral force (force applied by actuator at beam-to-column connection) versus drift (displacement of beam-to-column connection with respect to column base. This force is essentially the base shear force (but for a small inertia force of moving parts, estimated to be less than 65lbs).
3. Loop of damper force versus damper displacement.
4. Graph of damper displacement versus drift (lateral displacement of the frame).

The sign convention adopted for the presentation of the test results is: (a) positive frame displacement and frame lateral force when the drift is to the right per Figure 3-1, (b) positive damper displacement and damper force when the damper is in extension (piston rod moves out), (c) the base shear force is negative when the drift of the frame is positive (note that base shear is in opposite sign with lateral force which is assumed as actuator force in the strong-floor testing).

Results for the four tested cases are presented in Figures 3-5 to 3-8 in motion of amplitude of 1in and frequencies of 0.05Hz (quasi-static) and 2.0Hz (dynamic). At the frequency of 0.05Hz there is practically no damping force so that the behavior of the un-damped frame is revealed. Each of these figures includes information on the magnification factor: (a) as calculated by Equation (1-9) without due consideration for frame deformation effects, f_{THEORY}, (b) as calculated by a computational model of the tested frame in program SAP2000 (Computer and Structures, 2006), f_{COMP} (from Table 2-1), and (c) based on the measurements of displacements during testing under quasi-static and dynamic conditions, f_{EXP}. This factor was determined as the ratio of the damper peak displacement (u_D) to the frame peak drift (u). There are two values shown in the figures for the experimental value because the damper displacements differ depending on the direction of motion as explained below. Note that values of f_{COMP} reported in Table 2-1 in which the frame model analyzed had the simple connections modelled as true pins and with due consideration of the frame deformations caused by the lateral frame deformation and the damper forces. Table 3-2 compares the values of the magnification obtained by analysis and experiment.

Table 3-2 Values of Magnification Factor

Model	**Theory (Eq.** (1-9)**)** f_{THEORY}	**Computational**[1] f_{COMP}	**Experimental**[2] **(quasi-static)** f_{EXP}	**Experimental**[2] **(dynamic)** f_{EXP}
Model 1, R-S	0.55	0.35	0.41/0.35	0.35/0.37
Model 2, R-S	0.69	0.91	0.94/0.80	0.79/0.75
Model 1, S-R	0.55	0.67	0.53/0.55	0.49/0.53
Model 2, S-R	0.69	0.68	0.80/0.77	0.67/0.68

[1]: Model includes effects of frame deformation; simple connections modelled as pins
[2]: Two values as peak damper displacement is different in two directions

The results in Figures 3-5 to Figure 3-8 and Table 3-2 reveal the following:

1. The lateral force-frame displacement loops (base shear vs drift relations) reveal the stiffness and damping characteristics of the tested frames. It is evident in the loops that there is little increase in energy dissipated per cycle in the case on Model-1, R-S (Figure 3-5) and also Model-1, S-R (Figure 3-6). This was expected as the actual magnification factor is small due to the effects of frame deformations. This is also evident in the small damper force measured in both cases and in the small damper displacement measured in Model-1, R-S (one with least magnification factor). By contrast, the loops in Figures 3-7 and 3-8 show a noticeable increase in energy dissipated at the higher frequency test when the damper is activated. Also, note in Figures 3-7 and 3-8 the larger damper force and displacement by comparison to those of the models in Figures 3-5 and 3-6.
2. The lateral frame force-displacement loops (base shear vs drift relations) of the frame with the damping system show a higher stiffness than the loops of the frame without the damping system (the latter presumed to be those of the frame driven under quasi-static

conditions so that the damping force is essentially zero). This is due to the introduction of stiffness by the damping system due to the effect of the deformation of the system to which the damper is attached (including the frame itself). This is a well understood phenomenon (e.g., Constantinou et al. 2001). It can be mitigated by connecting the damping system components directly to or as close as possible to beam-column joints.

3. The damper displacement-frame displacement curves show “hysteresis” that is due to sliding in some of the simple joints and supports of the tested model. This is evident in the fact that the damper displacement remains constant at large values and there is asymmetry with more displacement in one direction than the other. Slippage was inevitable as the diameter of holes was larger than the bolt diameter. For the tested model all holes where oversize (3/16th inch larger than bolt diameter) to allow for ease in assembly and adjustments during testing (particularly when some yielding and distortion occurred). About 3/16th inch (5mm) of sliding motion could occur at each joint. This led to asymmetry in behavior with the experimental magnification factor value being different depending on the direction of motion. Also, the magnification factor values were further affected (reduced) under dynamic conditions due to increase in slippage. Efforts to mitigate this problem included periodic tightening of bolts which was partially effective for short times but also affected the stiffness of the frame as the simple connections actually behaved as semi-rigid of variable stiffness depending on the degree of bolt tightening. This will be better observed in results of identification tests of the frame on the shake table. Generally, this created a complexity in predicting the response of the tested model as the properties of the frame kept changing.
4. The experimental value of the magnification factor is generally consistent with the value obtained by the computational model.

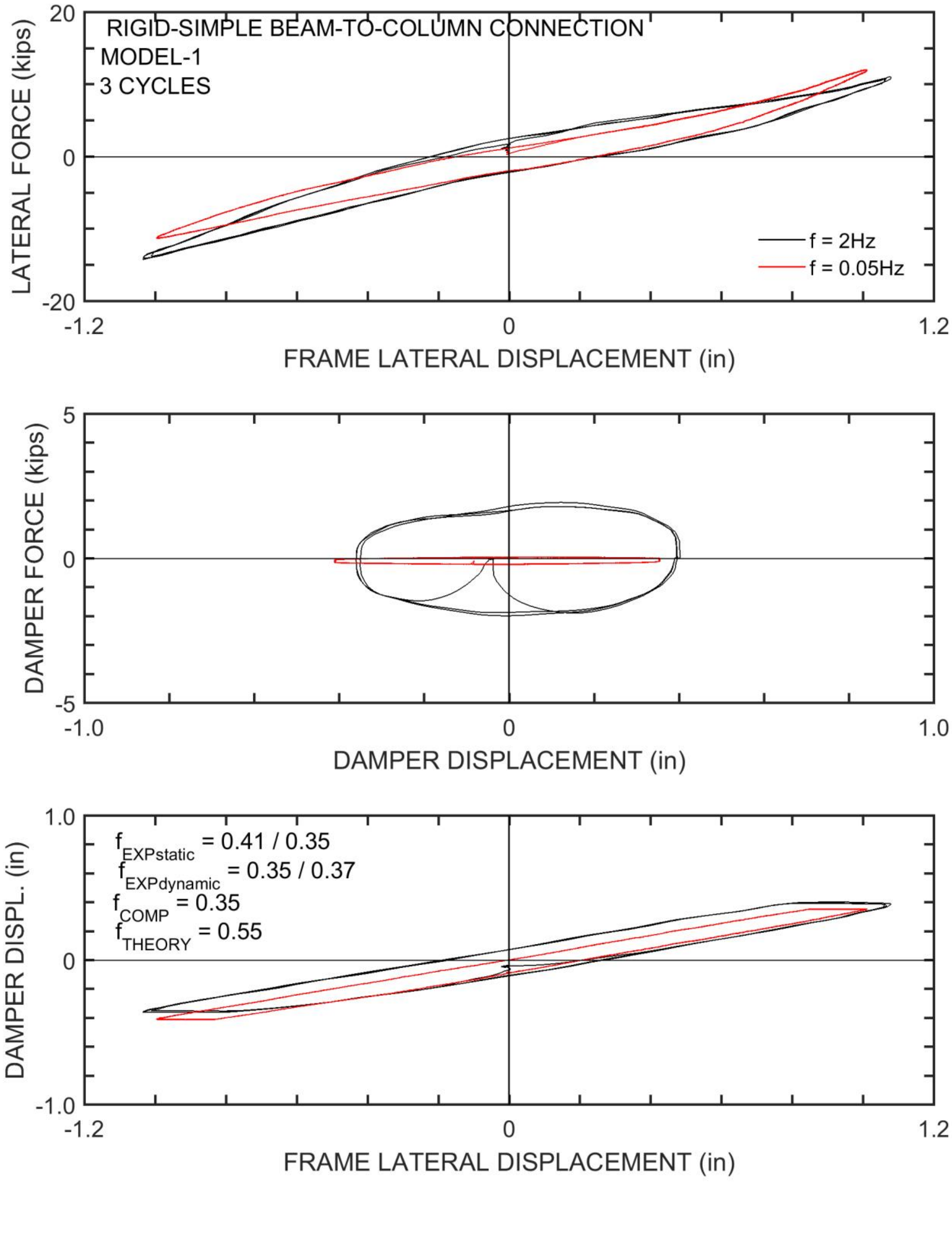

Figure 3-5 Recorded Response of Model 1 R-S Frame Subjected to Lateral Motion at the Joint

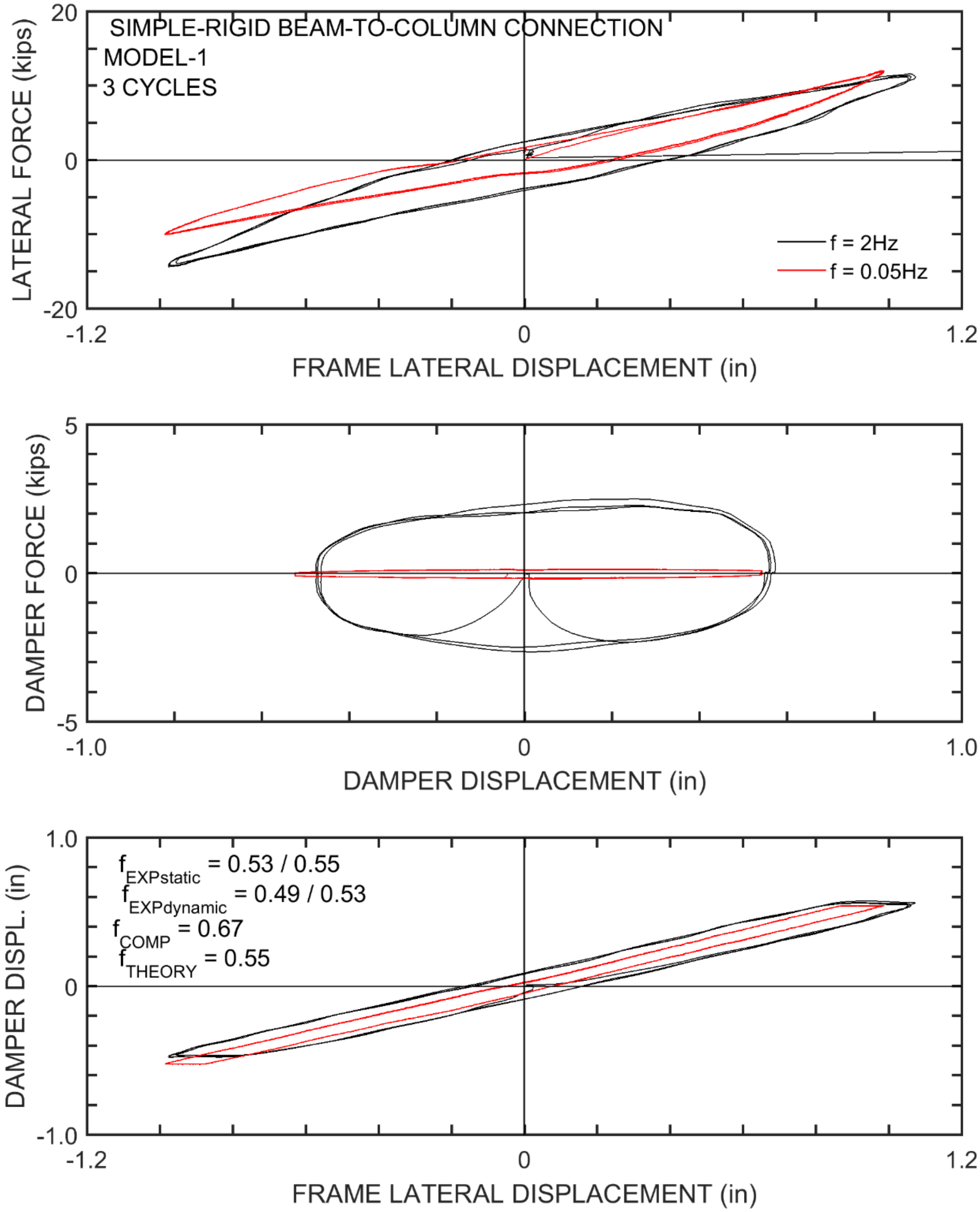

Figure 3-6 Recorded Response of Model 1 S-R Frame Subjected to Lateral Motion at the Joint

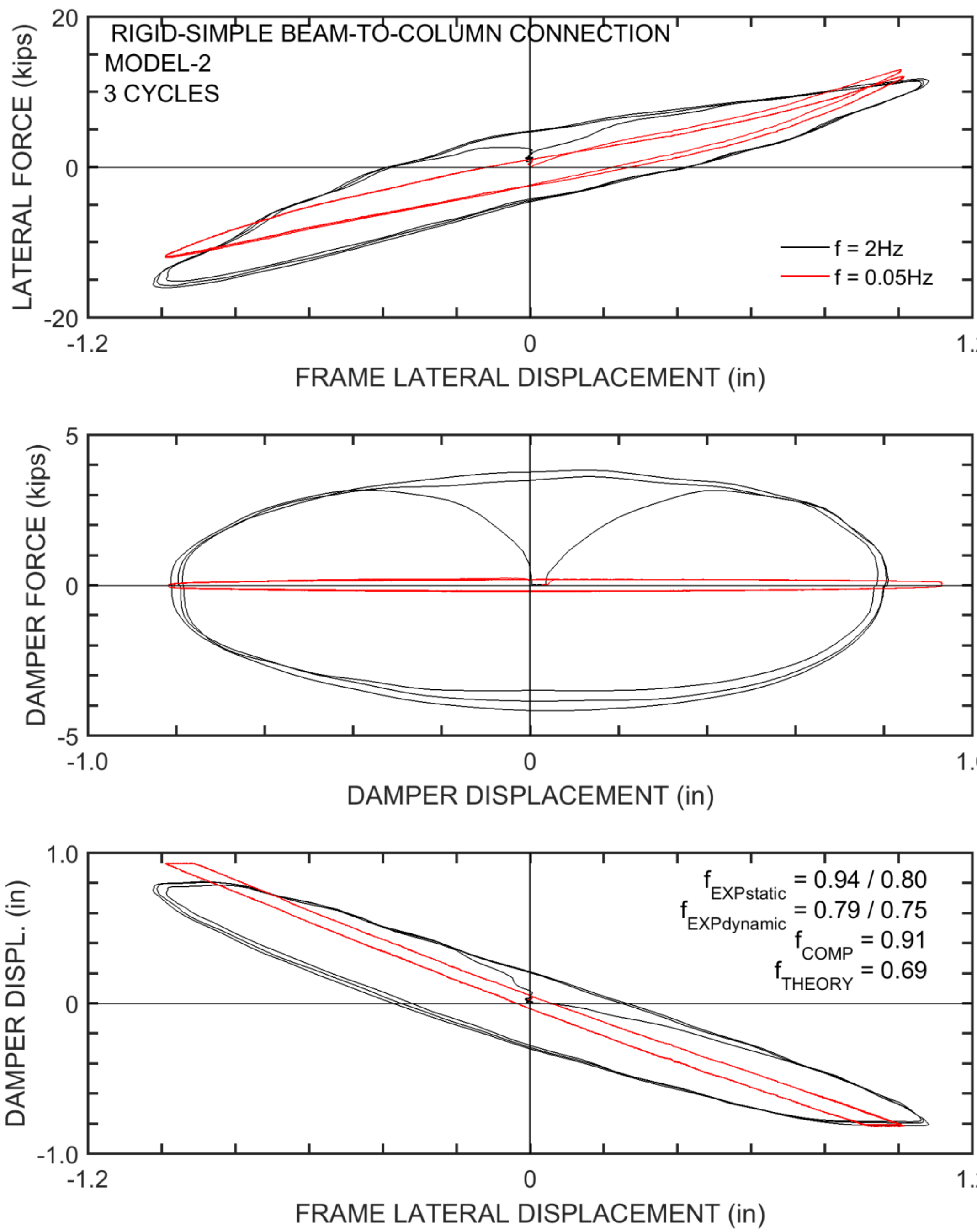

Figure 3-7 Recorded Response of Model 2 R-S Frame Subjected to Lateral Motion at the Joint

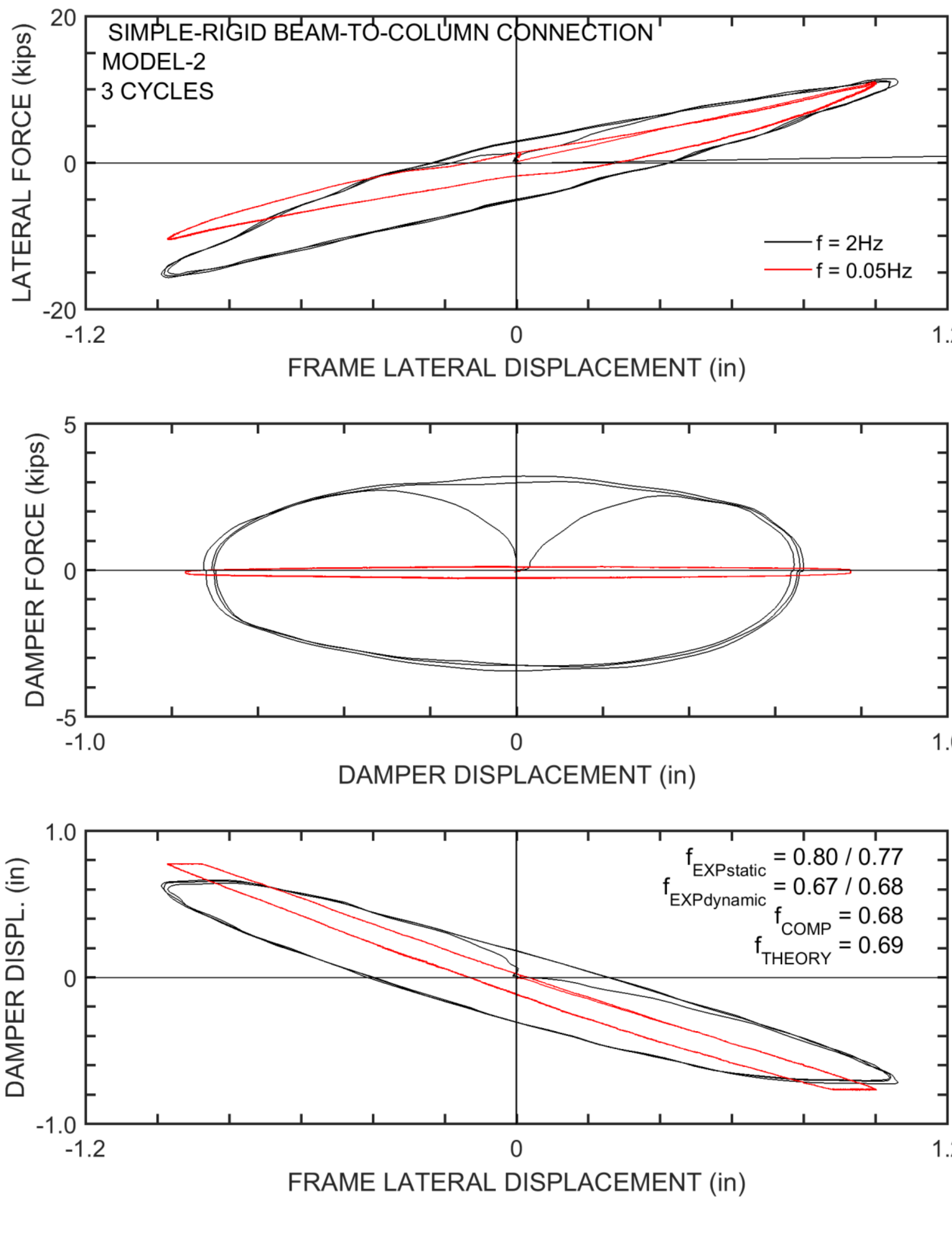

Figure 3-8 Recorded Response of Model 2 S-R Frame Subjected to Lateral Motion at the Joint

3.4 Analytical Prediction of Response

The tested frame was modelled and analyzed in computer program SAP2000. Figure 3-9 illustrates the computational model of the tested frame for the rigid-simple beam-to-column configuration (to avoid repetition, element list and their properties are presented in Section 5 in Table 5-2). The model featured true pins for the damping system elements. Moreover, all elements of the damping system were properly represented by beam elements to correctly account for their flexibilities. Supports 1 and 4 were modelled as pinned with an added elastic rotational spring to simulate the behavior of the supports. The simple beam-to-column 3 on the right was modelled as a pin with an added nonlinear rotational spring. The rotational stiffness of the added rotational springs at joints 1, 3 and 4 was assigned values to better approximate the measured stiffness of the tested frame. The hysteretic properties of joint 3 were assigned so that a representative hysteretic behavior was obtained as seen in the recorder base shear-frame displacements loops. However, the tested frame exhibited asymmetric behavior with more stiffness in one direction (see Figures 3-5 to 3-8) which could not be simulated in the described analytical model. The source of the asymmetry was slippage in the joints, a phenomenon which difficult to simulate as it depended on amount of torque put in the bolts (which was unknown), friction in the joints and allowance for motion in the oversize holes (which varied from test to test). Note that the asymmetry is much less in the frame tested under quasi-static conditions (essentially zero damping force) as a result of reduced slippage in the joints.

Figures 3-10 to 3-17 compare the experimental response of the tested frames to analytically predicted response in the tests at frequency of 1Hz and 2Hz, and amplitude of 1inch. These were the cases in which slippage in the joints of the model resulted in asymmetric hysteretic behavior. The computational prediction of the response of the tested frames is seen to be good despite the inability to model the asymmetry in stiffness and slippage in the joints. Note that this is a characteristic of the tested model while in actual applications the connections will be welded or with standard size holes, for which slippage in the joints will be smaller ($1/16^{th}$ inch rather than $3/16^{th}$ inch). The importance of joint slippage is better appreciated when one considers that the tested frame was at length scale of 2, so that the drift and damper displacement were half of those of actual buildings, whereas the slippage was as much as three times larger.

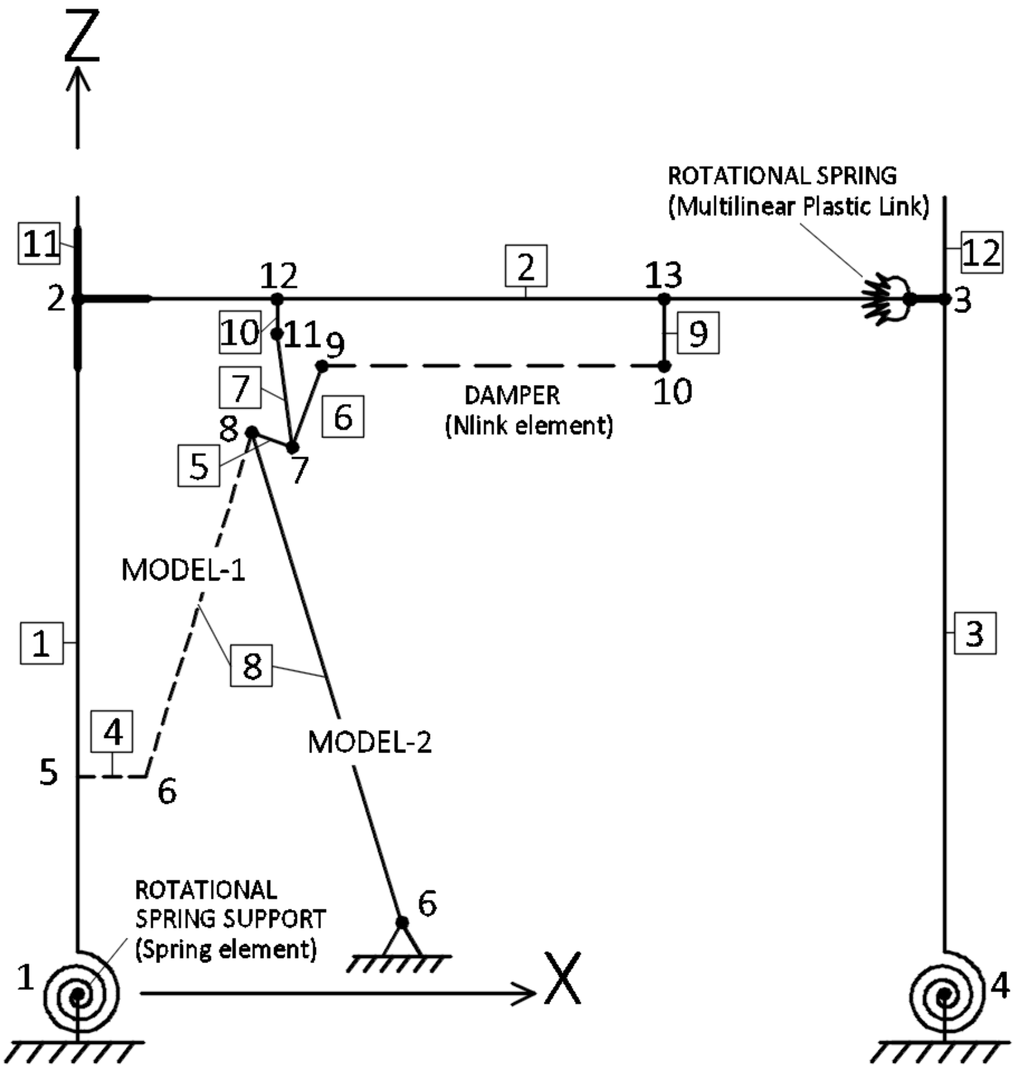

Figure 3-9 Analytical Model for Tested Model 2 R-S

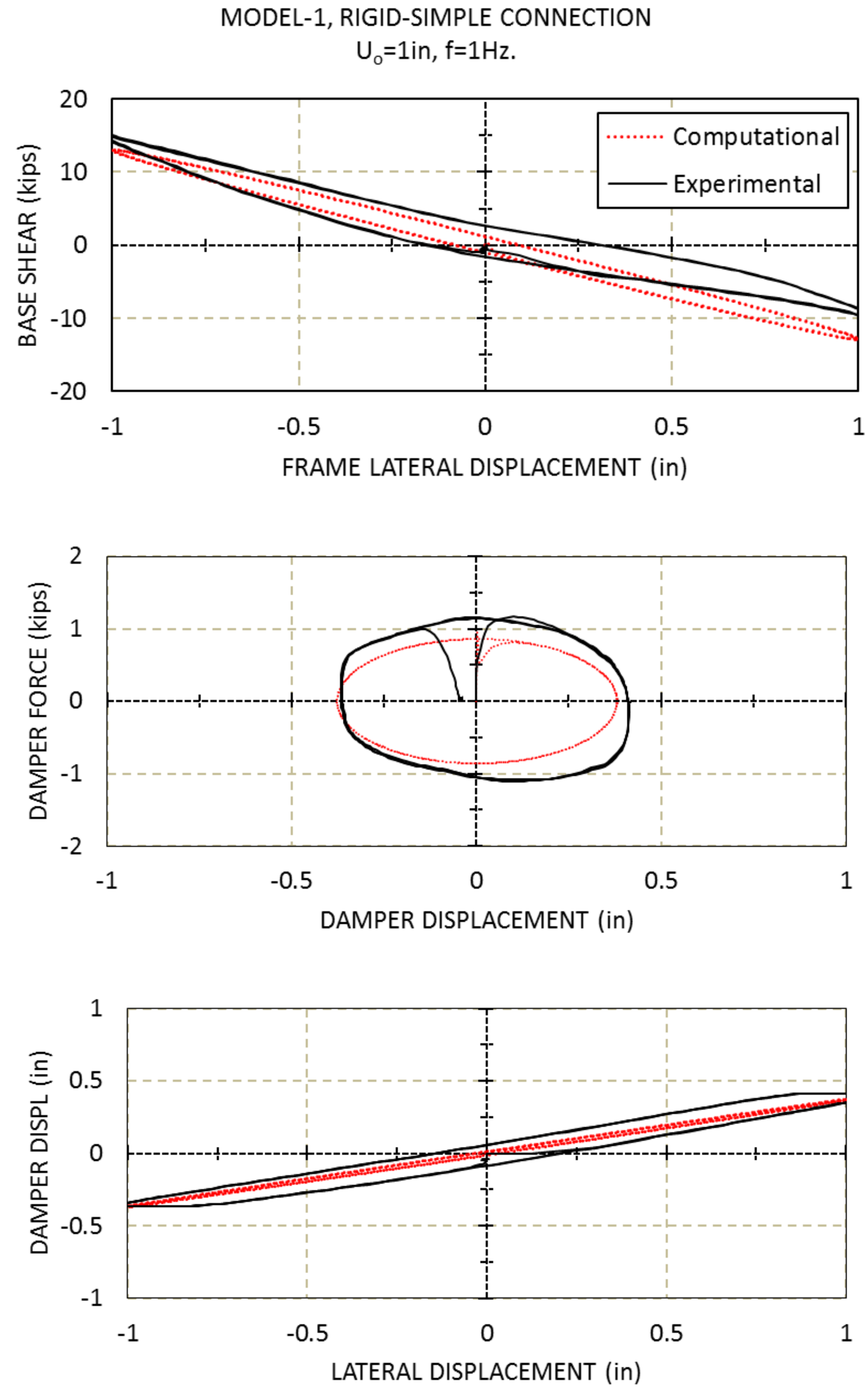

Figure 3-10 Measured and Predicted Single Frame Response of Model 1 R-S in Test of 1 inch Amplitude at 1Hz Frequency

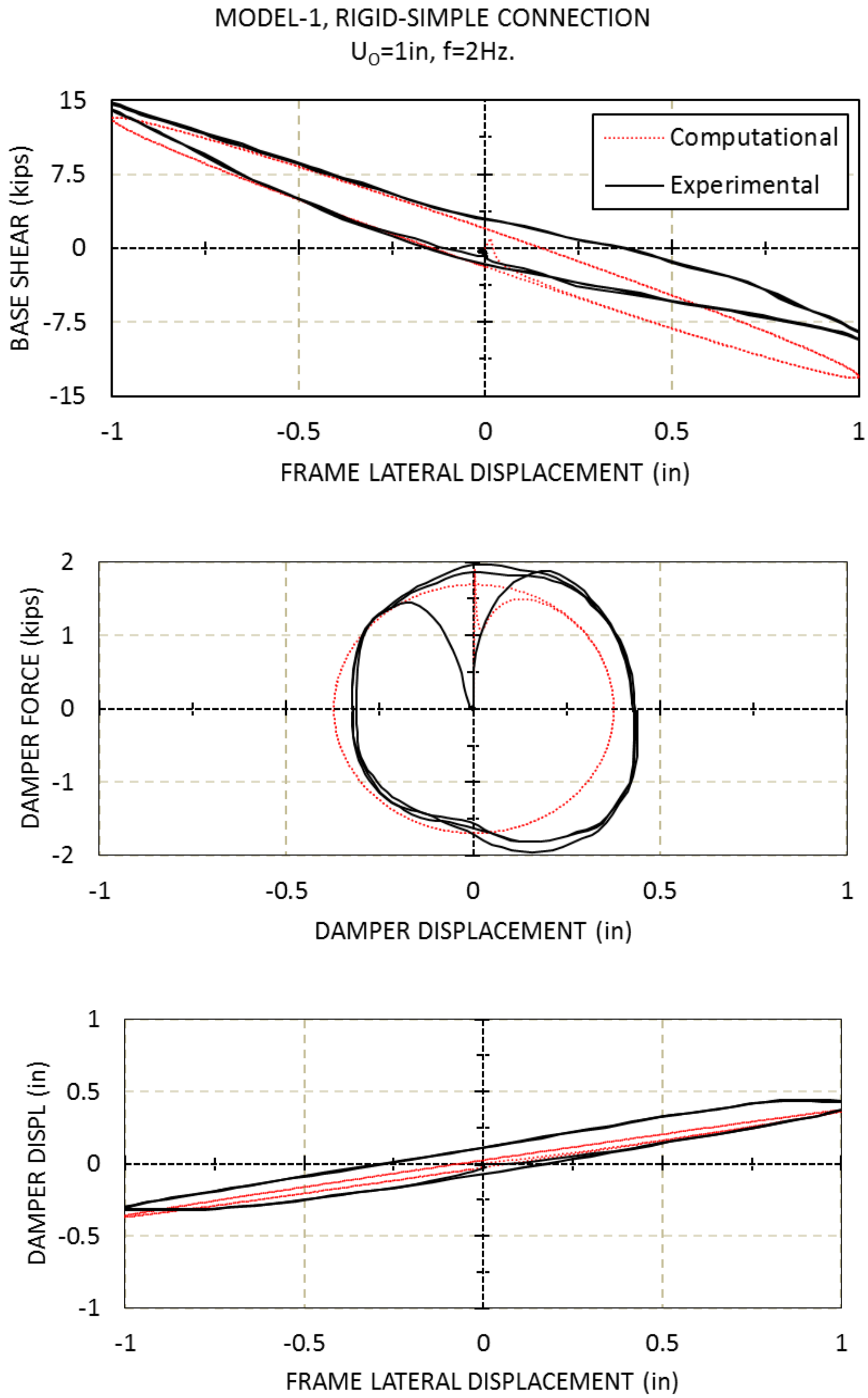

Figure 3-11 Measured and Predicted Single Frame Response of Model 1 R-S in Test of 1 inch Amplitude at 2Hz Frequency

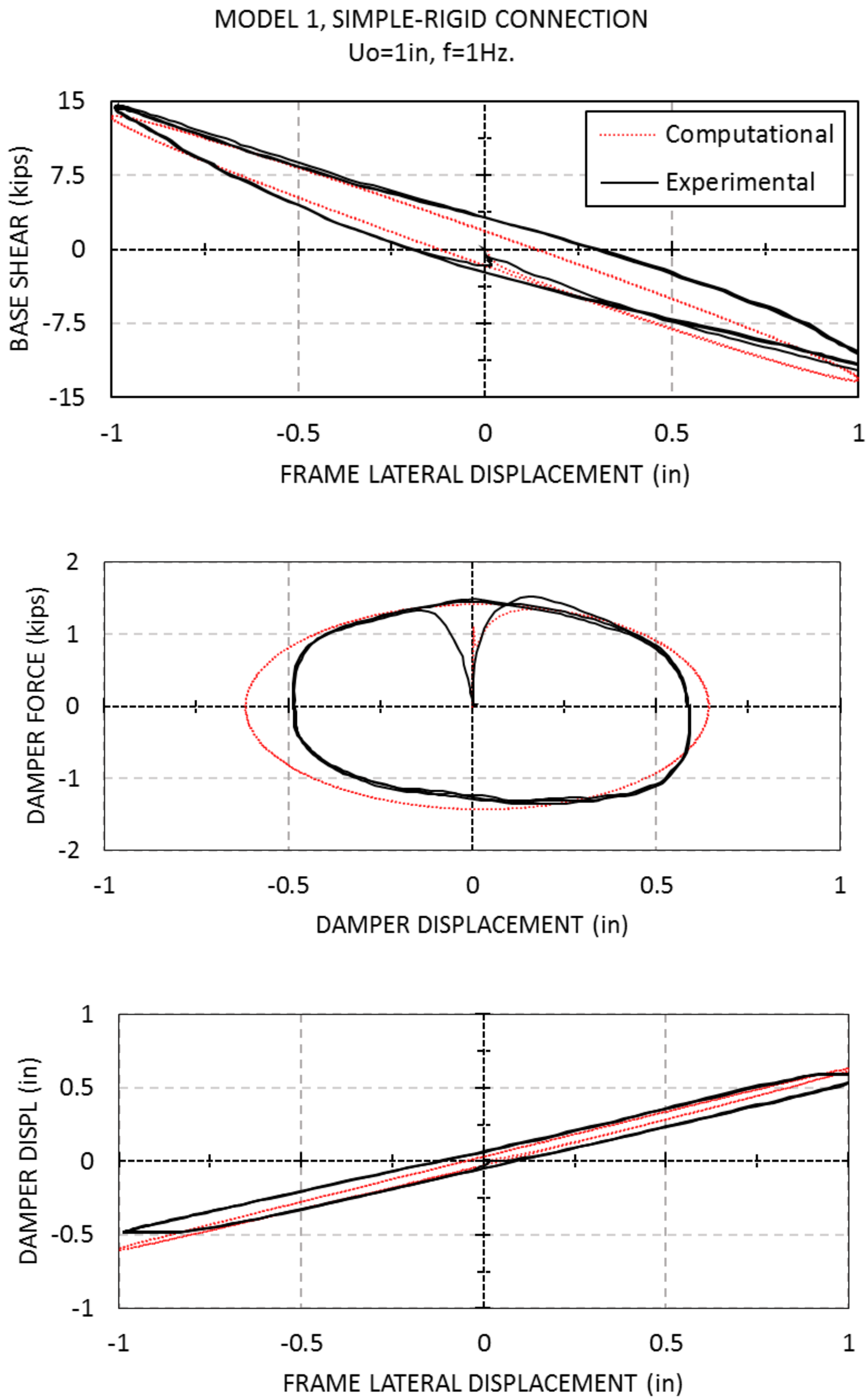

Figure 3-12 Measured and Predicted Single Frame Response of Model 1 S-R in test of 1 inch Amplitude at 1Hz Frequency

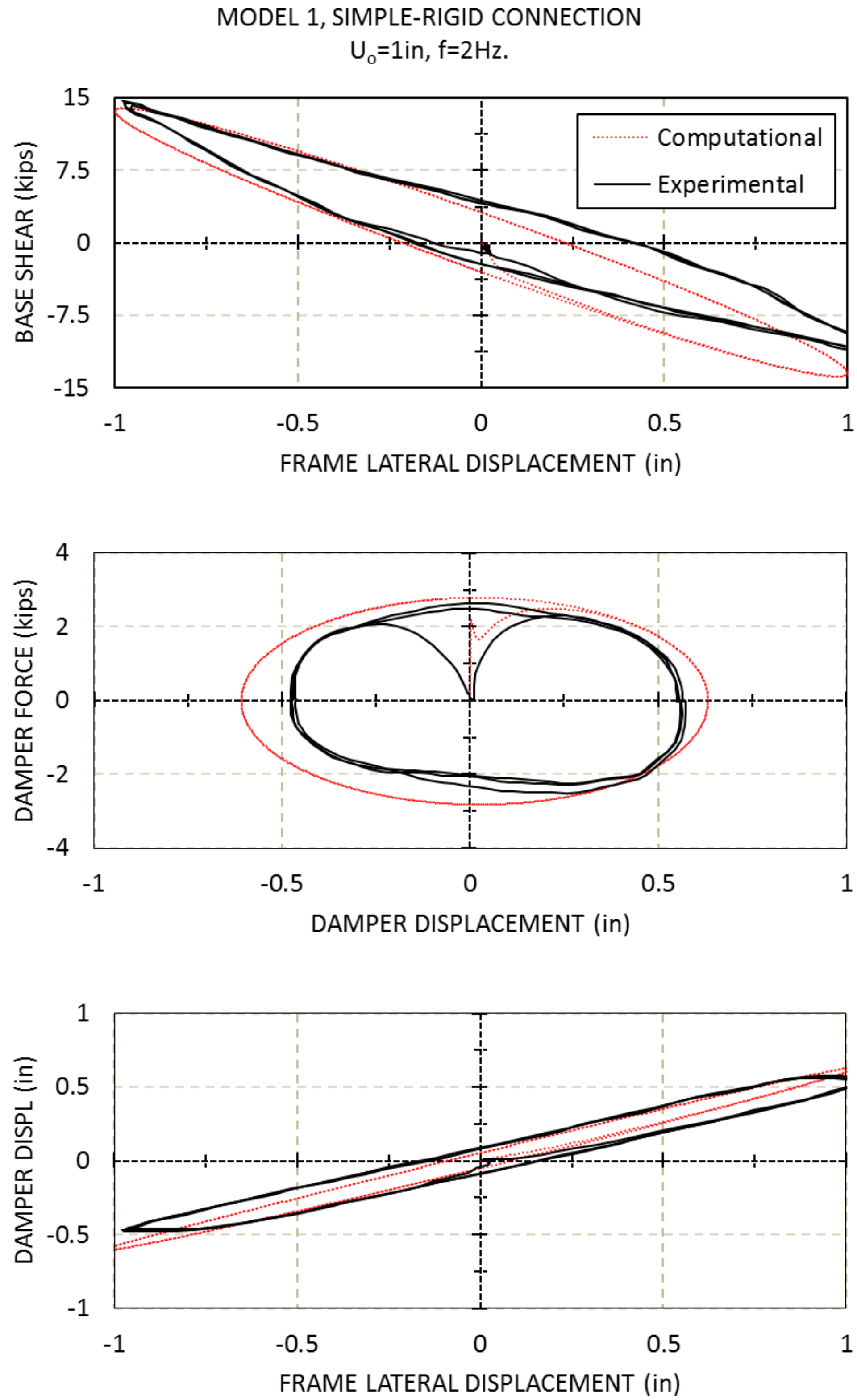

Figure 3-13 Measured and Predicted Single Frame Response of Model 1 S-R in Test of 1 inch Amplitude at 2Hz Frequency

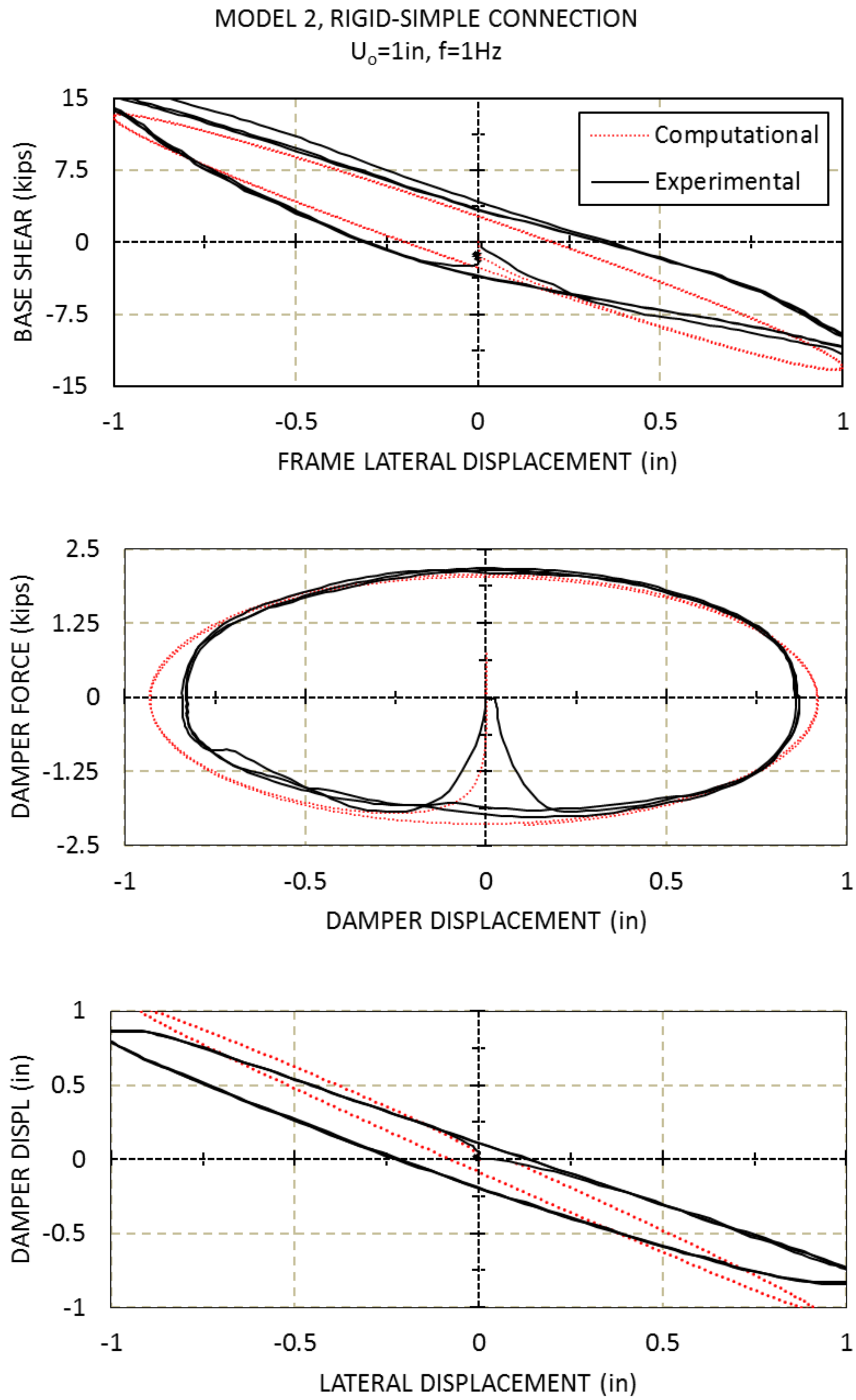

Figure 3-14 Measured and Predicted Single Frame Response of Model 2 R-S in Test of 1 inch Amplitude at 1Hz Frequency

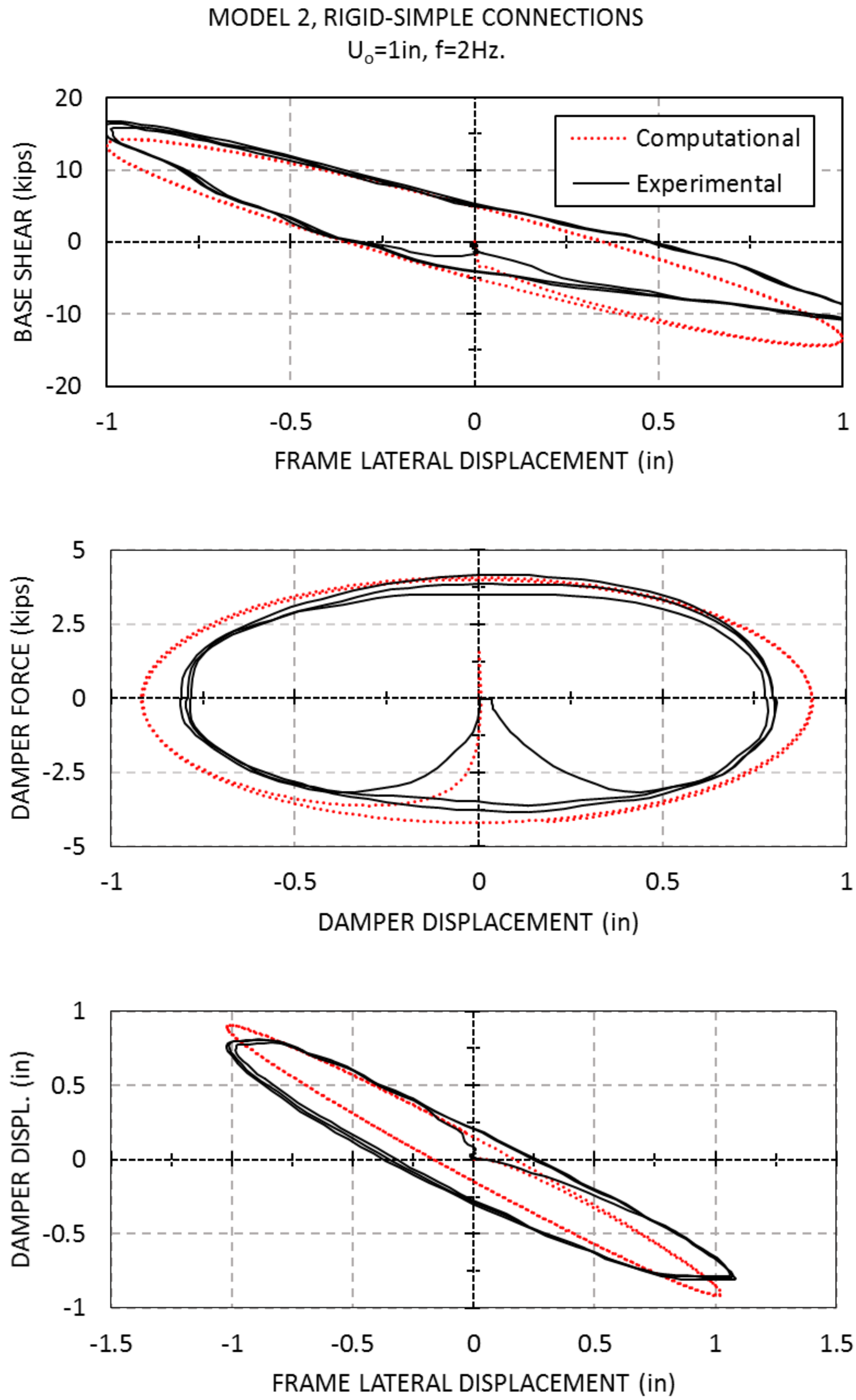

Figure 3-15 Measured and Predicted Single Frame Response of Model 2 R-S in Test of 1 inch Amplitude at 2Hz Frequency

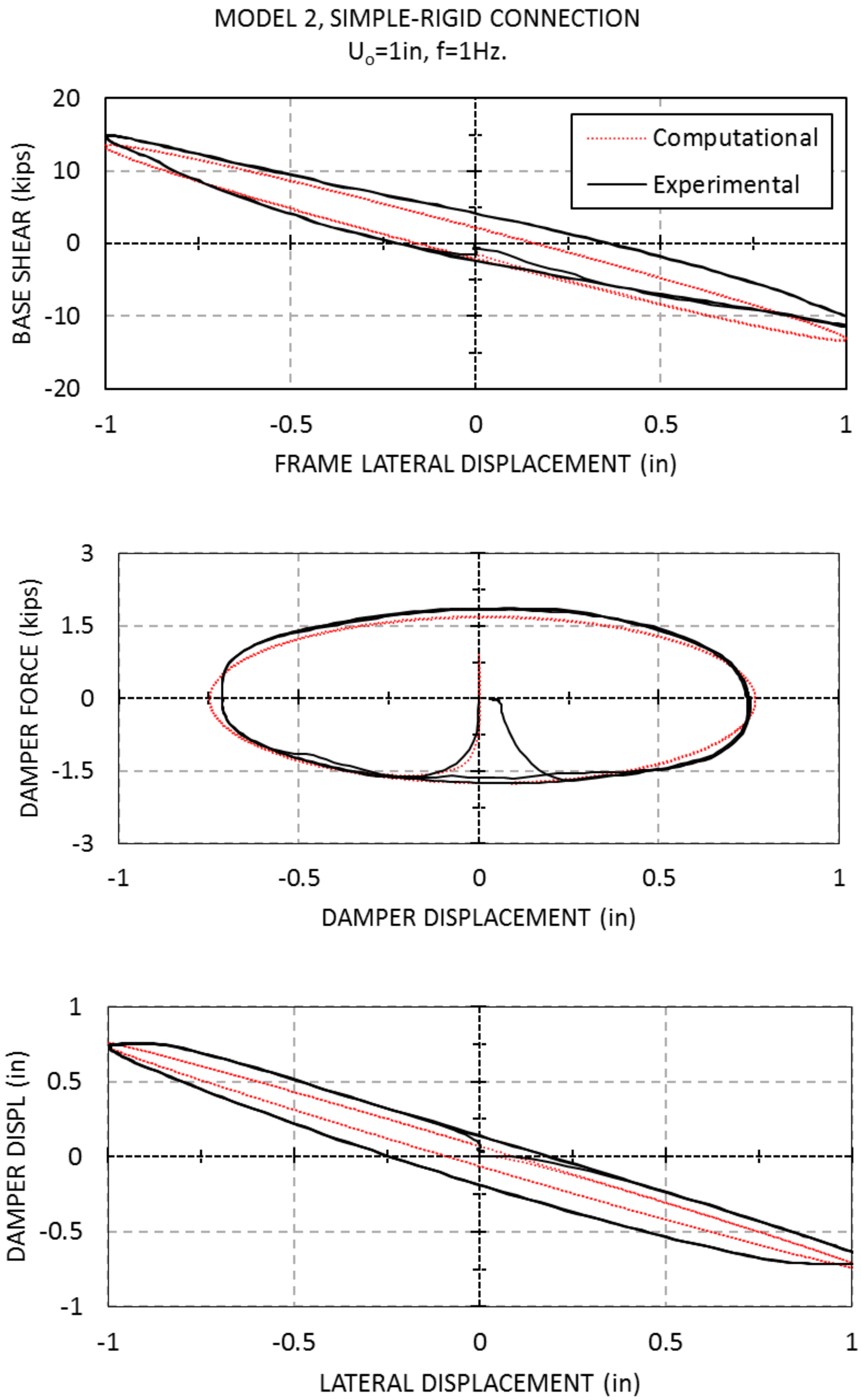

Figure 3-16 Measured and Predicted Single Frame Response of Model 2 S-R in Test of 1 inch Amplitude at 1Hz Frequency

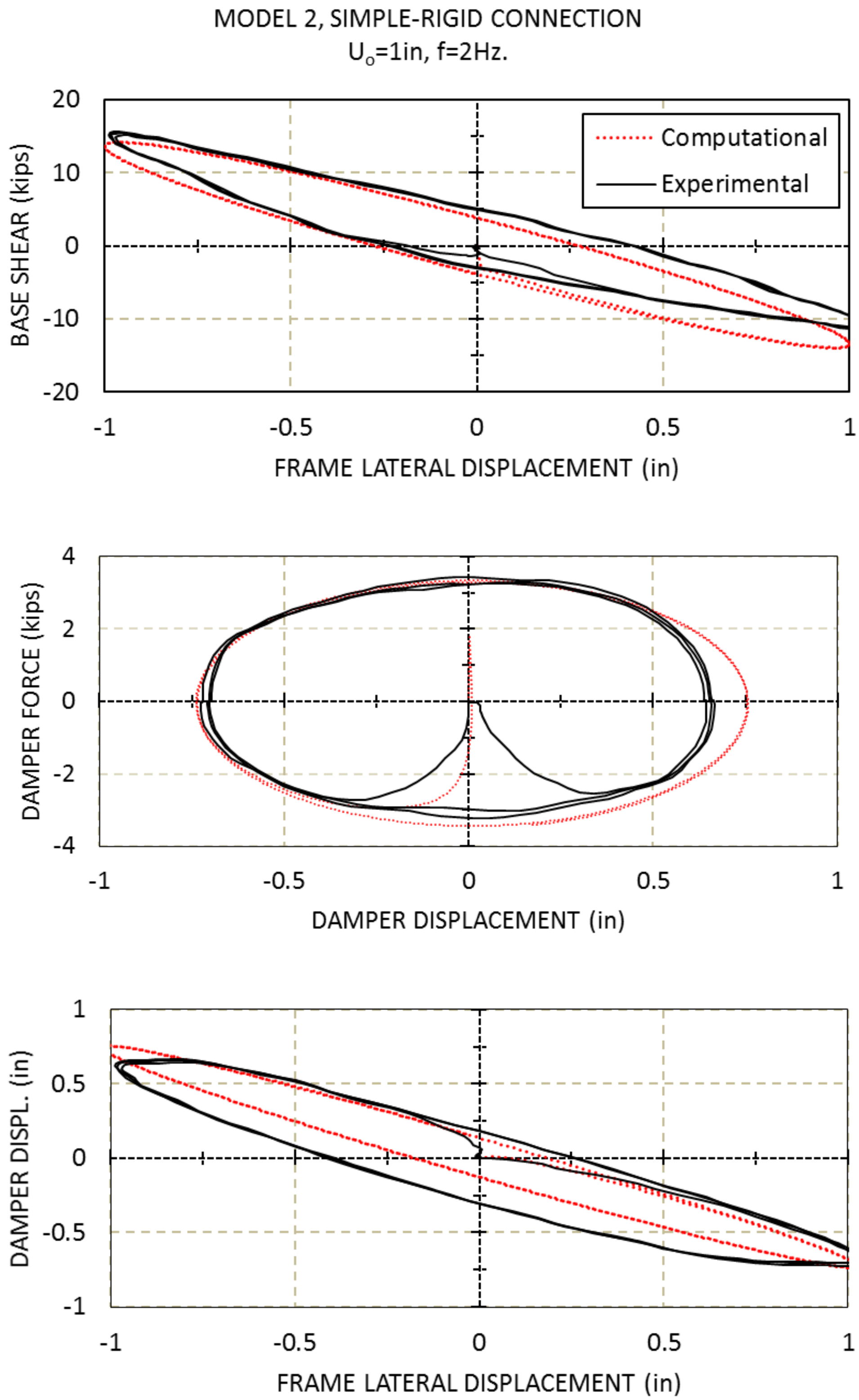

Figure 3-17 Measured and Predicted Single Frame Response of Model 2 S-R in Test of 1 inch Amplitude at 2Hz Frequency

This Page Intentionally Left Blank”

SECTION 4
EARTHQUAKE SIMULATOR TESTING OF MODEL STRUCTURE WITH OPEN SPACE DAMPING SYSTEM

4.1 Introduction

A model structure consisting of two identical frames and with a concrete block on top was tested on the earthquake simulator. Figure 4-1 shows the model on the earthquake simulator (the frame geometry is that shown in Figure 3-1). Testing of the model was conducted to observe the behavior of a structure with the open space damping system in historic earthquake motions and to acquire dynamic response data that can be used on the analytical model validation. In addition to the single frame features described in Section 3, the model structure had the following features:

1. The beam-to-column connection enabled testing with one rigid and one simple connection per frame (referred to as rigid-simple or R-S and simple-rigid or S-R configurations), and two rigid connections per frame (rigid-rigid or R-R configuration). In Model 3 (see Figure 3-1b) one connection could not be converted to rigid due to space limitations and the resulting connection is classified in this report as semi-rigid, with the resulting configurations referred to as rigid-semi-rigid or R-sR. Also, the column bases and the top of the columns to the concrete mass on top were built as simple connections.
2. Lateral stability of the test structure was provided by cross-bracing that could be tightened by turnbuckles as seen in Figure 4-1. It was observed that during testing the cross bracing tension gradually relaxed, requiring thus periodic adjustment. This phenomenon, together with differences between the two frames (due to the condition of the connections of the beam to the columns) in the principal (damped) direction led to some asymmetry and to torsional response. The extent of the problem varied as relaxation of the various bolted connections occurred during testing that was followed by periodic tightening of the bolts and turnbuckles.

3. The concrete mass used for earthquake simulator testing comprised of two blocks weighting a total of 32 kips (142.3kN), and was secured with rods atop of the four columns using rounded plates in order to achieve simple connections.

Testing conducted only in the horizontal direction; vertical component of the ground motion was not considered. A list of ground motions used in the earthquake-simulator testing and their characteristics are presented in Table 4-1. The table provides information on the peak values of acceleration, velocity, and displacement of the originally recorded motion, and the maximum scale factor used to scale the original records in acceleration amplitude. In the testing the motions were compressed in time by a factor of $\sqrt{2}$ due to similitude requirement of the model's length scale factor of 2.

Figure 4-1 Model Structure on Earthquake Simulator (shown configuration is Model 2, R-R)

The fidelity of the earthquake-simulator was investigated by comparison of 5-percent damped acceleration response spectra of the actual (target) ground motions and the spectra of the recorded acceleration motion of the extension table to which the model was attached (seen in Figure 4-1). Figure 4-2 compares the actual (target) and simulated response spectra of the ground motion records. The earthquake simulator reproduced the target motion comparatively well. Some discrepancies in the simulation is observed in the vicinity of the natural period of the model structure (~0.35 – 0.45sec) when the resonance frequency occurs, and structure-simulator interaction becomes predominant.

Table 4-1 Earthquake Motions Used in Earthquake-Simulator Testing and Characteristics in Prototype Scale (All Components are Horizontal)

NOTATION	RECORD	PEAK ACCEL. (g)	PEAK VEL. (in/sec)	PEAK DISPL. (in)	MAX. SCALE FACTOR
El Centro S00E	Imperial Valley, May 18, 1940, Component S00E	0.348	13.0	4.28	1.00
Taft 21	Kern County, July 21, 1952 Component 21	0.159	6.0	2.64	3.00
Pacoima 164	San Fernando, February 9, 1971, Component 164	1.22	45.0	4.26	0.75
Newhall 90	Northridge, January 17, 1994, LA County Fire Station, component 90	0.58	29.5	6.93	0.75

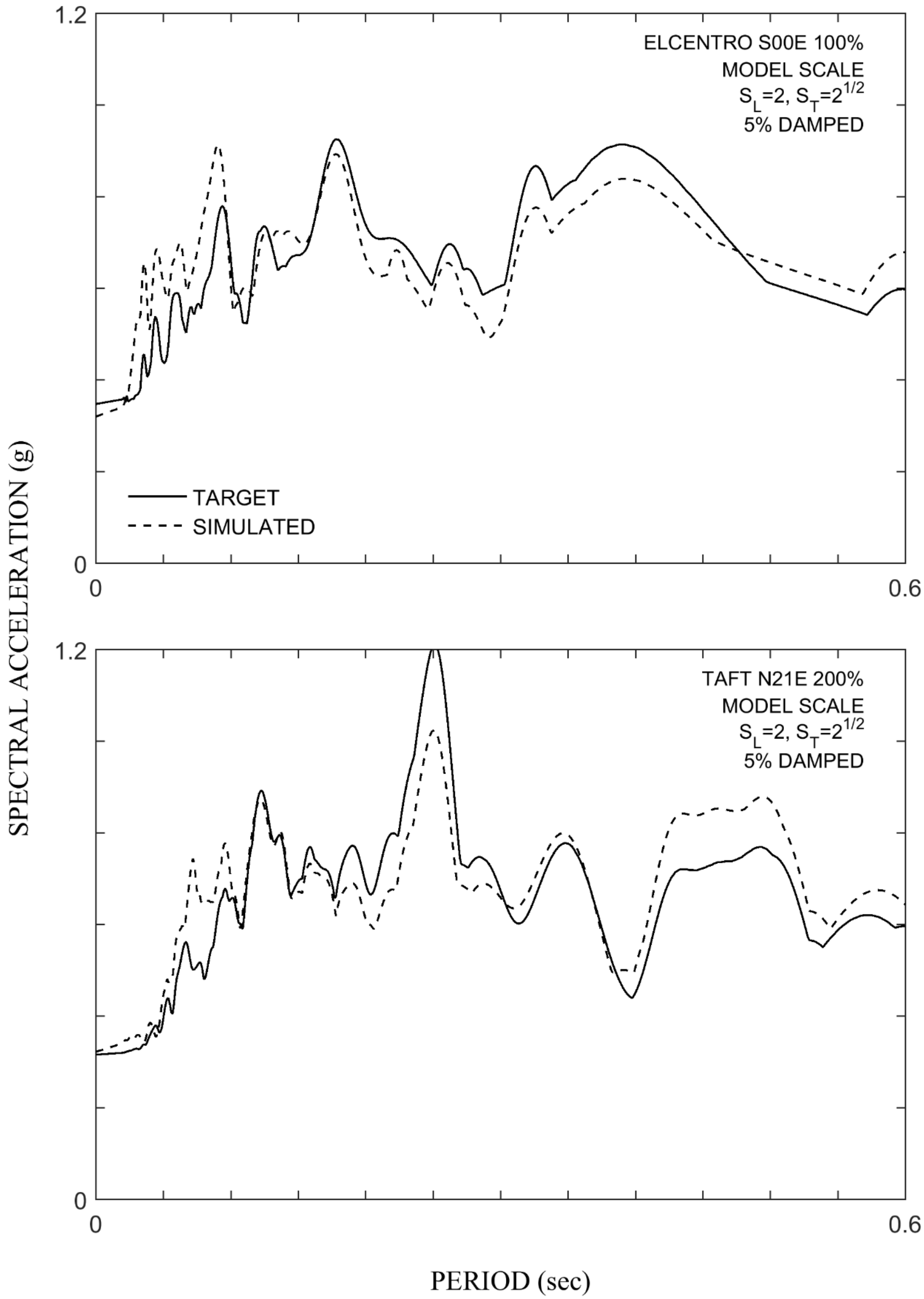

Figure 4-2 Response spectra in model scale of actual (target) ground motions and motions produced by earthquake simulator

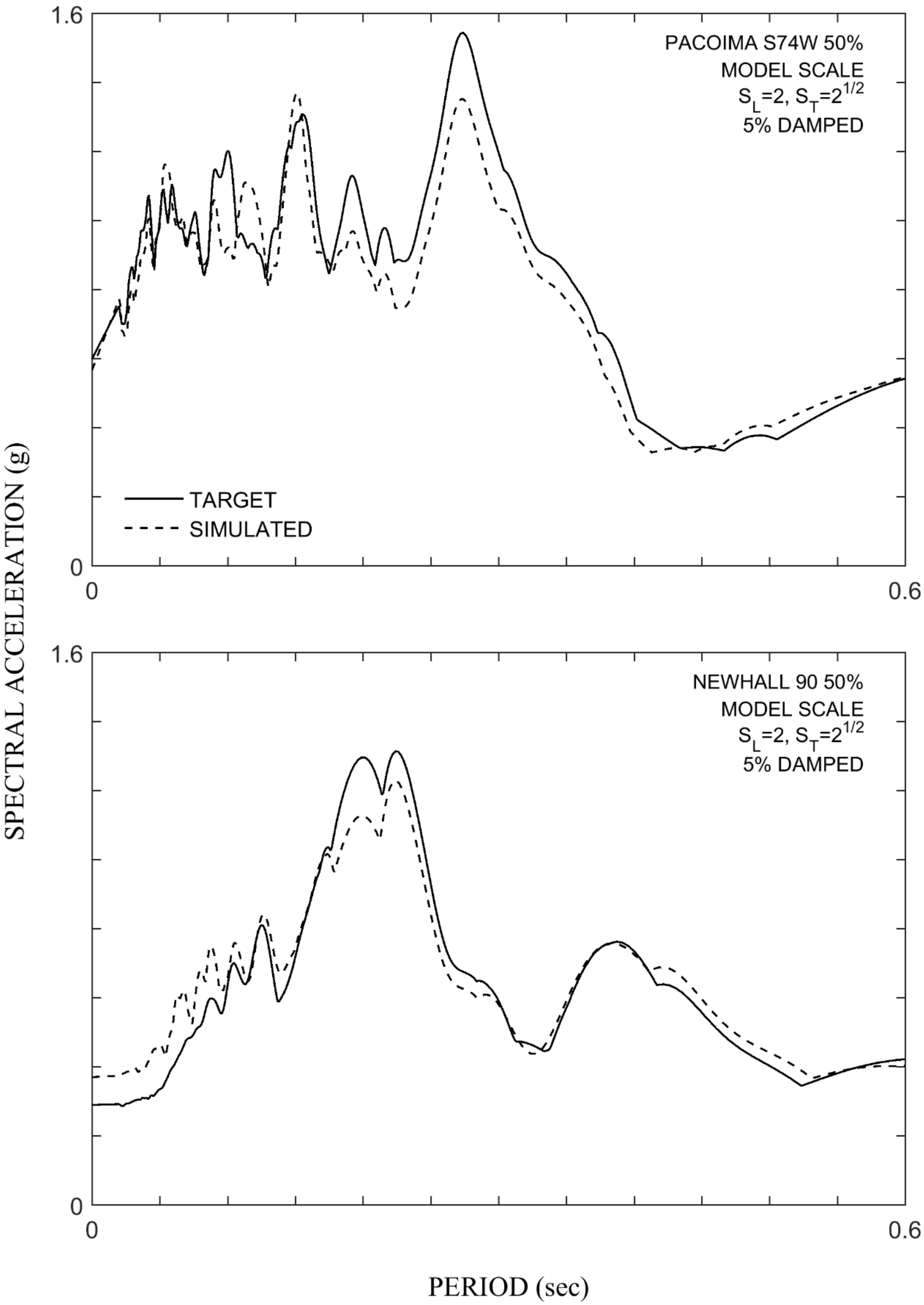

Figure 4-2 Cont'd. Response spectra in model scale of actual (target) ground motions and motions produced by earthquake simulator

4.2 Instrumentation of Model Structure for Earthquake Simulator Testing

The instrumentation consisted of accelerometers, displacement transducers, load cells and Krypton light emitting diodes or LED (used for a limited number of tests). The instrumentation scheme was similar to that of the previously tested scissor-jack damper system (Sigaher-Boyle et al., 2005). A list of monitored channels and their description are presented in Table 4-2. Figures 4-3 and 4-4 show the location of these instruments and the direction of recording. All measured signals were filtered using a low-pass filter with a cutoff frequency of 25 Hz.

Table 4-2 List of Instruments Used in Earthquake Simulator Testing

CHANNEL	INSTRUMENT	NOTATION	RESPONSE MEASURED	UNITS
1	/	TIME	Time	sec
2	Accelerometer	ABSH	Base Horizontal Accel. –S	g
3	Accelerometer	ABNH	Base Horizontal Accel.-N	g
4	Accelerometer	ABWSV	Base Vertical Accel.-WS	g
5	Accelerometer	ABWNV	Base Vertical Accel.-WN	g
6	Accelerometer	ABESV	Base Vertical Accel.-ES	g
7	Accelerometer	ACTS	Column Top Horiz. Accel.-S	g
8	Accelerometer	ACJS	Column Joint Horiz. Accel.-S	g
9	Accelerometer	ACTN	Column Top Horiz. Accel.-N	g
10	Accelerometer	ACJN	Column Joint Horiz. Accel.-N	g
11	Accelerometer	ACTTE	Column Top Tarnsv. Accel.-E	g
12	Accelerometer	ACTTW	Column Top Tarnsv. Accel.-W	g
13	Accelerometer	ACTVS	Column Top Vert. Accel.-S	g
14	Accelerometer	ACTVN	Column Top Vert. Accel.-N	g
15	Accelerometer	ATBH	Top Block Horiz. Accel.	g
16[1]	Load Cell	Dp_Frc_S	Damper Force-S	kip
17[1]	Load Cell	Dp_Frc_N	Damper Force-N	kip
18	Disp. Transducer	DBS	Base Horiz. Displ.-S	in
19	Disp. Transducer	DBN	Base Horiz. Displ.-N	in
20	Disp. Transducer	DTS	Column Top Horiz. Displ.-S	in
21	Disp. Transducer	DJS	Column Joint Horiz. Displ.-S	in
22	Disp. Transducer	DTN	Column Top Horiz. Displ.-N	in
23	Disp. Transducer	DJN	Column Joint Horiz. Displ.-N	in

Table 4-2 Cont'd. List of Instruments Used in Earthquake Simulator Testing

CHANNEL	INSTRUMENT	NOTATION	RESPONSE MEASURED	UNITS
24	Disp. Transducer	DTBH	Top Block Horiz. Displ.	in
25	Disp. Transducer	Dp_Dsp_S	Damper Displ.-S	in
26	Disp. Transducer	Dp_Dsp_N	Damper Displ.-N	in
27	LED	DRPPS	Rocker Plate Pivot Pin.-S	in
28	LED	DRPLS	Rocker Plate Left Pin.-S	in
29	LED	DRPTS	Rocker Plate Top Pin .-S	in
30	LED	DRPPN	Rocker Plate Pivot Pin.-N	in
31	LED	DRPLN	Rocker Plate Left Pin.-N	in
32	LED	DRPTN	Rocker Plate Top Pin .-N	in
33[2]	LED	DRS	Rod bottom joint-S	in
34[2]	LED	DRN	Rod bottom joint-N	in
35[3]	Disp. Transducer	DLAT	Table Horiz. Displ.	in
36[3]	Disp. Transducer	SPEXTXS	Extens. Table Horiz. Displ.-S	in
37[3]	Disp. Transducer	SPEXTXN	Extens. Table Horiz. Displ.-N	in
38[3]	Disp. Transducer	SPEXTY	Extens. Table Transv. Displ.	in
39[3]	Disp. Transducer	SPEXTZ	Extens. Table Vert. Displ.	in
40[3]	Accelerometer	ATBLX	Shake Table Horiz.Accel.	g
41[3]	Accelerometer	ATBLY	Shake Table Transv.Accel.	g
42[3]	Accelerometer	ATBLZ	Shake Table Vert.Accel.	g
43[3]	Accelerometer	AEXTX	Extens. Table Horiz.Accel.	g
44[3]	Accelerometer	AEXTY	Extens. Table Transv.Accel.	g
45[3]	Accelerometer	AEXTZ	Extens. Table Vert.Accel.	g

E = East, W = West, N = North, S = South, SE = South East, SW = South West,

NE = North East

1 Load cells were used for measuring the damper force only in Model 1 and Model 2

2 Needed for Model-1

3 Instruments used to control earthquake simulator

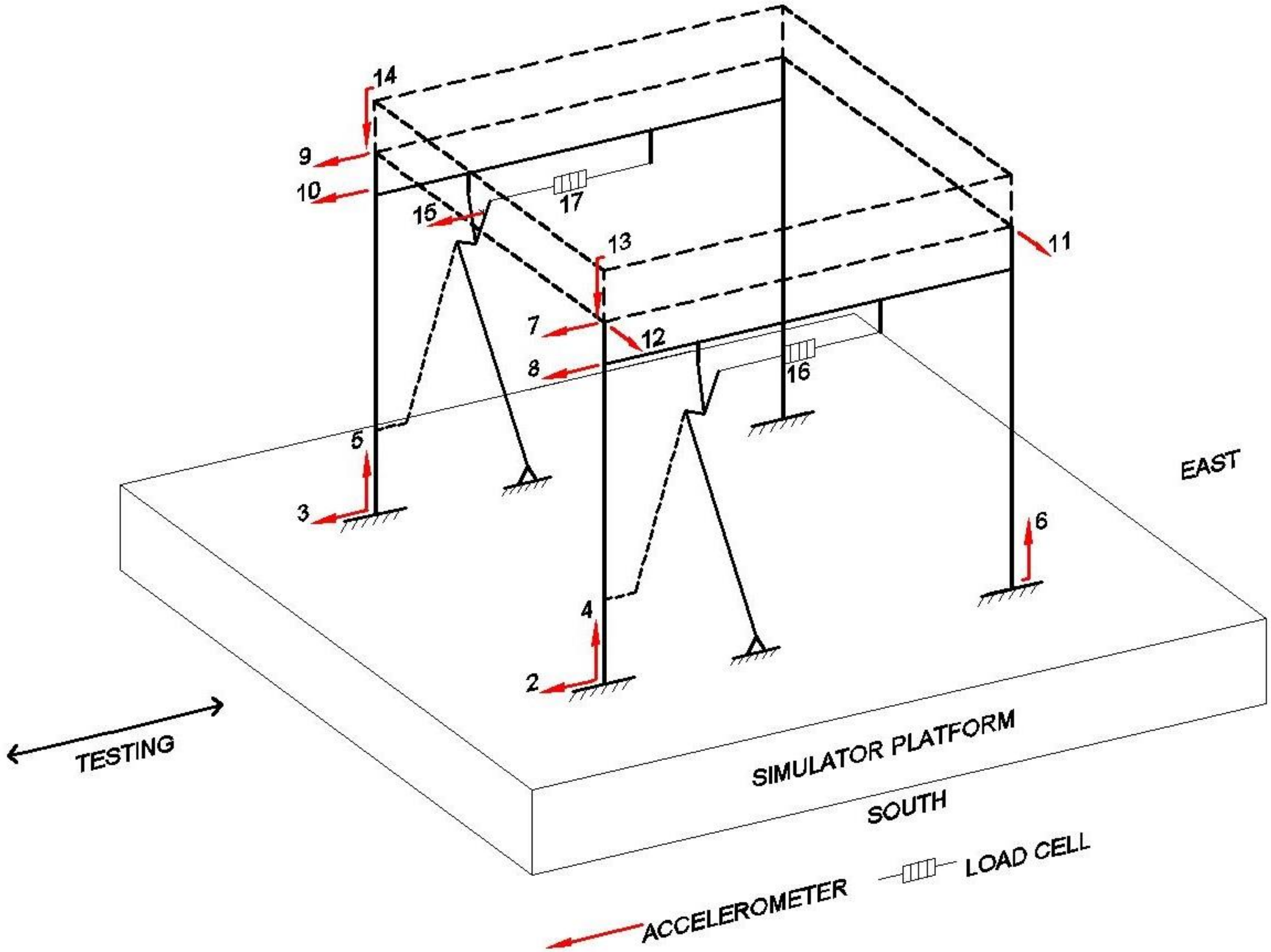

Figure 4-3 Accelerometer and Load Cell Instrumentation Diagram of Tested Structure

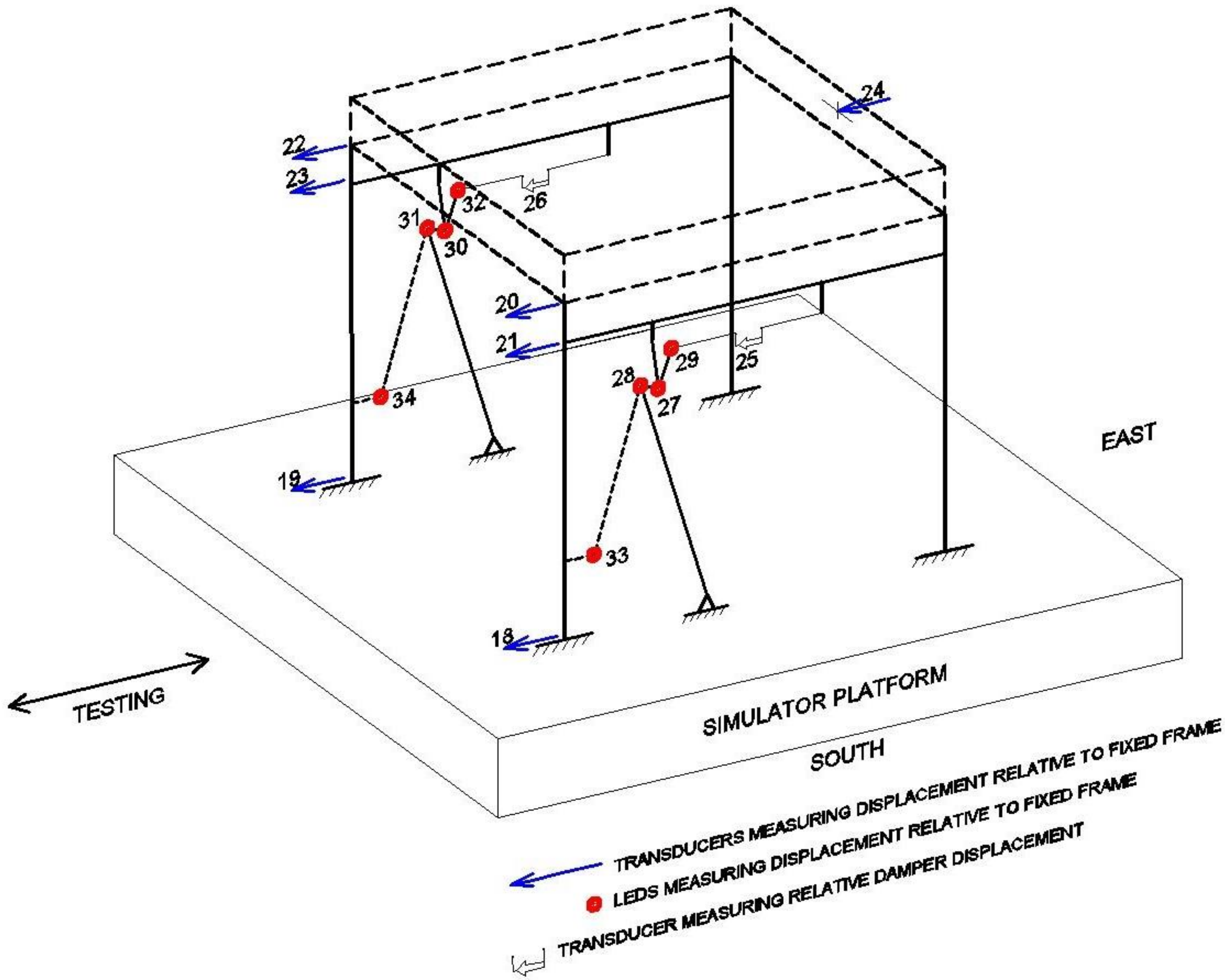

Figure 4-4 Displacement Transducer and LED Instrumentation Diagram of Tested Structure

4.3 Identification of Dynamic Properties of Model Structure

The model as shown in Figure 4-1 consisting of two frames and a 32kips (142.3kN) concrete mass on top of the columns was placed on the shake table in its dynamic characteristics identified. The base of the model was driven in banded white noise excitation within a frequency range of 0-25Hz and acceleration amplitude of 0.05 to 0.3g in several tests. Transfer functions were then constructed as the ratio of the Fourier transforms of the acceleration recorded at the column top (where the concrete mass is connected to the frame) to the acceleration recoded at the column base. The average acceleration histories recorded at the two frames (average of ACTS-ACTN, and average of ABHS-ABHN, see Figure 4-3 and Table 4-2) were used as some torsion occurred. The amplitude of the transfer function was used to obtain the frame characteristics in terms of the fundamental frequency and damping ratio by treating the tested system as a single-degree-of-freedom system (SDOF). This is reasonably acceptable assumption for the tested structure except for the problem of torsional response which was somehow alleviated by averaging the recorded acceleration histories of the two frames.

Assuming that damping is relatively small, the peak of the transfer functions reveals the location of the fundamental frequency of the SDOF system. The damping ratio ξ is related to the peak value of the transfer function T_{peak} and given by Equation (4-1).

$$\xi = \sqrt{\frac{1}{4\left(T_{peak}^2 - 1\right)}} \tag{4-1}$$

Figure 4-5 presents representative amplitude of transfer function vs frequency plots for the five tested systems with the damping system at white noise acceleration amplitude of 0.3g. The five systems are identified by model (1, 2 or 3 per Figure 3-1), beam-to-column connections and placement of the connection (left or right frame joint). The graphs also include the transfer function plots for the structure without the damping system at white noise acceleration amplitude of 0.1 to 0.3g. All transfer functions were obtained in tests that followed several seismic tests. The fundamental frequency and damping ratio of the model were obtained from the location and value of the single dominant peak in the transfer function amplitude per Equation (4-1). The values are presented in Table 4-3. The transfer function amplitude function shown for the un-damped rigid-semi-rigid frame has two dominant peaks, indicating strong torsional response. The damping ratio could not be estimated from this graph on the basis of Equation (4-1) as the equation does not apply to a multi-degree-of-freedom system. The frequency was estimated on the basis of the second peak location.

Table 4-3 Identified Characteristics of Model Structure with and without Damping System

Model	Beam-to-Column Connections (left and right)	Fundamental Frequency (Hz)	Damping Ratio
Without Damping System	Simple-Rigid	2.30[1]	0.011[1]
	Rigid-Simple	2.20	0.017
	Rigid-Rigid	2.98	0.029
	Rigid-Semi-rigid	2.40	NA
1	Simple-Rigid	2.21	0.087
2	Rigid-Simple	2.60	0.102
	Simple-Rigid	2.30	0.068
	Rigid-Rigid	3.00	0.075
3	Rigid-Semi-rigid	2.56	0.117
[1]: In another test frequency was 2.20Hz and damping was 0.023			

The un-damped frame has low damping of the order of 0.01 to 0.03 depending on the conditions of testing. The effect of the damping system is evident in the increase in damping and to a small extent in the increase in frequency (however, it should be noted that frequency was also affected by degree of bolt tightening). The increase in frequency is the result of viscoelastic behavior caused by the frame and damping system assembly deformation under the action of the inertia and damping forces. The damping ratio could be predicted by:

$$\beta = \frac{T C_o f^2 g \phi_1^2}{4\pi W \phi_2^2} \qquad (4\text{-}2)$$

Equation (4-2) is a modification of Equation (1-3) to account for the fact that mass of the single degree of freedom system undergoes a different displacement than the beam to which the damping system is connected to. In Equation (4-2), ϕ_1 is the modal displacement of the beam-to-column joint and ϕ_2 is the modal displacement of the center of mass of the concrete block,

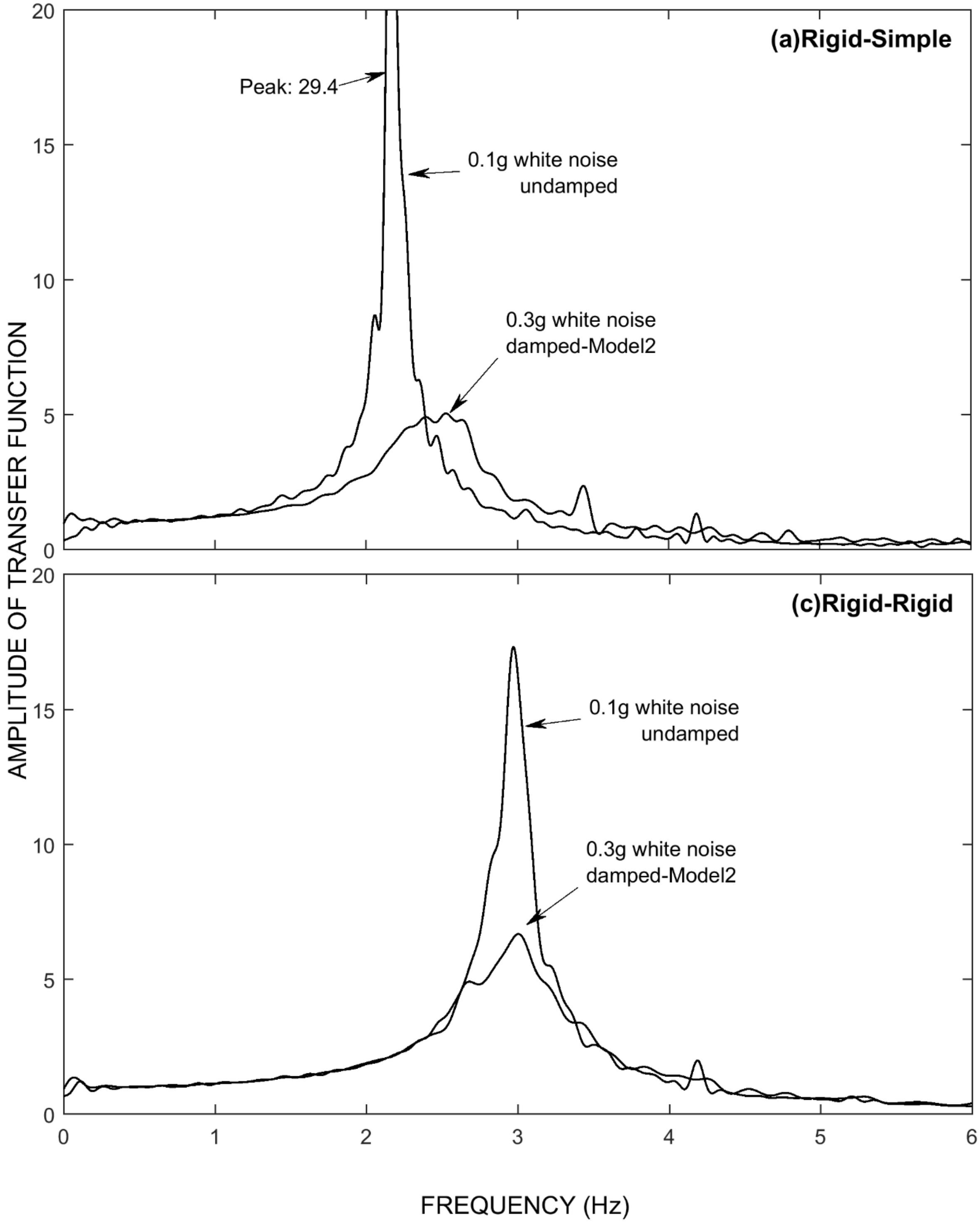

Figure 4-5 Amplitude of Transfer Functions of Model Structure with and without Damping System

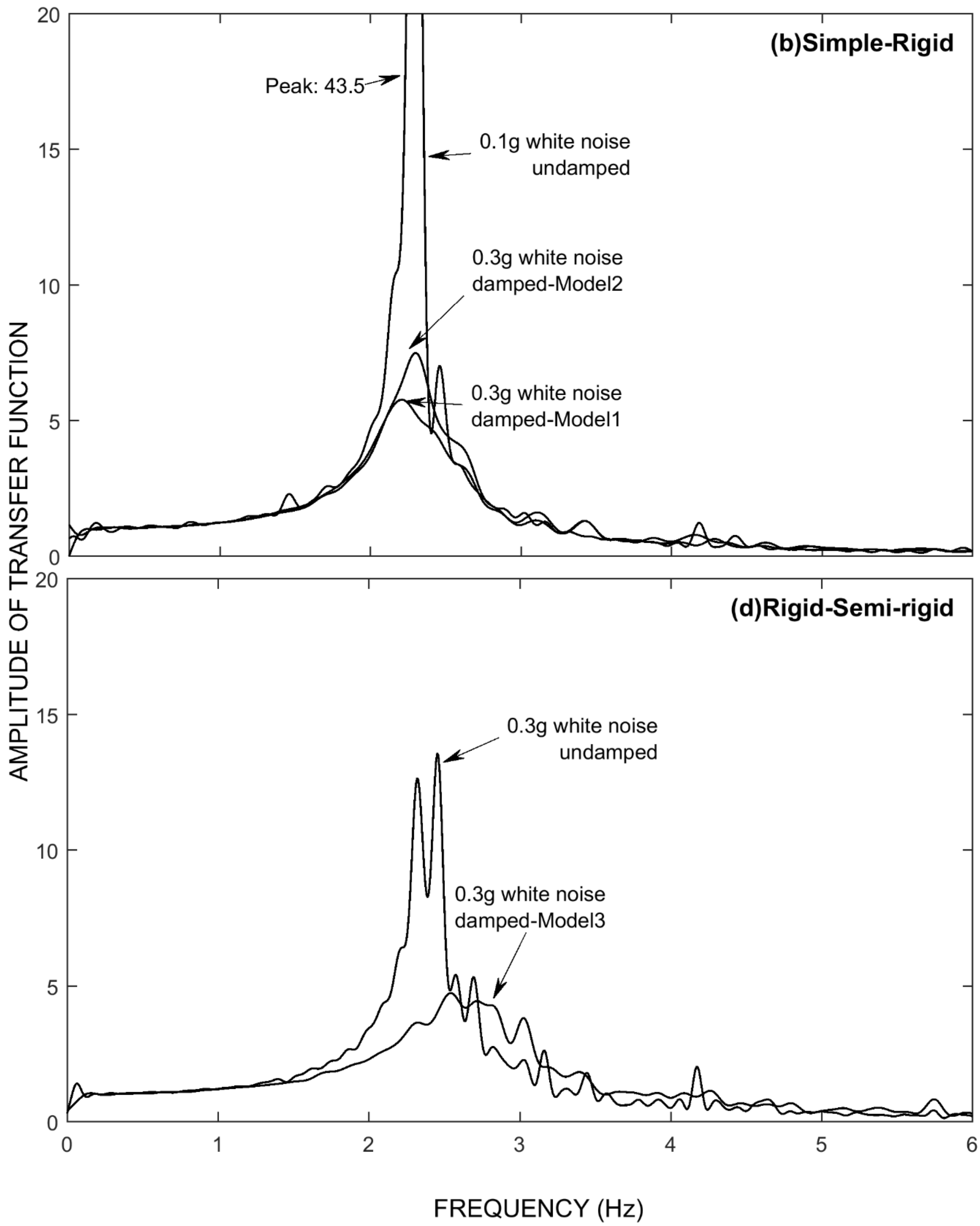

Figure 4-5 Cont'd. Amplitude of Transfer Functions of Model Structure with and without Damping System

which presumably is the same as that of the column top when assuming simple connection between the concrete mass and the column top. Approximately, ϕ_1/ϕ_2 is equal to H_1/H_2, where H_2 is the height of the column (*=90.63inch*-see Figure 3-1) and H_1 is the height of the beam-to-column joint (*=75.13inch*-see Figure 3-1). Use of Equation (4-2) for Model 2 in the Rigid-Simple configuration and utilizing the identified frequency of *2.60Hz*, so that *T=0.385sec*, *W=32.8kips*(*145.9kN*), $H_1/H_2=0.83$, C_o=2*x0.36=0.72kip-sec/in* (*2x0.063=0.126kN-sec/mm*) and the measured value of the magnification factor under dynamic conditions in Table 3-2 *f=0.75* (least of values in two directions under dynamic conditions), the added damping ratio is calculated as $\beta=0.100$. Adding about *0.015* for the inherent damping, the damping ratio is *0.115*, which compares well with the experimental value of *0.102* in the identification tests. However, use of the computed value of the magnification factor *f=0.91* per Table 3-2 would have resulted in a total damping ratio of about *0.16* rather than *0.115*. As explained earlier, the value of the magnification factor has been affected by slippage in the joints as demonstrated in the test data of Figure 3-5 to 3-8.

The problem of slippage in the joints together with loosening and periodic tightening of the bolted connections resulted in continuous changes in the properties of the tested frame during the history of the experiments. As an example, Figure 4-6 presents transfer functions of one of the tested damped configurations over a period of several days starting with a test prior to any seismic tests and ending with a test after completing all seismic tests. The peak value, the test number (numbered consecutively) and the test data date are used to identify each curve. Note that several tests were conducted in-between the identification tests shown in Figure 4-6. The changing properties of the frame are evident in Figure 4-6.

4.4 Earthquake Simulator Test Results

A summary of selected results in the earthquake simulator testing is presented in Table 4-4. The table contains the following:

1. The system tested and test number. The models tested are identified as M2R-S for Model 2 with Rigid-Simple connections on the left and right, respectively, M2S-R for Model 2 with Simple-Rigid connections, M3R-sR for Model 3 with Rigid-Semi-Rigid connections,

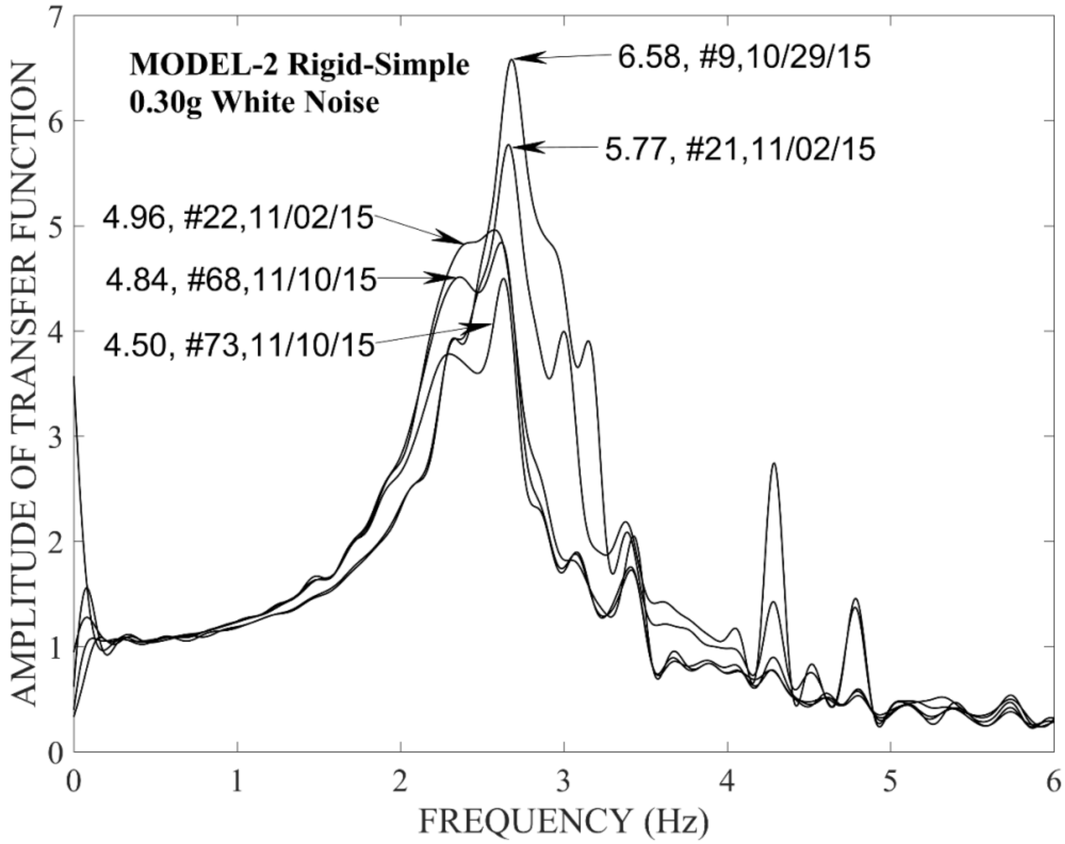

Figure 4-6 Transfer Functions of Model 2 Rigid-Simple Configuration in Several Tests

etc. Note that systems M1S-R, M2S-R, M2R-S, M2R-R and M3R-sR were tested, whereas system M1R-S was not tested as it was known to have a low magnification factor. Description of seismic excitation, which includes the excitation name, component, and acceleration amplitude scale. For example, EL CENTRO S00E 50% implies that the record was component S00E of the El Centro earthquake, scaled in amplitude of acceleration to 50-percent of the actual record.

3. Peak values of the earthquake simulator displacement, velocity and acceleration. The peak simulator displacement was obtained from instrument DBE (see Table 4-2), the peak velocity was derived from numerical differentiation of the displacement record, and the peak acceleration was obtained from instrument AEXTX (see Table 4-2).

4. Peak frame response (average of the south and north frame) in terms of drift (displacement of the beam-to-column joint with respect to column base), beam-to-column acceleration, damper displacement and damper force.
5. Values of the magnification factor determined separately for motion towards the left and for motion towards the right, then using the maximum value between the two and then averaging the values at south and north frames so that any torsion effects are removed. More details of values of the magnification factor are presented in Appendix C.

The peak frame response values are the average of the two quantities measured at the two frames of the model. The two values differed due to asymmetry in the model caused by slight variations in stiffness of the two frames, slippage in the joints (which was not the same in the two frames), degree of tightening of the bolts of joints of the two frames and amount of tension in the transverse cross-bracing of the structure. The reported magnification factor is simply the ratio of the peak damper displacement to the peak frame drift. As discussed earlier in this report when the frame testing was described, the magnification factor is dependent on the frame deformations and on slippage in the joints. The latter is affected by the direction and the amplitude of motion. That is, the magnification factor changes during motion and the reported value should be viewed as a representative single value. Other selected results are presented in Appendix C. The results in the appendix include histories of the joint acceleration, frame drift and damper deformation, and loops of damper force versus damper deformation. Also, Appendix D presents drawings of the model as assembled on the earthquake simulator.

The measured values of magnification factor lie in the range of 0.65 to 0.77 for Model 2 R-S, 0.48 to 0.56 for Model 2 S-R, 0.49 to 0.56 for Model 1 S-R, 0.54 to 0.63 for Model 2 R-R and 0.82 to 0.84 for Model 3 R-sR. The values of the magnification factor for the tested systems are consistent with those reported in Table 3-2 as obtained in the cyclic testing of individual frames under dynamic conditions (0.75 for M2R-S, 0.67 for M2S-R, 0.49 for M1S-R). The values measured in the shake table testing of system M2S-R are lower than those from the individual frame testing with the likely reason being differences in the condition of the simple connections. Moreover, for system Model 3 R-sR, which has not been cyclically tested, the magnification factor is higher than the other systems due to the fact that it is unaffected by the beam deformations. Measured values of magnification factor for the Model 3 R-sR configuration are in the range of 0.82 and 0.84 compared to the value of 0.91 predicted by a computational model of the frame including the effects of frame deformations due to the inertia and damping forces. The difference between the experimental and computational values is due again to slippage in the bolted joints that could not be analytically accounted for, and due to differences in the stiffness of the frame between the physical model and the computational model.

Table 4-4 Peak Response of Model Structure in Earthquake-Simulator Testing

System	Test #	Excitation	Peak Earthquake Simulator Motion			Drift (inch)	Accel (g)	Damper Displ. (inch)	Damper Force (kip)	Magnif. Factor
			Displ. (inch)	Veloc. (inch/sec)	Accel. (g)					
M2R-S	11	TAFT N21E 200%	1.97	7.42	0.29	0.51	0.37	0.35	2.38	0.69
	13	EL CENTRO S00E 50%	0.87	4.30	0.18	0.46	0.32	0.30	1.82	0.65
	14	EL CENTRO S00E 100%	1.96	8.58	0.33	0.86	0.55	0.61	3.22	0.71
	19	PACOIMA S74W 50%	3.12	13.44	0.45	0.44	0.34	0.33	1.92	0.75
	23	PACOIMA S74W 75%	4.70	20.16	0.72	0.68	0.50	0.51	2.95	0.75
	70	PACOIMA S74W 100%	6.32	27.17	1.01	1.05	0.65	0.79	3.70	0.75
	71	NEWHALL 90 75%	2.43	12.32	0.60	0.87	0.54	0.67	4.22	0.77
M2S-R	38	TAFT N21E 200%	1.94	7.36	0.29	0.90	0.52	0.44	2.53	0.51
	35	EL CENTRO S00E 50%	0.99	4.41	0.18	0.55	0.32	0.26	1.43	0.48
	63	EL CENTRO S00E 100%	1.95	8.71	0.30	1.03	0.56	0.58	2.90	0.56
	36	PACOIMA S74W 50%	3.12	13.60	0.45	0.48	0.31	0.21	1.48	0.49
	64	PACOIMA S74W 75%	4.72	20.18	0.71	0.78	0.49	0.42	2.12	0.55
M1S-R	42	EL CENTRO S00E 50%	0.99	4.35	0.17	0.52	0.29	0.26	1.34	0.50
	44	PACOIMA S74W 50%	3.12	13.40	0.44	0.47	0.31	0.25	1.49	0.54
	45	PACOIMA S74W 75%	4.69	20.16	0.70	0.75	0.48	0.40	2.05	0.53
	48	NEWHALL 90 50%	1.59	8.12	0.36	0.66	0.40	0.32	2.27	0.49
	54	TAFT N21E 200%	1.94	7.32	0.29	0.91	0.50	0.49	2.17	0.55
	55	PACOIMA S74W 75%	4.73	20.42	0.71	0.79	0.48	0.44	1.90	0.56
M2R-R	26	EL CENTRO S00E 50%	0.85	4.65	0.19	0.33	0.32	0.18	1.46	0.54
	66	TAFT N21E 200%	1.98	7.39	0.28	0.55	0.50	0.31	2.35	0.58
	67	PACOIMA S74W 75%	4.76	20.16	0.75	0.77	0.68	0.48	3.45	0.63
M3R-sR	83	EL CENTRO S00E 100%	1.95	8.70	0.34	0.77	0.61	0.64	NA	0.82
	84	PACOIMA S74W 75%	4.74	20.20	0.71	0.74	0.54	0.62	NA	0.84

This Page Intentionally Left Blank”

SECTION 5
ANALYTICAL PREDICTION OF RESPONSE

5.1 Analytical Model

Dynamic analysis of the tested structure was performed in computer program SAP2000. Figure 5-1 depicts the analytical model used in the cases of Model 1 and Model 2, Rigid-Simple configuration. Note that each simple connection (beam-to-column and the two column bases) was modeled as a pin with a rotational spring (partial fixity in SAP2000) of which the stiffness was determined so that the fundamental frequency was close to the one measured in the identification tests of the structure without the damping system (see Table 4-3). All connections of the damping system were modelled as true pins. Also, the connection of each column top to the concrete mass was modelled as a true pin (in reality it is not). Inherent damping of 2% of critical in each mode of vibration was assigned to the model. Only one of the two frames was modeled. Masses, calculated from the added concrete blocks and the tributary weights of the elements, were lumped at the joints, as shown in Figure 5-2. Joint coordinates including lumped masses are listed in Table 5-1. Element properties in the SAP2000 model are listed in Table 5-2. The viscous damper was modeled as nonlinear link element (Damper-Exponential in SAP2000) with a damping coefficient of 0.36 kip-sec/in and damping exponent of unity. Nonlinear modal time history analysis (known as fast nonlinear analysis) was used for the solution, which is limited to small deformation theory.

5.2 Response History Analysis Results

Figure 5-3 to 5-6 present comparisons of analytical and experimental results in eight selected tests of the five tested systems. The compared results are acceleration and drift histories, damper force-displacement loops and base shear normalized by weight W vs drift loops (W is the tributary weight of one frame=16.4kip or 72.95kN) versus drift. The predicted acceleration and drift histories and the base shear-drift loops are in good agreement with the experimental response. The damper force-displacement loops were not predicted well by the analytical model due to primary overestimation of the damper displacement (and thus also damper velocity). This is the results of overestimation of the magnification factor due to inability to account for joint slippage and for hysteretic behavior in the “simple” frame joints (which were dependent on the degree of bolt tension, and kept changing during testing) in the analytical model. It may be noted in Figure 5-3 to 5-6 that the analytical model predicts a damper displacement of as much as 0.2inches (5mm) more than the observed value, which is consistent with what was possible slippage in the oversize-hole connections (3/16th inch or 5mm).

Slippage in the joints together with oversized holes was a characteristic of the tested model while in actual applications the connections will be welded or with standard size holes, for which slippage in the joints will be of the order of $1/16^{th}$ inch (1.5mm) rather than $3/16^{th}$ inch (5mm). The importance of joint slippage is better appreciated when one considers that the tested model was at length scale of 2, so that the drift and damper displacement were half of those of actual buildings, whereas the slippage was as much as three times larger.

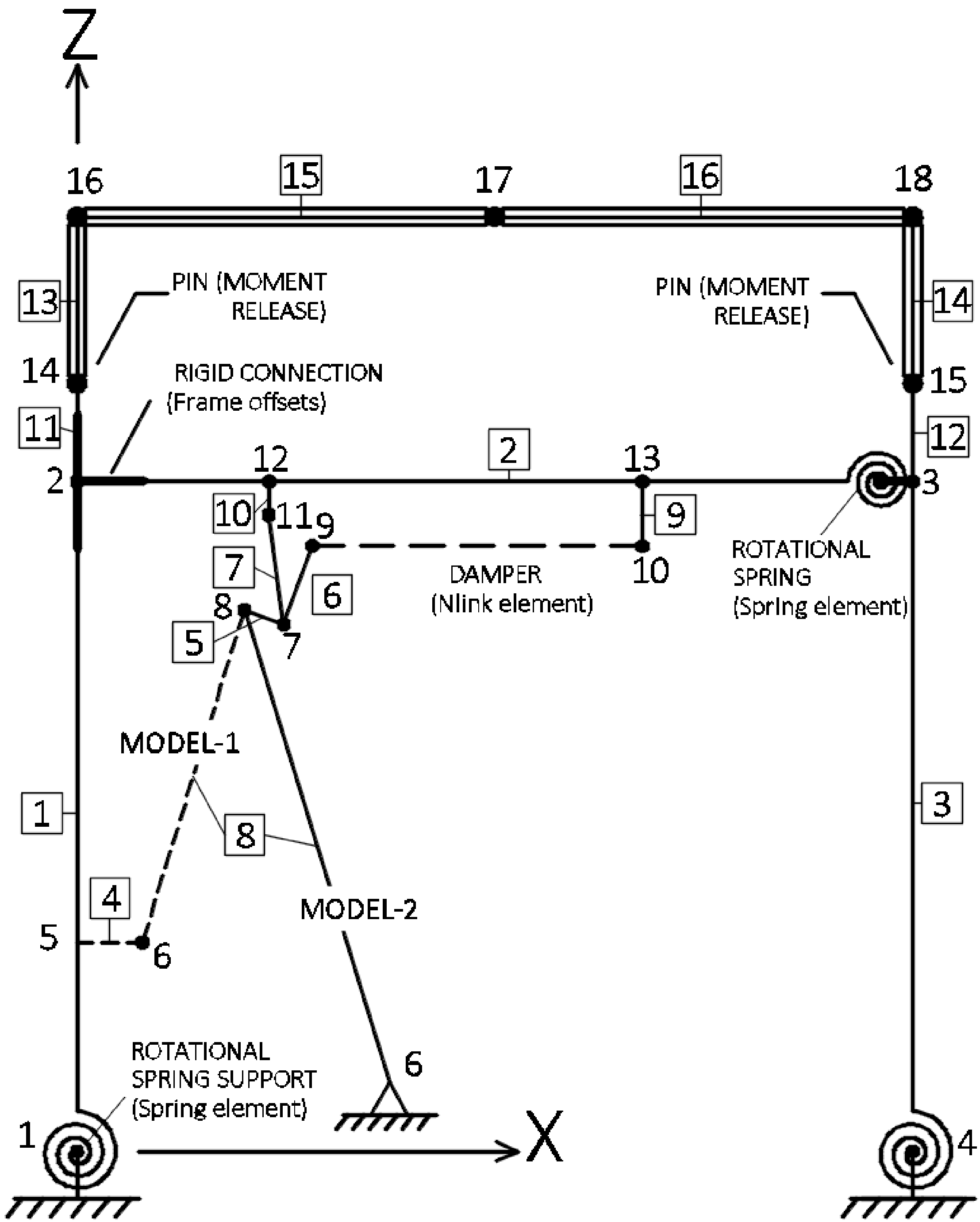

Figure 5-1 Illustration of Analysis Model in SAP2000 for Case of Model 1 or Model 2 in Rigid-Simple Configuration of Tested Structure

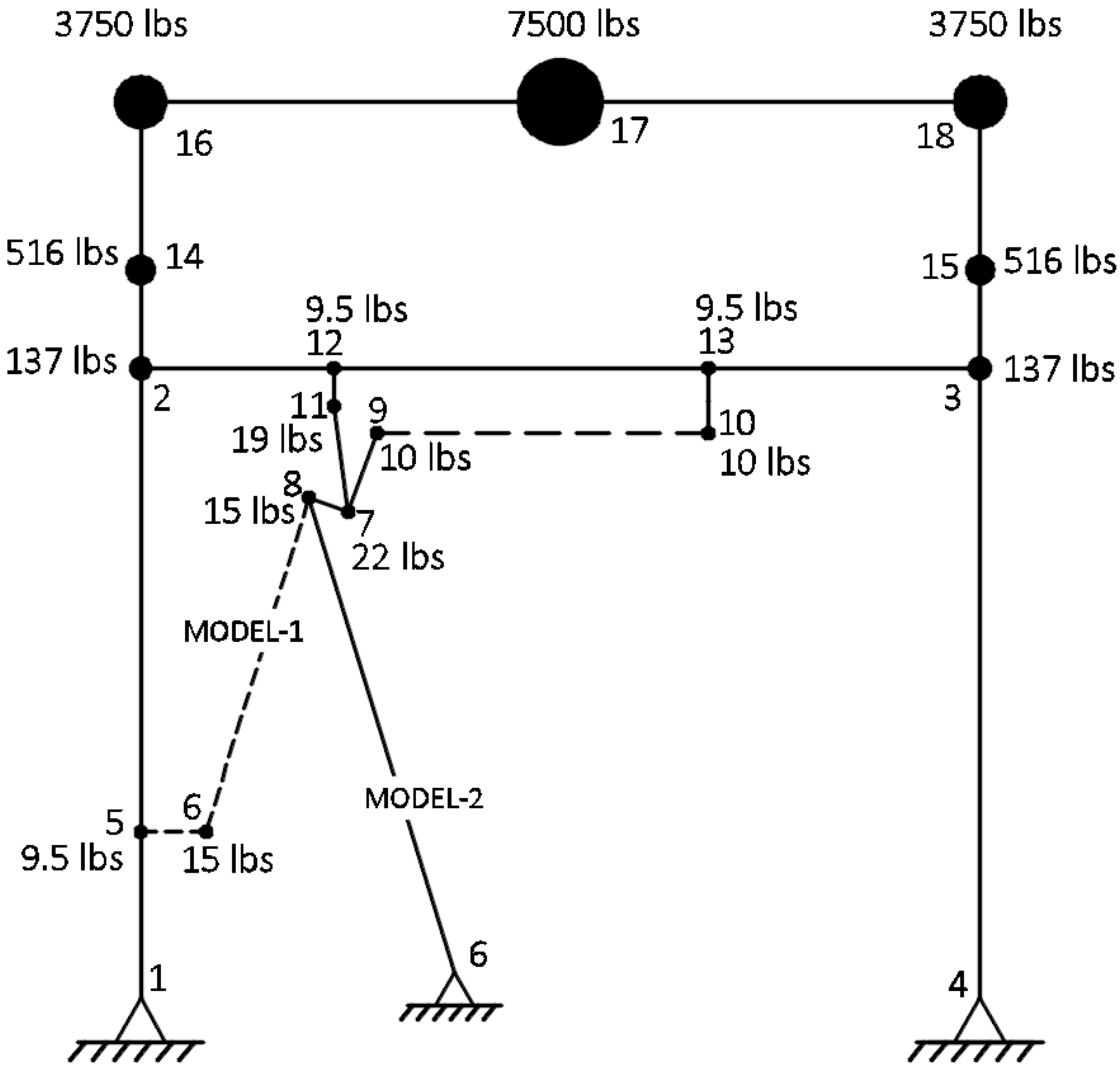

Figure 5-2 Lumped Weights in SAP2000 Model of Tested Structure

Table 5-1 Joint Coordinates and Lumped Joint Weights in SAP2000 Model

Joint	X (in)	Z (in)	Weight (lb)
1	0	0	0
2	0	75.125	137
3	100	75.125	137
4	100	0	0
5	*0/NA	*19.832/ NA	*9.5/NA
6	*0/37.478	*19.832/3.05	*15/0
7	24.57	57.995	22
8	19.881	59.73	15
9	28.046	67.357	10
10	67.627	67.375	10
11	22.827	71.125	19
12	22.827	75.125	9.5
13	67.627	75.125	9.5
14	0	90.625	516
15	100	90.625	516
16	0	116.425	3750
17	50	116.425	7500
18	100	116.425	3750
*First value is for Model 1, second value is for Model 2			

Table 5-2 Element Properties in SAP2000 Model

Element	Start Joint	End Joint	Section	Area (in^2)	I_{zz} (in^4)	Shear Area (in^2)
1	1	2	W8X15	4.44	48	1.99
2	2	3	W8X13	3.84	39.6	1.84
3	3	4	W8X15	4.44	48	1.99
4	5	6	RIGID	100	100	100
5	7	8	RIGID	100	100	100
6	7	9	RIGID	100	100	100
7	7	11	PLATE	2	3.6	100
8	6	8	BEAM	3.14	10	10
9	10	13	RIGID	100	100	100
10	11	12	RIGID	100	100	100
11	2	14	W8X15	4.44	48	1.99
12	3	15	W8X15	4.44	48	1.99
13	14	16	RIGID	1000	10000	1000
14	15	18	RIGID	1000	10000	1000
15	16	17	RIGID	1000	10000	1000
16	17	18	RIGID	1000	10000	1000
NLINK	6	10	C = 0.36 kip-sec/in			
SPRING	3	-	K_{rot} = 20000 kip-in/radian			
SPRING	1	-	K_{rot} = 6000 kip-in/radian			
SPRING	4	-	K_{rot} = 6000 kip-in/radian			

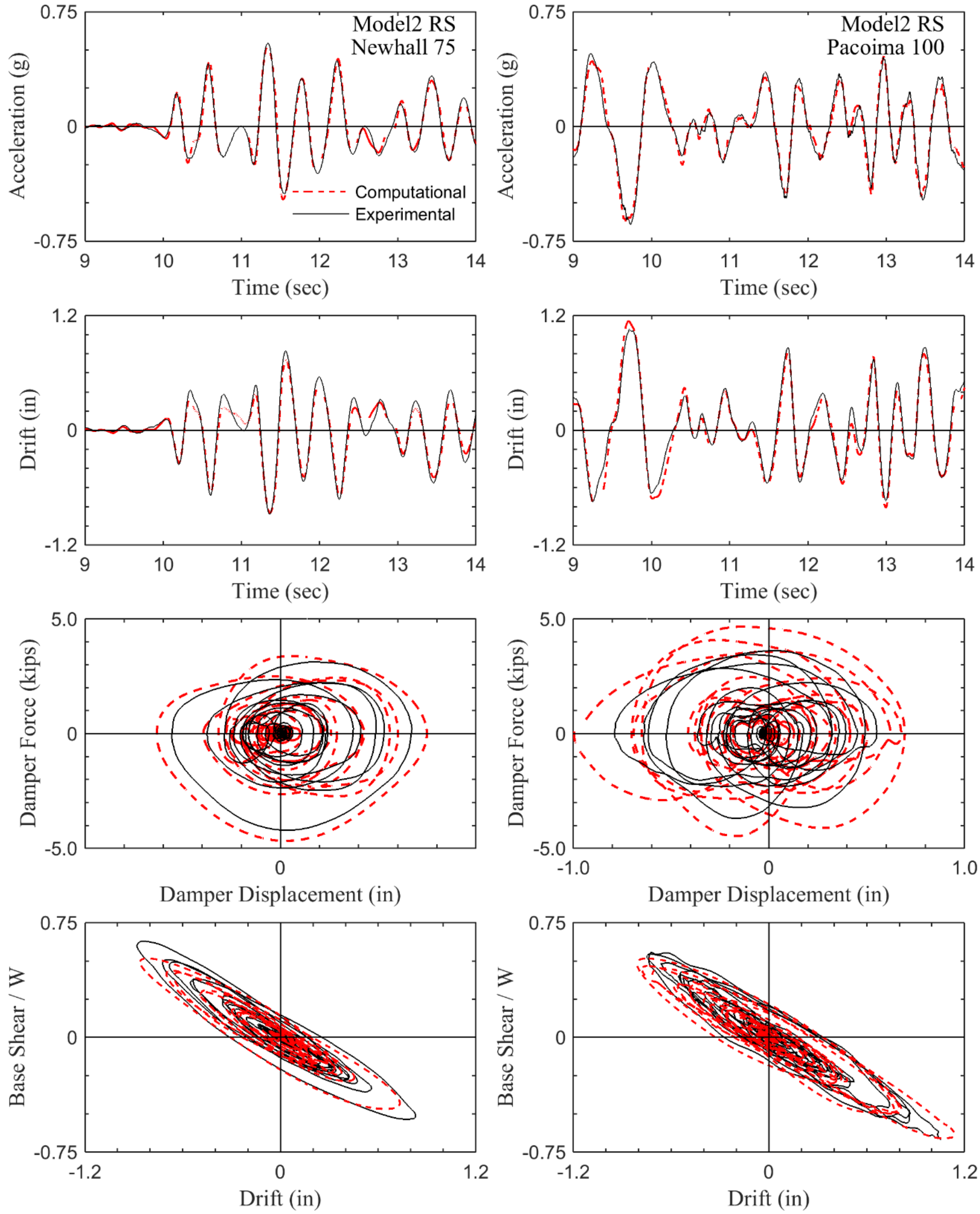

Figure 5-3 Comparison of Experimental and Analytical Results for Model 2 R-S in Two Tests

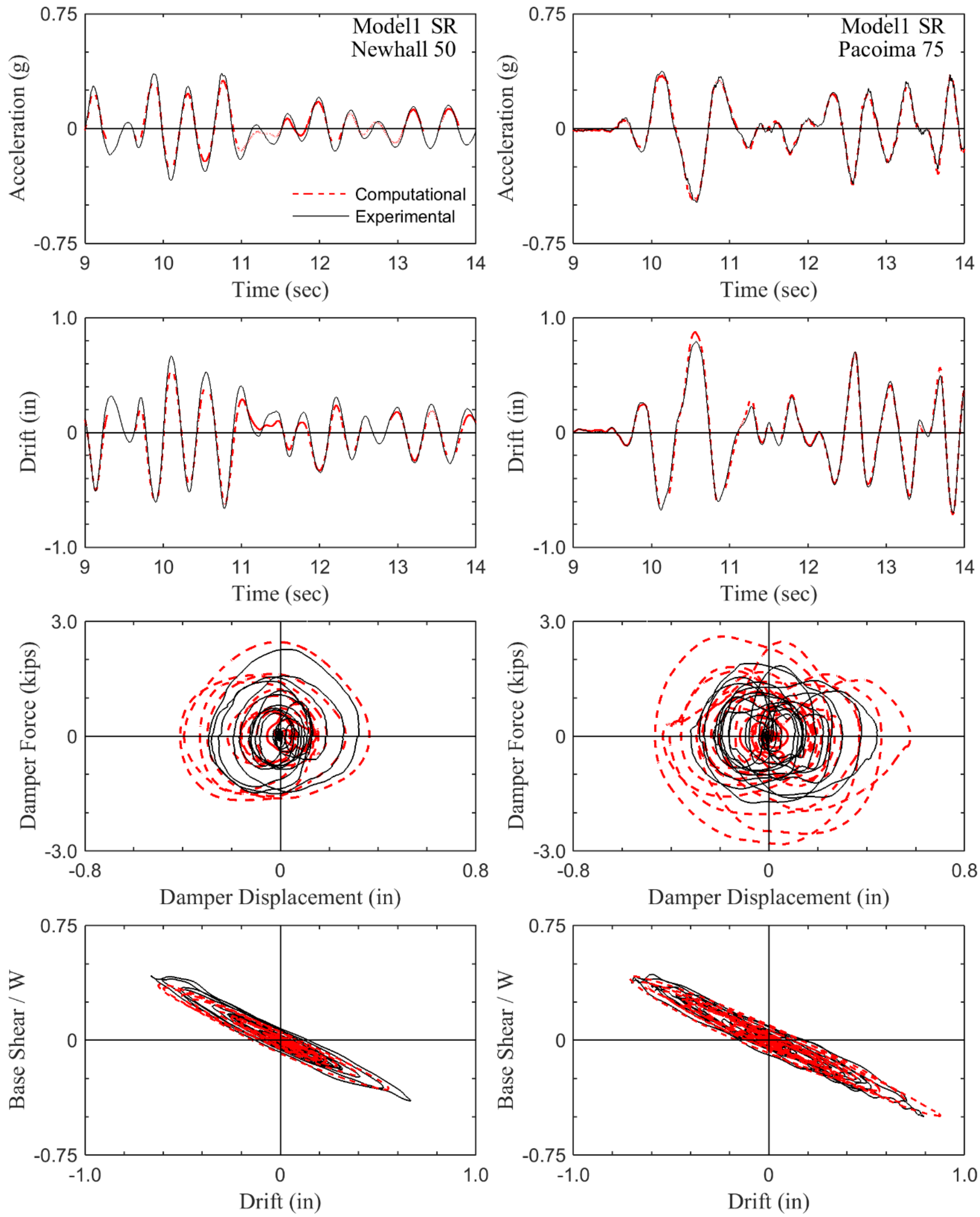

Figure 5-4 Comparison of Experimental and Analytical Results for Model 1 S-R in Two Tests

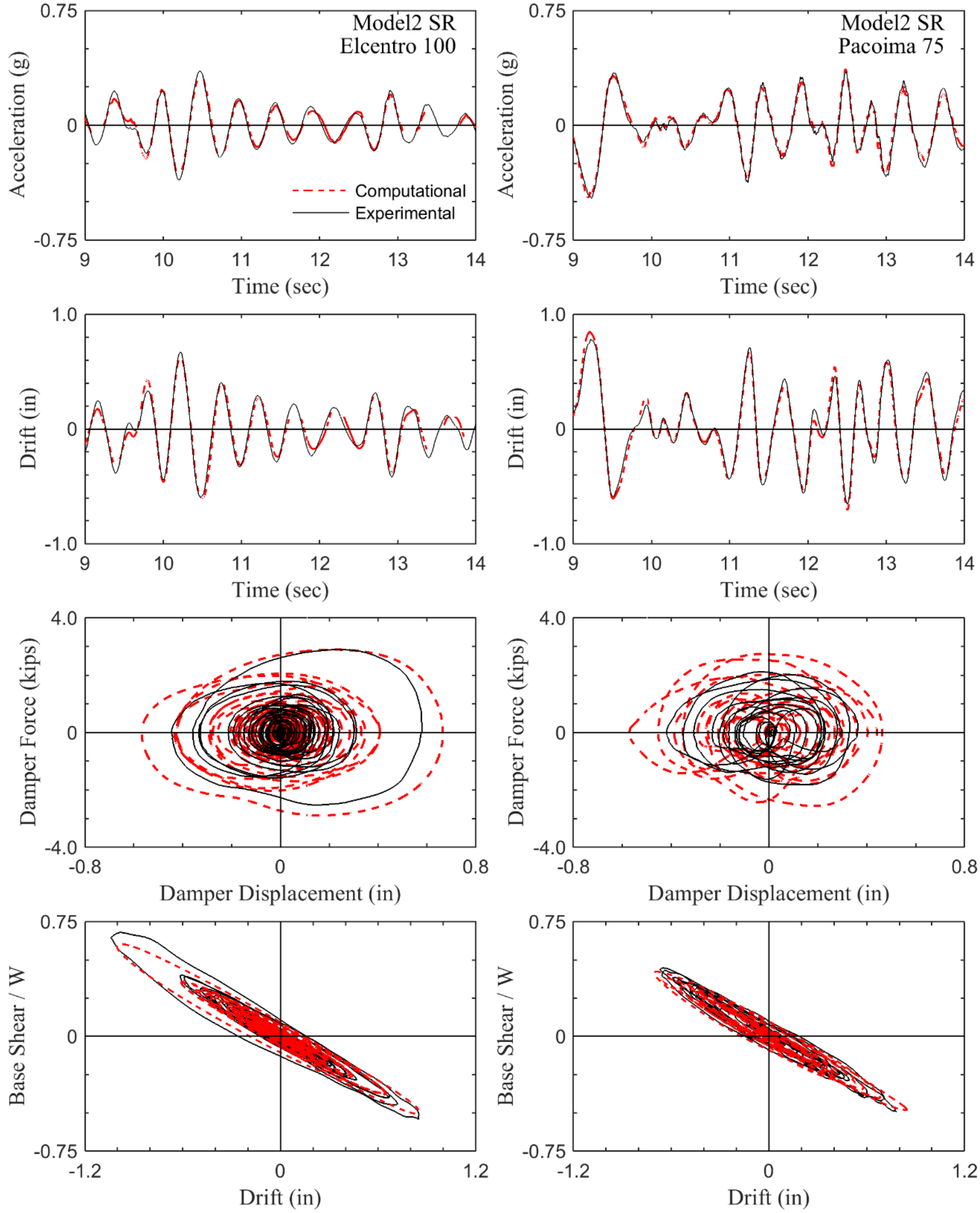

Figure 5-5 Comparison of Experimental and Analytical Results for Model 2 S-R in Two Tests

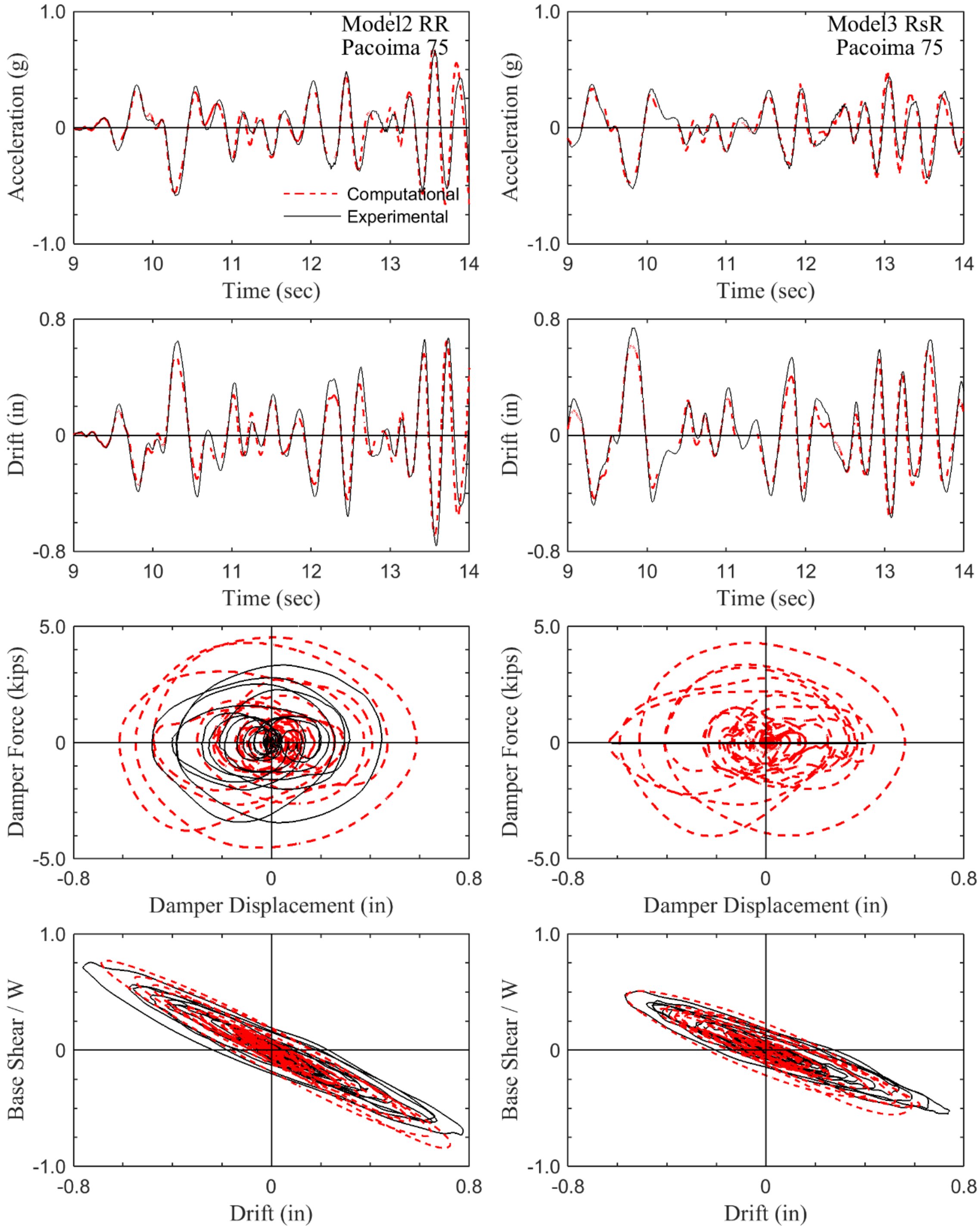

Figure 5-6 Earthquake Simulator Test Results for Model 2 R-R and Model 3 R-sR in Pacoima Motion

SECTION 6

SUMMARY AND CONCLUSIONS

A damping system has been described which allows for open space configuration that is most desirable by architects, owners and engineers. The configuration features a damper that may be installed parallel to the beam and which is connected to a column or the beam below through an inclined lever mechanism and a vertically inclined brace. The magnification factor accomplished by this configuration is close to that of the commonly used diagonal configuration, although larger values may be achieved at the expense of reduction in the open space characteristics.

A theory has been presented to predict the magnification factor of the system, defined as the ratio of the damper displacement to the frame drift, which is needed in predicting the damping ratio of the structure. It has been shown that the magnification factor is significantly affected by the beam deformations at the locations where the system is attached. However, the magnification factor is practically unaffected by the level of the damper forces (as large as 25% of the base shear force) and by large deformation effects up to a story drift of 4% of the story height.

Verification of the theory has been presented by comparison of theoretical predictions of the magnification factor to results of computational analysis of a sample frame in program SAP2000. This frame is a half-length scale model of a portal frame built for testing of the open space damping system.

An experimental study of the open space damping system has been presented. The experiments were conducted in order to demonstrate the increase in damping afforded by the damping system and to acquire data on dynamic response for validating the developed computational models for analysis. On the basis of the presented results, it may be concluded that the behavior of structures with the open space damping system can be predicted with sufficient accuracy for practical applications using readily available computational tools. In general, the prediction of drift and acceleration histories of response was in good agreement with the recorded response. However, damper displacements were generally over-predicted by as much as 0.2in (5mm), a value which is consistent with what was possible slippage in the oversize-hole connections of the tested frame ($3/16^{th}$ inch or 5mm).

The difficulties encountered with slippage in the joints were a characteristic of the tested model rather than of actual structures of which connections are typically welded or, when simple, they employ standard holes (rather than the slotted holes used in the model) and thus slippage is much less. Nevertheless, any uncertainty in properties needs to be accounted for by bounding analysis in which more than one models of analysis are used and the maximum response is utilized in design.

SECTION 7
REFERENCES

Baquero Mosquera, J. S., Almazán, J. L., and Tapia, N. F. (2016). "Amplification system for concentrated and distributed energy dissipation devices." *Earthquake Engineering and Structural Dynamics*.

Christopoulos, C., and Filiatrault, A. (2006). *Principles of passive supplemental damping and seismic isolation*, IUSS Press, Pavia.

Computers and Structures, Inc. (2015). "Integrated Finite Element Analysis and Design of Structures, Basic Analysis Reference Manual." *Berkeley, CA, USA.*

Constantinou, M. C., Soong, T. T., and Dargush, G. F. (1998). *Passive energy dissipation systems for structural design and retrofit*, Multidisciplinary Center for Earthquake Engineering Research Buffalo, New York.

Constantinou, M. C., Tsopelas, P., Hammel, W., and Sigaher, A. N. (2001). "Toggle-brace-damper seismic energy dissipations systems." *J. Struct. Eng.*, 127(2), 105-112.

Federal Emergency Management Agency (FEMA) (2015). "NEHRP recommended seismic provisions for new buildings and other structures", FEMA-P-1050, Volume I, Commentary to Chapter 18, Washington, DC.

Hibino, H., Kawamura, S., Hisano, M., Yamasa, M., and Kawamura, H. (1990). "Study on Response Control System of Structures Utilizing Damping Amplifier."Japan, 9p.

Kang, J. D., and Tagawa, H. (2013). "Seismic response of steel structures with seesaw systems using viscoelastic dampers." *Earthquake Engineering & Structural Dynamics*, 42(5), 779-794.

Rahimian, A.A., (2002), "Coupled Truss Systems with Damping for Seismic Protection of Buildings", *U.S. Patent 6,397,528 B1*, assigned to the Cantor Seinuk Group, P.C., New York, N.Y.

McNamara, R., Huang, C. and Wan, V. (2000). "Viscous-Damper with Motion Amplification Device for High Rise Building Applications." Structures Congress, Philadelphia, PA, May 8-10.

Sarkisian, M., Lee, P., Garai, R., Tsui, A. and Constantinou, M.C. (2015). " Controlling Wind in Tall and Flexible Structure With Viscous Damping Devices."Proceedings, SEAOC 2015 Convention, September 9-12, Seattle, WA.

Sarlis, A.A., Pasala, D.T.R., Constantinou, M.C., Reinhorn, A.M., Nagarajaiah, S. and Taylor, D. (2013). "Negative stiffness device for seismic protection of structures." *Technical Report MCEER-13-0005*, *Multidisciplinary Center for Earthquake Engineering Research.* State University of New York at Buffalo, Buffalo, NY.

Sigaher-Boyle, A. N., Constantinou, M.C. (2005). "*Scissor-jack damper energy dissipation system.*" *Technical Report MCEER-04-0010,* Multidisciplinary Center for Earthquake Engineering, Buffalo, N.Y.

Sigaher, A. N., and Constantinou, M. C. (2003). "Scissor-jack-damper energy dissipation system." *Earthquake Spectra*, 19(1), 133-158.

Soong, T. T., and Dargush, G. F. (1997). *Passive energy dissipation systems in structural engineering*, Wiley.

Symans, M., Charney, F., Whittaker, A., Constantinou, M., Kircher, C., Johnson, M., and McNamara, R. (2008). "Energy dissipation systems for seismic applications: current practice and recent developments." *J. Struct. Eng.*, 134(1), 3-21.

APPENDIX A
DERIVATION OF MAGNIFICATION FACTOR

Consider Figure 1-6. The movement of brace EC and rocker plate CAB is further illustrated in Figure A-1 for the case without frame deformation effects. Note that the original configuration (prior to frame lateral motion) is shown in dashed lines, and the final configuration (after the frame experiences lateral motion) is shown in solid lines. Members are considered inextensible so that the lengths of brace EC (L_{EC}) and of members CA (L) and AB (h) are constant. Note that the horizontal displacements of points A and D are the same as the drift u. Expressions for the displacements of points A, B, C and D, obtained entirely on the basis of kinematics, are shown in the Figure 12. Note also that counter-clockwise rotations are positive.

The coordinates of points $C\ and\ C'$ are, respectively, given by $(X_C, Y_C) = (L_{EC}\sin\theta_2, L_{EC}\cos\theta_2)$ and $(X_C', Y_C') = (L_{EC}\sin\theta_2', L_{EC}\cos\theta_2')$. It follows from the figure above that $Y_C' = L_{EC}\cos\theta_2' = Y_C + L\sin(\theta+\theta_3) - L\sin\theta$. Also, $X_C' = L_{EC}\sin\theta_2' = X_C + u + Lcos\theta_3 - L\cos(\theta+\theta_3)$. The cosine and sine of angle θ_2' are given by the following equations after using $X_C = L_{EC}\sin\theta_2$ and $Y_C = L_{EC}\cos\theta_2$:

$$\cos(\theta_2') = \frac{Y_{C'}}{L_{EC}} = \cos\theta_2 + \frac{L}{L_{EC}}\sin(\theta+\theta_3) - \frac{L}{L_{EC}}\sin\theta \quad \text{(A-1)}$$

$$\sin\theta_2' = \frac{X_{C'}}{L_{EC}} = \sin\theta_2 + \frac{u}{L_{EC}} + \frac{Lcos\theta_3}{L_{EC}} - \frac{L}{L_{EC}}\cos(\theta+\theta_3) \quad \text{(A-2)}$$

Angle θ_2' is eliminated from Equations (A-1) and (A-2) by use of $cos^2(\theta_2') + sin^2(\theta_2') = 1$ and after some algebra, the following is derived:

$$\frac{u^2}{L_{EC}} + \frac{2uL}{L_{EC}}(\cos\theta_3 - \cos(\theta_3-\theta)) + 2usin\theta_2 + 2Lsin(\theta-\theta_2+\theta_3) + 2Lsin(\theta_2-\theta_3) = 0 \quad \text{(A-3)}$$

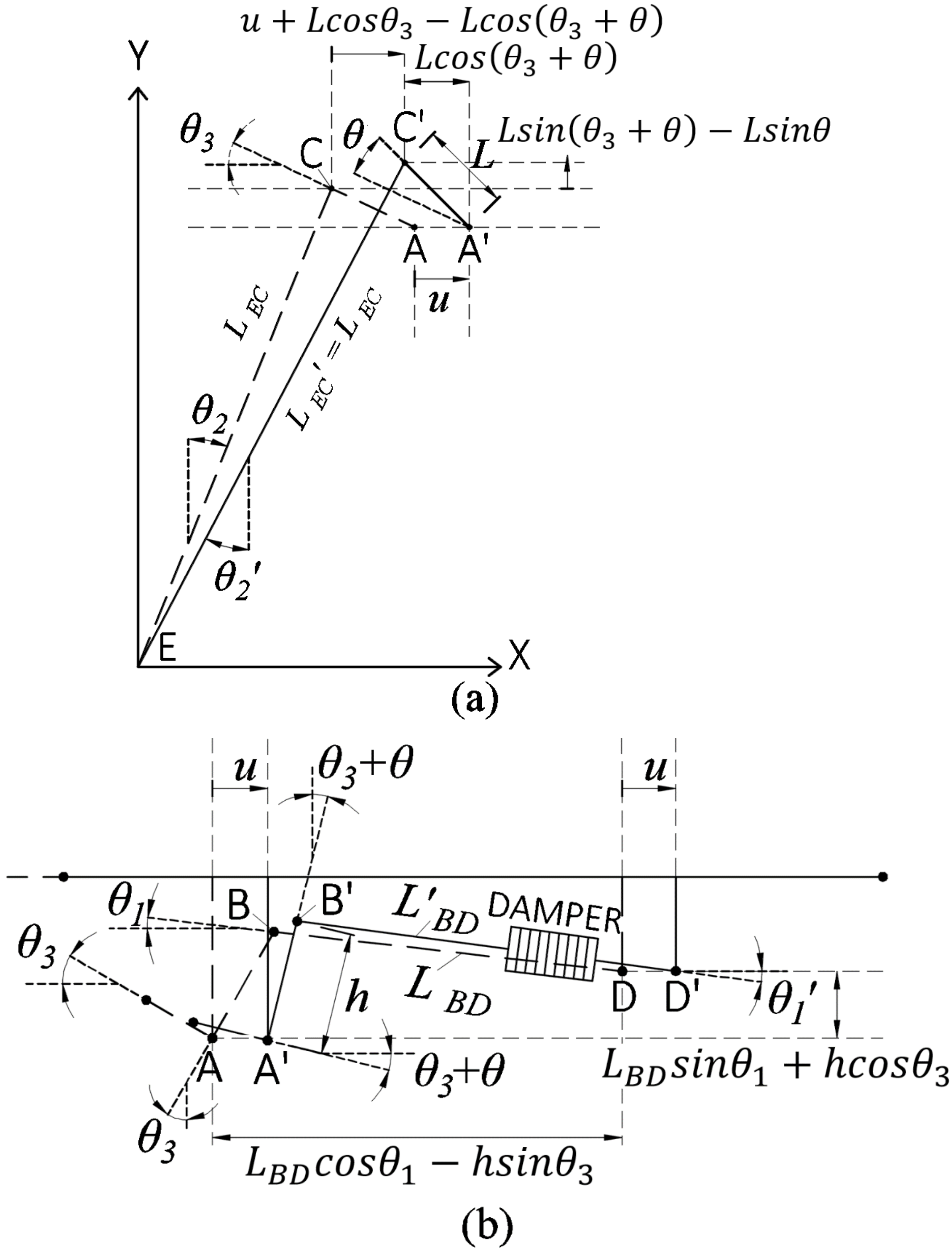

Figure A-1: Illustration of an Initial and Deformed Geometry of an Open Space System without Frame Deformation: (a) Rotation of Point A; (b) Damper Motion

Assuming small rotations so that $\sin(\theta)\sim\theta$ and $\cos(\theta)\sim 1$, Equation (A-3) reduces to

$$\frac{u^2}{L_{EC}}+2u\theta\frac{\mathrm{L}}{L_{EC}}sin\theta_3+2L\theta\cos(\theta_2-\theta_3)+2u\sin\theta_2=0 \qquad \text{(A-4)}$$

Terms involving u^2 and $u\theta$ are higher order terms so that for small displacements and rotations, Equation (A-4) reduces to

$$u\sin\theta_2+\mathrm{L}\theta\cos(\theta_2-\theta_3)=0 \qquad \text{(A-5)}$$

Solving for θ yields

$$\theta=-\frac{usin\theta_2}{Lcos(\theta_2-\theta_3)} \qquad \text{(A-6)}$$

The magnification factor is $f=(L_{B'D'}-L_{BD})/u$, where $(L_{B'D'}-L_{BD})$ is the damper deformation u_D and u is the drift, which is related to angle θ through Equation (A-6). Consider now the coordinates of points D and D'. Per Figure A-1(b), they are $(X_D,Y_D)=(X_A-hsin\theta_3+L_{BD}cos\theta_1,\ Y_A+h\cos\theta_3+L_{BD}sin\theta_1)$ and $(X'_D,Y'_D)=(X'_A-h\sin(\theta_3+\theta)+L_{B'D'}\cos\theta'_1,\ Y'_A+h\cos(\theta_3+\theta)+L_{B'D'}sin\theta'_1)$. Note that from the kinematics of the Figure A-2(b), $X'_D-X'_A=X_D-X_A$, and $Y'_D-Y'_A=Y_D-Y_A$. Using these relations, the following equations are derived.

$$L_{B'D'}cos\theta'_1=L_{BD}cos\theta_1+hsin(\theta+\theta_3)-hsin\theta_3 \qquad \text{(A-7)}$$

$$L_{B'D'}sin\theta'_1=L_{BD}sin\theta_1-hcos(\theta+\theta_3)+hcos\theta_3 \qquad \text{(A-8)}$$

Angle θ'_1 is eliminated from Equations (A-7) and (A-8) by use of $cos^2(\theta'_1)+sin^2(\theta'_1)=1$ and after some algebra, the following is derived:

$$L_{B'D'}{}^2 - L_{BD}^2 = 2h^2 - 2h^2 cos\theta + 2L_{BD} hsin(\theta_1 - \theta_3) + 2L_{BD} hsin(\theta - \theta_1 + \theta_3) \tag{A-9}$$

Expanding the terms in Equation (A-9) and for small rotations so that $\sin(\theta) \sim \theta$ and $\cos(\theta) \sim 1$, the following is derived

$$(L_{B'D'} - L_{BD})(L_{B'D'} + L_{BD}) = 2L_{BD} h\theta \cos(\theta_1 - \theta_3) \tag{A-10}$$

In (A-10) $L_{B'D'} - L_{BD}$ is the damper deformation, u_D. Further recognizing that for small rotations, $L_{B'D'} + L_{BD} \sim 2L_{BD}$, the damper deformation is given by

$$u_D = L_{B'D'} - L_{BD} = h\theta \cos(\theta_1 - \theta_3) \tag{A-11}$$

Finally, from Equations (A-10) and (A-11) the magnification factor is obtained as

$$f = \frac{u_D}{u} = \left| \frac{hcos(\theta_1 - \theta_3) sin\theta_2}{Lcos(\theta_2 - \theta_3)} \right| \tag{A-12}$$

APPENDIX B

RESULTS OF TESTING OF INDIVIDUAL FRAMES

MODEL 1, RIGID-SIMPLE CONNECTION
U_o=0.5in, f=1Hz.

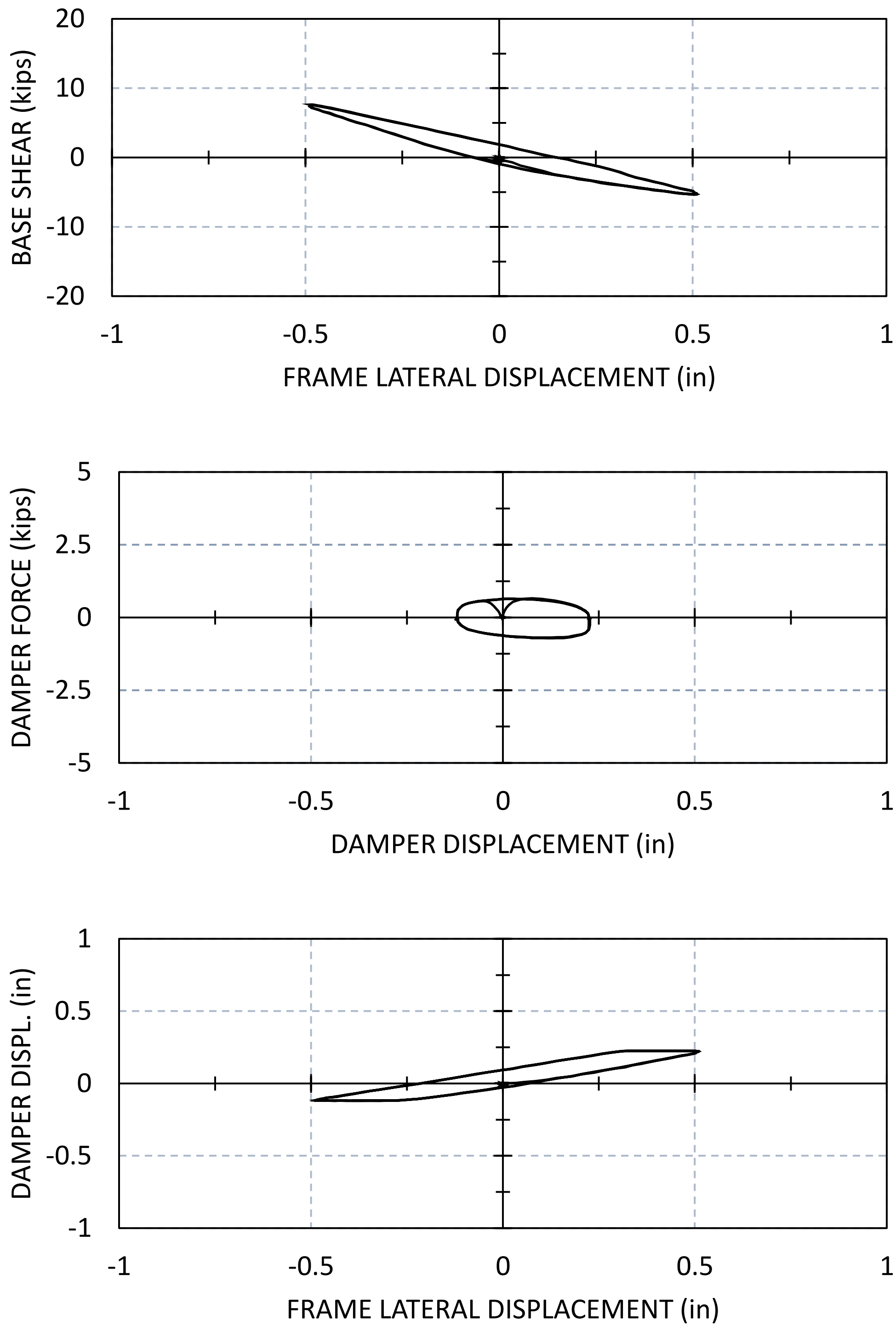

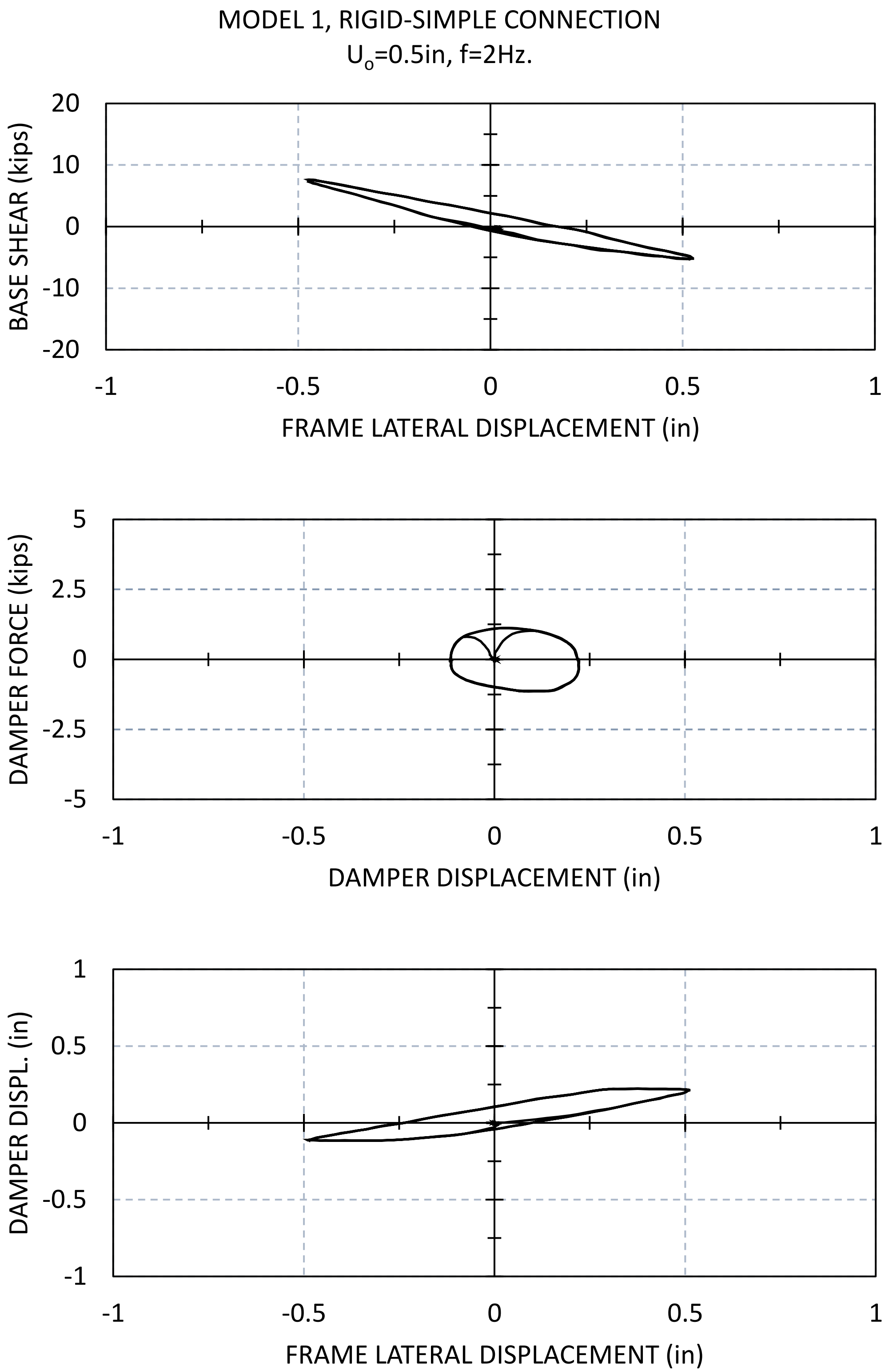
MODEL 1, RIGID-SIMPLE CONNECTION
Uo=0.5in, f=2Hz.
BASE SHEAR (kips)
20
10
0
-10
-20
-1
-0.5
0
0.5
1
FRAME LATERAL DISPLACEMENT (in)
DAMPER FORCE (kips)
5
2.5
0
-2.5
-5
-1
-0.5
0
0.5
1
DAMPER DISPLACEMENT (in)
DAMPER DISPL. (in)
1
0.5
0
-0.5
-1
-1
-0.5
0
0.5
1
FRAME LATERAL DISPLACEMENT (in)

MODEL 1, RIGID-SIMPLE CONNECTION

U_o=1in, f=0.05Hz.

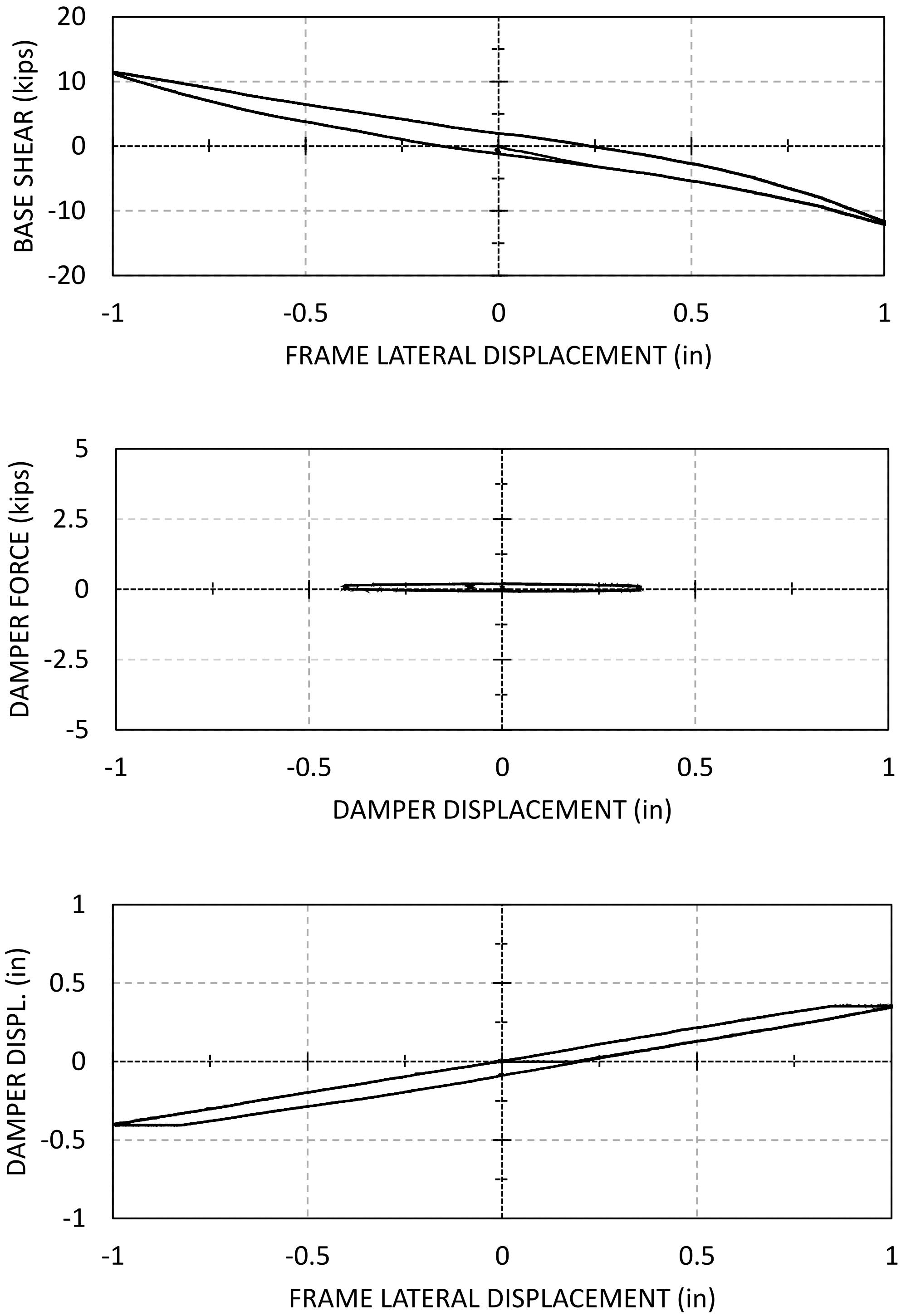

MODEL 1, RIGID-SIMPLE CONNECTION
U_o=1in, f=1Hz.

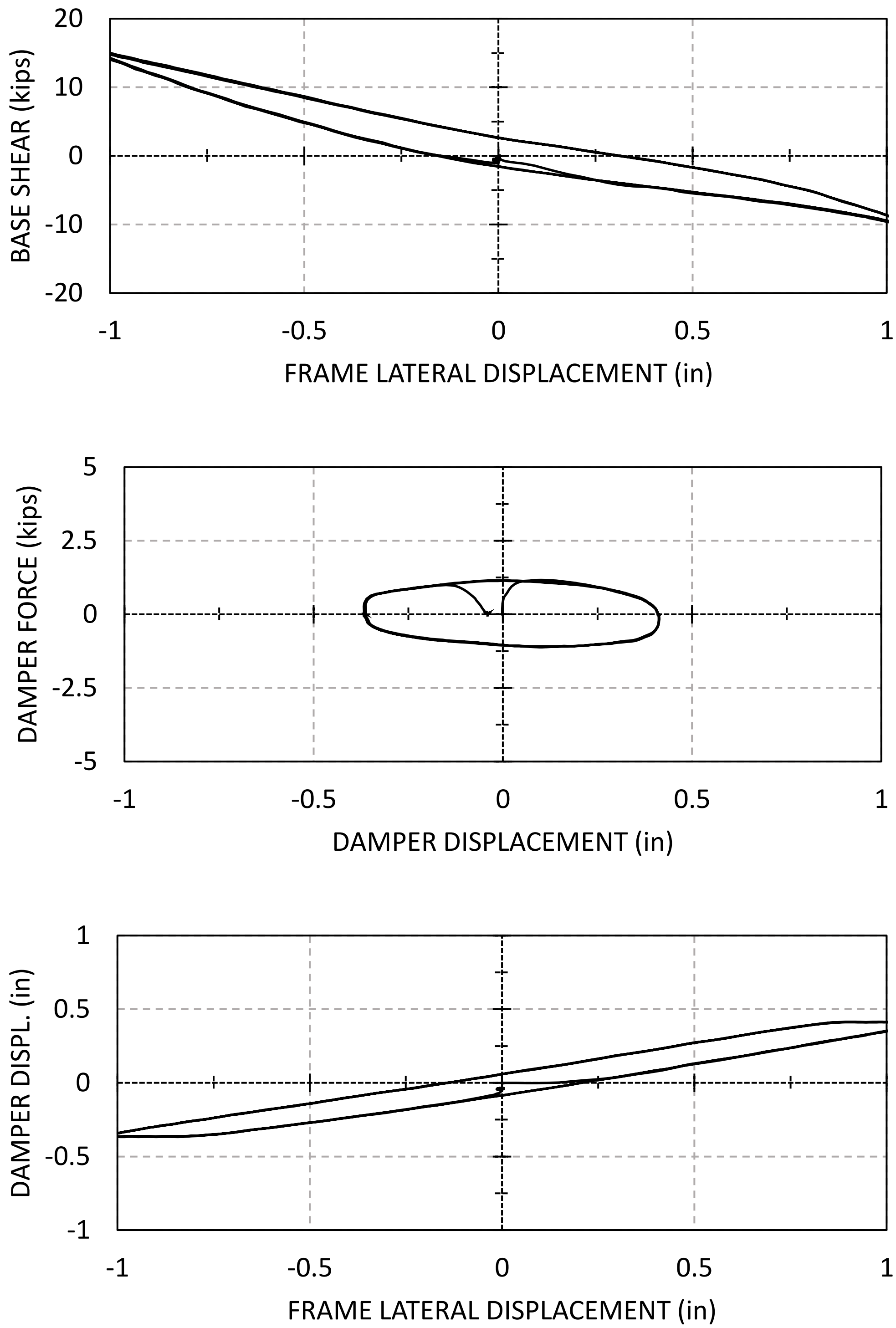

MODEL 1, RIGID-SIMPLE CONNECTION

U_o=1in, f=2Hz.

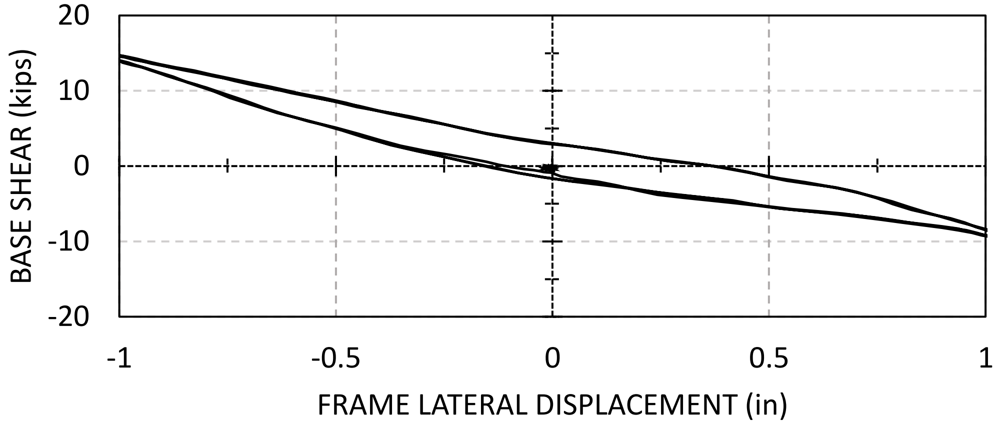

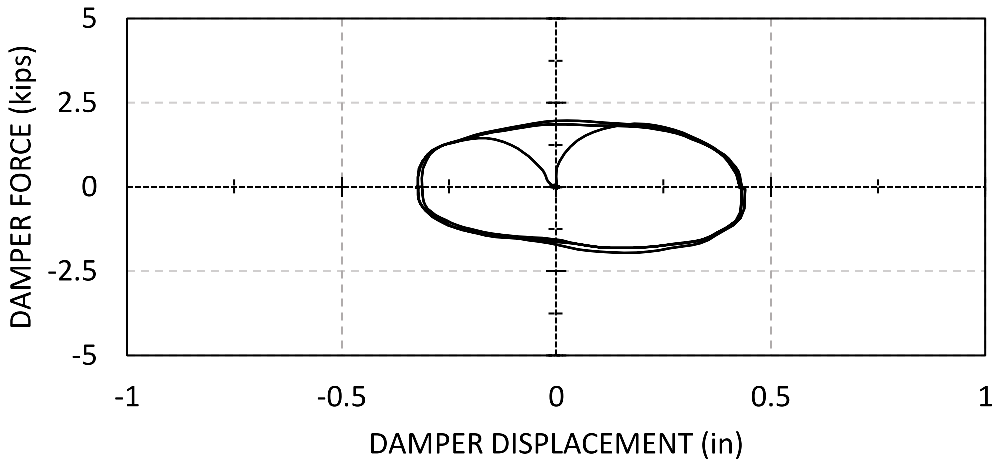

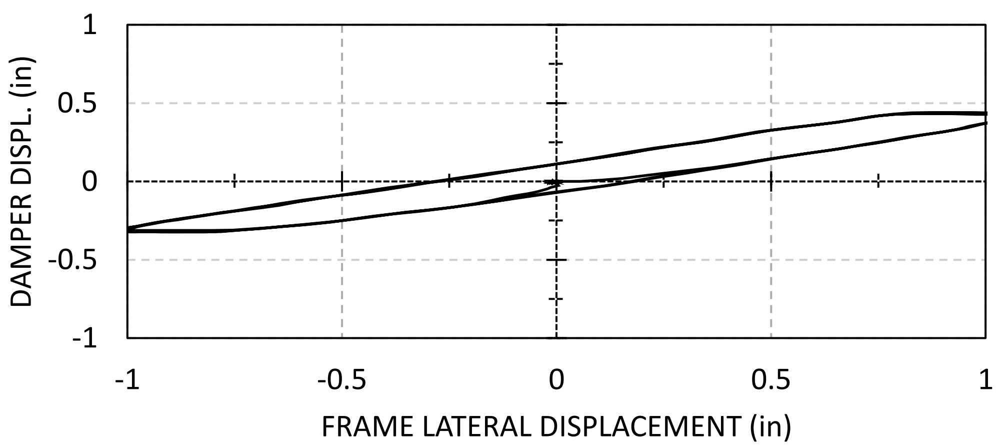

MODEL 1, SIMPLE-RIGID CONNECTION
U_o=1in, f=0.05Hz.

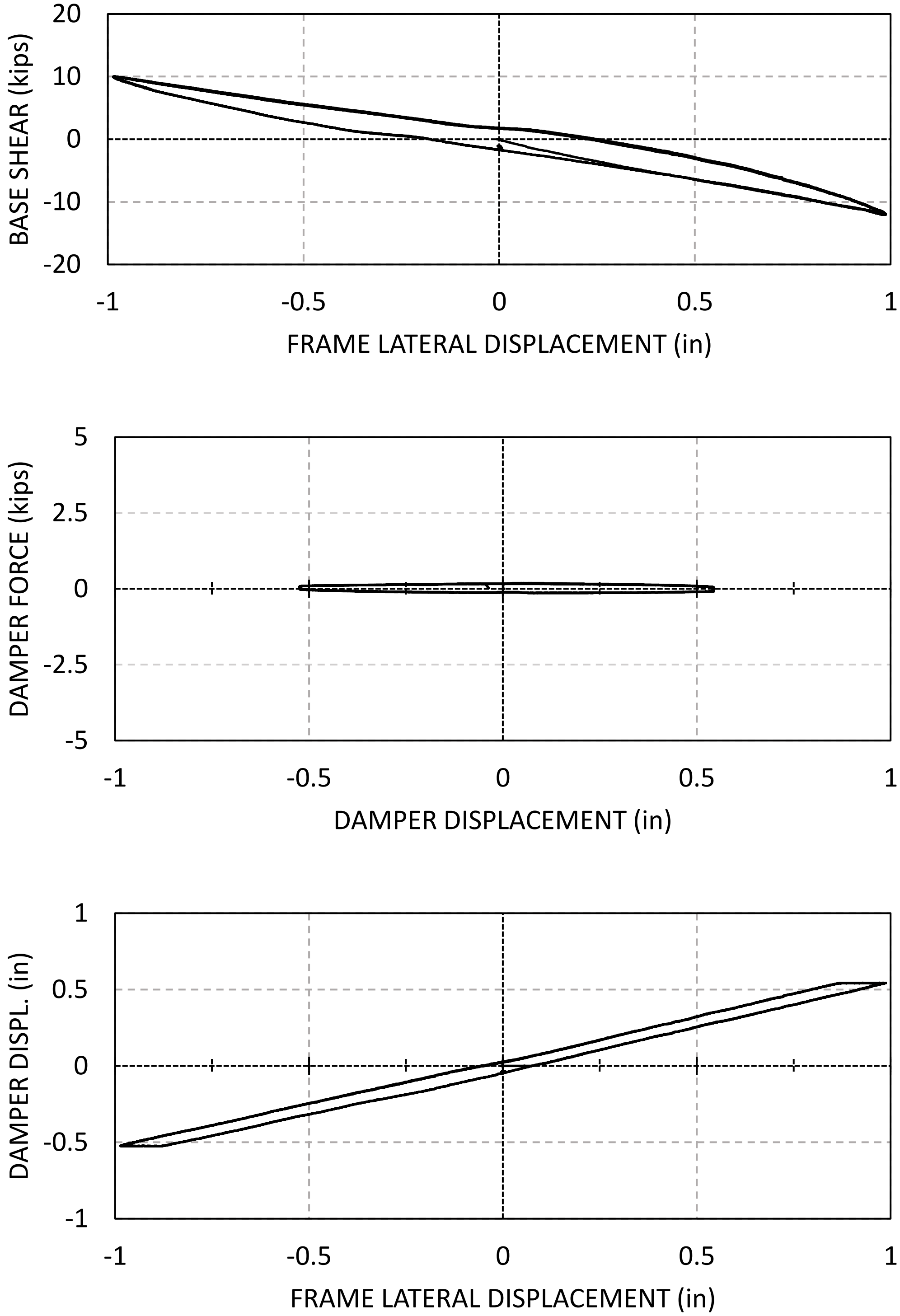

MODEL 1, SIMPLE-RIGID CONNECTION

U_o=1in, f=1Hz.

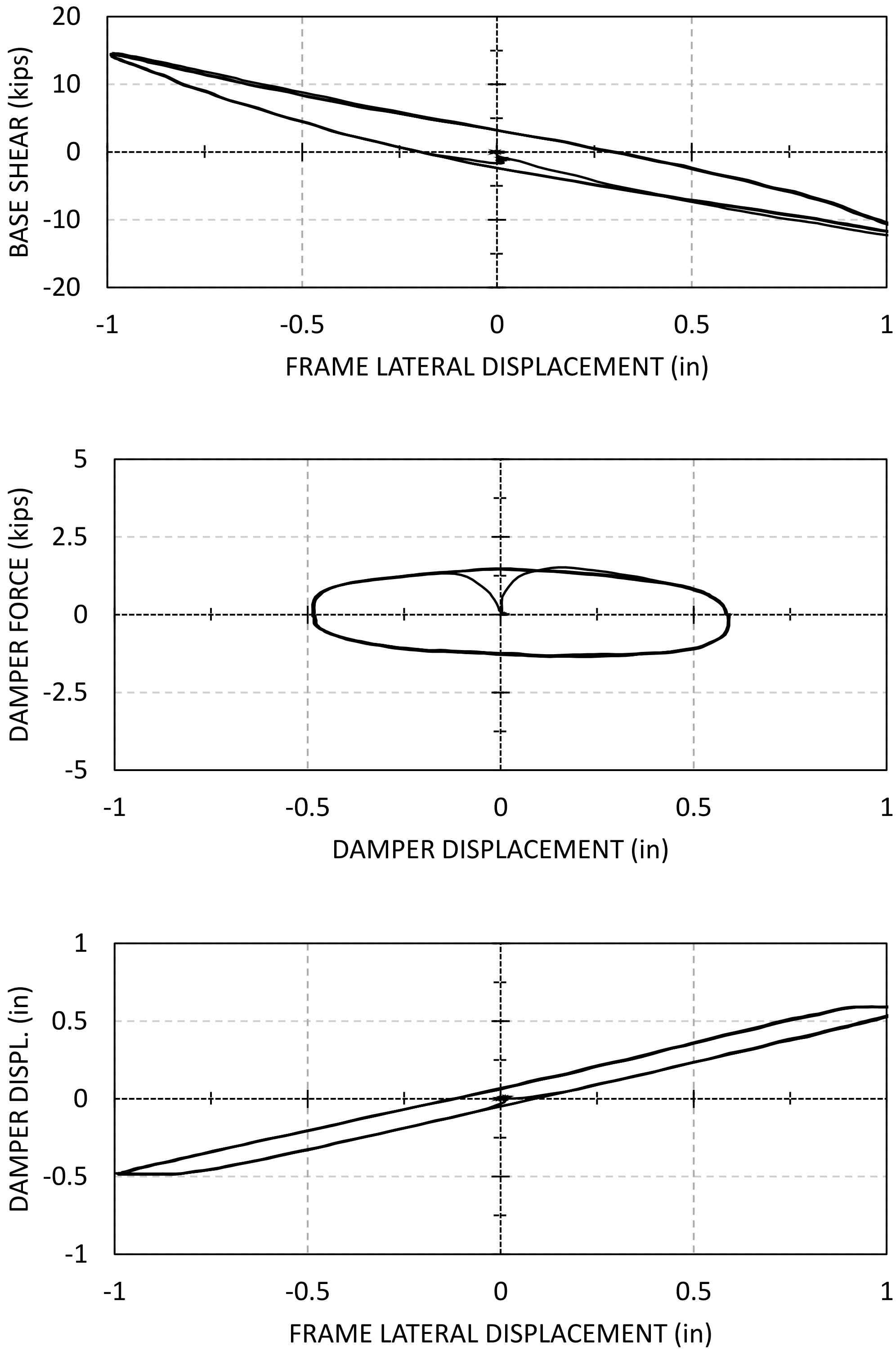

MODEL 1, SIMPLE-RIGID CONNECTION

U_o=1in, f=2Hz.

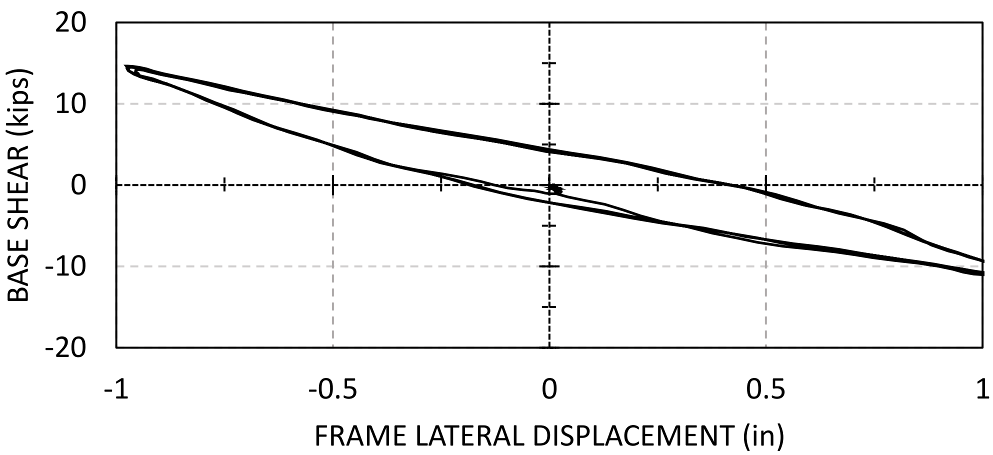

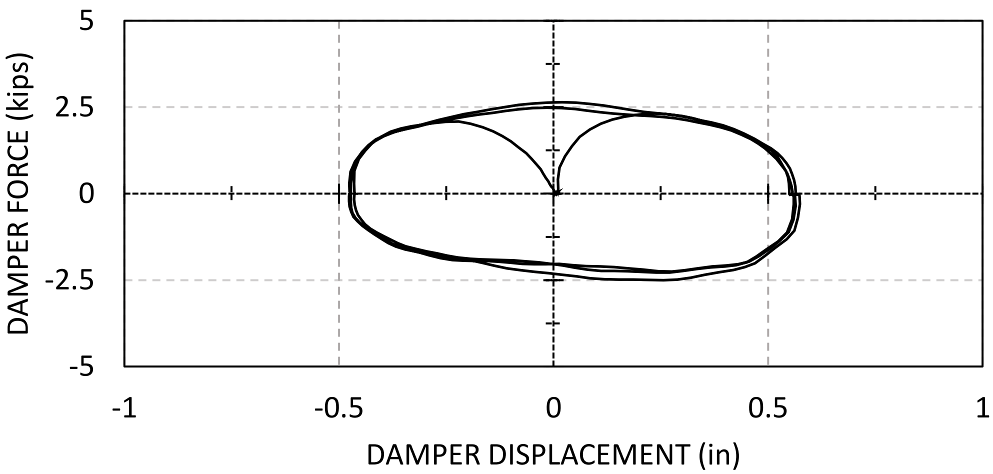

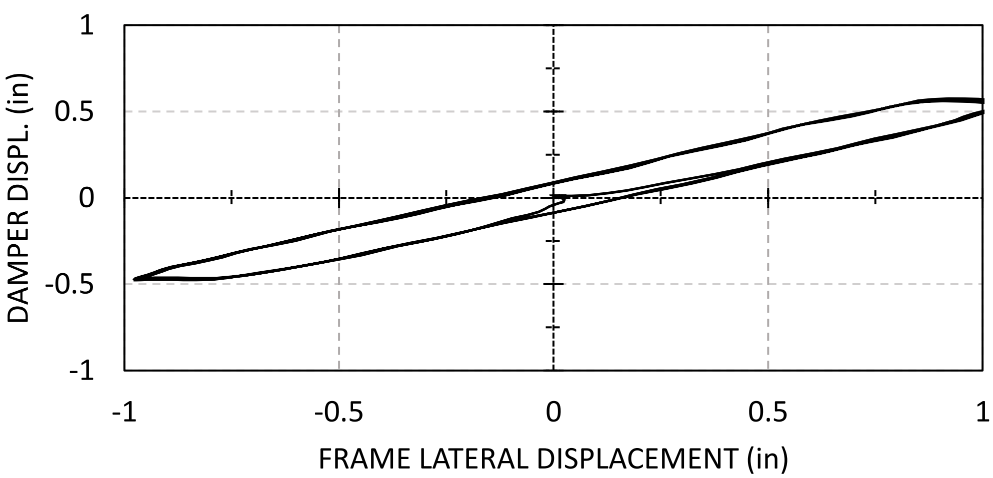

MODEL 2, RIGID-SIMPLE CONNECTION
U_o=0.5in, f=1Hz.

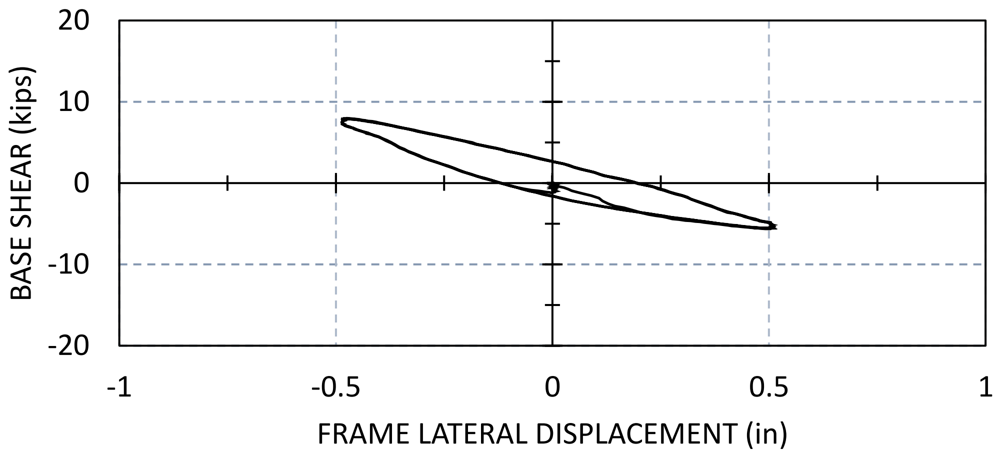

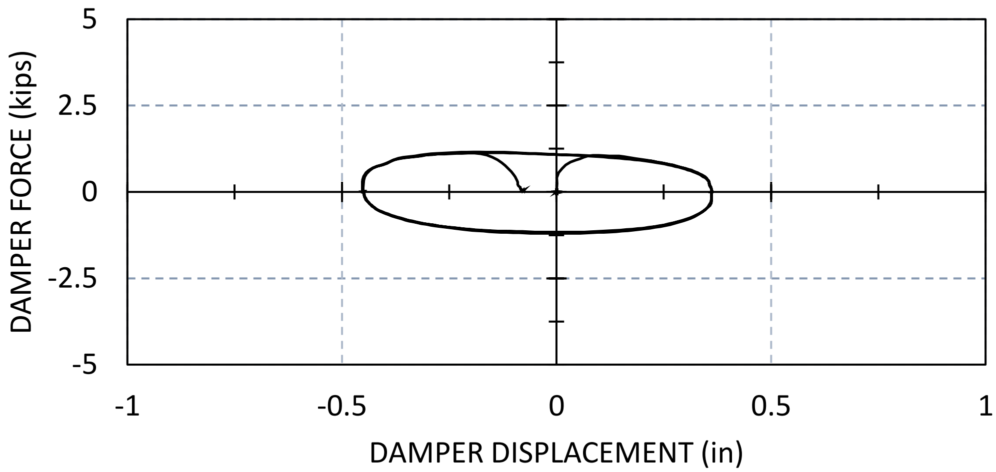

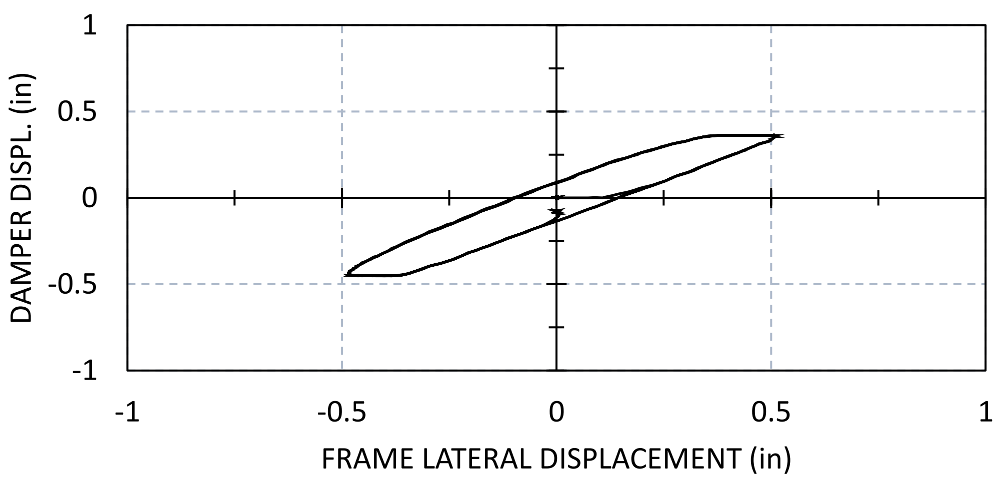

MODEL 2, RIGID-SIMPLE CONNECTION

U_o=0.5in, f=2Hz.

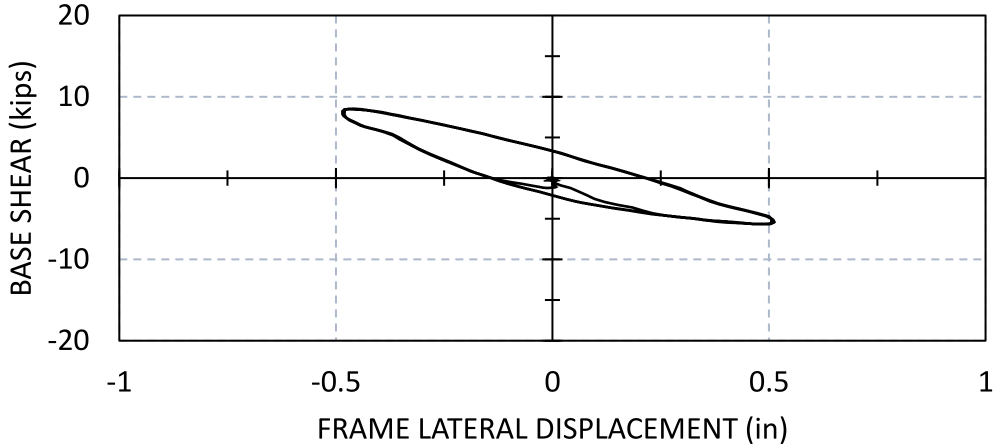

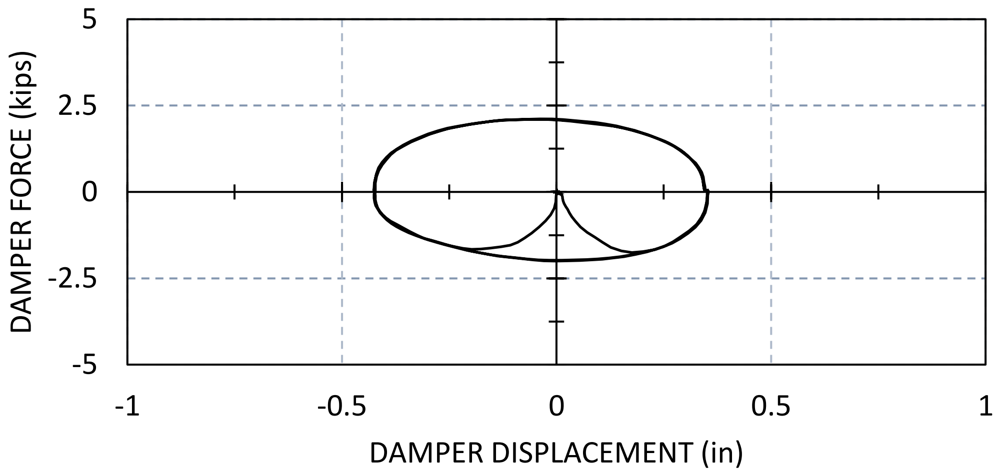

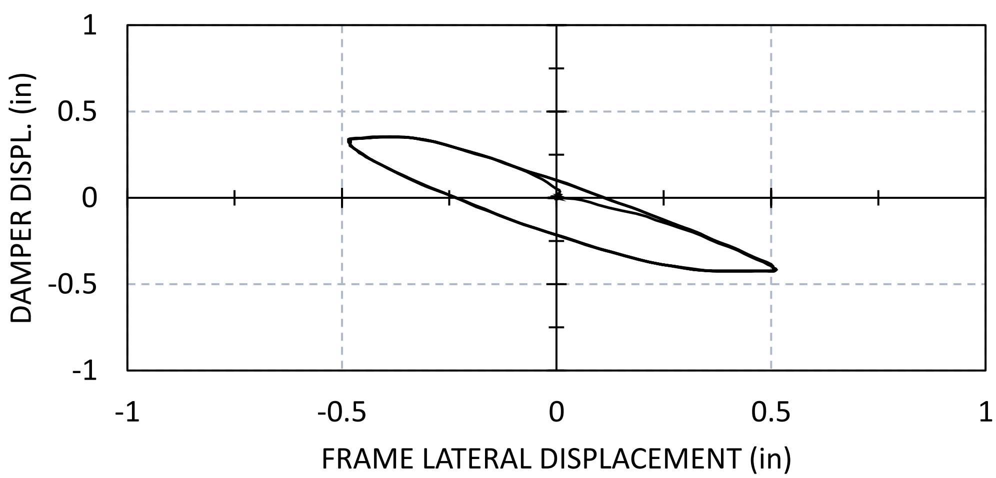

MODEL 2, RIGID-SIMPLE CONNECTION
U_o=1in, f=0.05Hz.

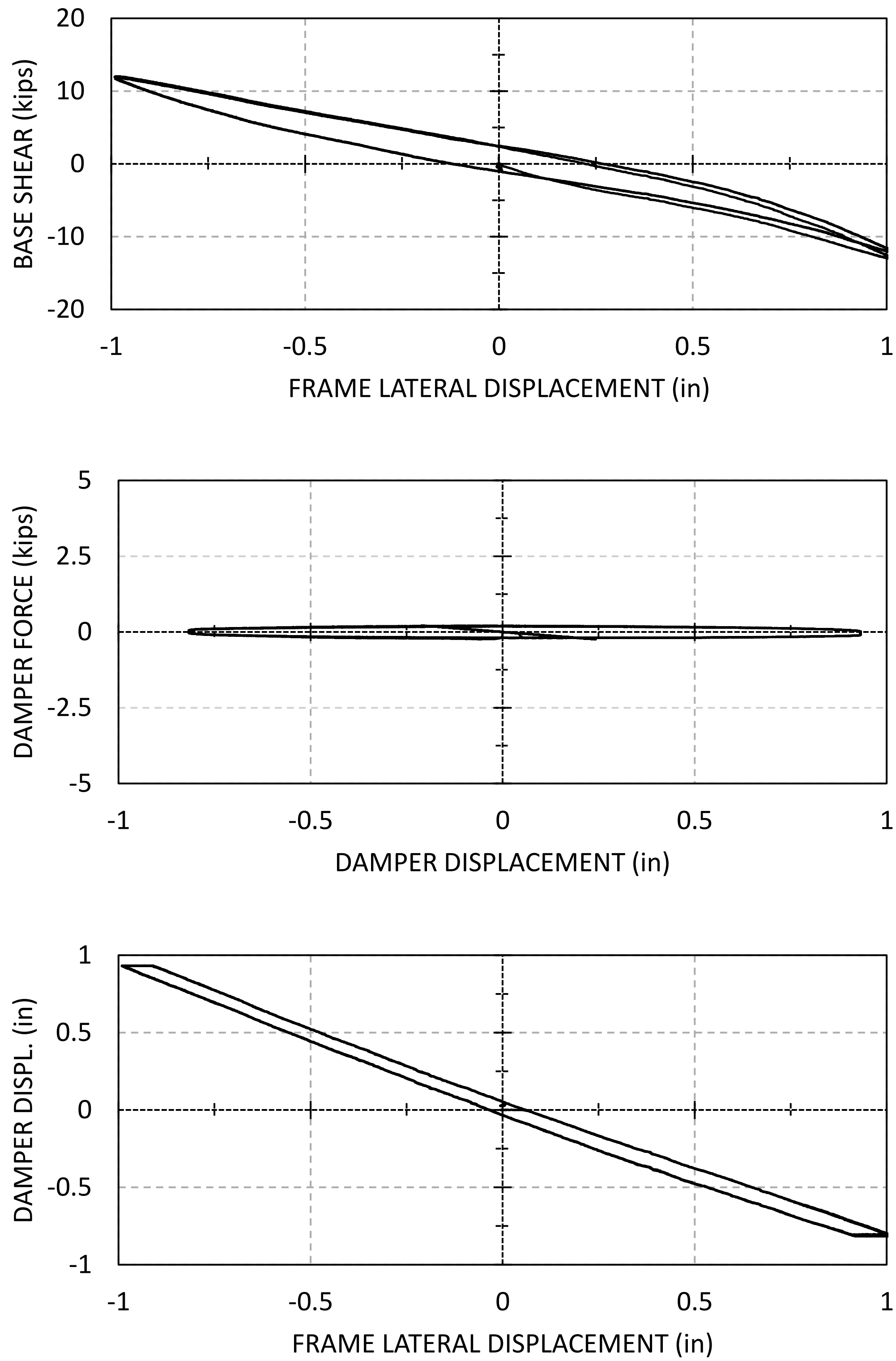

MODEL 2, RIGID-SIMPLE CONNECTION
U_o=1in, f=1Hz

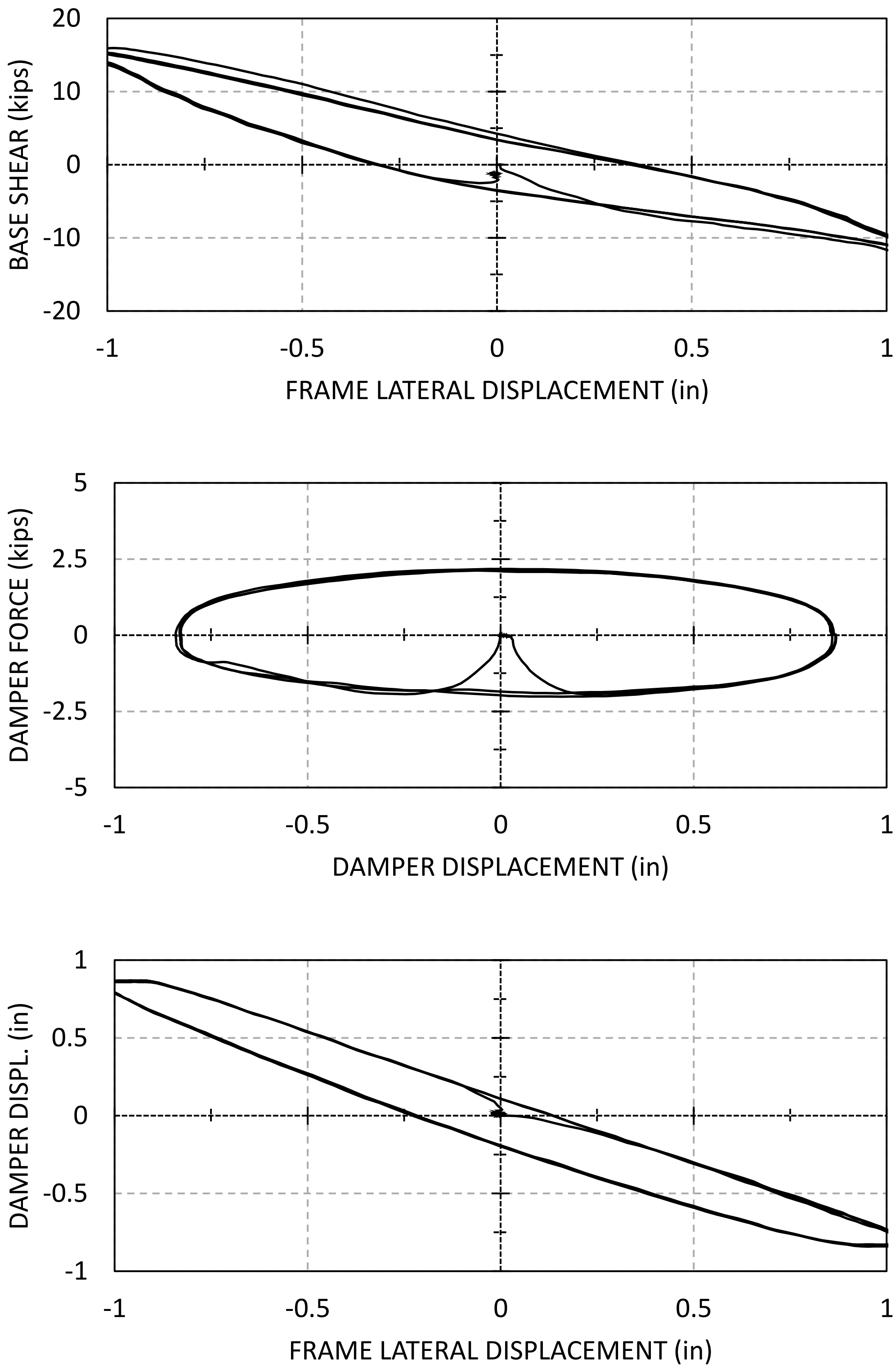

MODEL 2, RIGID-SIMPLE CONNECTIONS
U_o=1in, f=2Hz.

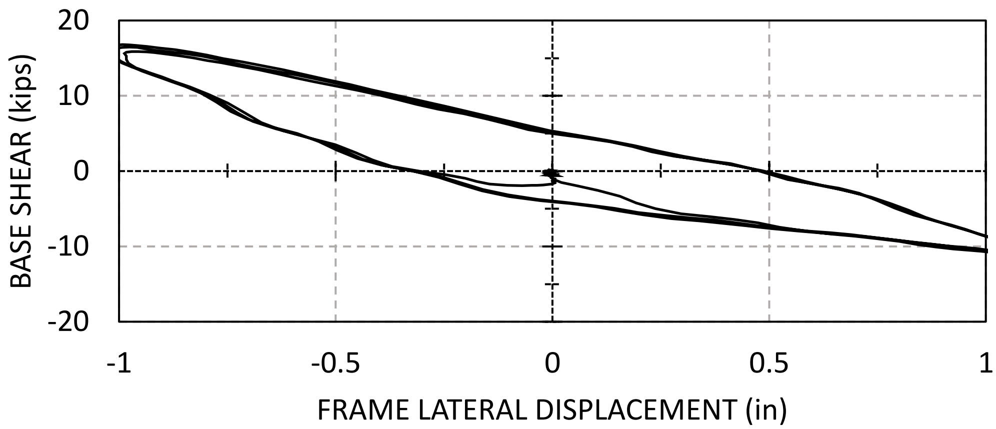

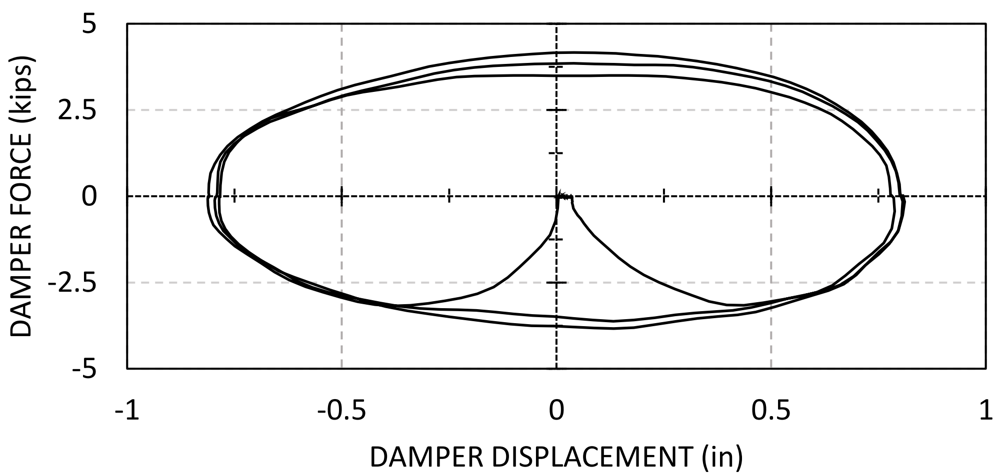

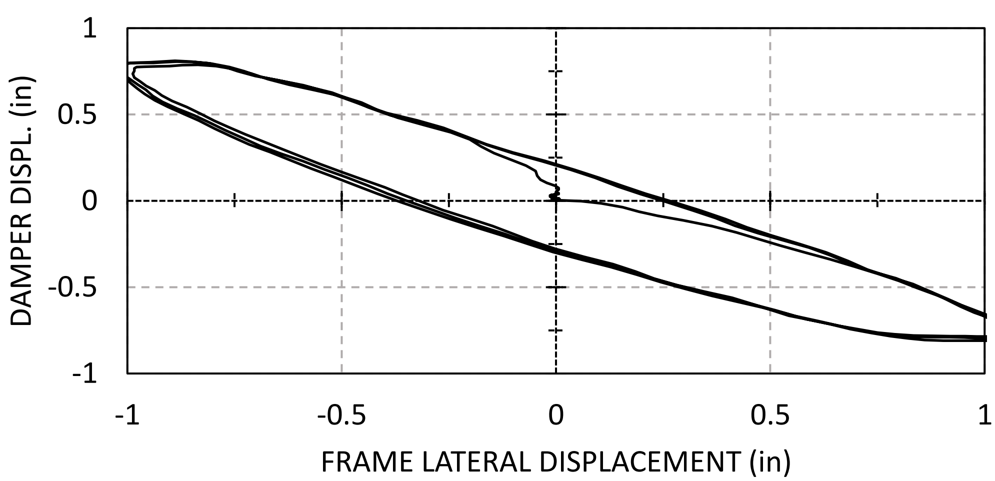

MODEL 2, SIMPLE-RIGID CONNECTION
U_o=1in, f=0.05Hz.

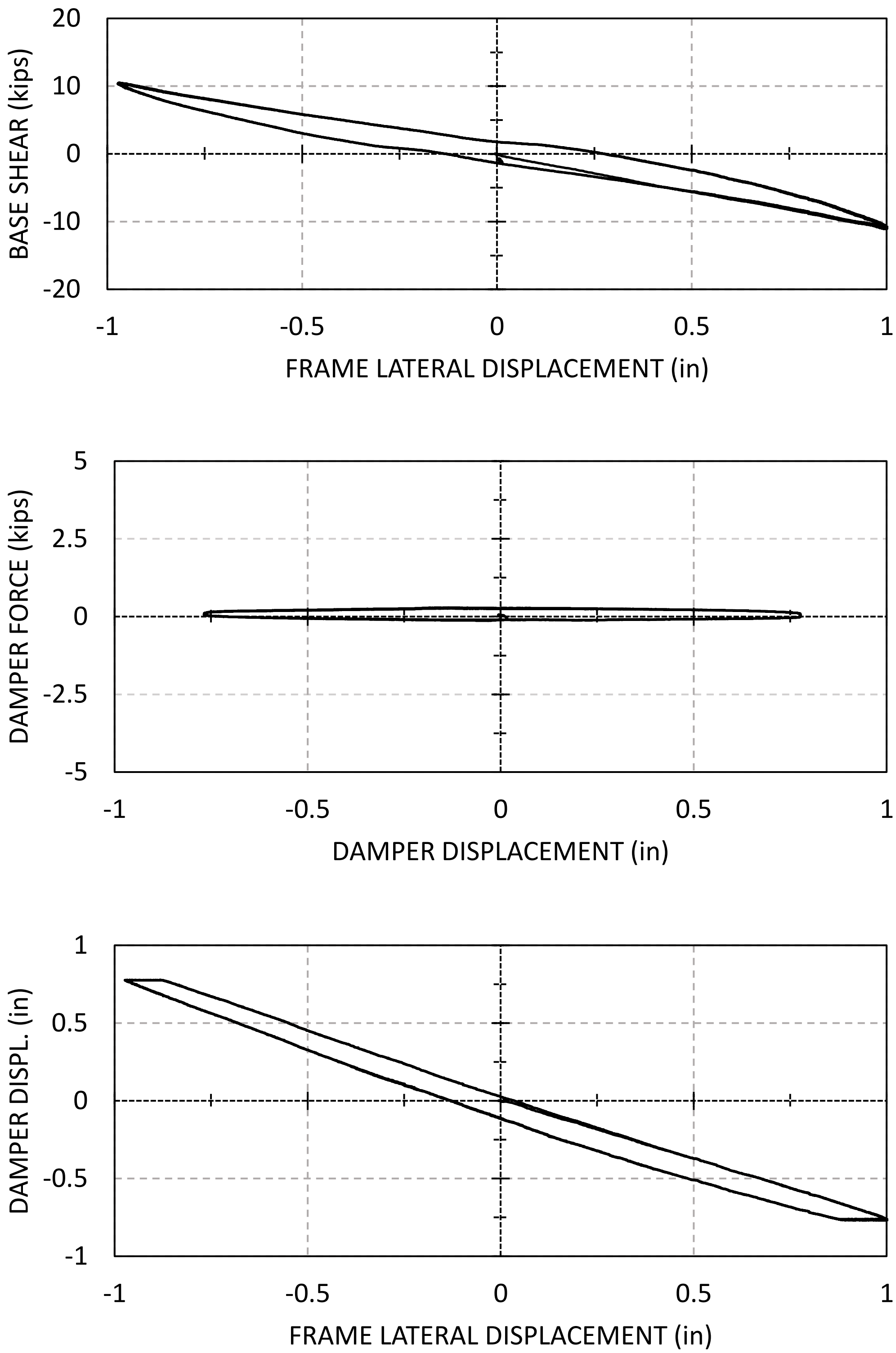

MODEL 2, SIMPLE-RIGID CONNECTION
U_o=1in, f=1Hz.

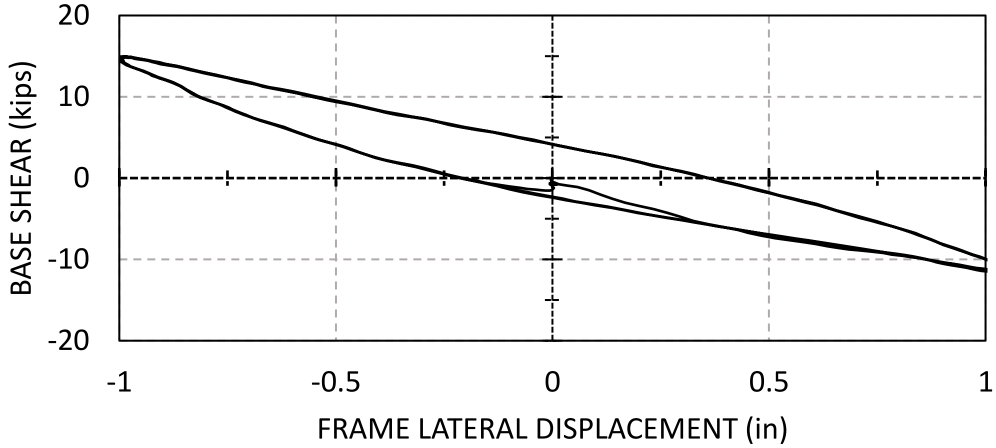

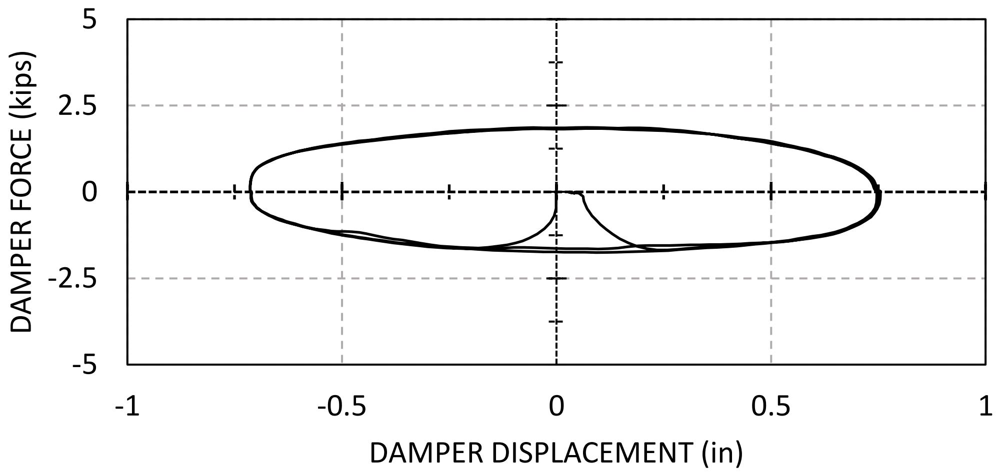

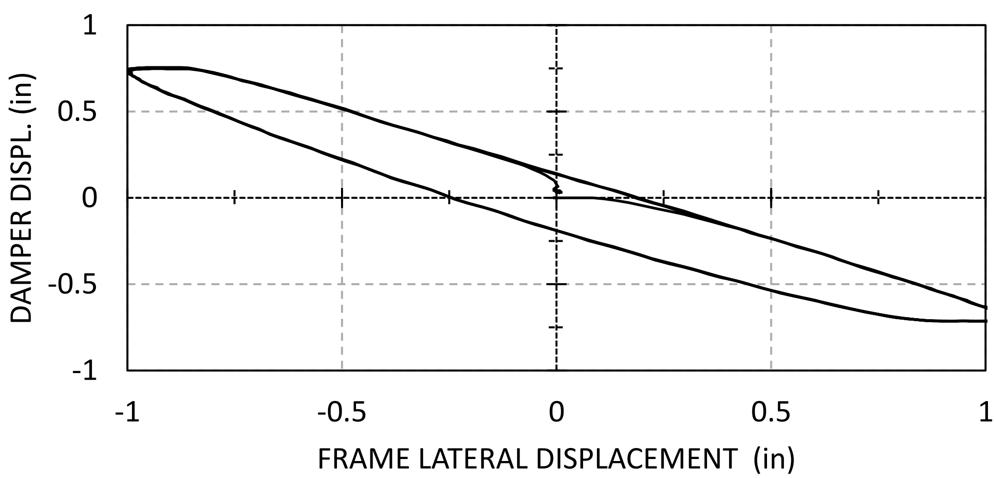

MODEL 2, SIMPLE-RIGID CONNECTION
U_o=1in, f=2Hz.

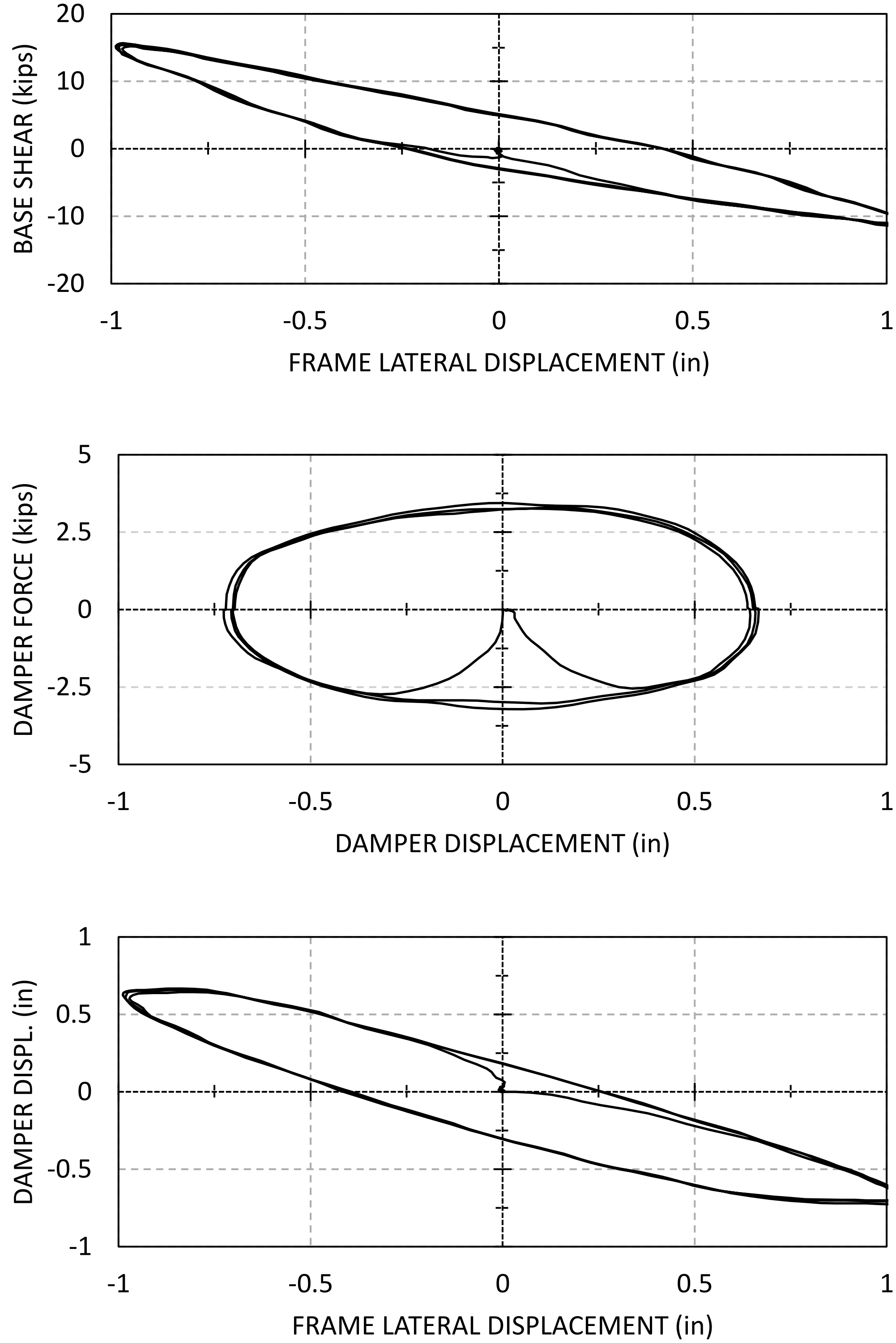

This Page Intentionally Left Blank”

APPENDIX C

EARTHQUAKE SIMULATOR TEST RESULTS

DATE	TEST #	FRAME MODEL	TEST NAME	EXCITATION	EQ. SIMULATOR PEAK VALUES			FRAME PEAK VALUES				DAMPER PEAK VALUES				MAGNIFICATION FACTOR	
					DISPL. (in)	VELOC. (in/sec)	ACCEL. (g)	DRIFT (in)		ACCELERATION (g)		DISPLACEMENT (in)		FORCE (kips)			
								Avg(+)	Avg(-)	Avg(+)	Avg(-)	Avg(+)	Avg(-)	Avg(+)	Avg(-)	Avg(+)	Avg(-)
10/30/2015	11	M2 R-S	osts2s2	TAFT N21E 200%	1.97	7.42	0.29	0.51	-0.49	0.36	-0.37	0.33	-0.35	2.38	-1.95	0.69	0.67
10/30/2015	13	M2 R-S	osts2s4	EL CENTRO S00E 50%	0.87	4.30	0.18	0.37	-0.46	0.32	-0.26	0.30	-0.23	1.57	-1.82	0.61	0.65
10/30/2015	14	M2 R-S	osts2s5	EL CENTRO S00E 100%	1.96	8.57	0.33	0.61	-0.86	0.55	-0.43	0.61	-0.42	2.95	-3.22	0.70	0.71
10/30/2015	19	M2 R-S	osts2s10	PACOIMA S74W 50%	3.12	13.43	0.45	0.44	-0.39	0.26	-0.34	0.24	-0.33	1.80	-1.92	0.75	0.62
11/2/2015	23	M2 R-S	osts2s12	PACOIMA S74W 75%	4.70	20.15	0.72	0.68	-0.58	0.38	-0.50	0.40	-0.51	2.85	-2.95	0.75	0.68
11/10/2015	70	M2 R-S	osts14s02	PACOIMA S74W 100%	6.32	27.15	1.01	1.05	-0.74	0.48	-0.65	0.55	-0.79	3.62	-3.70	0.75	0.75
11/10/2015	71	M2 R-S	osts14s03	NEWHALL 90 75%	2.43	12.31	0.60	0.82	-0.87	0.54	-0.44	0.67	-0.56	3.12	-4.22	0.68	0.77
11/3/2015	38	M2 S-R	osts6s04	TAFT N21E 200%	1.94	7.35	0.29	0.88	-0.90	0.52	-0.50	0.42	-0.44	2.53	-1.99	0.51	0.46
11/2/2015	35	M2 S-R	osts6s01	EL CENTRO S00E 50%	0.99	4.41	0.18	0.47	-0.55	0.32	-0.29	0.26	-0.21	1.43	-1.38	0.43	0.48
11/10/2015	63	M2 S-R	osts12s01	EL CENTRO S00E 100%	1.95	8.70	0.30	0.85	-1.03	0.56	-0.48	0.58	-0.44	2.90	-2.52	0.52	0.56
11/2/2015	36	M2 S-R	osts6s02	PACOIMA S74W 50%	3.12	13.59	0.45	0.48	-0.44	0.28	-0.31	0.21	-0.20	1.48	-1.22	0.42	0.49
11/10/2015	64	M2 S-R	osts12s02	PACOIMA S74W 75%	4.72	20.16	0.71	0.78	-0.66	0.40	-0.49	0.36	-0.42	2.12	-1.82	0.54	0.55
11/3/2015	42	M1 S-R	osts7s01	EL CENTRO S00E 50%	0.99	4.35	0.17	0.47	-0.52	0.29	-0.26	0.23	-0.26	1.34	-1.32	0.48	0.50
11/4/2015	44	M1 S-R	osts7s03	PACOIMA S74W 50%	3.12	13.39	0.44	0.47	-0.44	0.27	-0.31	0.25	-0.22	1.37	-1.49	0.54	0.50
11/4/2015	45	M1 S-R	osts7s04	PACOIMA S74W 75%	4.69	20.14	0.70	0.75	-0.65	0.39	-0.48	0.40	-0.32	1.98	-2.05	0.53	0.49
11/4/2015	48	M1 S-R	osts7s07	NEWHALL 90 50%	1.59	8.12	0.36	0.66	-0.65	0.40	-0.34	0.32	-0.29	2.27	-1.51	0.49	0.45
11/9/2015	54	M1 S-R	osts9s01	TAFT N21E 200%	1.94	7.32	0.29	0.90	-0.91	0.50	-0.50	0.49	-0.30	2.17	-2.13	0.55	0.33
11/9/2015	55	M1 S-R	osts9s02	PACOIMA S74W 75%	4.73	20.41	0.71	0.79	-0.69	0.37	-0.48	0.44	-0.32	1.90	-1.74	0.56	0.46
11/2/2015	26	M2 R-R	osts3s01	EL CENTRO S00E 50%	0.85	4.64	0.19	0.33	-0.31	0.32	-0.32	0.14	-0.18	1.04	-1.46	0.54	0.45
11/10/2015	66	M2 R-R	osts13s01	TAFT N21E 200%	1.98	7.38	0.28	0.53	-0.55	0.50	-0.47	0.31	-0.31	2.35	-1.83	0.58	0.55
11/10/2015	67	M2 R-R	osts13s02	PACOIMA S74W 75%	4.75	20.15	0.75	0.77	-0.75	0.68	-0.66	0.44	-0.48	3.34	-3.45	0.63	0.59
11/11/2015	83	M3 R-sR	osts18s02	EL CENTRO S00E 100%	1.95	8.69	0.34	0.61	-0.77	0.61	-0.42	0.64	-0.48	-0.03	-0.03	0.77	0.82
11/11/2015	84	M3 R-sR	osts18s03	PACOIMA S74W 75%	4.74	20.19	0.71	0.74	-0.56	0.45	-0.54	0.40	-0.62	-0.03	-0.03	0.84	0.72

Avg=Average value between two frames, (+): positive is towards the right, (-): negative is towards the left

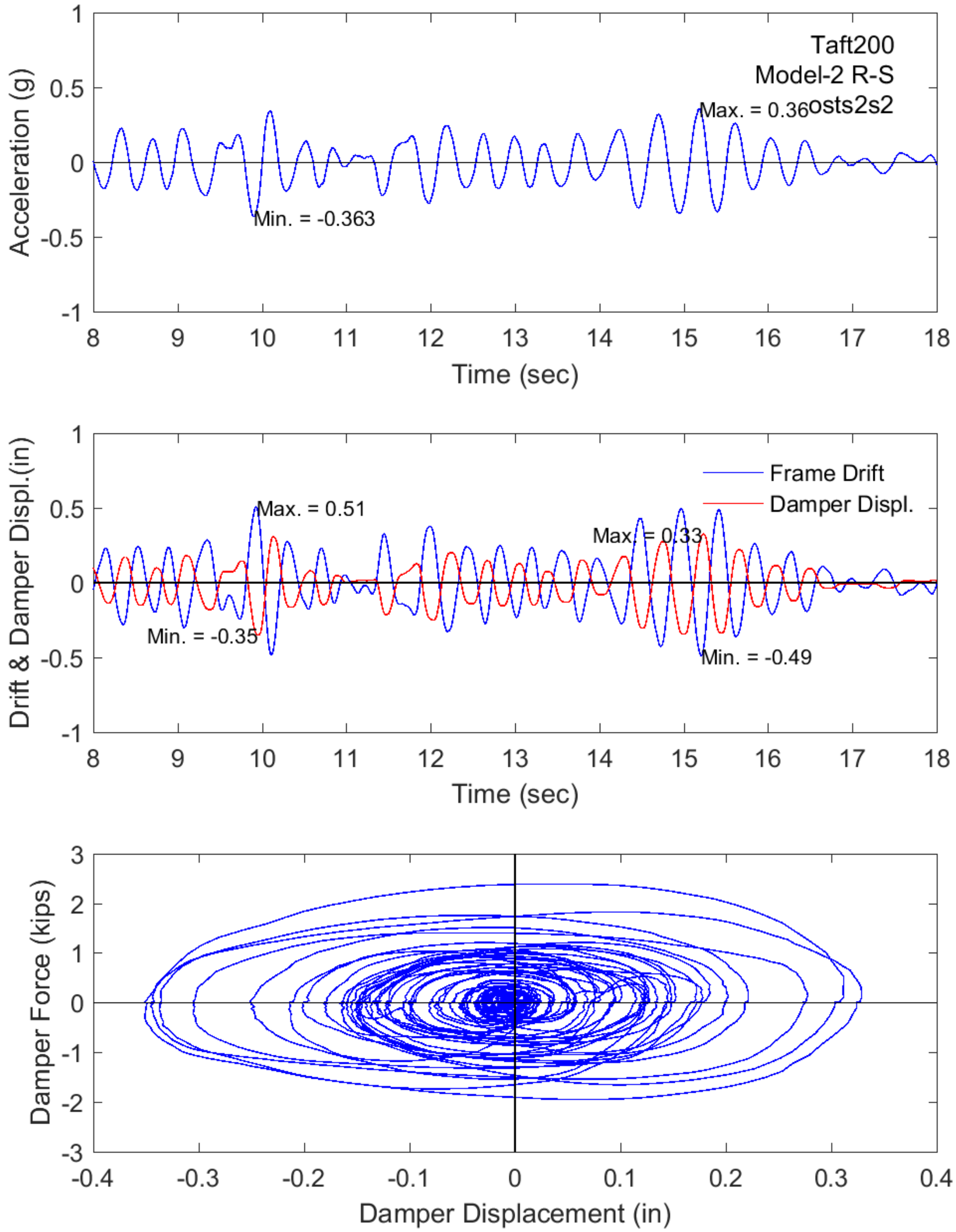
Taft200
Model-2 R-S
osts2s2
Max. = 0.36
Min. = -0.363
Acceleration (g)
Time (sec)
Frame Drift
Damper Displ.
Max. = 0.51
Max. = 0.33
Min. = -0.35
Min. = -0.49
Drift & Damper Displ.(in)
Time (sec)
Damper Force (kips)
Damper Displacement (in)

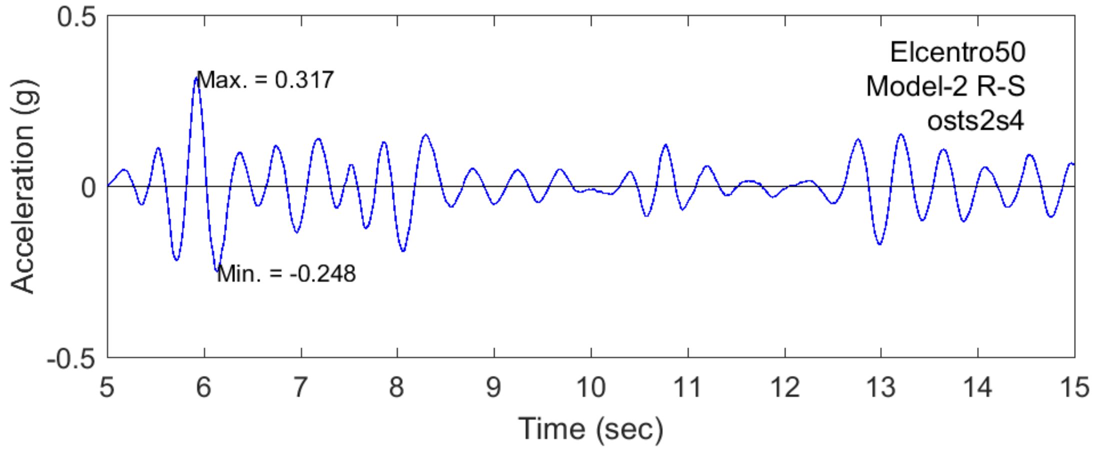

0.5
0
-0.5
Acceleration (g)
Max. = 0.317
Min. = -0.248
Elcentro50
Model-2 R-S
osts2s4
5
6
7
8
9
10
11
12
13
14
15
Time (sec)

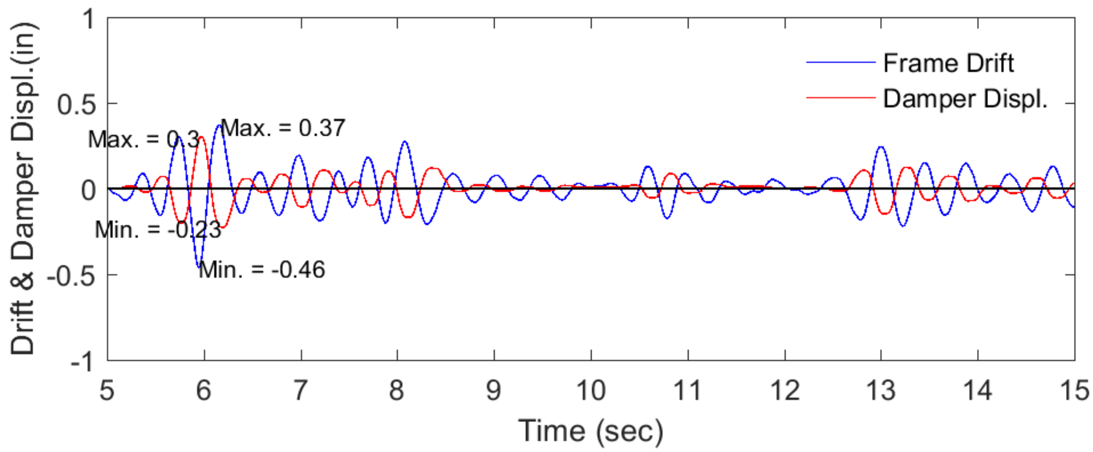

1
0.5
0
-0.5
-1
Drift & Damper Displ.(in)
Frame Drift
Damper Displ.
Max. = 0.3
Max. = 0.37
Min. = -0.23
Min. = -0.46
5
6
7
8
9
10
11
12
13
14
15
Time (sec)

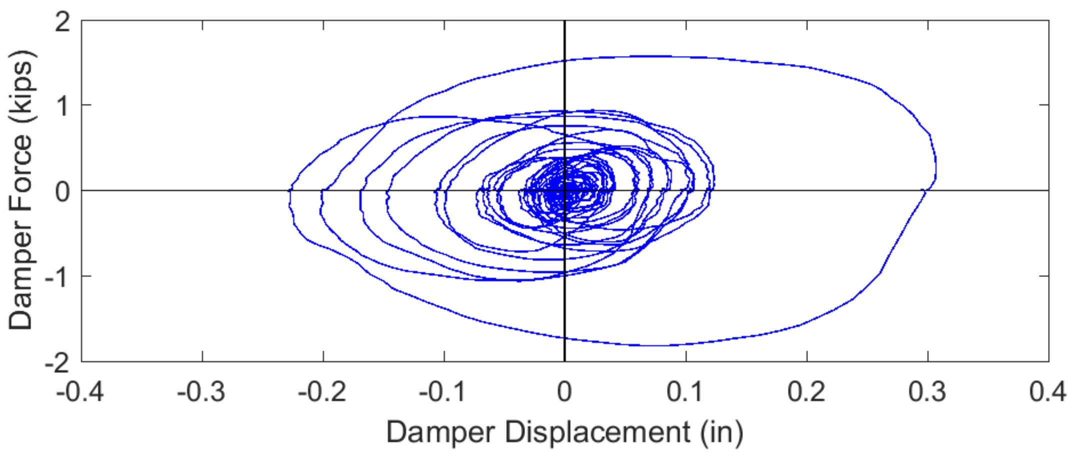

2
1
0
-1
-2
Damper Force (kips)
-0.4
-0.3
-0.2
-0.1
0
0.1
0.2
0.3
0.4
Damper Displacement (in)

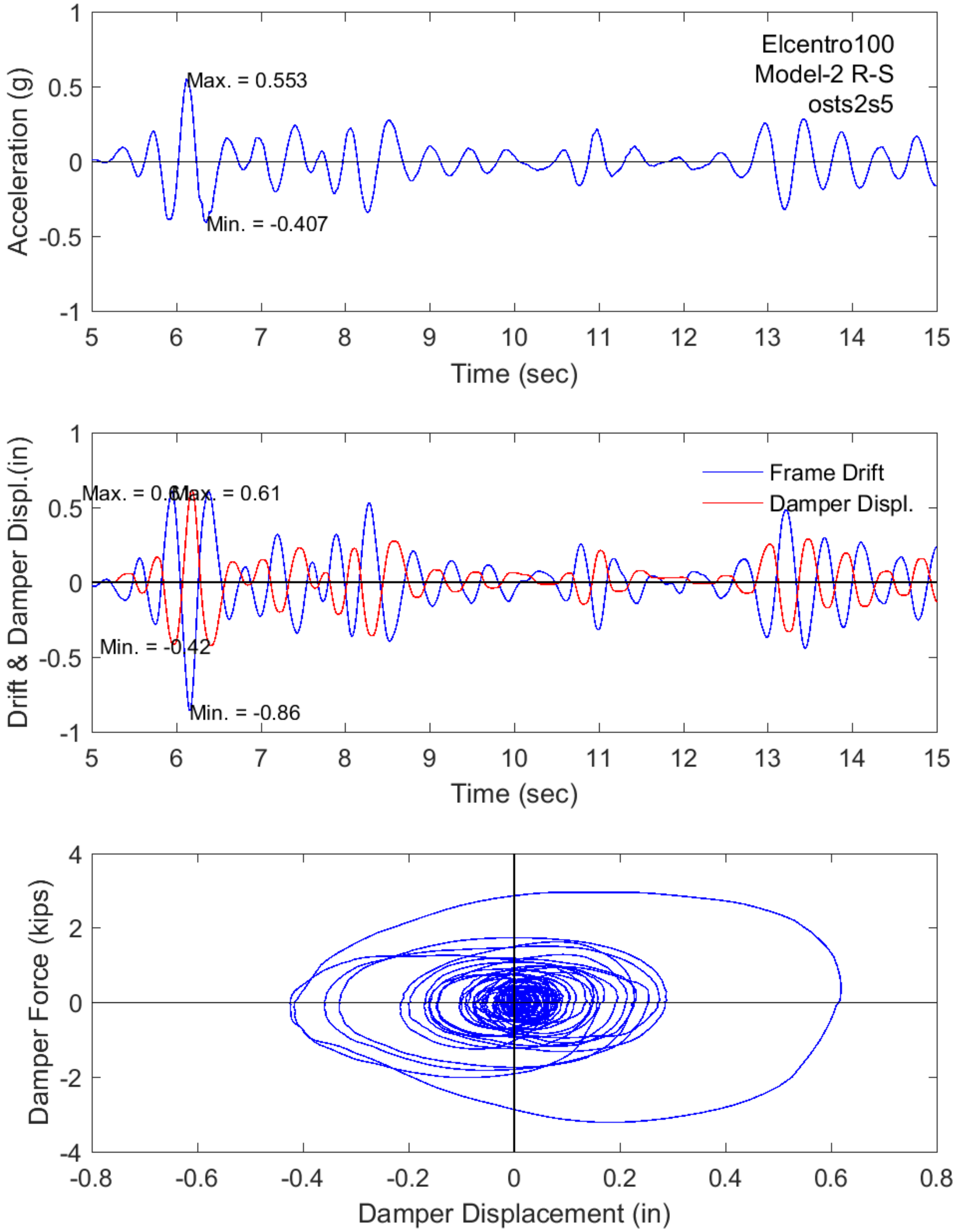
Elcentro100
Model-2 R-S
osts2s5
Max. = 0.553
Min. = -0.407
Acceleration (g)
Time (sec)
Frame Drift
Damper Displ.
Max. = 0.61
Min. = -0.42
Min. = -0.86
Drift & Damper Displ.(in)
Time (sec)
Damper Force (kips)
Damper Displacement (in)

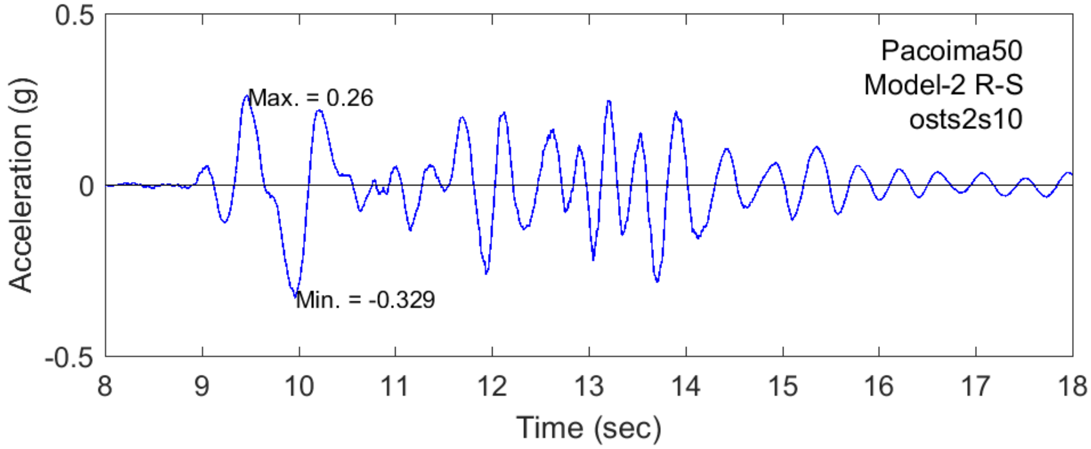
Pacoima50
Model-2 R-S
osts2s10
Max. = 0.26
Min. = -0.329
Acceleration (g)
0.5
0
-0.5
8
9
10
11
12
13
14
15
16
17
18
Time (sec)

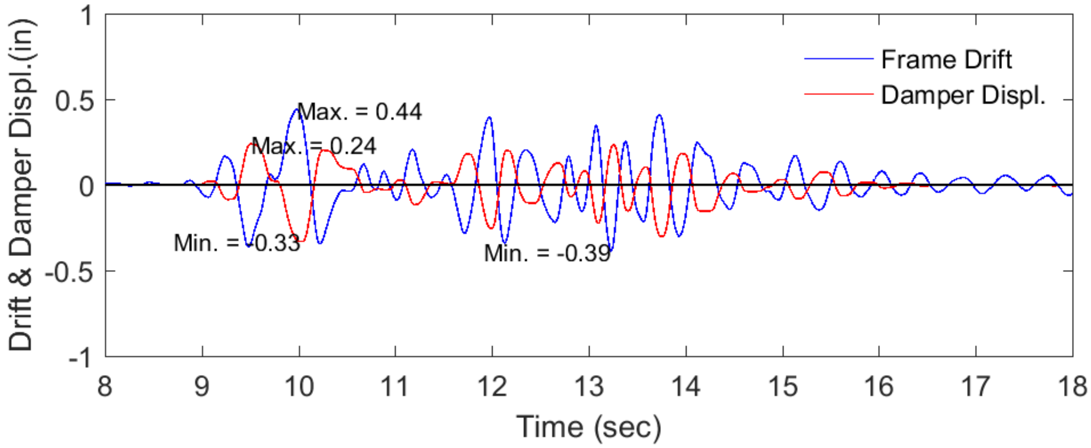
Frame Drift
Damper Displ.
Max. = 0.44
Max. = 0.24
Min. = -0.33
Min. = -0.39
Drift & Damper Displ.(in)
1
0.5
0
-0.5
-1
8
9
10
11
12
13
14
15
16
17
18
Time (sec)

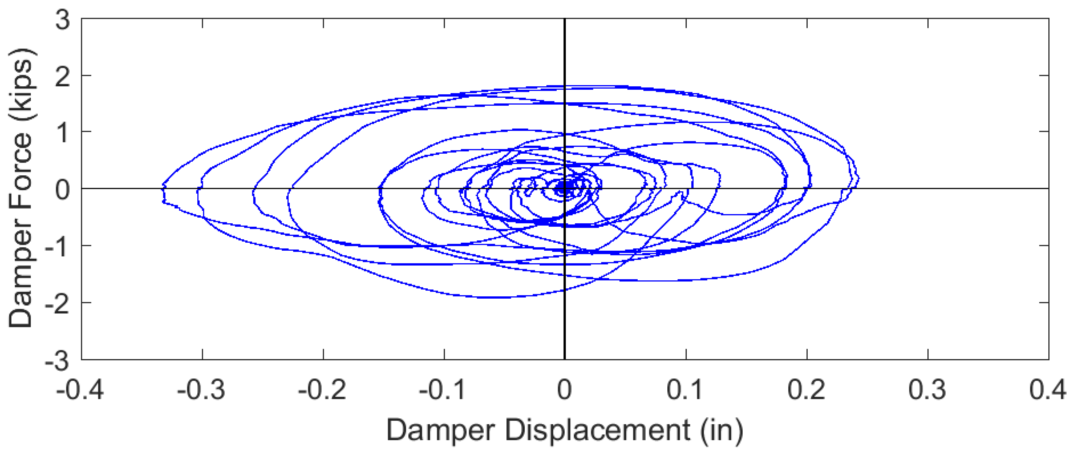
Damper Force (kips)
3
2
1
0
-1
-2
-3
-0.4
-0.3
-0.2
-0.1
0
0.1
0.2
0.3
0.4
Damper Displacement (in)

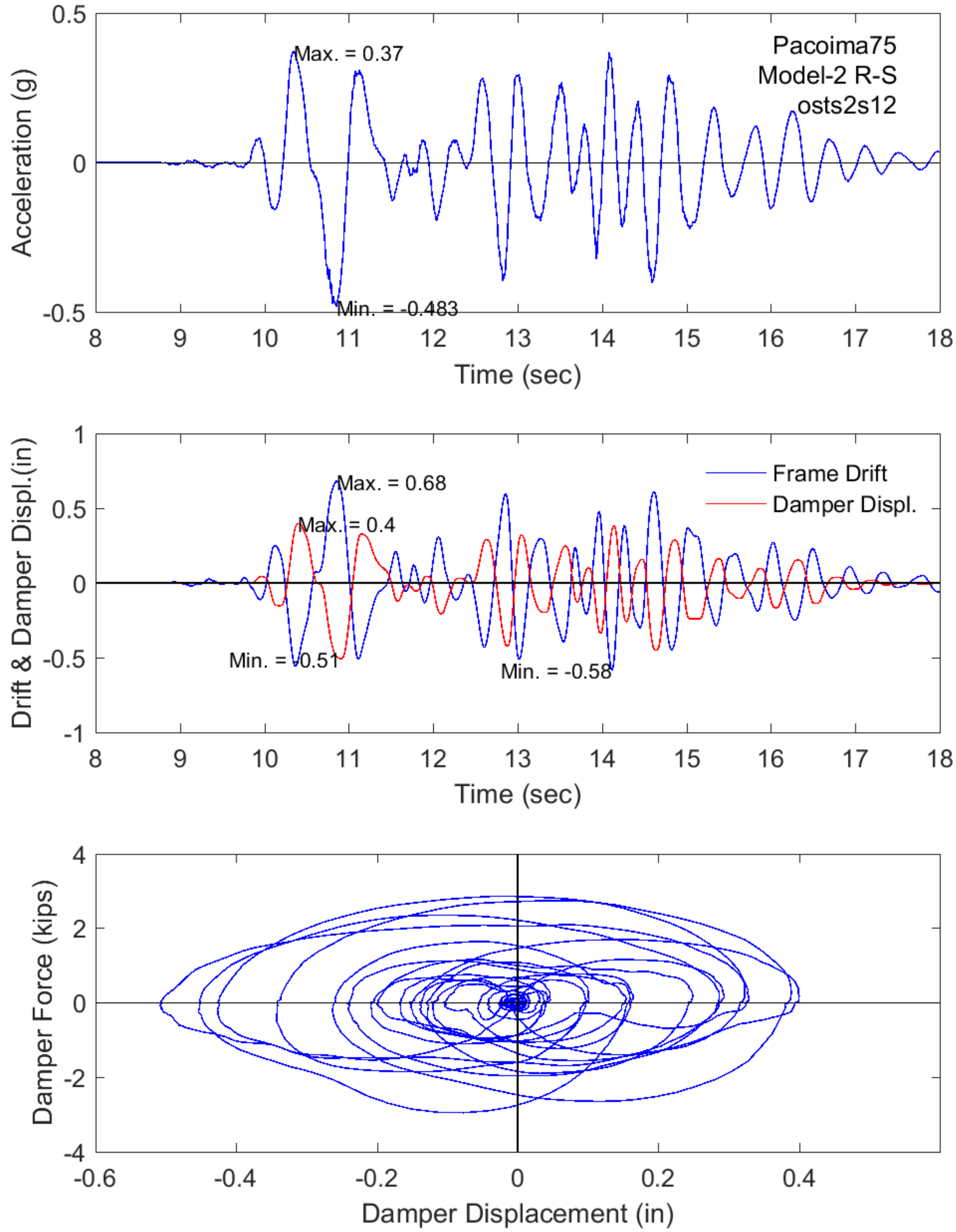

Pacoima75
Model-2 R-S
osts2s12
Max. = 0.37
Min. = -0.483
Acceleration (g)
Time (sec)
Frame Drift
Damper Displ.
Max. = 0.68
Max. = 0.4
Min. = -0.51
Min. = -0.58
Drift & Damper Displ.(in)
Time (sec)
Damper Force (kips)
Damper Displacement (in)

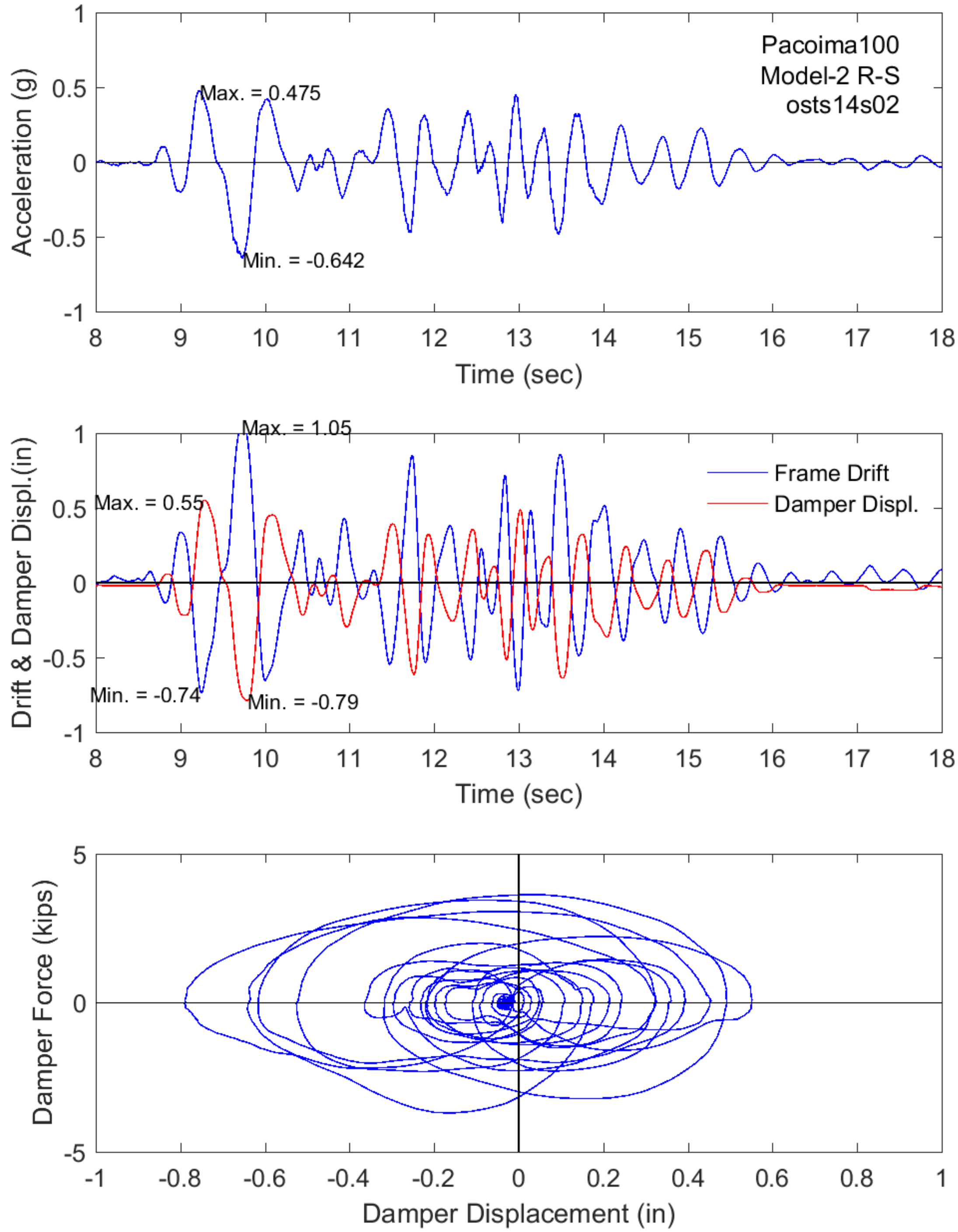

Pacoima100
Model-2 R-S
osts14s02
Max. = 0.475
Min. = -0.642
Acceleration (g)
Time (sec)
Max. = 1.05
Max. = 0.55
Min. = -0.74
Min. = -0.79
Frame Drift
Damper Displ.
Drift & Damper Displ.(in)
Time (sec)
Damper Force (kips)
Damper Displacement (in)

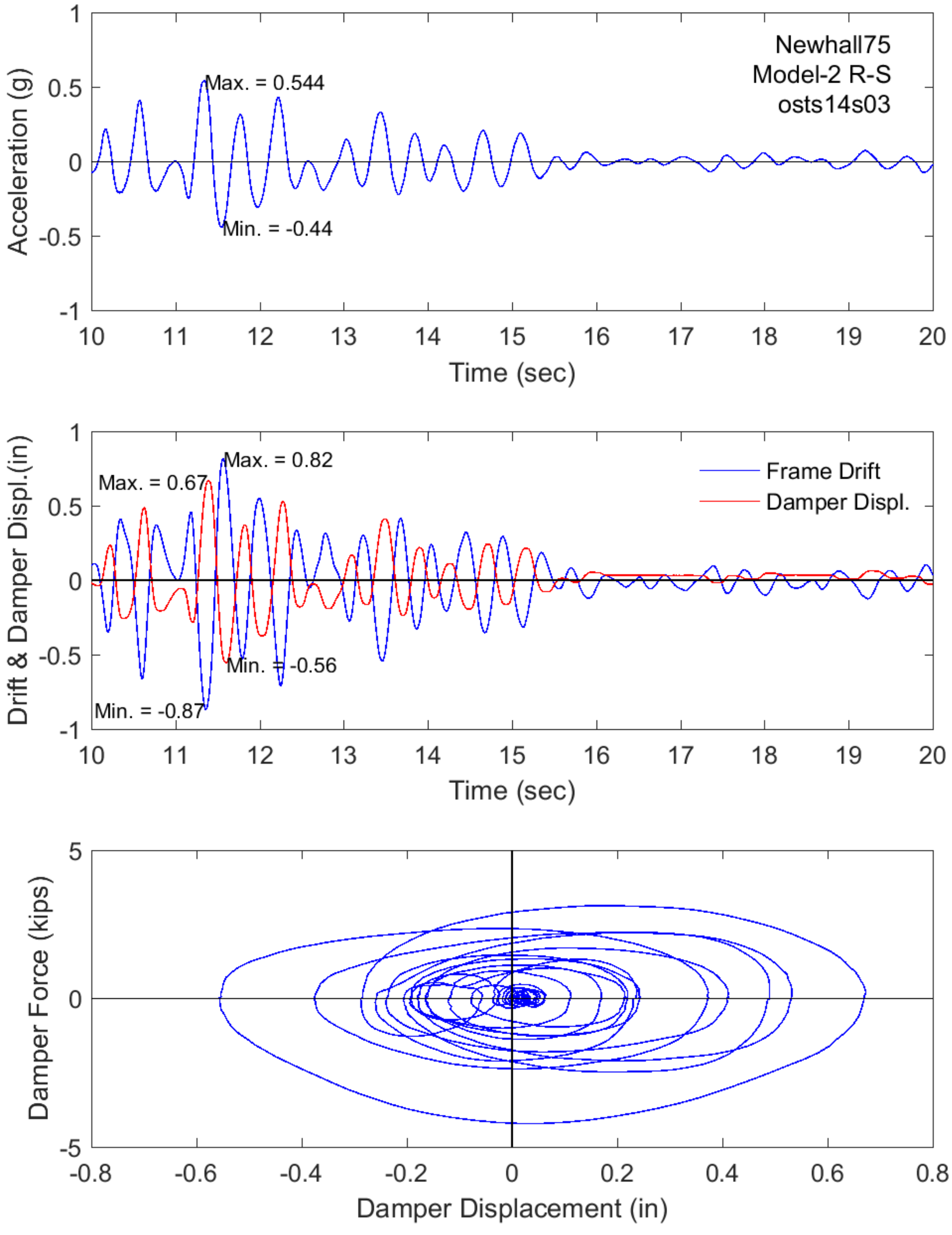

Newhall75
Model-2 R-S
osts14s03
Max. = 0.544
Min. = -0.44
Acceleration (g)
Time (sec)
Frame Drift
Damper Displ.
Max. = 0.67
Max. = 0.82
Min. = -0.56
Min. = -0.87
Drift & Damper Displ.(in)
Time (sec)
Damper Force (kips)
Damper Displacement (in)

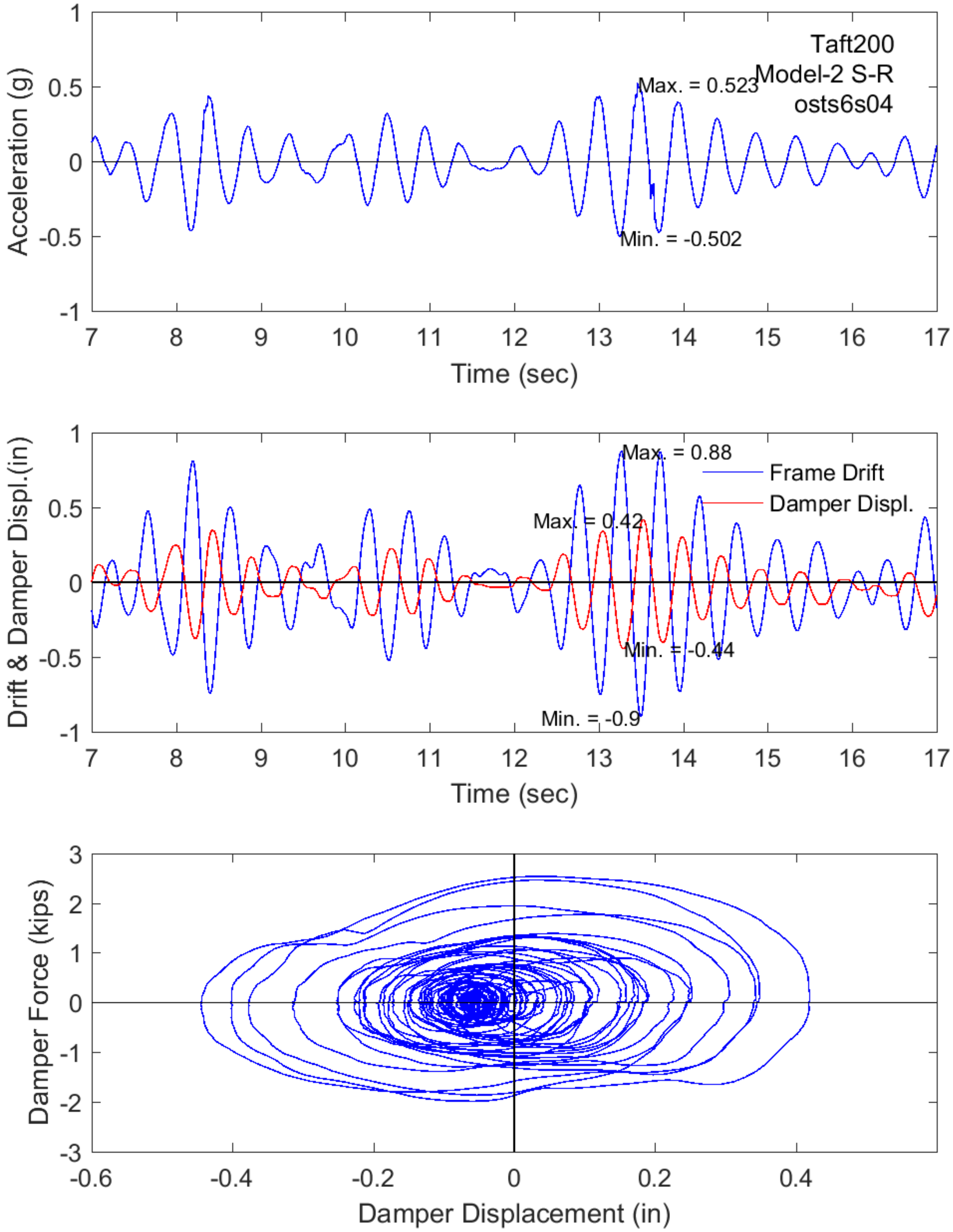
Taft200
Model-2 S-R
osts6s04
Max. = 0.523
Min. = -0.502
Acceleration (g)
Time (sec)
Max. = 0.88
Max. = 0.42
Min. = -0.44
Min. = -0.9
Frame Drift
Damper Displ.
Drift & Damper Displ.(in)
Time (sec)
Damper Force (kips)
Damper Displacement (in)

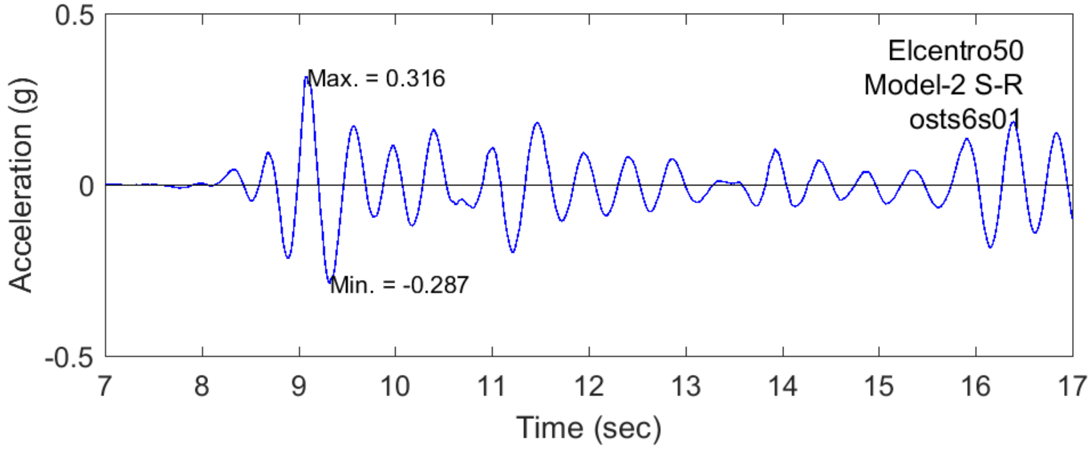

Elcentro50
Model-2 S-R
osts6s01
Max. = 0.316
Min. = -0.287
Acceleration (g)
Time (sec)

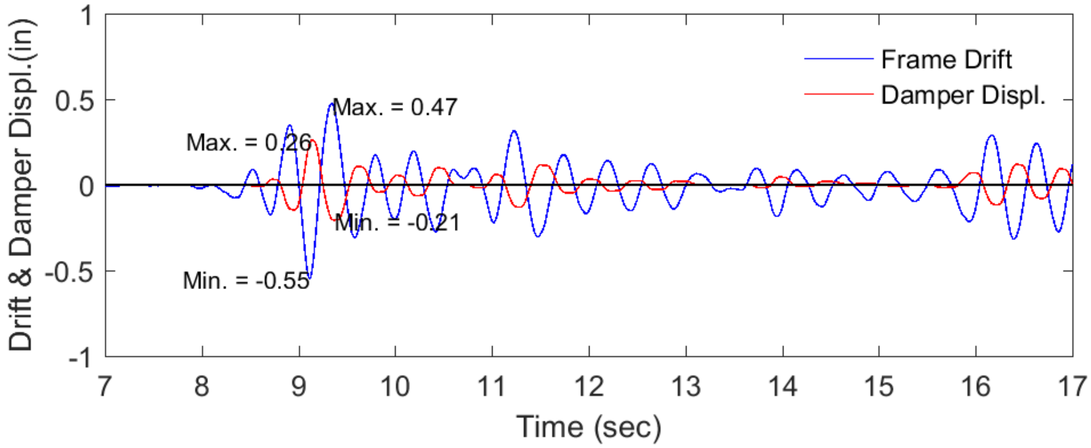

Frame Drift
Damper Displ.
Max. = 0.47
Max. = 0.26
Min. = -0.21
Min. = -0.55
Drift & Damper Displ.(in)
Time (sec)

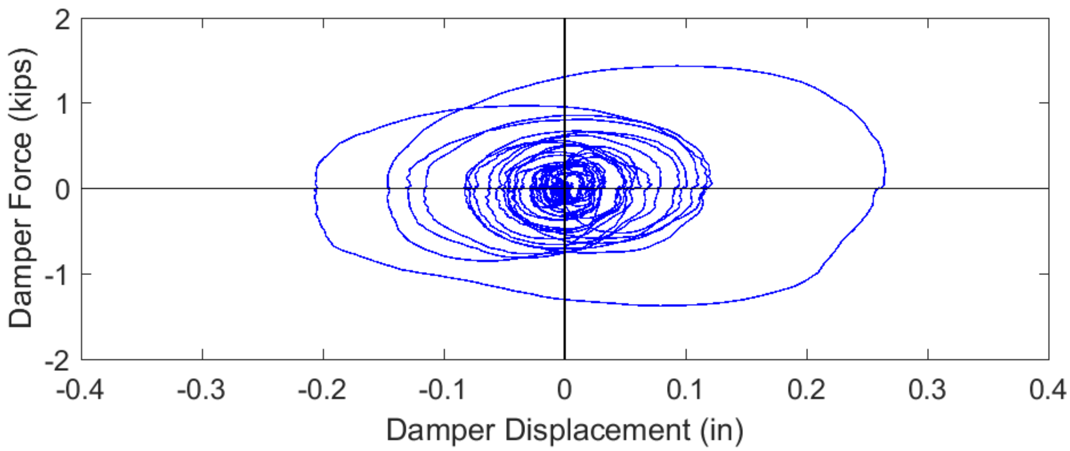

Damper Force (kips)
Damper Displacement (in)

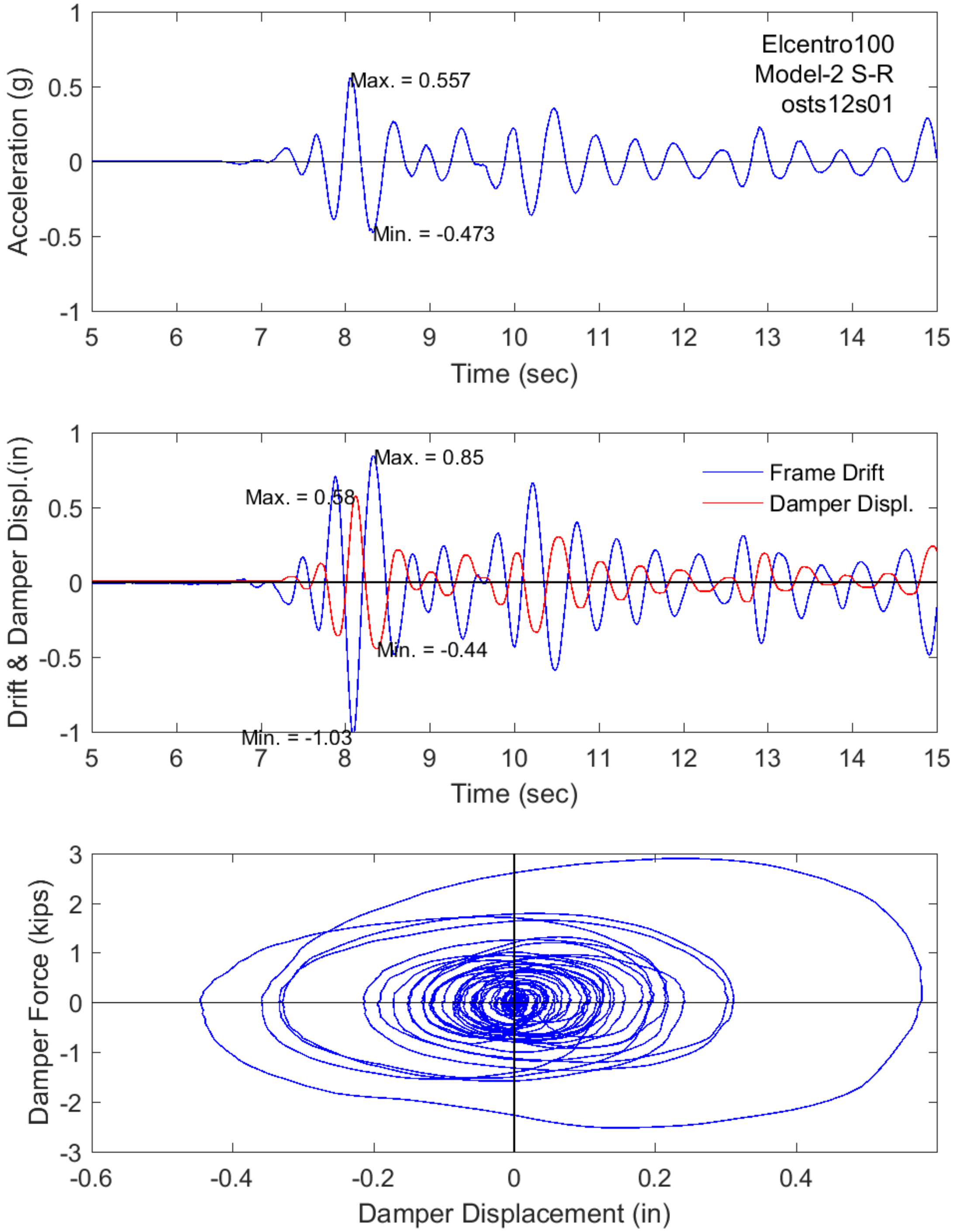
Elcentro100
Model-2 S-R
osts12s01
Max. = 0.557
Min. = -0.473
Acceleration (g)
Time (sec)
Max. = 0.85
Max. = 0.58
Min. = -0.44
Min. = -1.03
Frame Drift
Damper Displ.
Drift & Damper Displ.(in)
Time (sec)
Damper Force (kips)
Damper Displacement (in)

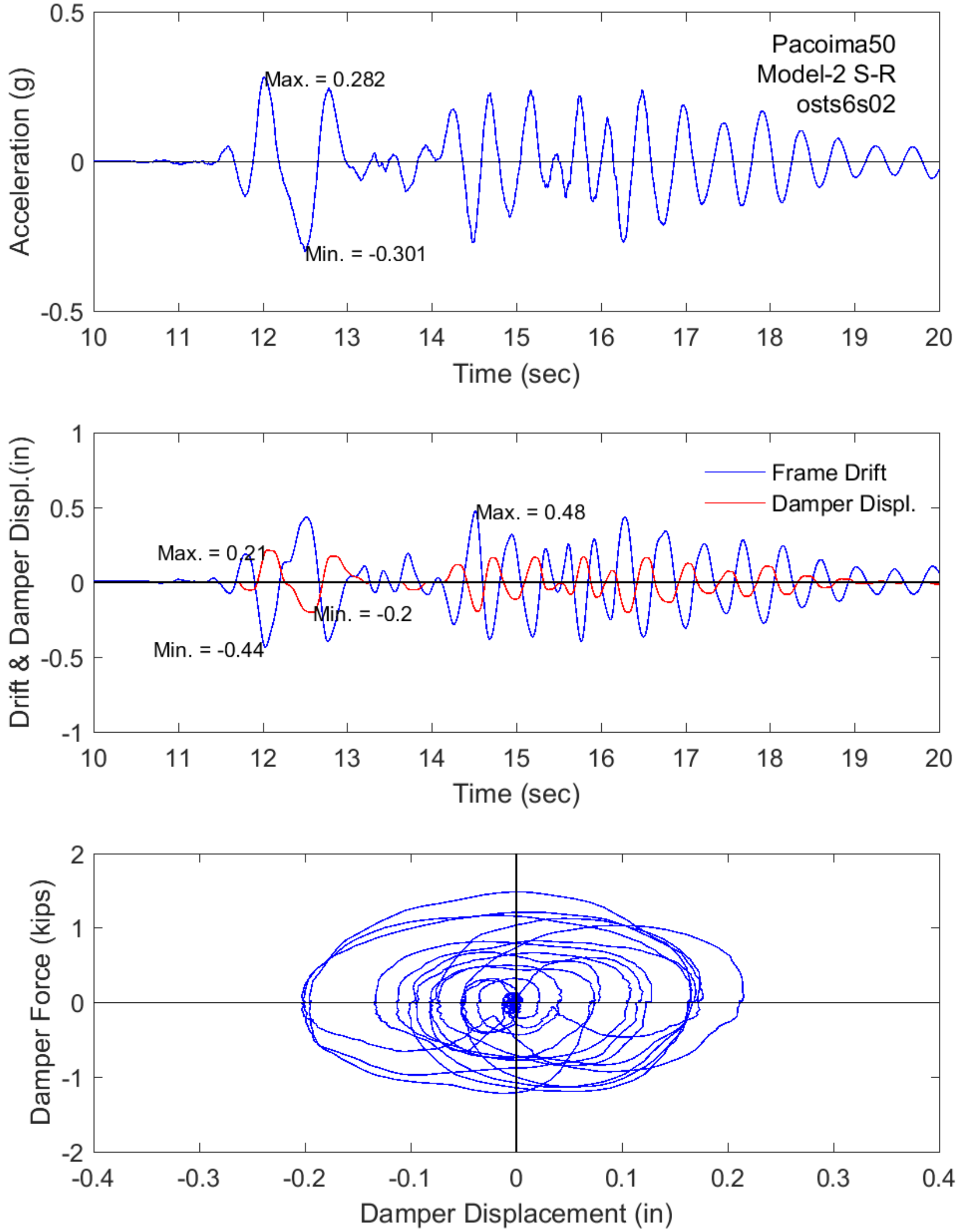

Pacoima50
Model-2 S-R
osts6s02
Max. = 0.282
Min. = -0.301
Acceleration (g)
Time (sec)
Frame Drift
Damper Displ.
Max. = 0.48
Max. = 0.21
Min. = -0.2
Min. = -0.44
Drift & Damper Displ.(in)
Time (sec)
Damper Force (kips)
Damper Displacement (in)

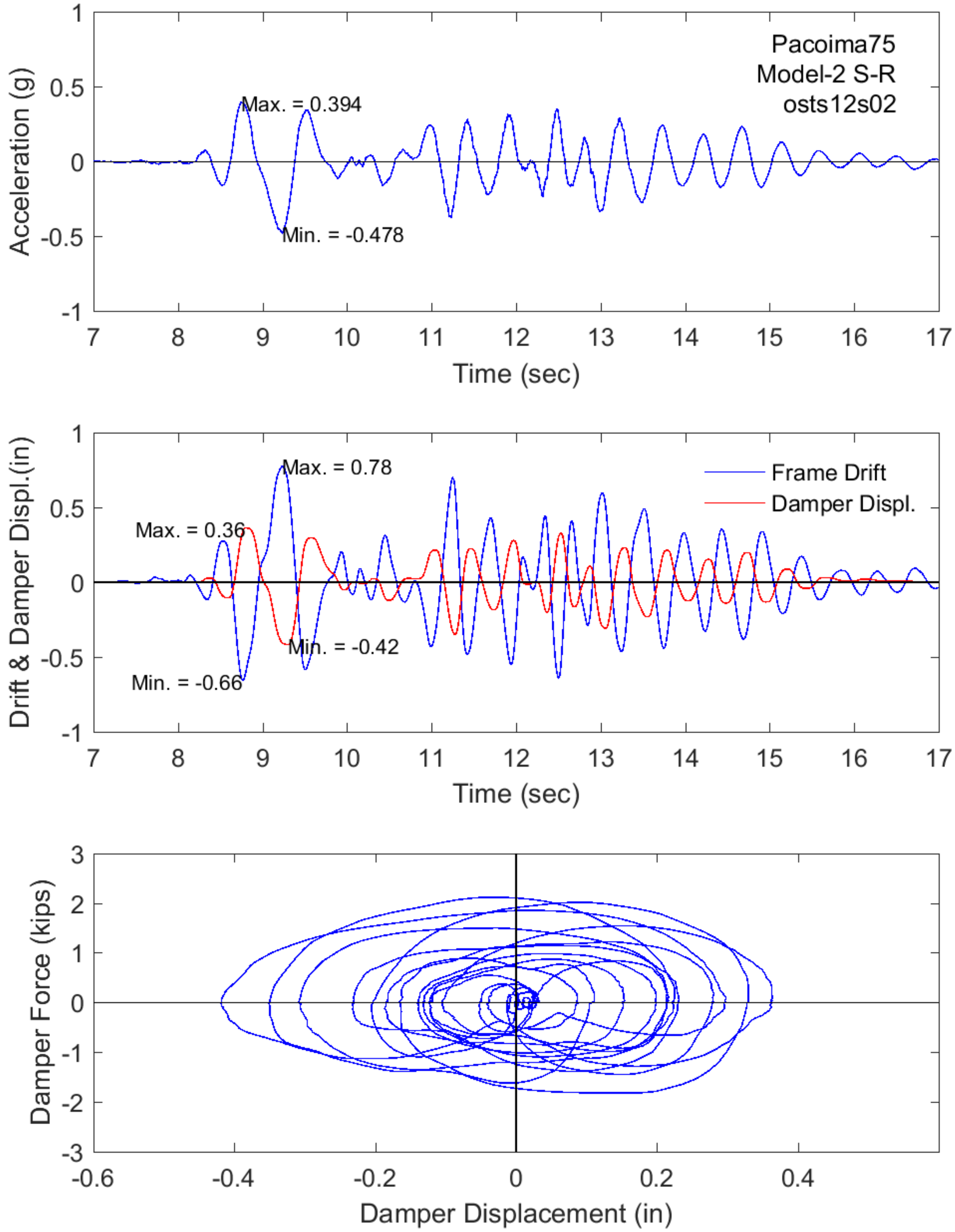
Pacoima75
Model-2 S-R
osts12s02
Max. = 0.394
Min. = -0.478
Acceleration (g)
Time (sec)
Max. = 0.78
Max. = 0.36
Min. = -0.42
Min. = -0.66
Frame Drift
Damper Displ.
Drift & Damper Displ.(in)
Time (sec)
Damper Force (kips)
Damper Displacement (in)

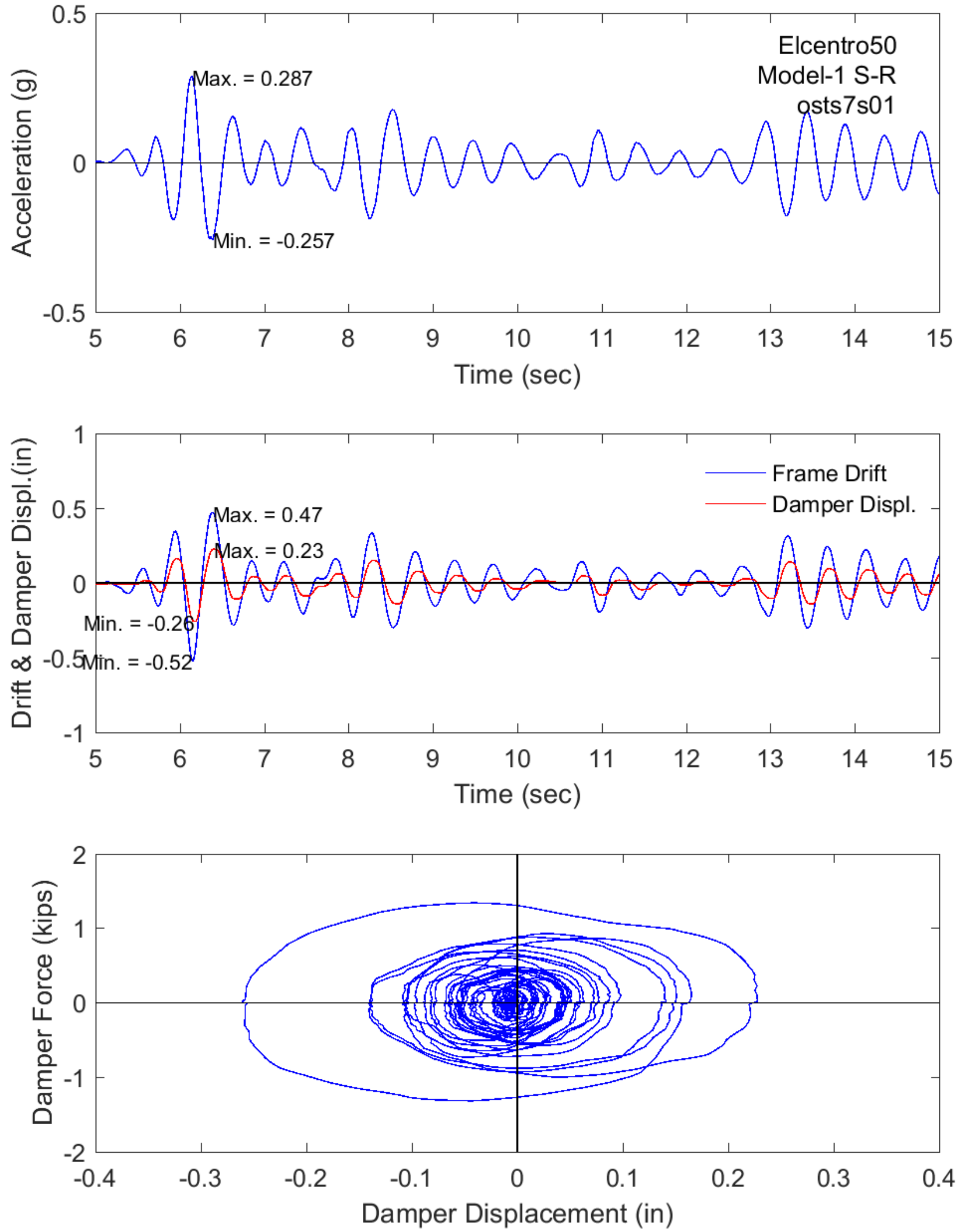
Elcentro50
Model-1 S-R
osts7s01
Max. = 0.287
Min. = -0.257
Acceleration (g)
Time (sec)
Frame Drift
Damper Displ.
Max. = 0.47
Max. = 0.23
Min. = -0.26
Min. = -0.52
Drift & Damper Displ.(in)
Time (sec)
Damper Force (kips)
Damper Displacement (in)

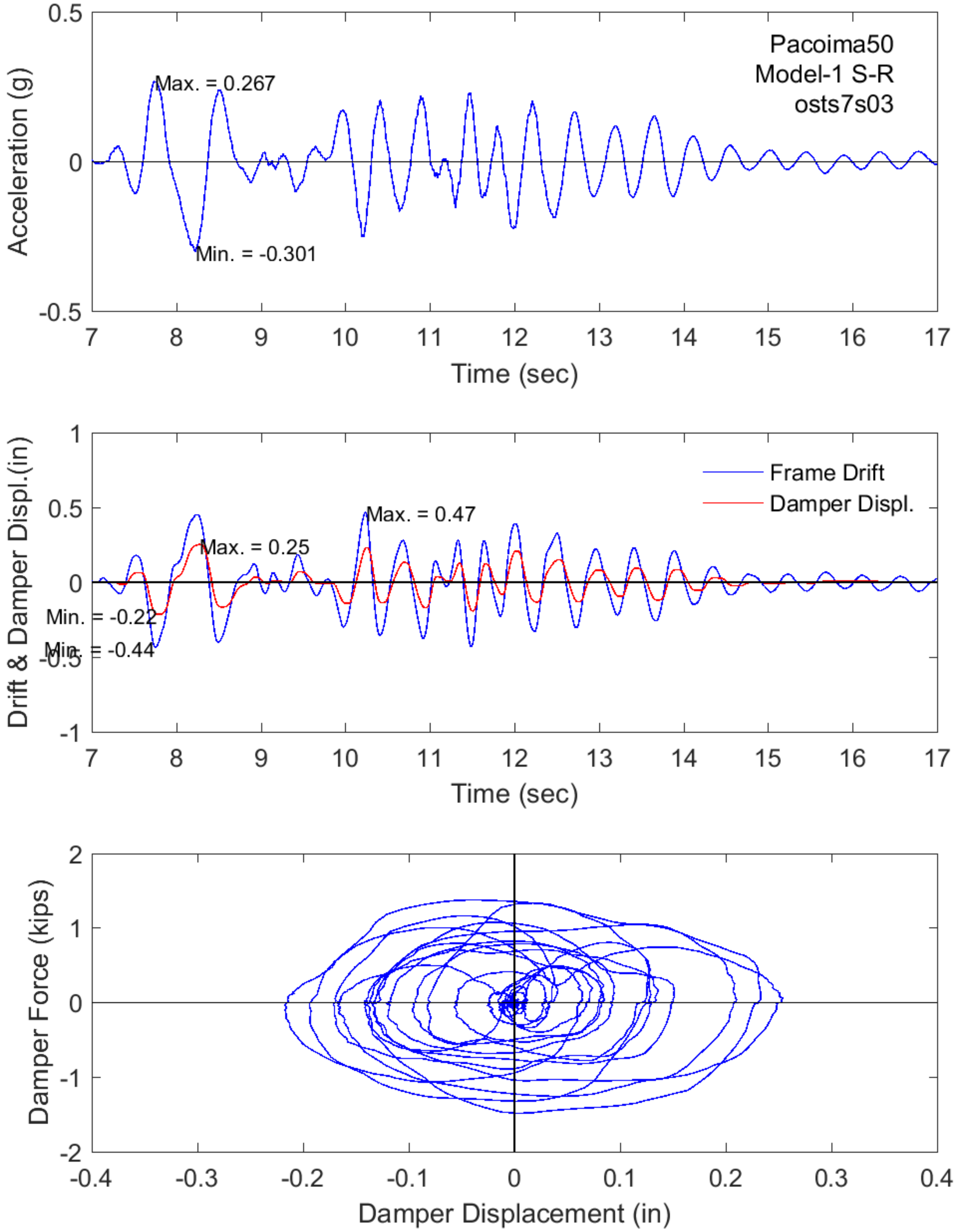
Pacoima50
Model-1 S-R
osts7s03
Max. = 0.267
Min. = -0.301
Acceleration (g)
Time (sec)
Frame Drift
Damper Displ.
Max. = 0.47
Max. = 0.25
Min. = -0.22
Min. = -0.44
Drift & Damper Displ.(in)
Time (sec)
Damper Force (kips)
Damper Displacement (in)

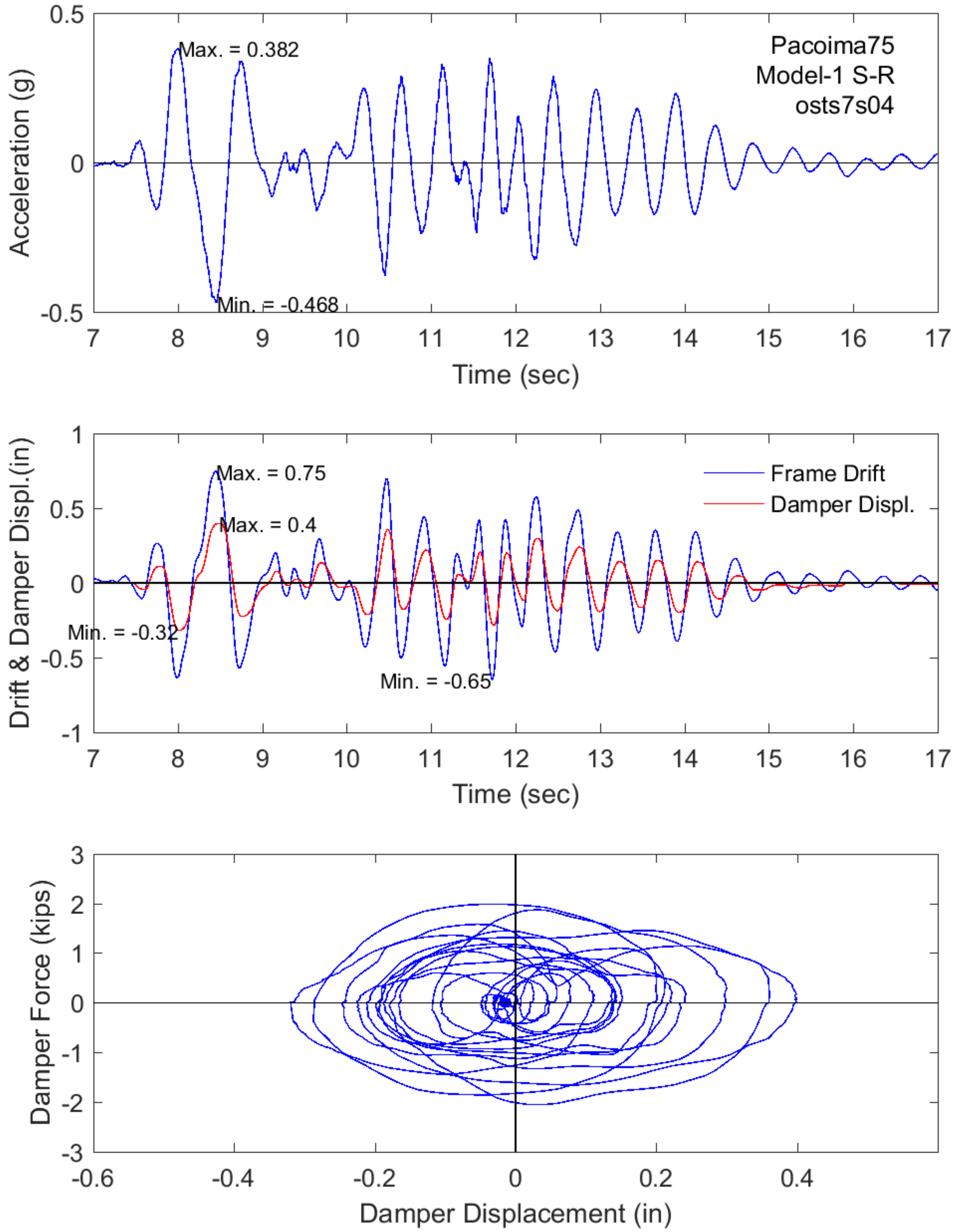
Pacoima75
Model-1 S-R
osts7s04
Max. = 0.382
Min. = -0.468
Acceleration (g)
Time (sec)
Frame Drift
Damper Displ.
Max. = 0.75
Max. = 0.4
Min. = -0.32
Min. = -0.65
Drift & Damper Displ.(in)
Time (sec)
Damper Force (kips)
Damper Displacement (in)

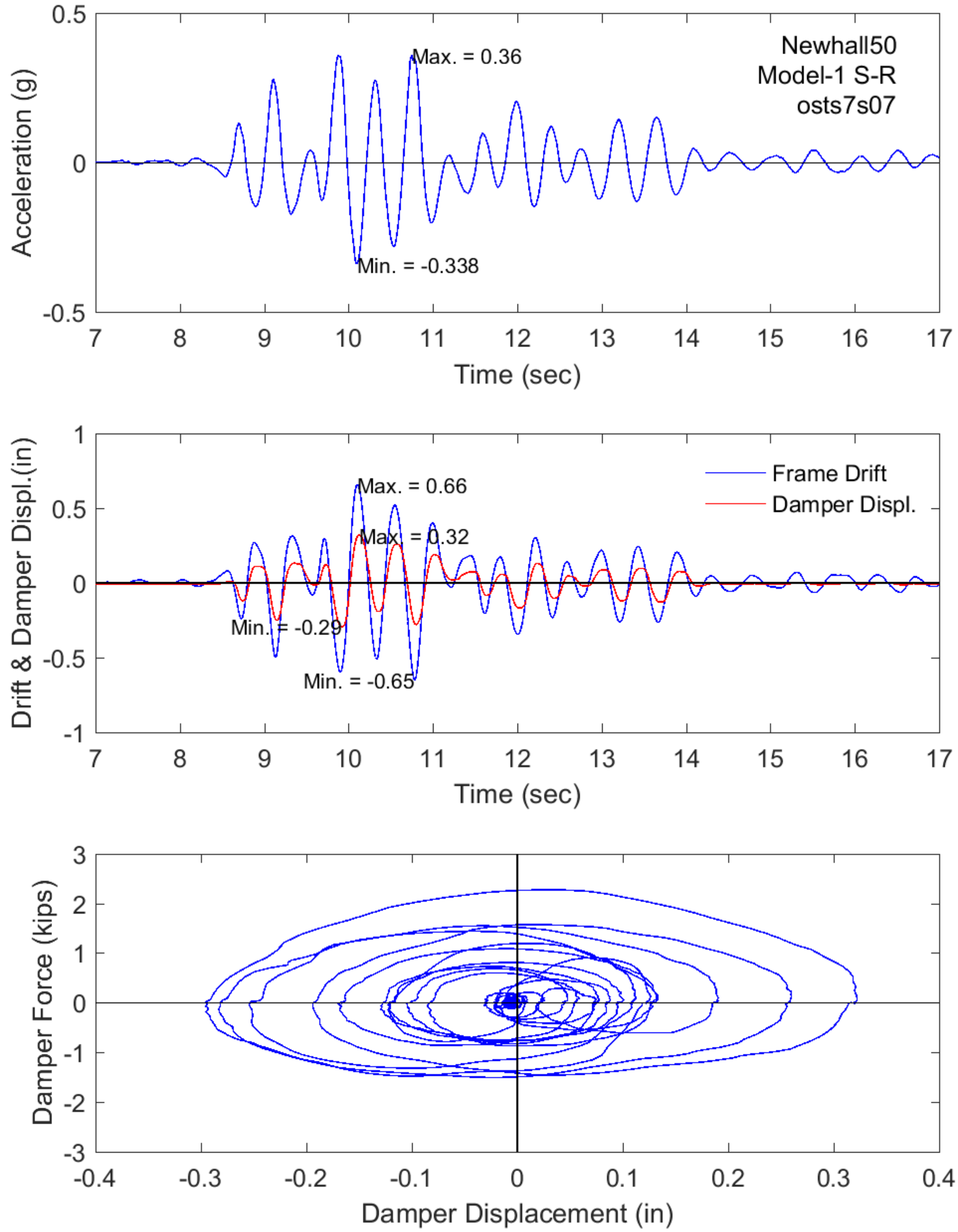

Newhall50
Model-1 S-R
osts7s07
Max. = 0.36
Min. = -0.338
Acceleration (g)
Time (sec)
Frame Drift
Damper Displ.
Max. = 0.66
Max. = 0.32
Min. = -0.29
Min. = -0.65
Drift & Damper Displ.(in)
Time (sec)
Damper Force (kips)
Damper Displacement (in)

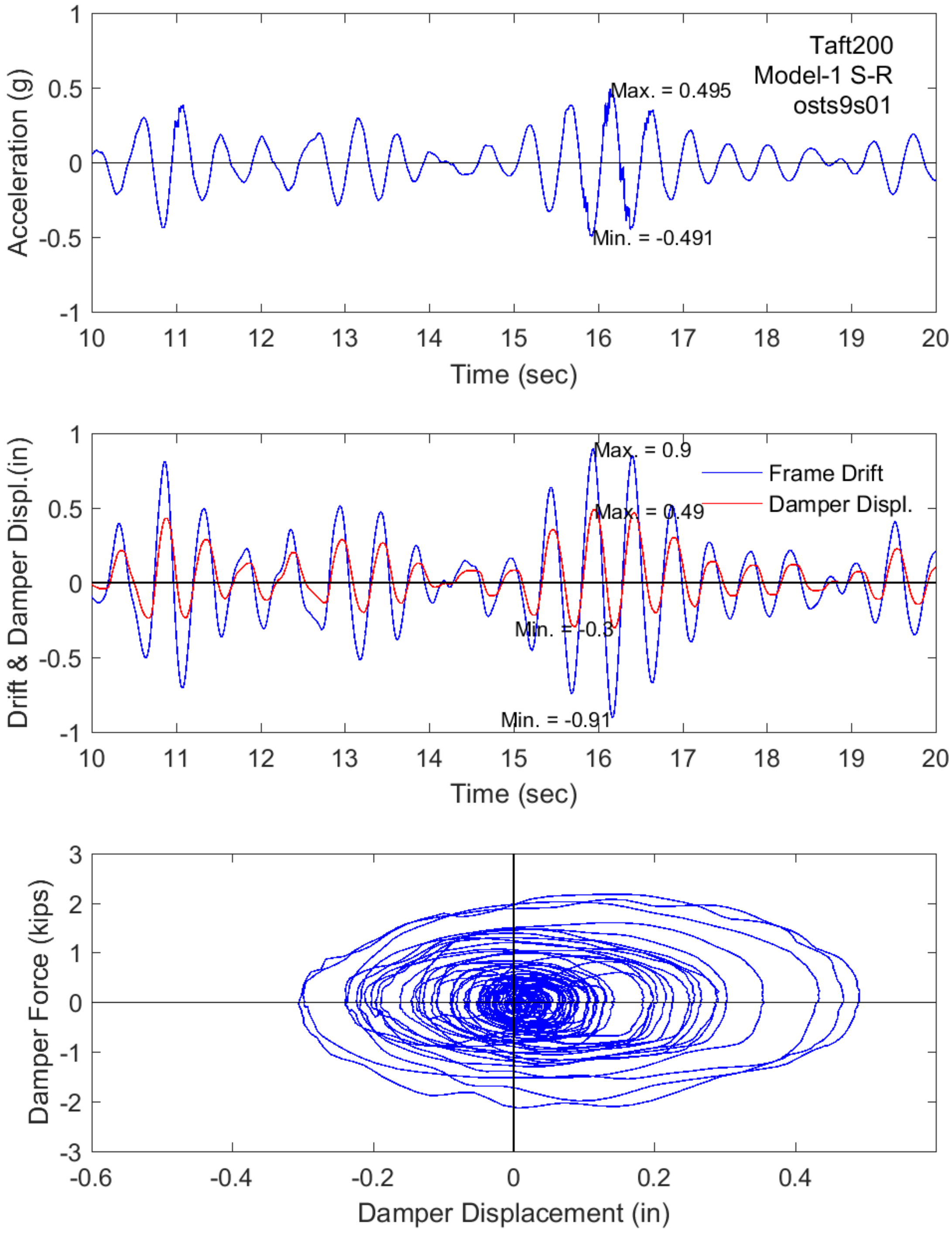
Taft200
Model-1 S-R
osts9s01
Max. = 0.495
Min. = -0.491
Acceleration (g)
Time (sec)
Max. = 0.9
Max. = 0.49
Frame Drift
Damper Displ.
Min. = -0.3
Min. = -0.91
Drift & Damper Displ.(in)
Time (sec)
Damper Force (kips)
Damper Displacement (in)

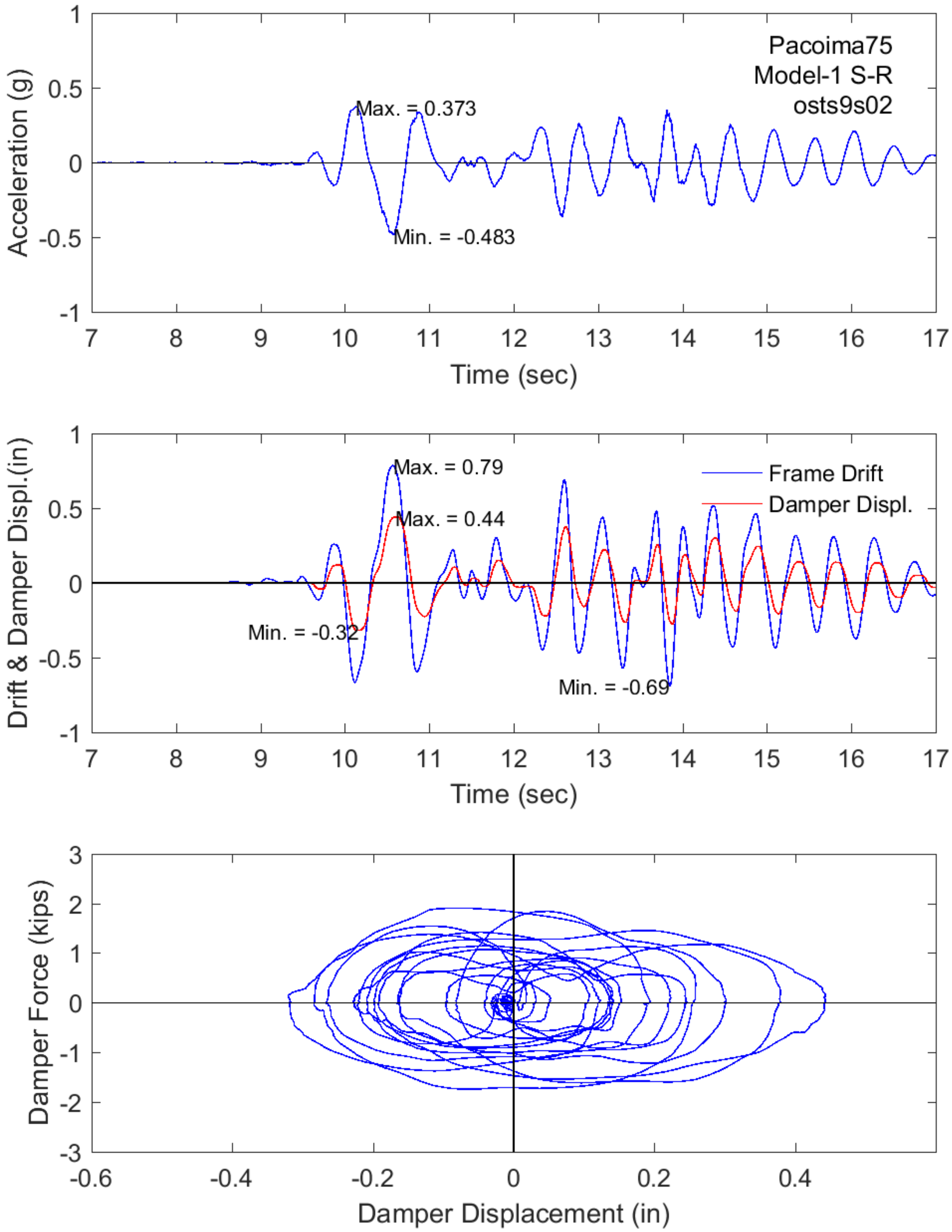
Pacoima75
Model-1 S-R
osts9s02
Max. = 0.373
Min. = -0.483
Acceleration (g)
Time (sec)
Max. = 0.79
Max. = 0.44
Min. = -0.32
Min. = -0.69
Frame Drift
Damper Displ.
Drift & Damper Displ.(in)
Time (sec)
Damper Force (kips)
Damper Displacement (in)

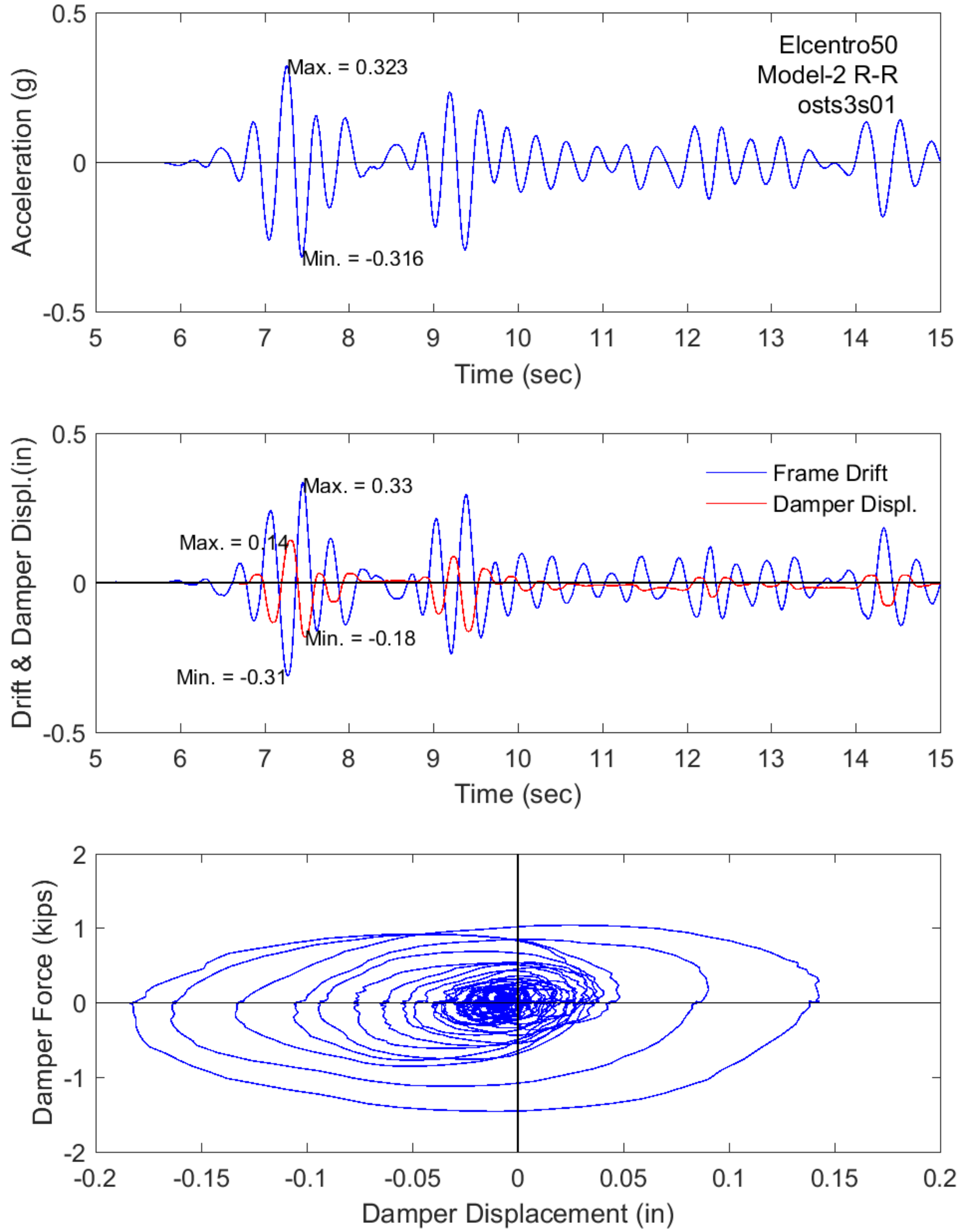
Elcentro50
Model-2 R-R
osts3s01
Max. = 0.323
Min. = -0.316
Acceleration (g)
Time (sec)
Frame Drift
Damper Displ.
Max. = 0.33
Max. = 0.14
Min. = -0.18
Min. = -0.31
Drift & Damper Displ.(in)
Time (sec)
Damper Force (kips)
Damper Displacement (in)

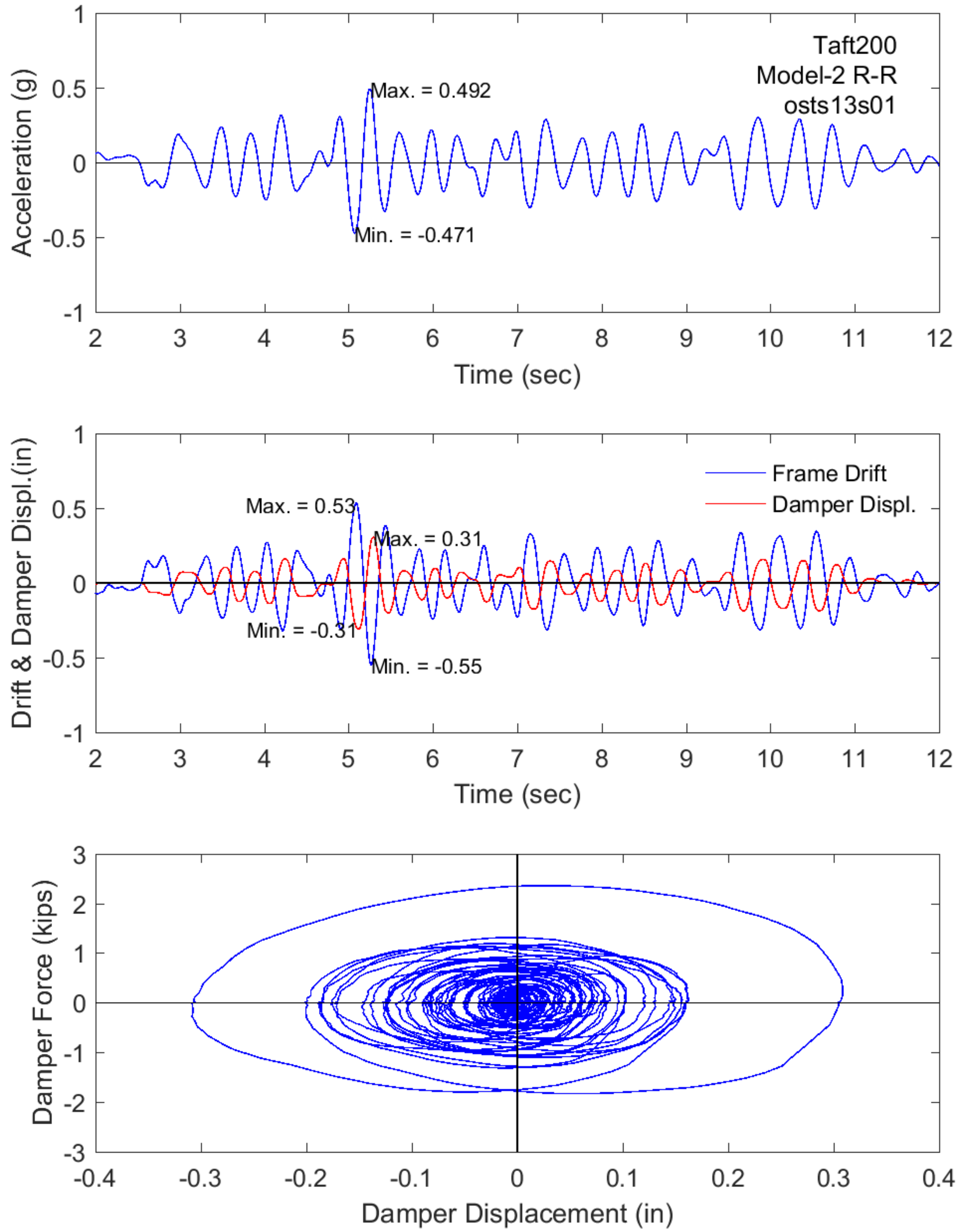
Taft200
Model-2 R-R
osts13s01
Max. = 0.492
Min. = -0.471
Acceleration (g)
Time (sec)
Frame Drift
Damper Displ.
Max. = 0.53
Max. = 0.31
Min. = -0.31
Min. = -0.55
Drift & Damper Displ.(in)
Time (sec)
Damper Force (kips)
Damper Displacement (in)

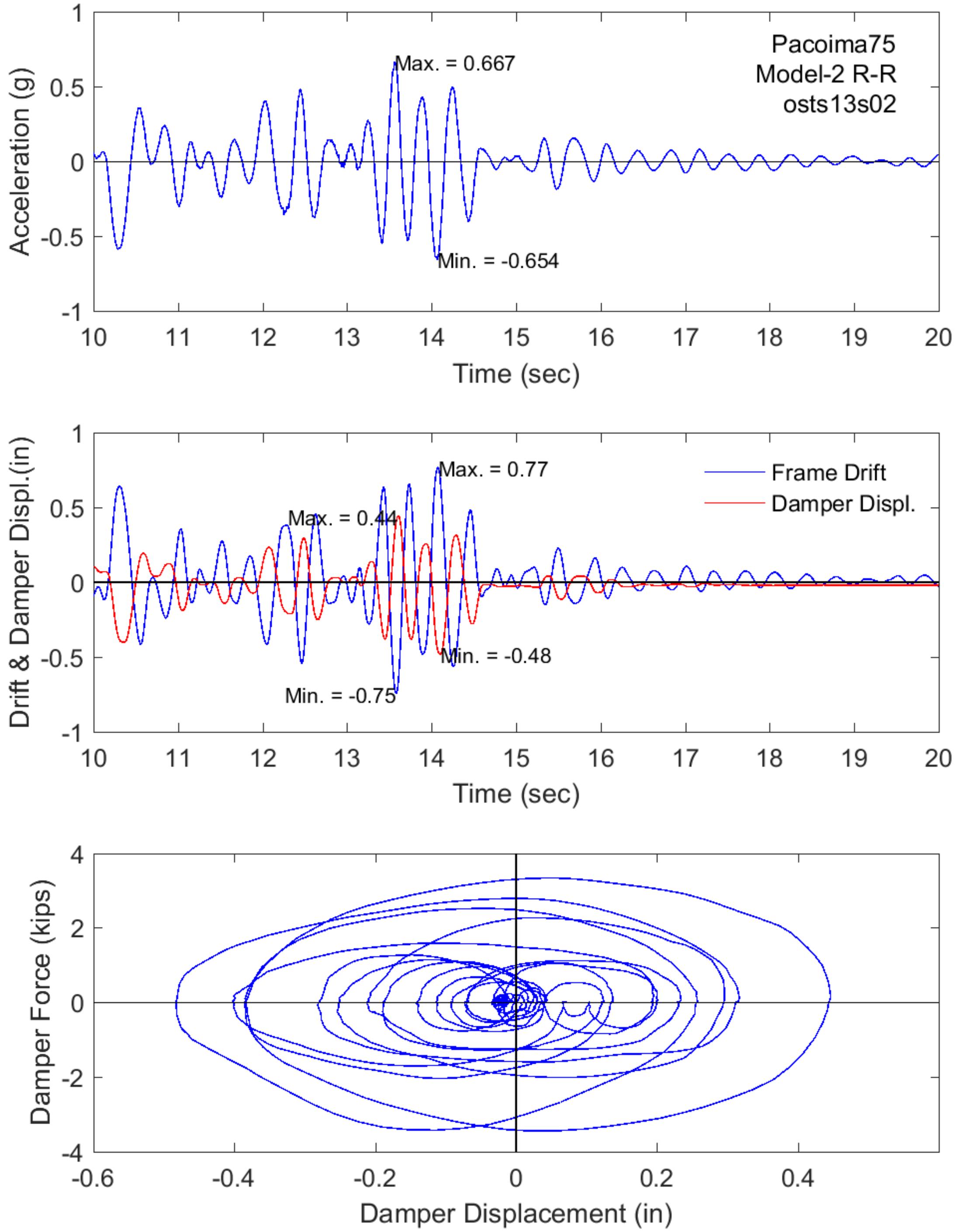

Pacoima75
Model-2 R-R
osts13s02
Max. = 0.667
Min. = -0.654
Acceleration (g)
Time (sec)
Frame Drift
Damper Displ.
Max. = 0.77
Max. = 0.44
Min. = -0.48
Min. = -0.75
Drift & Damper Displ.(in)
Time (sec)
Damper Force (kips)
Damper Displacement (in)

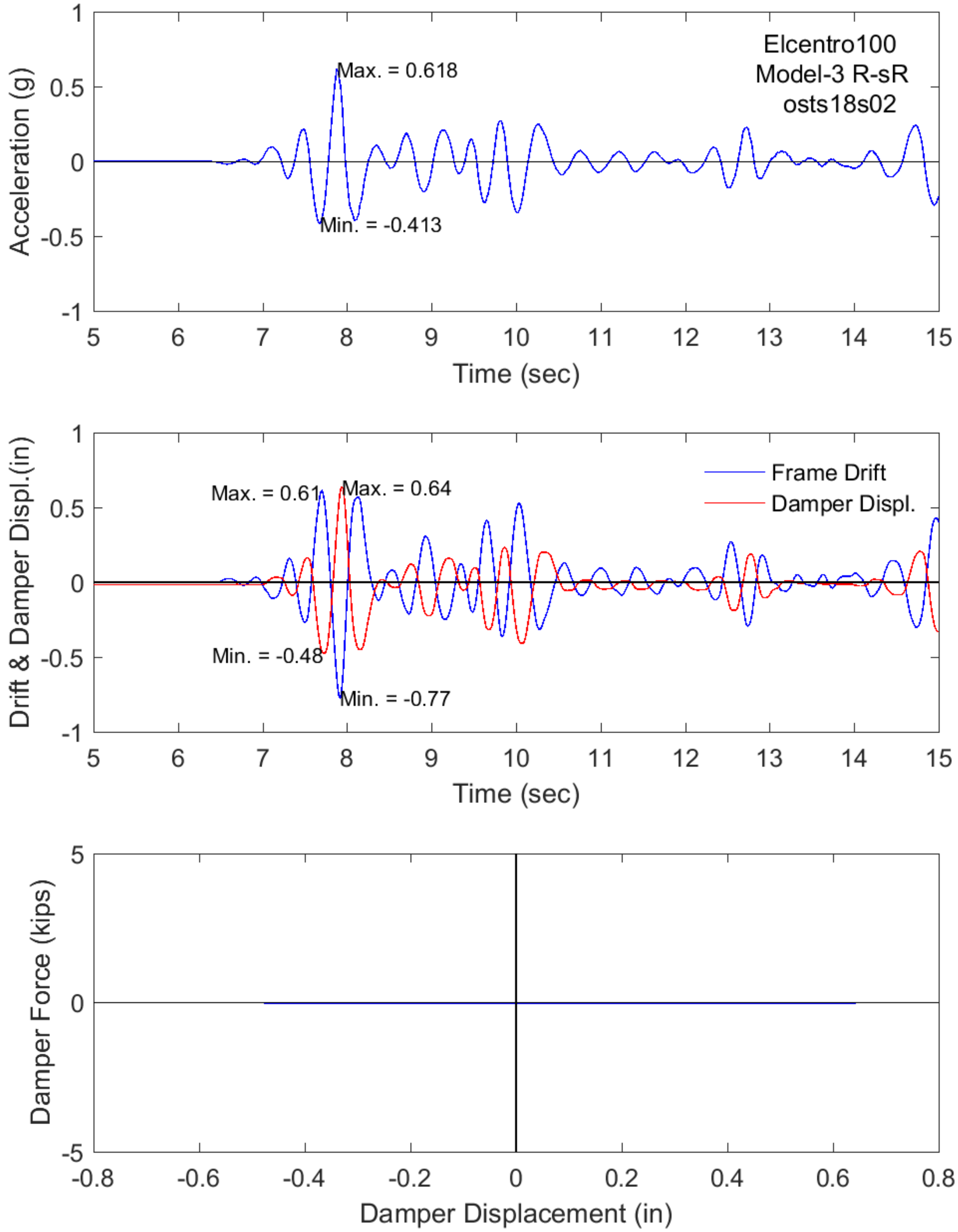
Elcentro100
Model-3 R-sR
osts18s02
Max. = 0.618
Min. = -0.413
Acceleration (g)
Time (sec)
Frame Drift
Damper Displ.
Max. = 0.61
Max. = 0.64
Min. = -0.48
Min. = -0.77
Drift & Damper Displ.(in)
Time (sec)
Damper Force (kips)
Damper Displacement (in)

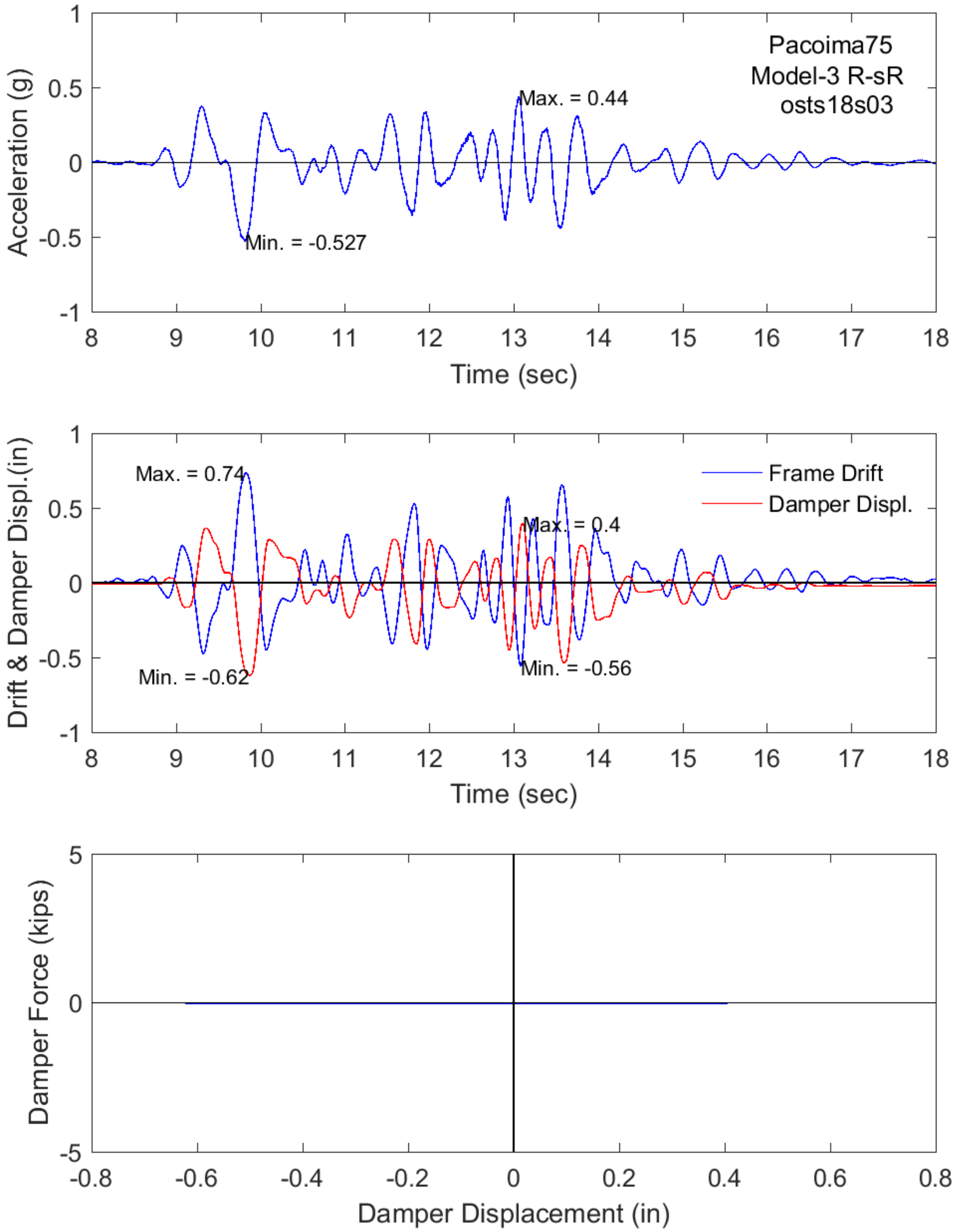

Pacoima75
Model-3 R-sR
osts18s03
Max. = 0.44
Min. = -0.527
Acceleration (g)
Time (sec)
Frame Drift
Damper Displ.
Max. = 0.74
Max. = 0.4
Min. = -0.62
Min. = -0.56
Drift & Damper Displ.(in)
Time (sec)
Damper Force (kips)
Damper Displacement (in)

This Page Intentionally Left Blank”

APPENDIX D

EARTHQUAKE SIMULATOR TEST DRAWINGS

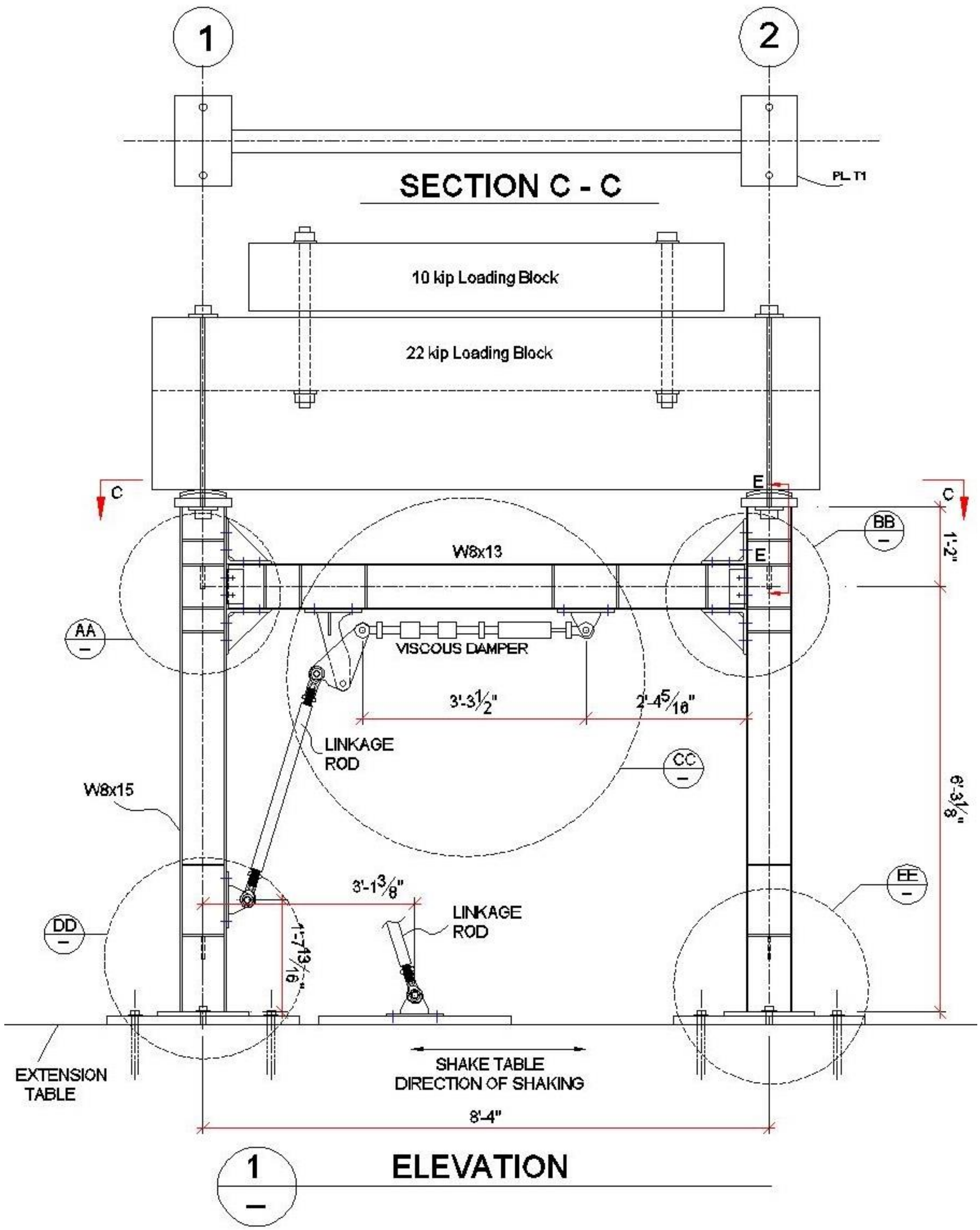
1
2
SECTION C - C
PL T1
10 kip Loading Block
22 kip Loading Block
C
C
E
E
BB
1'-2"
W8x13
AA
VISCOUS DAMPER
3'-3 1/2"
2'-4 5/16"
LINKAGE ROD
CC
W8x15
6'-3 1/8"
EE
3'-1 3/8"
LINKAGE ROD
DD
1'-7 13/16"
EXTENSION TABLE
SHAKE TABLE DIRECTION OF SHAKING
8'-4"
1
ELEVATION

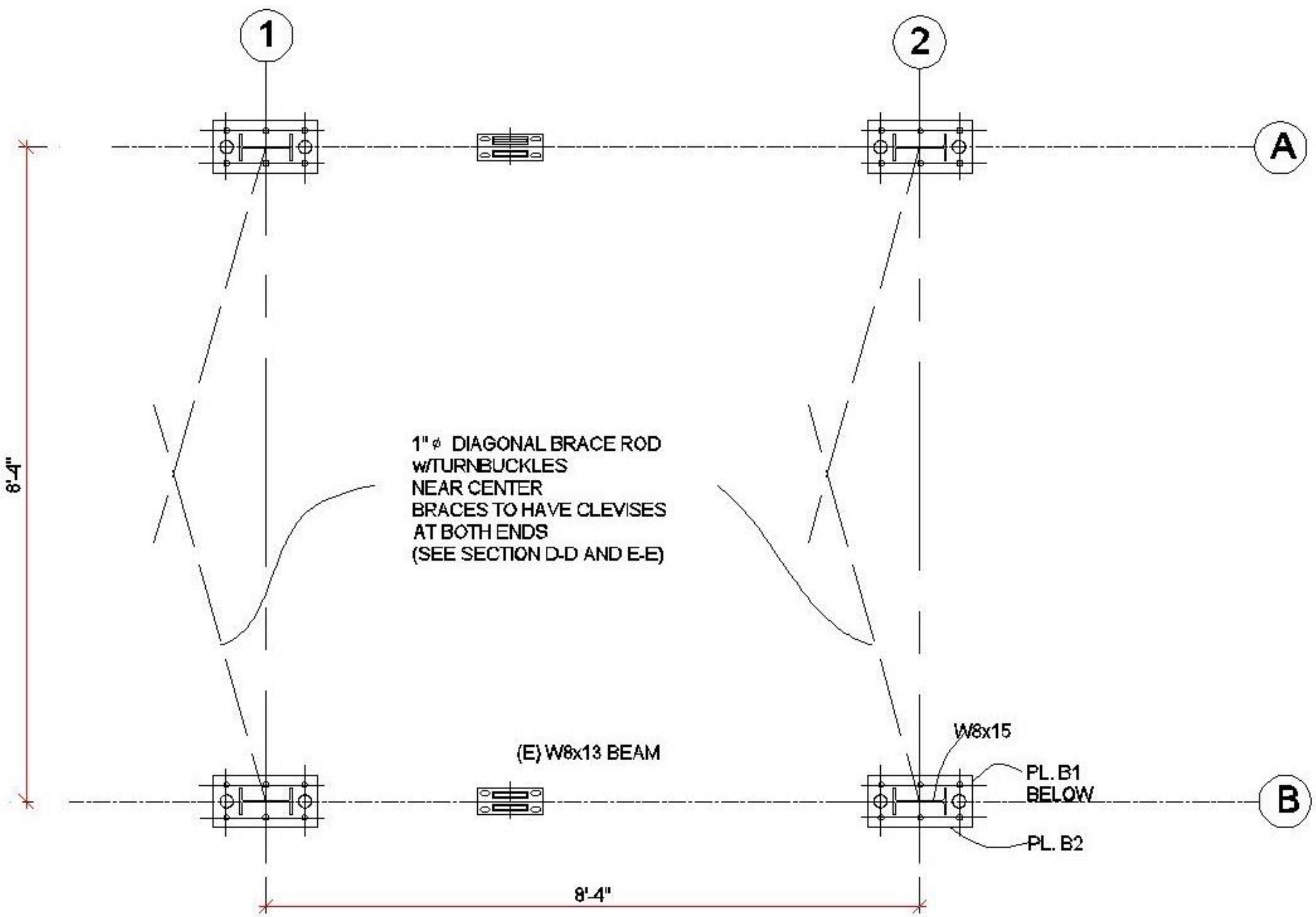
1
2
A
B
8'-4"
1"ø DIAGONAL BRACE ROD
w/TURNBUCKLES
NEAR CENTER
BRACES TO HAVE CLEVISES
AT BOTH ENDS
(SEE SECTION D-D AND E-E)
(E) W8x13 BEAM
W8x15
PL. B1
BELOW
PL. B2
8'-4"

1
–

PLAN

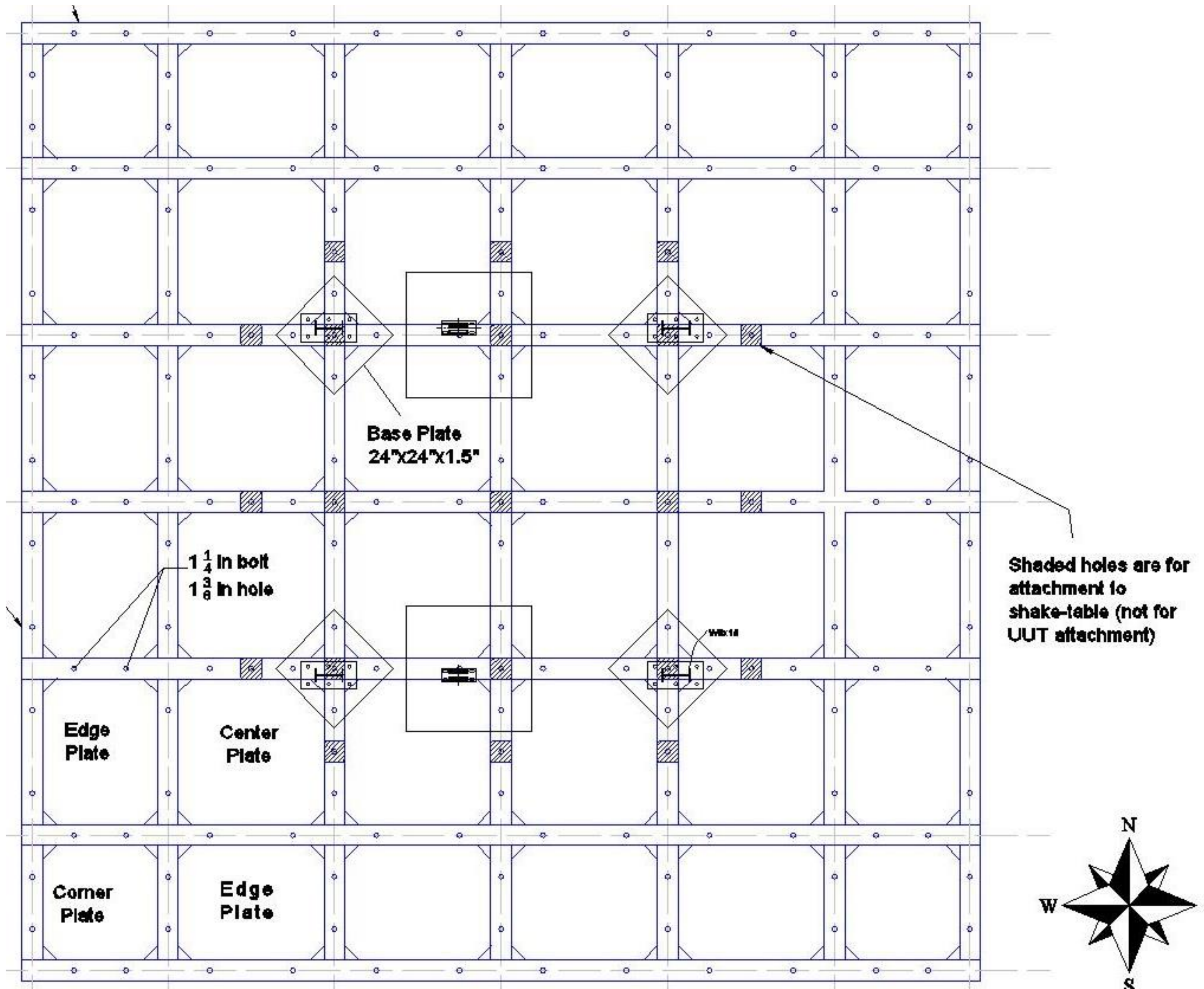

1
–
EXTENSION TABLE PLAN

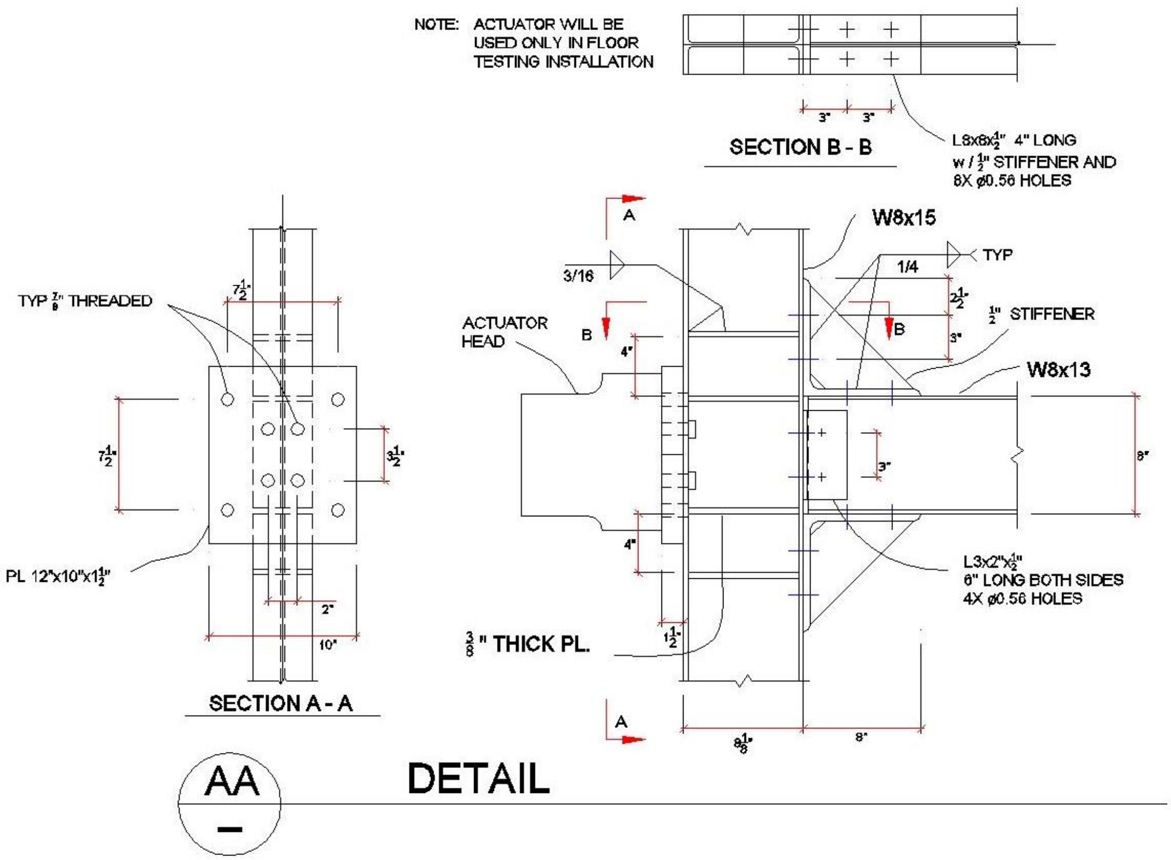
NOTE: ACTUATOR WILL BE
USED ONLY IN FLOOR
TESTING INSTALLATION
SECTION B - B
3"
3"
L8x8x½" 4" LONG
w / ½" STIFFENER AND
8X ø0.56 HOLES
W8x15
1/4
TYP
3/16
ACTUATOR
HEAD
½" STIFFENER
W8x13
TYP ⅞" THREADED
PL 12"x10"x1½"
L3x2"x½"
6" LONG BOTH SIDES
4X ø0.56 HOLES
⅜" THICK PL.
SECTION A - A
AA
DETAIL

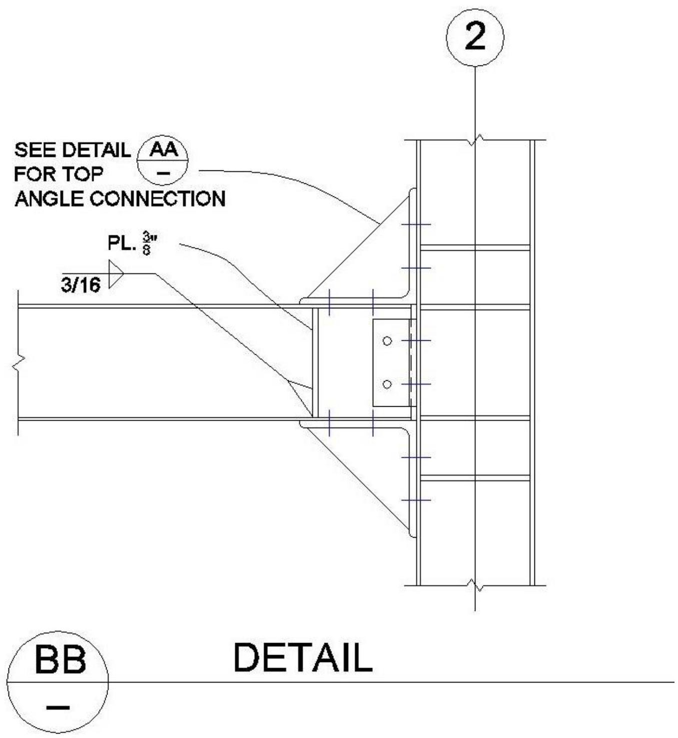
2
SEE DETAIL AA
FOR TOP
ANGLE CONNECTION
PL. ⅜"
3/16
BB
DETAIL

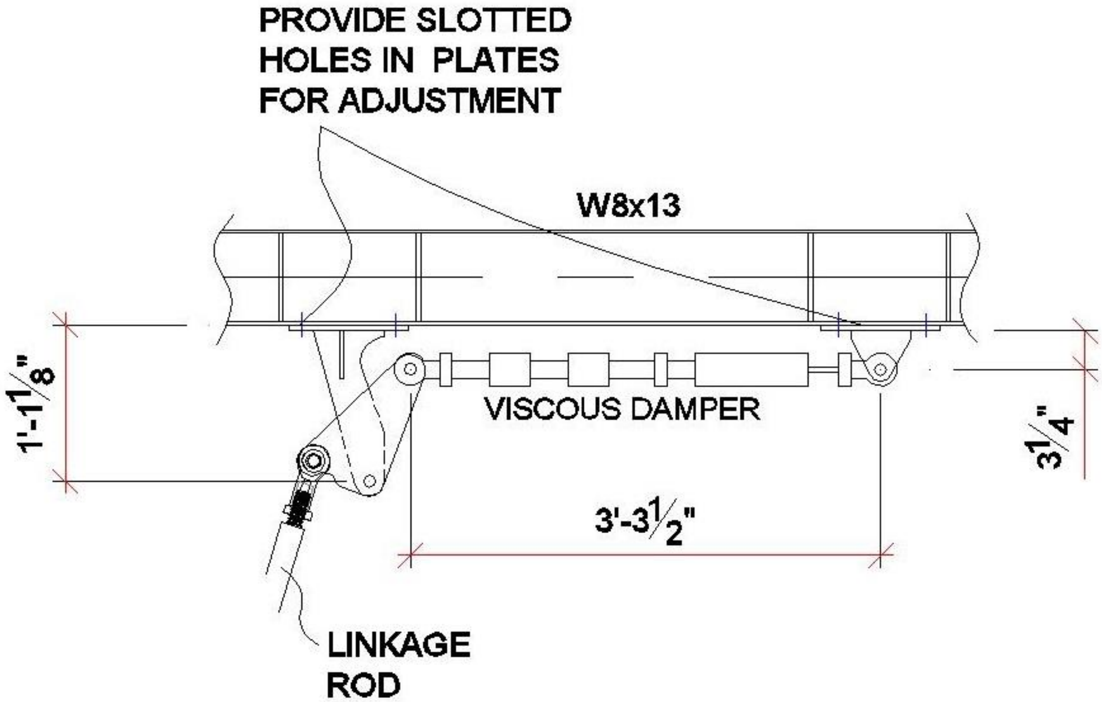

CC DETAIL

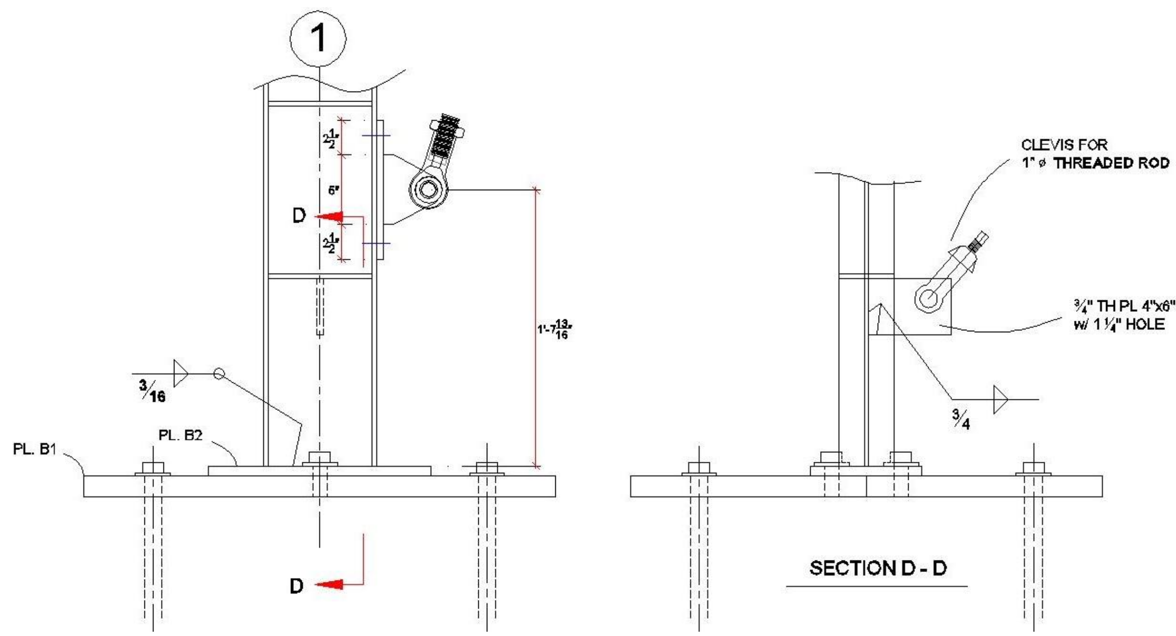

DD DETAIL

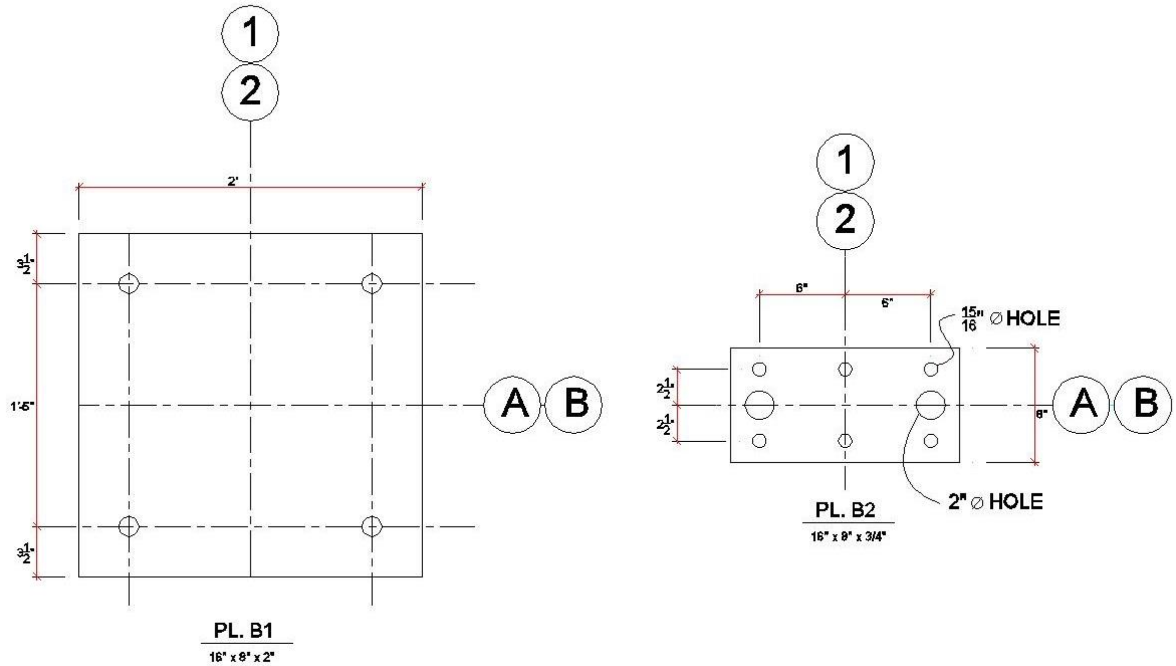

GG DETAIL FOR PL. B1 AND B2

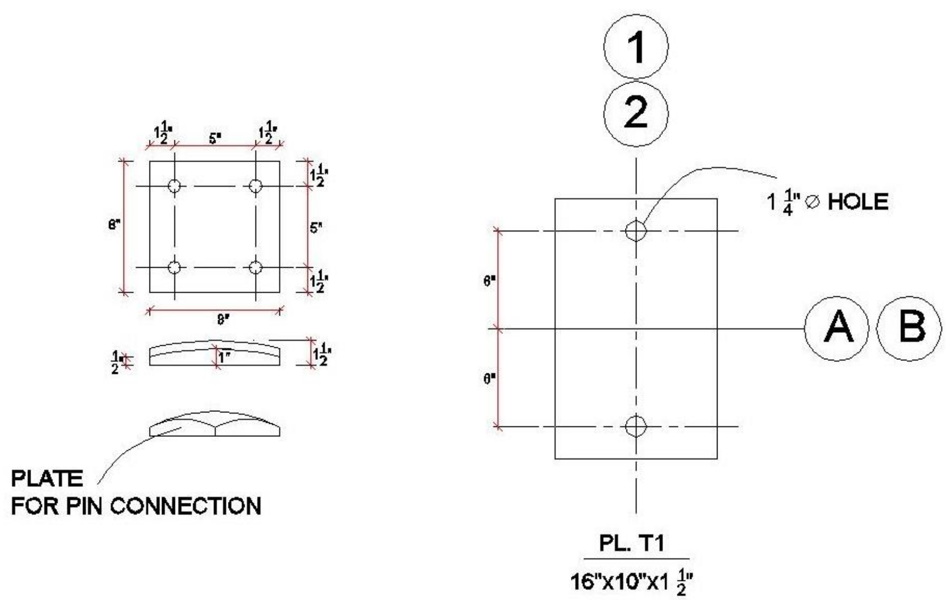

FF DETAIL FOR PL. T1

“This Page Intentionally Left Blank”

MCEER Technical Reports

MCEER publishes technical reports on a variety of subjects written by authors funded through MCEER. These reports are available from both MCEER Publications and the National Technical Information Service (NTIS). Requests for reports should be directed to MCEER Publications, MCEER, University at Buffalo, State University of New York, 133A Ketter Hall, Buffalo, New York 14260. Reports can also be requested through NTIS, P.O. Box 1425, Springfield, Virginia 22151. NTIS accession numbers are shown in parenthesis, if available.

NCEER-87-0001 "First-Year Program in Research, Education and Technology Transfer," 3/5/87, (PB88-134275, A04, MF-A01).

NCEER-87-0002 "Experimental Evaluation of Instantaneous Optimal Algorithms for Structural Control," by R.C. Lin, T.T. Soong and A.M. Reinhorn, 4/20/87, (PB88-134341, A04, MF-A01).

NCEER-87-0003 "Experimentation Using the Earthquake Simulation Facilities at University at Buffalo," by A.M. Reinhorn and R.L. Ketter, not available.

NCEER-87-0004 "The System Characteristics and Performance of a Shaking Table," by J.S. Hwang, K.C. Chang and G.C. Lee, 6/1/87, (PB88-134259, A03, MF-A01). This report is available only through NTIS (see address given above).

NCEER-87-0005 "A Finite Element Formulation for Nonlinear Viscoplastic Material Using a Q Model," by O. Gyebi and G. Dasgupta, 11/2/87, (PB88-213764, A08, MF-A01).

NCEER-87-0006 "Symbolic Manipulation Program (SMP) - Algebraic Codes for Two and Three Dimensional Finite Element Formulations," by X. Lee and G. Dasgupta, 11/9/87, (PB88-218522, A05, MF-A01).

NCEER-87-0007 "Instantaneous Optimal Control Laws for Tall Buildings Under Seismic Excitations," by J.N. Yang, A. Akbarpour and P. Ghaemmaghami, 6/10/87, (PB88-134333, A06, MF-A01). This report is only available through NTIS (see address given above).

NCEER-87-0008 "IDARC: Inelastic Damage Analysis of Reinforced Concrete Frame - Shear-Wall Structures," by Y.J. Park, A.M. Reinhorn and S.K. Kunnath, 7/20/87, (PB88-134325, A09, MF-A01). This report is only available through NTIS (see address given above).

NCEER-87-0009 "Liquefaction Potential for New York State: A Preliminary Report on Sites in Manhattan and Buffalo," by M. Budhu, V. Vijayakumar, R.F. Giese and L. Baumgras, 8/31/87, (PB88-163704, A03, MF-A01). This report is available only through NTIS (see address given above).

NCEER-87-0010 "Vertical and Torsional Vibration of Foundations in Inhomogeneous Media," by A.S. Veletsos and K.W. Dotson, 6/1/87, (PB88-134291, A03, MF-A01). This report is only available through NTIS (see address given above).

NCEER-87-0011 "Seismic Probabilistic Risk Assessment and Seismic Margins Studies for Nuclear Power Plants," by Howard H.M. Hwang, 6/15/87, (PB88-134267, A03, MF-A01). This report is only available through NTIS (see address given above).

NCEER-87-0012 "Parametric Studies of Frequency Response of Secondary Systems Under Ground-Acceleration Excitations," by Y. Yong and Y.K. Lin, 6/10/87, (PB88-134309, A03, MF-A01). This report is only available through NTIS (see address given above).

NCEER-87-0013 "Frequency Response of Secondary Systems Under Seismic Excitation," by J.A. HoLung, J. Cai and Y.K. Lin, 7/31/87, (PB88-134317, A05, MF-A01). This report is only available through NTIS (see address given above).

NCEER-87-0014 "Modelling Earthquake Ground Motions in Seismically Active Regions Using Parametric Time Series Methods," by G.W. Ellis and A.S. Cakmak, 8/25/87, (PB88-134283, A08, MF-A01). This report is only available through NTIS (see address given above).

NCEER-87-0015 "Detection and Assessment of Seismic Structural Damage," by E. DiPasquale and A.S. Cakmak, 8/25/87, (PB88-163712, A05, MF-A01). This report is only available through NTIS (see address given above).

NCEER-87-0016 "Pipeline Experiment at Parkfield, California," by J. Isenberg and E. Richardson, 9/15/87, (PB88-163720, A03, MF-A01). This report is available only through NTIS (see address given above).

NCEER-87-0017 "Digital Simulation of Seismic Ground Motion," by M. Shinozuka, G. Deodatis and T. Harada, 8/31/87, (PB88-155197, A04, MF-A01). This report is available only through NTIS (see address given above).

NCEER-87-0018 "Practical Considerations for Structural Control: System Uncertainty, System Time Delay and Truncation of Small Control Forces," J.N. Yang and A. Akbarpour, 8/10/87, (PB88-163738, A08, MF-A01). This report is only available through NTIS (see address given above).

NCEER-87-0019 "Modal Analysis of Nonclassically Damped Structural Systems Using Canonical Transformation," by J.N. Yang, S. Sarkani and F.X. Long, 9/27/87, (PB88-187851, A04, MF-A01).

NCEER-87-0020 "A Nonstationary Solution in Random Vibration Theory," by J.R. Red-Horse and P.D. Spanos, 11/3/87, (PB88-163746, A03, MF-A01).

NCEER-87-0021 "Horizontal Impedances for Radially Inhomogeneous Viscoelastic Soil Layers," by A.S. Veletsos and K.W. Dotson, 10/15/87, (PB88-150859, A04, MF-A01).

NCEER-87-0022 "Seismic Damage Assessment of Reinforced Concrete Members," by Y.S. Chung, C. Meyer and M. Shinozuka, 10/9/87, (PB88-150867, A05, MF-A01). This report is available only through NTIS (see address given above).

NCEER-87-0023 "Active Structural Control in Civil Engineering," by T.T. Soong, 11/11/87, (PB88-187778, A03, MF-A01).

NCEER-87-0024 "Vertical and Torsional Impedances for Radially Inhomogeneous Viscoelastic Soil Layers," by K.W. Dotson and A.S. Veletsos, 12/87, (PB88-187786, A03, MF-A01).

NCEER-87-0025 "Proceedings from the Symposium on Seismic Hazards, Ground Motions, Soil-Liquefaction and Engineering Practice in Eastern North America," October 20-22, 1987, edited by K.H. Jacob, 12/87, (PB88-188115, A23, MF-A01). This report is available only through NTIS (see address given above).

NCEER-87-0026 "Report on the Whittier-Narrows, California, Earthquake of October 1, 1987," by J. Pantelic and A. Reinhorn, 11/87, (PB88-187752, A03, MF-A01). This report is available only through NTIS (see address given above).

NCEER-87-0027 "Design of a Modular Program for Transient Nonlinear Analysis of Large 3-D Building Structures," by S. Srivastav and J.F. Abel, 12/30/87, (PB88-187950, A05, MF-A01). This report is only available through NTIS (see address given above).

NCEER-87-0028 "Second-Year Program in Research, Education and Technology Transfer," 3/8/88, (PB88-219480, A04, MF-A01).

NCEER-88-0001 "Workshop on Seismic Computer Analysis and Design of Buildings With Interactive Graphics," by W. McGuire, J.F. Abel and C.H. Conley, 1/18/88, (PB88-187760, A03, MF-A01). This report is only available through NTIS (see address given above).

NCEER-88-0002 "Optimal Control of Nonlinear Flexible Structures," by J.N. Yang, F.X. Long and D. Wong, 1/22/88, (PB88-213772, A06, MF-A01).

NCEER-88-0003 "Substructuring Techniques in the Time Domain for Primary-Secondary Structural Systems," by G.D. Manolis and G. Juhn, 2/10/88, (PB88-213780, A04, MF-A01).

NCEER-88-0004 "Iterative Seismic Analysis of Primary-Secondary Systems," by A. Singhal, L.D. Lutes and P.D. Spanos, 2/23/88, (PB88-213798, A04, MF-A01).

NCEER-88-0005 "Stochastic Finite Element Expansion for Random Media," by P.D. Spanos and R. Ghanem, 3/14/88, (PB88-213806, A03, MF-A01).

NCEER-88-0006 "Combining Structural Optimization and Structural Control," by F.Y. Cheng and C.P. Pantelides, 1/10/88, (PB88-213814, A05, MF-A01).

NCEER-88-0007 "Seismic Performance Assessment of Code-Designed Structures," by H.H-M. Hwang, J-W. Jaw and H-J. Shau, 3/20/88, (PB88-219423, A04, MF-A01). This report is only available through NTIS (see address given above).

NCEER-88-0008 "Reliability Analysis of Code-Designed Structures Under Natural Hazards," by H.H-M. Hwang, H. Ushiba and M. Shinozuka, 2/29/88, (PB88-229471, A07, MF-A01). This report is only available through NTIS (see address given above).

NCEER-88-0009 "Seismic Fragility Analysis of Shear Wall Structures," by J-W Jaw and H.H-M. Hwang, 4/30/88, (PB89-102867, A04, MF-A01).

NCEER-88-0010 "Base Isolation of a Multi-Story Building Under a Harmonic Ground Motion - A Comparison of Performances of Various Systems," by F-G Fan, G. Ahmadi and I.G. Tadjbakhsh, 5/18/88, (PB89-122238, A06, MF-A01). This report is only available through NTIS (see address given above).

NCEER-88-0011 "Seismic Floor Response Spectra for a Combined System by Green's Functions," by F.M. Lavelle, L.A. Bergman and P.D. Spanos, 5/1/88, (PB89-102875, A03, MF-A01).

NCEER-88-0012 "A New Solution Technique for Randomly Excited Hysteretic Structures," by G.Q. Cai and Y.K. Lin, 5/16/88, (PB89-102883, A03, MF-A01).

NCEER-88-0013 "A Study of Radiation Damping and Soil-Structure Interaction Effects in the Centrifuge," by K. Weissman, supervised by J.H. Prevost, 5/24/88, (PB89-144703, A06, MF-A01).

NCEER-88-0014 "Parameter Identification and Implementation of a Kinematic Plasticity Model for Frictional Soils," by J.H. Prevost and D.V. Griffiths, not available.

NCEER-88-0015 "Two- and Three- Dimensional Dynamic Finite Element Analyses of the Long Valley Dam," by D.V. Griffiths and J.H. Prevost, 6/17/88, (PB89-144711, A04, MF-A01).

NCEER-88-0016 "Damage Assessment of Reinforced Concrete Structures in Eastern United States," by A.M. Reinhorn, M.J. Seidel, S.K. Kunnath and Y.J. Park, 6/15/88, (PB89-122220, A04, MF-A01). This report is only available through NTIS (see address given above).

NCEER-88-0017 "Dynamic Compliance of Vertically Loaded Strip Foundations in Multilayered Viscoelastic Soils," by S. Ahmad and A.S.M. Israil, 6/17/88, (PB89-102891, A04, MF-A01).

NCEER-88-0018 "An Experimental Study of Seismic Structural Response With Added Viscoelastic Dampers," by R.C. Lin, Z. Liang, T.T. Soong and R.H. Zhang, 6/30/88, (PB89-122212, A05, MF-A01). This report is available only through NTIS (see address given above).

NCEER-88-0019 "Experimental Investigation of Primary - Secondary System Interaction," by G.D. Manolis, G. Juhn and A.M. Reinhorn, 5/27/88, (PB89-122204, A04, MF-A01).

NCEER-88-0020 "A Response Spectrum Approach For Analysis of Nonclassically Damped Structures," by J.N. Yang, S. Sarkani and F.X. Long, 4/22/88, (PB89-102909, A04, MF-A01).

NCEER-88-0021 "Seismic Interaction of Structures and Soils: Stochastic Approach," by A.S. Veletsos and A.M. Prasad, 7/21/88, (PB89-122196, A04, MF-A01). This report is only available through NTIS (see address given above).

NCEER-88-0022 "Identification of the Serviceability Limit State and Detection of Seismic Structural Damage," by E. DiPasquale and A.S. Cakmak, 6/15/88, (PB89-122188, A05, MF-A01). This report is available only through NTIS (see address given above).

NCEER-88-0023 "Multi-Hazard Risk Analysis: Case of a Simple Offshore Structure," by B.K. Bhartia and E.H. Vanmarcke, 7/21/88, (PB89-145213, A05, MF-A01).

NCEER-88-0024 "Automated Seismic Design of Reinforced Concrete Buildings," by Y.S. Chung, C. Meyer and M. Shinozuka, 7/5/88, (PB89-122170, A06, MF-A01). This report is available only through NTIS (see address given above).

NCEER-88-0025 "Experimental Study of Active Control of MDOF Structures Under Seismic Excitations," by L.L. Chung, R.C. Lin, T.T. Soong and A.M. Reinhorn, 7/10/88, (PB89-122600, A04, MF-A01).

NCEER-88-0026 "Earthquake Simulation Tests of a Low-Rise Metal Structure," by J.S. Hwang, K.C. Chang, G.C. Lee and R.L. Ketter, 8/1/88, (PB89-102917, A04, MF-A01).

NCEER-88-0027 "Systems Study of Urban Response and Reconstruction Due to Catastrophic Earthquakes," by F. Kozin and H.K. Zhou, 9/22/88, (PB90-162348, A04, MF-A01).

NCEER-88-0028 "Seismic Fragility Analysis of Plane Frame Structures," by H.H-M. Hwang and Y.K. Low, 7/31/88, (PB89-131445, A06, MF-A01).

NCEER-88-0029 "Response Analysis of Stochastic Structures," by A. Kardara, C. Bucher and M. Shinozuka, 9/22/88, (PB89-174429, A04, MF-A01).

NCEER-88-0030 "Nonnormal Accelerations Due to Yielding in a Primary Structure," by D.C.K. Chen and L.D. Lutes, 9/19/88, (PB89-131437, A04, MF-A01).

NCEER-88-0031 "Design Approaches for Soil-Structure Interaction," by A.S. Veletsos, A.M. Prasad and Y. Tang, 12/30/88, (PB89-174437, A03, MF-A01). This report is available only through NTIS (see address given above).

NCEER-88-0032 "A Re-evaluation of Design Spectra for Seismic Damage Control," by C.J. Turkstra and A.G. Tallin, 11/7/88, (PB89-145221, A05, MF-A01).

NCEER-88-0033 "The Behavior and Design of Noncontact Lap Splices Subjected to Repeated Inelastic Tensile Loading," by V.E. Sagan, P. Gergely and R.N. White, 12/8/88, (PB89-163737, A08, MF-A01).

NCEER-88-0034 "Seismic Response of Pile Foundations," by S.M. Mamoon, P.K. Banerjee and S. Ahmad, 11/1/88, (PB89-145239, A04, MF-A01).

NCEER-88-0035 "Modeling of R/C Building Structures With Flexible Floor Diaphragms (IDARC2)," by A.M. Reinhorn, S.K. Kunnath and N. Panahshahi, 9/7/88, (PB89-207153, A07, MF-A01).

NCEER-88-0036 "Solution of the Dam-Reservoir Interaction Problem Using a Combination of FEM, BEM with Particular Integrals, Modal Analysis, and Substructuring," by C-S. Tsai, G.C. Lee and R.L. Ketter, 12/31/88, (PB89-207146, A04, MF-A01).

NCEER-88-0037 "Optimal Placement of Actuators for Structural Control," by F.Y. Cheng and C.P. Pantelides, 8/15/88, (PB89-162846, A05, MF-A01).

NCEER-88-0038 "Teflon Bearings in Aseismic Base Isolation: Experimental Studies and Mathematical Modeling," by A. Mokha, M.C. Constantinou and A.M. Reinhorn, 12/5/88, (PB89-218457, A10, MF-A01). This report is available only through NTIS (see address given above).

NCEER-88-0039 "Seismic Behavior of Flat Slab High-Rise Buildings in the New York City Area," by P. Weidlinger and M. Ettouney, 10/15/88, (PB90-145681, A04, MF-A01).

NCEER-88-0040 "Evaluation of the Earthquake Resistance of Existing Buildings in New York City," by P. Weidlinger and M. Ettouney, 10/15/88, not available.

NCEER-88-0041 "Small-Scale Modeling Techniques for Reinforced Concrete Structures Subjected to Seismic Loads," by W. Kim, A. El-Attar and R.N. White, 11/22/88, (PB89-189625, A05, MF-A01).

NCEER-88-0042 "Modeling Strong Ground Motion from Multiple Event Earthquakes," by G.W. Ellis and A.S. Cakmak, 10/15/88, (PB89-174445, A03, MF-A01).

NCEER-88-0043 "Nonstationary Models of Seismic Ground Acceleration," by M. Grigoriu, S.E. Ruiz and E. Rosenblueth, 7/15/88, (PB89-189617, A04, MF-A01).

NCEER-88-0044 "SARCF User's Guide: Seismic Analysis of Reinforced Concrete Frames," by Y.S. Chung, C. Meyer and M. Shinozuka, 11/9/88, (PB89-174452, A08, MF-A01).

NCEER-88-0045 "First Expert Panel Meeting on Disaster Research and Planning," edited by J. Pantelic and J. Stoyle, 9/15/88, (PB89-174460, A05, MF-A01).

NCEER-88-0046 "Preliminary Studies of the Effect of Degrading Infill Walls on the Nonlinear Seismic Response of Steel Frames," by C.Z. Chrysostomou, P. Gergely and J.F. Abel, 12/19/88, (PB89-208383, A05, MF-A01).

NCEER-88-0047 "Reinforced Concrete Frame Component Testing Facility - Design, Construction, Instrumentation and Operation," by S.P. Pessiki, C. Conley, T. Bond, P. Gergely and R.N. White, 12/16/88, (PB89-174478, A04, MF-A01).

NCEER-89-0001 "Effects of Protective Cushion and Soil Compliancy on the Response of Equipment Within a Seismically Excited Building," by J.A. HoLung, 2/16/89, (PB89-207179, A04, MF-A01).

NCEER-89-0002 "Statistical Evaluation of Response Modification Factors for Reinforced Concrete Structures," by H.H-M. Hwang and J-W. Jaw, 2/17/89, (PB89-207187, A05, MF-A01).

NCEER-89-0003 "Hysteretic Columns Under Random Excitation," by G-Q. Cai and Y.K. Lin, 1/9/89, (PB89-196513, A03, MF-A01).

NCEER-89-0004 "Experimental Study of `Elephant Foot Bulge' Instability of Thin-Walled Metal Tanks," by Z-H. Jia and R.L. Ketter, 2/22/89, (PB89-207195, A03, MF-A01).

NCEER-89-0005 "Experiment on Performance of Buried Pipelines Across San Andreas Fault," by J. Isenberg, E. Richardson and T.D. O'Rourke, 3/10/89, (PB89-218440, A04, MF-A01). This report is available only through NTIS (see address given above).

NCEER-89-0006 "A Knowledge-Based Approach to Structural Design of Earthquake-Resistant Buildings," by M. Subramani, P. Gergely, C.H. Conley, J.F. Abel and A.H. Zaghw, 1/15/89, (PB89-218465, A06, MF-A01).

NCEER-89-0007 "Liquefaction Hazards and Their Effects on Buried Pipelines," by T.D. O'Rourke and P.A. Lane, 2/1/89, (PB89-218481, A09, MF-A01).

NCEER-89-0008 "Fundamentals of System Identification in Structural Dynamics," by H. Imai, C-B. Yun, O. Maruyama and M. Shinozuka, 1/26/89, (PB89-207211, A04, MF-A01).

NCEER-89-0009 "Effects of the 1985 Michoacan Earthquake on Water Systems and Other Buried Lifelines in Mexico," by A.G. Ayala and M.J. O'Rourke, 3/8/89, (PB89-207229, A06, MF-A01).

NCEER-89-R010 "NCEER Bibliography of Earthquake Education Materials," by K.E.K. Ross, Second Revision, 9/1/89, (PB90-125352, A05, MF-A01). This report is replaced by NCEER-92-0018.

NCEER-89-0011 "Inelastic Three-Dimensional Response Analysis of Reinforced Concrete Building Structures (IDARC-3D), Part I - Modeling," by S.K. Kunnath and A.M. Reinhorn, 4/17/89, (PB90-114612, A07, MF-A01). This report is available only through NTIS (see address given above).

NCEER-89-0012 "Recommended Modifications to ATC-14," by C.D. Poland and J.O. Malley, 4/12/89, (PB90-108648, A15, MF-A01).

NCEER-89-0013 "Repair and Strengthening of Beam-to-Column Connections Subjected to Earthquake Loading," by M. Corazao and A.J. Durrani, 2/28/89, (PB90-109885, A06, MF-A01).

NCEER-89-0014 "Program EXKAL2 for Identification of Structural Dynamic Systems," by O. Maruyama, C-B. Yun, M. Hoshiya and M. Shinozuka, 5/19/89, (PB90-109877, A09, MF-A01).

NCEER-89-0015 "Response of Frames With Bolted Semi-Rigid Connections, Part I - Experimental Study and Analytical Predictions," by P.J. DiCorso, A.M. Reinhorn, J.R. Dickerson, J.B. Radziminski and W.L. Harper, 6/1/89, not available.

NCEER-89-0016 "ARMA Monte Carlo Simulation in Probabilistic Structural Analysis," by P.D. Spanos and M.P. Mignolet, 7/10/89, (PB90-109893, A03, MF-A01).

NCEER-89-P017 "Preliminary Proceedings from the Conference on Disaster Preparedness - The Place of Earthquake Education in Our Schools," Edited by K.E.K. Ross, 6/23/89, (PB90-108606, A03, MF-A01).

NCEER-89-0017 "Proceedings from the Conference on Disaster Preparedness - The Place of Earthquake Education in Our Schools," Edited by K.E.K. Ross, 12/31/89, (PB90-207895, A012, MF-A02). This report is available only through NTIS (see address given above).

NCEER-89-0018 "Multidimensional Models of Hysteretic Material Behavior for Vibration Analysis of Shape Memory Energy Absorbing Devices, by E.J. Graesser and F.A. Cozzarelli, 6/7/89, (PB90-164146, A04, MF-A01).

NCEER-89-0019 "Nonlinear Dynamic Analysis of Three-Dimensional Base Isolated Structures (3D-BASIS)," by S. Nagarajaiah, A.M. Reinhorn and M.C. Constantinou, 8/3/89, (PB90-161936, A06, MF-A01). This report has been replaced by NCEER-93-0011.

NCEER-89-0020 "Structural Control Considering Time-Rate of Control Forces and Control Rate Constraints," by F.Y. Cheng and C.P. Pantelides, 8/3/89, (PB90-120445, A04, MF-A01).

NCEER-89-0021 "Subsurface Conditions of Memphis and Shelby County," by K.W. Ng, T-S. Chang and H-H.M. Hwang, 7/26/89, (PB90-120437, A03, MF-A01).

NCEER-89-0022 "Seismic Wave Propagation Effects on Straight Jointed Buried Pipelines," by K. Elhmadi and M.J. O'Rourke, 8/24/89, (PB90-162322, A10, MF-A02).

NCEER-89-0023 "Workshop on Serviceability Analysis of Water Delivery Systems," edited by M. Grigoriu, 3/6/89, (PB90-127424, A03, MF-A01).

NCEER-89-0024 "Shaking Table Study of a 1/5 Scale Steel Frame Composed of Tapered Members," by K.C. Chang, J.S. Hwang and G.C. Lee, 9/18/89, (PB90-160169, A04, MF-A01).

NCEER-89-0025 "DYNA1D: A Computer Program for Nonlinear Seismic Site Response Analysis - Technical Documentation," by Jean H. Prevost, 9/14/89, (PB90-161944, A07, MF-A01). This report is available only through NTIS (see address given above).

NCEER-89-0026 "1:4 Scale Model Studies of Active Tendon Systems and Active Mass Dampers for Aseismic Protection," by A.M. Reinhorn, T.T. Soong, R.C. Lin, Y.P. Yang, Y. Fukao, H. Abe and M. Nakai, 9/15/89, (PB90-173246, A10, MF-A02). This report is available only through NTIS (see address given above).

NCEER-89-0027 "Scattering of Waves by Inclusions in a Nonhomogeneous Elastic Half Space Solved by Boundary Element Methods," by P.K. Hadley, A. Askar and A.S. Cakmak, 6/15/89, (PB90-145699, A07, MF-A01).

NCEER-89-0028 "Statistical Evaluation of Deflection Amplification Factors for Reinforced Concrete Structures," by H.H.M. Hwang, J-W. Jaw and A.L. Ch'ng, 8/31/89, (PB90-164633, A05, MF-A01).

NCEER-89-0029 "Bedrock Accelerations in Memphis Area Due to Large New Madrid Earthquakes," by H.H.M. Hwang, C.H.S. Chen and G. Yu, 11/7/89, (PB90-162330, A04, MF-A01).

NCEER-89-0030 "Seismic Behavior and Response Sensitivity of Secondary Structural Systems," by Y.Q. Chen and T.T. Soong, 10/23/89, (PB90-164658, A08, MF-A01).

NCEER-89-0031 "Random Vibration and Reliability Analysis of Primary-Secondary Structural Systems," by Y. Ibrahim, M. Grigoriu and T.T. Soong, 11/10/89, (PB90-161951, A04, MF-A01).

NCEER-89-0032 "Proceedings from the Second U.S. - Japan Workshop on Liquefaction, Large Ground Deformation and Their Effects on Lifelines, September 26-29, 1989," Edited by T.D. O'Rourke and M. Hamada, 12/1/89, (PB90-209388, A22, MF-A03).

NCEER-89-0033 "Deterministic Model for Seismic Damage Evaluation of Reinforced Concrete Structures," by J.M. Bracci, A.M. Reinhorn, J.B. Mander and S.K. Kunnath, 9/27/89, (PB91-108803, A06, MF-A01).

NCEER-89-0034 "On the Relation Between Local and Global Damage Indices," by E. DiPasquale and A.S. Cakmak, 8/15/89, (PB90-173865, A05, MF-A01).

NCEER-89-0035 "Cyclic Undrained Behavior of Nonplastic and Low Plasticity Silts," by A.J. Walker and H.E. Stewart, 7/26/89, (PB90-183518, A10, MF-A01).

NCEER-89-0036 "Liquefaction Potential of Surficial Deposits in the City of Buffalo, New York," by M. Budhu, R. Giese and L. Baumgrass, 1/17/89, (PB90-208455, A04, MF-A01).

NCEER-89-0037 "A Deterministic Assessment of Effects of Ground Motion Incoherence," by A.S. Veletsos and Y. Tang, 7/15/89, (PB90-164294, A03, MF-A01).

NCEER-89-0038 "Workshop on Ground Motion Parameters for Seismic Hazard Mapping," July 17-18, 1989, edited by R.V. Whitman, 12/1/89, (PB90-173923, A04, MF-A01).

NCEER-89-0039 "Seismic Effects on Elevated Transit Lines of the New York City Transit Authority," by C.J. Costantino, C.A. Miller and E. Heymsfield, 12/26/89, (PB90-207887, A06, MF-A01).

NCEER-89-0040 "Centrifugal Modeling of Dynamic Soil-Structure Interaction," by K. Weissman, Supervised by J.H. Prevost, 5/10/89, (PB90-207879, A07, MF-A01).

NCEER-89-0041 "Linearized Identification of Buildings With Cores for Seismic Vulnerability Assessment," by I-K. Ho and A.E. Aktan, 11/1/89, (PB90-251943, A07, MF-A01).

NCEER-90-0001 "Geotechnical and Lifeline Aspects of the October 17, 1989 Loma Prieta Earthquake in San Francisco," by T.D. O'Rourke, H.E. Stewart, F.T. Blackburn and T.S. Dickerman, 1/90, (PB90-208596, A05, MF-A01).

NCEER-90-0002 "Nonnormal Secondary Response Due to Yielding in a Primary Structure," by D.C.K. Chen and L.D. Lutes, 2/28/90, (PB90-251976, A07, MF-A01).

NCEER-90-0003 "Earthquake Education Materials for Grades K-12," by K.E.K. Ross, 4/16/90, (PB91-251984, A05, MF-A05). This report has been replaced by NCEER-92-0018.

NCEER-90-0004 "Catalog of Strong Motion Stations in Eastern North America," by R.W. Busby, 4/3/90, (PB90-251984, A05, MF-A01).

NCEER-90-0005 "NCEER Strong-Motion Data Base: A User Manual for the GeoBase Release (Version 1.0 for the Sun3)," by P. Friberg and K. Jacob, 3/31/90 (PB90-258062, A04, MF-A01).

NCEER-90-0006 "Seismic Hazard Along a Crude Oil Pipeline in the Event of an 1811-1812 Type New Madrid Earthquake," by H.H.M. Hwang and C-H.S. Chen, 4/16/90, (PB90-258054, A04, MF-A01).

NCEER-90-0007 "Site-Specific Response Spectra for Memphis Sheahan Pumping Station," by H.H.M. Hwang and C.S. Lee, 5/15/90, (PB91-108811, A05, MF-A01).

NCEER-90-0008 "Pilot Study on Seismic Vulnerability of Crude Oil Transmission Systems," by T. Ariman, R. Dobry, M. Grigoriu, F. Kozin, M. O'Rourke, T. O'Rourke and M. Shinozuka, 5/25/90, (PB91-108837, A06, MF-A01).

NCEER-90-0009 "A Program to Generate Site Dependent Time Histories: EQGEN," by G.W. Ellis, M. Srinivasan and A.S. Cakmak, 1/30/90, (PB91-108829, A04, MF-A01).

NCEER-90-0010 "Active Isolation for Seismic Protection of Operating Rooms," by M.E. Talbott, Supervised by M. Shinozuka, 6/8/9, (PB91-110205, A05, MF-A01).

NCEER-90-0011 "Program LINEARID for Identification of Linear Structural Dynamic Systems," by C-B. Yun and M. Shinozuka, 6/25/90, (PB91-110312, A08, MF-A01).

NCEER-90-0012 "Two-Dimensional Two-Phase Elasto-Plastic Seismic Response of Earth Dams," by A.N. Yiagos, Supervised by J.H. Prevost, 6/20/90, (PB91-110197, A13, MF-A02).

NCEER-90-0013 "Secondary Systems in Base-Isolated Structures: Experimental Investigation, Stochastic Response and Stochastic Sensitivity," by G.D. Manolis, G. Juhn, M.C. Constantinou and A.M. Reinhorn, 7/1/90, (PB91-110320, A08, MF-A01).

NCEER-90-0014 "Seismic Behavior of Lightly-Reinforced Concrete Column and Beam-Column Joint Details," by S.P. Pessiki, C.H. Conley, P. Gergely and R.N. White, 8/22/90, (PB91-108795, A11, MF-A02).

NCEER-90-0015 "Two Hybrid Control Systems for Building Structures Under Strong Earthquakes," by J.N. Yang and A. Danielians, 6/29/90, (PB91-125393, A04, MF-A01).

NCEER-90-0016 "Instantaneous Optimal Control with Acceleration and Velocity Feedback," by J.N. Yang and Z. Li, 6/29/90, (PB91-125401, A03, MF-A01).

NCEER-90-0017 "Reconnaissance Report on the Northern Iran Earthquake of June 21, 1990," by M. Mehrain, 10/4/90, (PB91-125377, A03, MF-A01).

NCEER-90-0018 "Evaluation of Liquefaction Potential in Memphis and Shelby County," by T.S. Chang, P.S. Tang, C.S. Lee and H. Hwang, 8/10/90, (PB91-125427, A09, MF-A01).

NCEER-90-0019 "Experimental and Analytical Study of a Combined Sliding Disc Bearing and Helical Steel Spring Isolation System," by M.C. Constantinou, A.S. Mokha and A.M. Reinhorn, 10/4/90, (PB91-125385, A06, MF-A01). This report is available only through NTIS (see address given above).

NCEER-90-0020 "Experimental Study and Analytical Prediction of Earthquake Response of a Sliding Isolation System with a Spherical Surface," by A.S. Mokha, M.C. Constantinou and A.M. Reinhorn, 10/11/90, (PB91-125419, A05, MF-A01).

NCEER-90-0021 "Dynamic Interaction Factors for Floating Pile Groups," by G. Gazetas, K. Fan, A. Kaynia and E. Kausel, 9/10/90, (PB91-170381, A05, MF-A01).

NCEER-90-0022 "Evaluation of Seismic Damage Indices for Reinforced Concrete Structures," by S. Rodriguez-Gomez and A.S. Cakmak, 9/30/90, PB91-171322, A06, MF-A01).

NCEER-90-0023 "Study of Site Response at a Selected Memphis Site," by H. Desai, S. Ahmad, E.S. Gazetas and M.R. Oh, 10/11/90, (PB91-196857, A03, MF-A01).

NCEER-90-0024 "A User's Guide to Strongmo: Version 1.0 of NCEER's Strong-Motion Data Access Tool for PCs and Terminals," by P.A. Friberg and C.A.T. Susch, 11/15/90, (PB91-171272, A03, MF-A01).

NCEER-90-0025 "A Three-Dimensional Analytical Study of Spatial Variability of Seismic Ground Motions," by L-L. Hong and A.H.-S. Ang, 10/30/90, (PB91-170399, A09, MF-A01).

NCEER-90-0026 "MUMOID User's Guide - A Program for the Identification of Modal Parameters," by S. Rodriguez-Gomez and E. DiPasquale, 9/30/90, (PB91-171298, A04, MF-A01).

NCEER-90-0027 "SARCF-II User's Guide - Seismic Analysis of Reinforced Concrete Frames," by S. Rodriguez-Gomez, Y.S. Chung and C. Meyer, 9/30/90, (PB91-171280, A05, MF-A01).

NCEER-90-0028 "Viscous Dampers: Testing, Modeling and Application in Vibration and Seismic Isolation," by N. Makris and M.C. Constantinou, 12/20/90 (PB91-190561, A06, MF-A01).

NCEER-90-0029 "Soil Effects on Earthquake Ground Motions in the Memphis Area," by H. Hwang, C.S. Lee, K.W. Ng and T.S. Chang, 8/2/90, (PB91-190751, A05, MF-A01).

NCEER-91-0001 "Proceedings from the Third Japan-U.S. Workshop on Earthquake Resistant Design of Lifeline Facilities and Countermeasures for Soil Liquefaction, December 17-19, 1990," edited by T.D. O'Rourke and M. Hamada, 2/1/91, (PB91-179259, A99, MF-A04).

NCEER-91-0002 "Physical Space Solutions of Non-Proportionally Damped Systems," by M. Tong, Z. Liang and G.C. Lee, 1/15/91, (PB91-179242, A04, MF-A01).

NCEER-91-0003 "Seismic Response of Single Piles and Pile Groups," by K. Fan and G. Gazetas, 1/10/91, (PB92-174994, A04, MF-A01).

NCEER-91-0004 "Damping of Structures: Part 1 - Theory of Complex Damping," by Z. Liang and G. Lee, 10/10/91, (PB92-197235, A12, MF-A03).

NCEER-91-0005 "3D-BASIS - Nonlinear Dynamic Analysis of Three Dimensional Base Isolated Structures: Part II," by S. Nagarajaiah, A.M. Reinhorn and M.C. Constantinou, 2/28/91, (PB91-190553, A07, MF-A01). This report has been replaced by NCEER-93-0011.

NCEER-91-0006 "A Multidimensional Hysteretic Model for Plasticity Deforming Metals in Energy Absorbing Devices," by E.J. Graesser and F.A. Cozzarelli, 4/9/91, (PB92-108364, A04, MF-A01).

NCEER-91-0007 "A Framework for Customizable Knowledge-Based Expert Systems with an Application to a KBES for Evaluating the Seismic Resistance of Existing Buildings," by E.G. Ibarra-Anaya and S.J. Fenves, 4/9/91, (PB91-210930, A08, MF-A01).

NCEER-91-0008 "Nonlinear Analysis of Steel Frames with Semi-Rigid Connections Using the Capacity Spectrum Method," by G.G. Deierlein, S-H. Hsieh, Y-J. Shen and J.F. Abel, 7/2/91, (PB92-113828, A05, MF-A01).

NCEER-91-0009 "Earthquake Education Materials for Grades K-12," by K.E.K. Ross, 4/30/91, (PB91-212142, A06, MF-A01). This report has been replaced by NCEER-92-0018.

NCEER-91-0010 "Phase Wave Velocities and Displacement Phase Differences in a Harmonically Oscillating Pile," by N. Makris and G. Gazetas, 7/8/91, (PB92-108356, A04, MF-A01).

NCEER-91-0011 "Dynamic Characteristics of a Full-Size Five-Story Steel Structure and a 2/5 Scale Model," by K.C. Chang, G.C. Yao, G.C. Lee, D.S. Hao and Y.C. Yeh," 7/2/91, (PB93-116648, A06, MF-A02).

NCEER-91-0012 "Seismic Response of a 2/5 Scale Steel Structure with Added Viscoelastic Dampers," by K.C. Chang, T.T. Soong, S-T. Oh and M.L. Lai, 5/17/91, (PB92-110816, A05, MF-A01).

NCEER-91-0013 "Earthquake Response of Retaining Walls; Full-Scale Testing and Computational Modeling," by S. Alampalli and A-W.M. Elgamal, 6/20/91, not available.

NCEER-91-0014 "3D-BASIS-M: Nonlinear Dynamic Analysis of Multiple Building Base Isolated Structures," by P.C. Tsopelas, S. Nagarajaiah, M.C. Constantinou and A.M. Reinhorn, 5/28/91, (PB92-113885, A09, MF-A02).

NCEER-91-0015 "Evaluation of SEAOC Design Requirements for Sliding Isolated Structures," by D. Theodossiou and M.C. Constantinou, 6/10/91, (PB92-114602, A11, MF-A03).

NCEER-91-0016 "Closed-Loop Modal Testing of a 27-Story Reinforced Concrete Flat Plate-Core Building," by H.R. Somaprasad, T. Toksoy, H. Yoshiyuki and A.E. Aktan, 7/15/91, (PB92-129980, A07, MF-A02).

NCEER-91-0017 "Shake Table Test of a 1/6 Scale Two-Story Lightly Reinforced Concrete Building," by A.G. El-Attar, R.N. White and P. Gergely, 2/28/91, (PB92-222447, A06, MF-A02).

NCEER-91-0018 "Shake Table Test of a 1/8 Scale Three-Story Lightly Reinforced Concrete Building," by A.G. El-Attar, R.N. White and P. Gergely, 2/28/91, (PB93-116630, A08, MF-A02).

NCEER-91-0019 "Transfer Functions for Rigid Rectangular Foundations," by A.S. Veletsos, A.M. Prasad and W.H. Wu, 7/31/91, not available.

NCEER-91-0020 "Hybrid Control of Seismic-Excited Nonlinear and Inelastic Structural Systems," by J.N. Yang, Z. Li and A. Danielians, 8/1/91, (PB92-143171, A06, MF-A02).

NCEER-91-0021 "The NCEER-91 Earthquake Catalog: Improved Intensity-Based Magnitudes and Recurrence Relations for U.S. Earthquakes East of New Madrid," by L. Seeber and J.G. Armbruster, 8/28/91, (PB92-176742, A06, MF-A02).

NCEER-91-0022 "Proceedings from the Implementation of Earthquake Planning and Education in Schools: The Need for Change - The Roles of the Changemakers," by K.E.K. Ross and F. Winslow, 7/23/91, (PB92-129998, A12, MF-A03).

NCEER-91-0023 "A Study of Reliability-Based Criteria for Seismic Design of Reinforced Concrete Frame Buildings," by H.H.M. Hwang and H-M. Hsu, 8/10/91, (PB92-140235, A09, MF-A02).

NCEER-91-0024 "Experimental Verification of a Number of Structural System Identification Algorithms," by R.G. Ghanem, H. Gavin and M. Shinozuka, 9/18/91, (PB92-176577, A18, MF-A04).

NCEER-91-0025 "Probabilistic Evaluation of Liquefaction Potential," by H.H.M. Hwang and C.S. Lee," 11/25/91, (PB92-143429, A05, MF-A01).

NCEER-91-0026 "Instantaneous Optimal Control for Linear, Nonlinear and Hysteretic Structures - Stable Controllers," by J.N. Yang and Z. Li, 11/15/91, (PB92-163807, A04, MF-A01).

NCEER-91-0027 "Experimental and Theoretical Study of a Sliding Isolation System for Bridges," by M.C. Constantinou, A. Kartoum, A.M. Reinhorn and P. Bradford, 11/15/91, (PB92-176973, A10, MF-A03).

NCEER-92-0001 "Case Studies of Liquefaction and Lifeline Performance During Past Earthquakes, Volume 1: Japanese Case Studies," Edited by M. Hamada and T. O'Rourke, 2/17/92, (PB92-197243, A18, MF-A04).

NCEER-92-0002 "Case Studies of Liquefaction and Lifeline Performance During Past Earthquakes, Volume 2: United States Case Studies," Edited by T. O'Rourke and M. Hamada, 2/17/92, (PB92-197250, A20, MF-A04).

NCEER-92-0003 "Issues in Earthquake Education," Edited by K. Ross, 2/3/92, (PB92-222389, A07, MF-A02).

NCEER-92-0004 "Proceedings from the First U.S. - Japan Workshop on Earthquake Protective Systems for Bridges," Edited by I.G. Buckle, 2/4/92, (PB94-142239, A99, MF-A06).

NCEER-92-0005 "Seismic Ground Motion from a Haskell-Type Source in a Multiple-Layered Half-Space," A.P. Theoharis, G. Deodatis and M. Shinozuka, 1/2/92, not available.

NCEER-92-0006 "Proceedings from the Site Effects Workshop," Edited by R. Whitman, 2/29/92, (PB92-197201, A04, MF-A01).

NCEER-92-0007 "Engineering Evaluation of Permanent Ground Deformations Due to Seismically-Induced Liquefaction," by M.H. Baziar, R. Dobry and A-W.M. Elgamal, 3/24/92, (PB92-222421, A13, MF-A03).

NCEER-92-0008 "A Procedure for the Seismic Evaluation of Buildings in the Central and Eastern United States," by C.D. Poland and J.O. Malley, 4/2/92, (PB92-222439, A20, MF-A04).

NCEER-92-0009 "Experimental and Analytical Study of a Hybrid Isolation System Using Friction Controllable Sliding Bearings," by M.Q. Feng, S. Fujii and M. Shinozuka, 5/15/92, (PB93-150282, A06, MF-A02).

NCEER-92-0010 "Seismic Resistance of Slab-Column Connections in Existing Non-Ductile Flat-Plate Buildings," by A.J. Durrani and Y. Du, 5/18/92, (PB93-116812, A06, MF-A02).

NCEER-92-0011 "The Hysteretic and Dynamic Behavior of Brick Masonry Walls Upgraded by Ferrocement Coatings Under Cyclic Loading and Strong Simulated Ground Motion," by H. Lee and S.P. Prawel, 5/11/92, not available.

NCEER-92-0012 "Study of Wire Rope Systems for Seismic Protection of Equipment in Buildings," by G.F. Demetriades, M.C. Constantinou and A.M. Reinhorn, 5/20/92, (PB93-116655, A08, MF-A02).

NCEER-92-0013 "Shape Memory Structural Dampers: Material Properties, Design and Seismic Testing," by P.R. Witting and F.A. Cozzarelli, 5/26/92, (PB93-116663, A05, MF-A01).

NCEER-92-0014 "Longitudinal Permanent Ground Deformation Effects on Buried Continuous Pipelines," by M.J. O'Rourke, and C. Nordberg, 6/15/92, (PB93-116671, A08, MF-A02).

NCEER-92-0015 "A Simulation Method for Stationary Gaussian Random Functions Based on the Sampling Theorem," by M. Grigoriu and S. Balopoulou, 6/11/92, (PB93-127496, A05, MF-A01).

NCEER-92-0016 "Gravity-Load-Designed Reinforced Concrete Buildings: Seismic Evaluation of Existing Construction and Detailing Strategies for Improved Seismic Resistance," by G.W. Hoffmann, S.K. Kunnath, A.M. Reinhorn and J.B. Mander, 7/15/92, (PB94-142007, A08, MF-A02).

NCEER-92-0017 "Observations on Water System and Pipeline Performance in the Limón Area of Costa Rica Due to the April 22, 1991 Earthquake," by M. O'Rourke and D. Ballantyne, 6/30/92, (PB93-126811, A06, MF-A02).

NCEER-92-0018 "Fourth Edition of Earthquake Education Materials for Grades K-12," Edited by K.E.K. Ross, 8/10/92, (PB93-114023, A07, MF-A02).

NCEER-92-0019 "Proceedings from the Fourth Japan-U.S. Workshop on Earthquake Resistant Design of Lifeline Facilities and Countermeasures for Soil Liquefaction," Edited by M. Hamada and T.D. O'Rourke, 8/12/92, (PB93-163939, A99, MF-E11).

NCEER-92-0020 "Active Bracing System: A Full Scale Implementation of Active Control," by A.M. Reinhorn, T.T. Soong, R.C. Lin, M.A. Riley, Y.P. Wang, S. Aizawa and M. Higashino, 8/14/92, (PB93-127512, A06, MF-A02).

NCEER-92-0021 "Empirical Analysis of Horizontal Ground Displacement Generated by Liquefaction-Induced Lateral Spreads," by S.F. Bartlett and T.L. Youd, 8/17/92, (PB93-188241, A06, MF-A02).

NCEER-92-0022 "IDARC Version 3.0: Inelastic Damage Analysis of Reinforced Concrete Structures," by S.K. Kunnath, A.M. Reinhorn and R.F. Lobo, 8/31/92, (PB93-227502, A07, MF-A02).

NCEER-92-0023 "A Semi-Empirical Analysis of Strong-Motion Peaks in Terms of Seismic Source, Propagation Path and Local Site Conditions, by M. Kamiyama, M.J. O'Rourke and R. Flores-Berrones, 9/9/92, (PB93-150266, A08, MF-A02).

NCEER-92-0024 "Seismic Behavior of Reinforced Concrete Frame Structures with Nonductile Details, Part I: Summary of Experimental Findings of Full Scale Beam-Column Joint Tests," by A. Beres, R.N. White and P. Gergely, 9/30/92, (PB93-227783, A05, MF-A01).

NCEER-92-0025 "Experimental Results of Repaired and Retrofitted Beam-Column Joint Tests in Lightly Reinforced Concrete Frame Buildings," by A. Beres, S. El-Borgi, R.N. White and P. Gergely, 10/29/92, (PB93-227791, A05, MF-A01).

NCEER-92-0026 "A Generalization of Optimal Control Theory: Linear and Nonlinear Structures," by J.N. Yang, Z. Li and S. Vongchavalitkul, 11/2/92, (PB93-188621, A05, MF-A01).

NCEER-92-0027 "Seismic Resistance of Reinforced Concrete Frame Structures Designed Only for Gravity Loads: Part I - Design and Properties of a One-Third Scale Model Structure," by J.M. Bracci, A.M. Reinhorn and J.B. Mander, 12/1/92, (PB94-104502, A08, MF-A02).

NCEER-92-0028 "Seismic Resistance of Reinforced Concrete Frame Structures Designed Only for Gravity Loads: Part II - Experimental Performance of Subassemblages," by L.E. Aycardi, J.B. Mander and A.M. Reinhorn, 12/1/92, (PB94-104510, A08, MF-A02).

NCEER-92-0029 "Seismic Resistance of Reinforced Concrete Frame Structures Designed Only for Gravity Loads: Part III - Experimental Performance and Analytical Study of a Structural Model," by J.M. Bracci, A.M. Reinhorn and J.B. Mander, 12/1/92, (PB93-227528, A09, MF-A01).

NCEER-92-0030 "Evaluation of Seismic Retrofit of Reinforced Concrete Frame Structures: Part I - Experimental Performance of Retrofitted Subassemblages," by D. Choudhuri, J.B. Mander and A.M. Reinhorn, 12/8/92, (PB93-198307, A07, MF-A02).

NCEER-92-0031 "Evaluation of Seismic Retrofit of Reinforced Concrete Frame Structures: Part II - Experimental Performance and Analytical Study of a Retrofitted Structural Model," by J.M. Bracci, A.M. Reinhorn and J.B. Mander, 12/8/92, (PB93-198315, A09, MF-A03).

NCEER-92-0032 "Experimental and Analytical Investigation of Seismic Response of Structures with Supplemental Fluid Viscous Dampers," by M.C. Constantinou and M.D. Symans, 12/21/92, (PB93-191435, A10, MF-A03). This report is available only through NTIS (see address given above).

NCEER-92-0033 "Reconnaissance Report on the Cairo, Egypt Earthquake of October 12, 1992," by M. Khater, 12/23/92, (PB93-188621, A03, MF-A01).

NCEER-92-0034 "Low-Level Dynamic Characteristics of Four Tall Flat-Plate Buildings in New York City," by H. Gavin, S. Yuan, J. Grossman, E. Pekelis and K. Jacob, 12/28/92, (PB93-188217, A07, MF-A02).

NCEER-93-0001 "An Experimental Study on the Seismic Performance of Brick-Infilled Steel Frames With and Without Retrofit," by J.B. Mander, B. Nair, K. Wojtkowski and J. Ma, 1/29/93, (PB93-227510, A07, MF-A02).

NCEER-93-0002 "Social Accounting for Disaster Preparedness and Recovery Planning," by S. Cole, E. Pantoja and V. Razak, 2/22/93, (PB94-142114, A12, MF-A03).

NCEER-93-0003 "Assessment of 1991 NEHRP Provisions for Nonstructural Components and Recommended Revisions," by T.T. Soong, G. Chen, Z. Wu, R-H. Zhang and M. Grigoriu, 3/1/93, (PB93-188639, A06, MF-A02).

NCEER-93-0004 "Evaluation of Static and Response Spectrum Analysis Procedures of SEAOC/UBC for Seismic Isolated Structures," by C.W. Winters and M.C. Constantinou, 3/23/93, (PB93-198299, A10, MF-A03).

NCEER-93-0005 "Earthquakes in the Northeast - Are We Ignoring the Hazard? A Workshop on Earthquake Science and Safety for Educators," edited by K.E.K. Ross, 4/2/93, (PB94-103066, A09, MF-A02).

NCEER-93-0006 "Inelastic Response of Reinforced Concrete Structures with Viscoelastic Braces," by R.F. Lobo, J.M. Bracci, K.L. Shen, A.M. Reinhorn and T.T. Soong, 4/5/93, (PB93-227486, A05, MF-A02).

NCEER-93-0007 "Seismic Testing of Installation Methods for Computers and Data Processing Equipment," by K. Kosar, T.T. Soong, K.L. Shen, J.A. HoLung and Y.K. Lin, 4/12/93, (PB93-198299, A07, MF-A02).

NCEER-93-0008 "Retrofit of Reinforced Concrete Frames Using Added Dampers," by A. Reinhorn, M. Constantinou and C. Li, not available.

NCEER-93-0009 "Seismic Behavior and Design Guidelines for Steel Frame Structures with Added Viscoelastic Dampers," by K.C. Chang, M.L. Lai, T.T. Soong, D.S. Hao and Y.C. Yeh, 5/1/93, (PB94-141959, A07, MF-A02).

NCEER-93-0010 "Seismic Performance of Shear-Critical Reinforced Concrete Bridge Piers," by J.B. Mander, S.M. Waheed, M.T.A. Chaudhary and S.S. Chen, 5/12/93, (PB93-227494, A08, MF-A02).

NCEER-93-0011 "3D-BASIS-TABS: Computer Program for Nonlinear Dynamic Analysis of Three Dimensional Base Isolated Structures," by S. Nagarajaiah, C. Li, A.M. Reinhorn and M.C. Constantinou, 8/2/93, (PB94-141819, A09, MF-A02).

NCEER-93-0012 "Effects of Hydrocarbon Spills from an Oil Pipeline Break on Ground Water," by O.J. Helweg and H.H.M. Hwang, 8/3/93, (PB94-141942, A06, MF-A02).

NCEER-93-0013 "Simplified Procedures for Seismic Design of Nonstructural Components and Assessment of Current Code Provisions," by M.P. Singh, L.E. Suarez, E.E. Matheu and G.O. Maldonado, 8/4/93, (PB94-141827, A09, MF-A02).

NCEER-93-0014 "An Energy Approach to Seismic Analysis and Design of Secondary Systems," by G. Chen and T.T. Soong, 8/6/93, (PB94-142767, A11, MF-A03).

NCEER-93-0015 "Proceedings from School Sites: Becoming Prepared for Earthquakes - Commemorating the Third Anniversary of the Loma Prieta Earthquake," Edited by F.E. Winslow and K.E.K. Ross, 8/16/93, (PB94-154275, A16, MF-A02).

NCEER-93-0016 "Reconnaissance Report of Damage to Historic Monuments in Cairo, Egypt Following the October 12, 1992 Dahshur Earthquake," by D. Sykora, D. Look, G. Croci, E. Karaesmen and E. Karaesmen, 8/19/93, (PB94-142221, A08, MF-A02).

NCEER-93-0017 "The Island of Guam Earthquake of August 8, 1993," by S.W. Swan and S.K. Harris, 9/30/93, (PB94-141843, A04, MF-A01).

NCEER-93-0018 "Engineering Aspects of the October 12, 1992 Egyptian Earthquake," by A.W. Elgamal, M. Amer, K. Adalier and A. Abul-Fadl, 10/7/93, (PB94-141983, A05, MF-A01).

NCEER-93-0019 "Development of an Earthquake Motion Simulator and its Application in Dynamic Centrifuge Testing," by I. Krstelj, Supervised by J.H. Prevost, 10/23/93, (PB94-181773, A-10, MF-A03).

NCEER-93-0020 "NCEER-Taisei Corporation Research Program on Sliding Seismic Isolation Systems for Bridges: Experimental and Analytical Study of a Friction Pendulum System (FPS)," by M.C. Constantinou, P. Tsopelas, Y-S. Kim and S. Okamoto, 11/1/93, (PB94-142775, A08, MF-A02).

NCEER-93-0021 "Finite Element Modeling of Elastomeric Seismic Isolation Bearings," by L.J. Billings, Supervised by R. Shepherd, 11/8/93, not available.

NCEER-93-0022 "Seismic Vulnerability of Equipment in Critical Facilities: Life-Safety and Operational Consequences," by K. Porter, G.S. Johnson, M.M. Zadeh, C. Scawthorn and S. Eder, 11/24/93, (PB94-181765, A16, MF-A03).

NCEER-93-0023 "Hokkaido Nansei-oki, Japan Earthquake of July 12, 1993, by P.I. Yanev and C.R. Scawthorn, 12/23/93, (PB94-181500, A07, MF-A01).

NCEER-94-0001 "An Evaluation of Seismic Serviceability of Water Supply Networks with Application to the San Francisco Auxiliary Water Supply System," by I. Markov, Supervised by M. Grigoriu and T. O'Rourke, 1/21/94, (PB94-204013, A07, MF-A02).

NCEER-94-0002 "NCEER-Taisei Corporation Research Program on Sliding Seismic Isolation Systems for Bridges: Experimental and Analytical Study of Systems Consisting of Sliding Bearings, Rubber Restoring Force Devices and Fluid Dampers," Volumes I and II, by P. Tsopelas, S. Okamoto, M.C. Constantinou, D. Ozaki and S. Fujii, 2/4/94, (PB94-181740, A09, MF-A02 and PB94-181757, A12, MF-A03).

NCEER-94-0003 "A Markov Model for Local and Global Damage Indices in Seismic Analysis," by S. Rahman and M. Grigoriu, 2/18/94, (PB94-206000, A12, MF-A03).

NCEER-94-0004 "Proceedings from the NCEER Workshop on Seismic Response of Masonry Infills," edited by D.P. Abrams, 3/1/94, (PB94-180783, A07, MF-A02).

NCEER-94-0005 "The Northridge, California Earthquake of January 17, 1994: General Reconnaissance Report," edited by J.D. Goltz, 3/11/94, (PB94-193943, A10, MF-A03).

NCEER-94-0006 "Seismic Energy Based Fatigue Damage Analysis of Bridge Columns: Part I - Evaluation of Seismic Capacity," by G.A. Chang and J.B. Mander, 3/14/94, (PB94-219185, A11, MF-A03).

NCEER-94-0007 "Seismic Isolation of Multi-Story Frame Structures Using Spherical Sliding Isolation Systems," by T.M. Al-Hussaini, V.A. Zayas and M.C. Constantinou, 3/17/94, (PB94-193745, A09, MF-A02).

NCEER-94-0008 "The Northridge, California Earthquake of January 17, 1994: Performance of Highway Bridges," edited by I.G. Buckle, 3/24/94, (PB94-193851, A06, MF-A02).

NCEER-94-0009 "Proceedings of the Third U.S.-Japan Workshop on Earthquake Protective Systems for Bridges," edited by I.G. Buckle and I. Friedland, 3/31/94, (PB94-195815, A99, MF-A06).

NCEER-94-0010 "3D-BASIS-ME: Computer Program for Nonlinear Dynamic Analysis of Seismically Isolated Single and Multiple Structures and Liquid Storage Tanks," by P.C. Tsopelas, M.C. Constantinou and A.M. Reinhorn, 4/12/94, (PB94-204922, A09, MF-A02).

NCEER-94-0011 "The Northridge, California Earthquake of January 17, 1994: Performance of Gas Transmission Pipelines," by T.D. O'Rourke and M.C. Palmer, 5/16/94, (PB94-204989, A05, MF-A01).

NCEER-94-0012 "Feasibility Study of Replacement Procedures and Earthquake Performance Related to Gas Transmission Pipelines," by T.D. O'Rourke and M.C. Palmer, 5/25/94, (PB94-206638, A09, MF-A02).

NCEER-94-0013 "Seismic Energy Based Fatigue Damage Analysis of Bridge Columns: Part II - Evaluation of Seismic Demand," by G.A. Chang and J.B. Mander, 6/1/94, (PB95-18106, A08, MF-A02).

NCEER-94-0014 "NCEER-Taisei Corporation Research Program on Sliding Seismic Isolation Systems for Bridges: Experimental and Analytical Study of a System Consisting of Sliding Bearings and Fluid Restoring Force/Damping Devices," by P. Tsopelas and M.C. Constantinou, 6/13/94, (PB94-219144, A10, MF-A03).

NCEER-94-0015 "Generation of Hazard-Consistent Fragility Curves for Seismic Loss Estimation Studies," by H. Hwang and J-R. Huo, 6/14/94, (PB95-181996, A09, MF-A02).

NCEER-94-0016 "Seismic Study of Building Frames with Added Energy-Absorbing Devices," by W.S. Pong, C.S. Tsai and G.C. Lee, 6/20/94, (PB94-219136, A10, A03).

NCEER-94-0017 "Sliding Mode Control for Seismic-Excited Linear and Nonlinear Civil Engineering Structures," by J. Yang, J. Wu, A. Agrawal and Z. Li, 6/21/94, (PB95-138483, A06, MF-A02).

NCEER-94-0018 "3D-BASIS-TABS Version 2.0: Computer Program for Nonlinear Dynamic Analysis of Three Dimensional Base Isolated Structures," by A.M. Reinhorn, S. Nagarajaiah, M.C. Constantinou, P. Tsopelas and R. Li, 6/22/94, (PB95-182176, A08, MF-A02).

NCEER-94-0019 "Proceedings of the International Workshop on Civil Infrastructure Systems: Application of Intelligent Systems and Advanced Materials on Bridge Systems," Edited by G.C. Lee and K.C. Chang, 7/18/94, (PB95-252474, A20, MF-A04).

NCEER-94-0020 "Study of Seismic Isolation Systems for Computer Floors," by V. Lambrou and M.C. Constantinou, 7/19/94, (PB95-138533, A10, MF-A03).

NCEER-94-0021 "Proceedings of the U.S.-Italian Workshop on Guidelines for Seismic Evaluation and Rehabilitation of Unreinforced Masonry Buildings," Edited by D.P. Abrams and G.M. Calvi, 7/20/94, (PB95-138749, A13, MF-A03).

NCEER-94-0022 "NCEER-Taisei Corporation Research Program on Sliding Seismic Isolation Systems for Bridges: Experimental and Analytical Study of a System Consisting of Lubricated PTFE Sliding Bearings and Mild Steel Dampers," by P. Tsopelas and M.C. Constantinou, 7/22/94, (PB95-182184, A08, MF-A02).

NCEER-94-0023 "Development of Reliability-Based Design Criteria for Buildings Under Seismic Load," by Y.K. Wen, H. Hwang and M. Shinozuka, 8/1/94, (PB95-211934, A08, MF-A02).

NCEER-94-0024 "Experimental Verification of Acceleration Feedback Control Strategies for an Active Tendon System," by S.J. Dyke, B.F. Spencer, Jr., P. Quast, M.K. Sain, D.C. Kaspari, Jr. and T.T. Soong, 8/29/94, (PB95-212320, A05, MF-A01).

NCEER-94-0025 "Seismic Retrofitting Manual for Highway Bridges," Edited by I.G. Buckle and I.F. Friedland, published by the Federal Highway Administration (PB95-212676, A15, MF-A03).

NCEER-94-0026 "Proceedings from the Fifth U.S.-Japan Workshop on Earthquake Resistant Design of Lifeline Facilities and Countermeasures Against Soil Liquefaction," Edited by T.D. O'Rourke and M. Hamada, 11/7/94, (PB95-220802, A99, MF-E08).

NCEER-95-0001 "Experimental and Analytical Investigation of Seismic Retrofit of Structures with Supplemental Damping: Part 1 - Fluid Viscous Damping Devices," by A.M. Reinhorn, C. Li and M.C. Constantinou, 1/3/95, (PB95-266599, A09, MF-A02).

NCEER-95-0002 "Experimental and Analytical Study of Low-Cycle Fatigue Behavior of Semi-Rigid Top-And-Seat Angle Connections," by G. Pekcan, J.B. Mander and S.S. Chen, 1/5/95, (PB95-220042, A07, MF-A02).

NCEER-95-0003 "NCEER-ATC Joint Study on Fragility of Buildings," by T. Anagnos, C. Rojahn and A.S. Kiremidjian, 1/20/95, (PB95-220026, A06, MF-A02).

NCEER-95-0004 "Nonlinear Control Algorithms for Peak Response Reduction," by Z. Wu, T.T. Soong, V. Gattulli and R.C. Lin, 2/16/95, (PB95-220349, A05, MF-A01).

NCEER-95-0005 "Pipeline Replacement Feasibility Study: A Methodology for Minimizing Seismic and Corrosion Risks to Underground Natural Gas Pipelines," by R.T. Eguchi, H.A. Seligson and D.G. Honegger, 3/2/95, (PB95-252326, A06, MF-A02).

NCEER-95-0006 "Evaluation of Seismic Performance of an 11-Story Frame Building During the 1994 Northridge Earthquake," by F. Naeim, R. DiSulio, K. Benuska, A. Reinhorn and C. Li, not available.

NCEER-95-0007 "Prioritization of Bridges for Seismic Retrofitting," by N. Basöz and A.S. Kiremidjian, 4/24/95, (PB95-252300, A08, MF-A02).

NCEER-95-0008 "Method for Developing Motion Damage Relationships for Reinforced Concrete Frames," by A. Singhal and A.S. Kiremidjian, 5/11/95, (PB95-266607, A06, MF-A02).

NCEER-95-0009 "Experimental and Analytical Investigation of Seismic Retrofit of Structures with Supplemental Damping: Part II - Friction Devices," by C. Li and A.M. Reinhorn, 7/6/95, (PB96-128087, A11, MF-A03).

NCEER-95-0010 "Experimental Performance and Analytical Study of a Non-Ductile Reinforced Concrete Frame Structure Retrofitted with Elastomeric Spring Dampers," by G. Pekcan, J.B. Mander and S.S. Chen, 7/14/95, (PB96-137161, A08, MF-A02).

NCEER-95-0011 "Development and Experimental Study of Semi-Active Fluid Damping Devices for Seismic Protection of Structures," by M.D. Symans and M.C. Constantinou, 8/3/95, (PB96-136940, A23, MF-A04).

NCEER-95-0012 "Real-Time Structural Parameter Modification (RSPM): Development of Innervated Structures," by Z. Liang, M. Tong and G.C. Lee, 4/11/95, (PB96-137153, A06, MF-A01).

NCEER-95-0013 "Experimental and Analytical Investigation of Seismic Retrofit of Structures with Supplemental Damping: Part III - Viscous Damping Walls," by A.M. Reinhorn and C. Li, 10/1/95, (PB96-176409, A11, MF-A03).

NCEER-95-0014 "Seismic Fragility Analysis of Equipment and Structures in a Memphis Electric Substation," by J-R. Huo and H.H.M. Hwang, 8/10/95, (PB96-128087, A09, MF-A02).

NCEER-95-0015 "The Hanshin-Awaji Earthquake of January 17, 1995: Performance of Lifelines," Edited by M. Shinozuka, 11/3/95, (PB96-176383, A15, MF-A03).

NCEER-95-0016 "Highway Culvert Performance During Earthquakes," by T.L. Youd and C.J. Beckman, available as NCEER-96-0015.

NCEER-95-0017 "The Hanshin-Awaji Earthquake of January 17, 1995: Performance of Highway Bridges," Edited by I.G. Buckle, 12/1/95, not available.

NCEER-95-0018 "Modeling of Masonry Infill Panels for Structural Analysis," by A.M. Reinhorn, A. Madan, R.E. Valles, Y. Reichmann and J.B. Mander, 12/8/95, (PB97-110886, MF-A01, A06).

NCEER-95-0019 "Optimal Polynomial Control for Linear and Nonlinear Structures," by A.K. Agrawal and J.N. Yang, 12/11/95, (PB96-168737, A07, MF-A02).

NCEER-95-0020 "Retrofit of Non-Ductile Reinforced Concrete Frames Using Friction Dampers," by R.S. Rao, P. Gergely and R.N. White, 12/22/95, (PB97-133508, A10, MF-A02).

NCEER-95-0021 "Parametric Results for Seismic Response of Pile-Supported Bridge Bents," by G. Mylonakis, A. Nikolaou and G. Gazetas, 12/22/95, (PB97-100242, A12, MF-A03).

NCEER-95-0022 "Kinematic Bending Moments in Seismically Stressed Piles," by A. Nikolaou, G. Mylonakis and G. Gazetas, 12/23/95, (PB97-113914, MF-A03, A13).

NCEER-96-0001 "Dynamic Response of Unreinforced Masonry Buildings with Flexible Diaphragms," by A.C. Costley and D.P. Abrams," 10/10/96, (PB97-133573, MF-A03, A15).

NCEER-96-0002 "State of the Art Review: Foundations and Retaining Structures," by I. Po Lam, not available.

NCEER-96-0003 "Ductility of Rectangular Reinforced Concrete Bridge Columns with Moderate Confinement," by N. Wehbe, M. Saiidi, D. Sanders and B. Douglas, 11/7/96, (PB97-133557, A06, MF-A02).

NCEER-96-0004 "Proceedings of the Long-Span Bridge Seismic Research Workshop," edited by I.G. Buckle and I.M. Friedland, not available.

NCEER-96-0005 "Establish Representative Pier Types for Comprehensive Study: Eastern United States," by J. Kulicki and Z. Prucz, 5/28/96, (PB98-119217, A07, MF-A02).

NCEER-96-0006 "Establish Representative Pier Types for Comprehensive Study: Western United States," by R. Imbsen, R.A. Schamber and T.A. Osterkamp, 5/28/96, (PB98-118607, A07, MF-A02).

NCEER-96-0007 "Nonlinear Control Techniques for Dynamical Systems with Uncertain Parameters," by R.G. Ghanem and M.I. Bujakov, 5/27/96, (PB97-100259, A17, MF-A03).

NCEER-96-0008 "Seismic Evaluation of a 30-Year Old Non-Ductile Highway Bridge Pier and Its Retrofit," by J.B. Mander, B. Mahmoodzadegan, S. Bhadra and S.S. Chen, 5/31/96, (PB97-110902, MF-A03, A10).

NCEER-96-0009 "Seismic Performance of a Model Reinforced Concrete Bridge Pier Before and After Retrofit," by J.B. Mander, J.H. Kim and C.A. Ligozio, 5/31/96, (PB97-110910, MF-A02, A10).

NCEER-96-0010 "IDARC2D Version 4.0: A Computer Program for the Inelastic Damage Analysis of Buildings," by R.E. Valles, A.M. Reinhorn, S.K. Kunnath, C. Li and A. Madan, 6/3/96, (PB97-100234, A17, MF-A03).

NCEER-96-0011 "Estimation of the Economic Impact of Multiple Lifeline Disruption: Memphis Light, Gas and Water Division Case Study," by S.E. Chang, H.A. Seligson and R.T. Eguchi, 8/16/96, (PB97-133490, A11, MF-A03).

NCEER-96-0012 "Proceedings from the Sixth Japan-U.S. Workshop on Earthquake Resistant Design of Lifeline Facilities and Countermeasures Against Soil Liquefaction, Edited by M. Hamada and T. O'Rourke, 9/11/96, (PB97-133581, A99, MF-A06).

NCEER-96-0013 "Chemical Hazards, Mitigation and Preparedness in Areas of High Seismic Risk: A Methodology for Estimating the Risk of Post-Earthquake Hazardous Materials Release," by H.A. Seligson, R.T. Eguchi, K.J. Tierney and K. Richmond, 11/7/96, (PB97-133565, MF-A02, A08).

NCEER-96-0014 "Response of Steel Bridge Bearings to Reversed Cyclic Loading," by J.B. Mander, D-K. Kim, S.S. Chen and G.J. Premus, 11/13/96, (PB97-140735, A12, MF-A03).

NCEER-96-0015 "Highway Culvert Performance During Past Earthquakes," by T.L. Youd and C.J. Beckman, 11/25/96, (PB97-133532, A06, MF-A01).

NCEER-97-0001 "Evaluation, Prevention and Mitigation of Pounding Effects in Building Structures," by R.E. Valles and A.M. Reinhorn, 2/20/97, (PB97-159552, A14, MF-A03).

NCEER-97-0002 "Seismic Design Criteria for Bridges and Other Highway Structures," by C. Rojahn, R. Mayes, D.G. Anderson, J. Clark, J.H. Hom, R.V. Nutt and M.J. O'Rourke, 4/30/97, (PB97-194658, A06, MF-A03).

NCEER-97-0003 "Proceedings of the U.S.-Italian Workshop on Seismic Evaluation and Retrofit," Edited by D.P. Abrams and G.M. Calvi, 3/19/97, (PB97-194666, A13, MF-A03).

NCEER-97-0004 "Investigation of Seismic Response of Buildings with Linear and Nonlinear Fluid Viscous Dampers," by A.A. Seleemah and M.C. Constantinou, 5/21/97, (PB98-109002, A15, MF-A03).

NCEER-97-0005 "Proceedings of the Workshop on Earthquake Engineering Frontiers in Transportation Facilities," edited by G.C. Lee and I.M. Friedland, 8/29/97, (PB98-128911, A25, MR-A04).

NCEER-97-0006 "Cumulative Seismic Damage of Reinforced Concrete Bridge Piers," by S.K. Kunnath, A. El-Bahy, A. Taylor and W. Stone, 9/2/97, (PB98-108814, A11, MF-A03).

NCEER-97-0007 "Structural Details to Accommodate Seismic Movements of Highway Bridges and Retaining Walls," by R.A. Imbsen, R.A. Schamber, E. Thorkildsen, A. Kartoum, B.T. Martin, T.N. Rosser and J.M. Kulicki, 9/3/97, (PB98-108996, A09, MF-A02).

NCEER-97-0008 "A Method for Earthquake Motion-Damage Relationships with Application to Reinforced Concrete Frames," by A. Singhal and A.S. Kiremidjian, 9/10/97, (PB98-108988, A13, MF-A03).

NCEER-97-0009 "Seismic Analysis and Design of Bridge Abutments Considering Sliding and Rotation," by K. Fishman and R. Richards, Jr., 9/15/97, (PB98-108897, A06, MF-A02).

NCEER-97-0010 "Proceedings of the FHWA/NCEER Workshop on the National Representation of Seismic Ground Motion for New and Existing Highway Facilities," edited by I.M. Friedland, M.S. Power and R.L. Mayes, 9/22/97, (PB98-128903, A21, MF-A04).

NCEER-97-0011 "Seismic Analysis for Design or Retrofit of Gravity Bridge Abutments," by K.L. Fishman, R. Richards, Jr. and R.C. Divito, 10/2/97, (PB98-128937, A08, MF-A02).

NCEER-97-0012 "Evaluation of Simplified Methods of Analysis for Yielding Structures," by P. Tsopelas, M.C. Constantinou, C.A. Kircher and A.S. Whittaker, 10/31/97, (PB98-128929, A10, MF-A03).

NCEER-97-0013 "Seismic Design of Bridge Columns Based on Control and Repairability of Damage," by C-T. Cheng and J.B. Mander, 12/8/97, (PB98-144249, A11, MF-A03).

NCEER-97-0014 "Seismic Resistance of Bridge Piers Based on Damage Avoidance Design," by J.B. Mander and C-T. Cheng, 12/10/97, (PB98-144223, A09, MF-A02).

NCEER-97-0015 "Seismic Response of Nominally Symmetric Systems with Strength Uncertainty," by S. Balopoulou and M. Grigoriu, 12/23/97, (PB98-153422, A11, MF-A03).

NCEER-97-0016 "Evaluation of Seismic Retrofit Methods for Reinforced Concrete Bridge Columns," by T.J. Wipf, F.W. Klaiber and F.M. Russo, 12/28/97, (PB98-144215, A12, MF-A03).

NCEER-97-0017 "Seismic Fragility of Existing Conventional Reinforced Concrete Highway Bridges," by C.L. Mullen and A.S. Cakmak, 12/30/97, (PB98-153406, A08, MF-A02).

NCEER-97-0018 "Loss Asssessment of Memphis Buildings," edited by D.P. Abrams and M. Shinozuka, 12/31/97, (PB98-144231, A13, MF-A03).

NCEER-97-0019 "Seismic Evaluation of Frames with Infill Walls Using Quasi-static Experiments," by K.M. Mosalam, R.N. White and P. Gergely, 12/31/97, (PB98-153455, A07, MF-A02).

NCEER-97-0020 "Seismic Evaluation of Frames with Infill Walls Using Pseudo-dynamic Experiments," by K.M. Mosalam, R.N. White and P. Gergely, 12/31/97, (PB98-153430, A07, MF-A02).

NCEER-97-0021 "Computational Strategies for Frames with Infill Walls: Discrete and Smeared Crack Analyses and Seismic Fragility," by K.M. Mosalam, R.N. White and P. Gergely, 12/31/97, (PB98-153414, A10, MF-A02).

NCEER-97-0022 "Proceedings of the NCEER Workshop on Evaluation of Liquefaction Resistance of Soils," edited by T.L. Youd and I.M. Idriss, 12/31/97, (PB98-155617, A15, MF-A03).

MCEER-98-0001 "Extraction of Nonlinear Hysteretic Properties of Seismically Isolated Bridges from Quick-Release Field Tests," by Q. Chen, B.M. Douglas, E.M. Maragakis and I.G. Buckle, 5/26/98, (PB99-118838, A06, MF-A01).

MCEER-98-0002 "Methodologies for Evaluating the Importance of Highway Bridges," by A. Thomas, S. Eshenaur and J. Kulicki, 5/29/98, (PB99-118846, A10, MF-A02).

MCEER-98-0003 "Capacity Design of Bridge Piers and the Analysis of Overstrength," by J.B. Mander, A. Dutta and P. Goel, 6/1/98, (PB99-118853, A09, MF-A02).

MCEER-98-0004 "Evaluation of Bridge Damage Data from the Loma Prieta and Northridge, California Earthquakes," by N. Basoz and A. Kiremidjian, 6/2/98, (PB99-118861, A15, MF-A03).

MCEER-98-0005 "Screening Guide for Rapid Assessment of Liquefaction Hazard at Highway Bridge Sites," by T. L. Youd, 6/16/98, (PB99-118879, A06, not available on microfiche).

MCEER-98-0006 "Structural Steel and Steel/Concrete Interface Details for Bridges," by P. Ritchie, N. Kauhl and J. Kulicki, 7/13/98, (PB99-118945, A06, MF-A01).

MCEER-98-0007 "Capacity Design and Fatigue Analysis of Confined Concrete Columns," by A. Dutta and J.B. Mander, 7/14/98, (PB99-118960, A14, MF-A03).

MCEER-98-0008 "Proceedings of the Workshop on Performance Criteria for Telecommunication Services Under Earthquake Conditions," edited by A.J. Schiff, 7/15/98, (PB99-118952, A08, MF-A02).

MCEER-98-0009 "Fatigue Analysis of Unconfined Concrete Columns," by J.B. Mander, A. Dutta and J.H. Kim, 9/12/98, (PB99-123655, A10, MF-A02).

MCEER-98-0010 "Centrifuge Modeling of Cyclic Lateral Response of Pile-Cap Systems and Seat-Type Abutments in Dry Sands," by A.D. Gadre and R. Dobry, 10/2/98, (PB99-123606, A13, MF-A03).

MCEER-98-0011 "IDARC-BRIDGE: A Computational Platform for Seismic Damage Assessment of Bridge Structures," by A.M. Reinhorn, V. Simeonov, G. Mylonakis and Y. Reichman, 10/2/98, (PB99-162919, A15, MF-A03).

MCEER-98-0012 "Experimental Investigation of the Dynamic Response of Two Bridges Before and After Retrofitting with Elastomeric Bearings," by D.A. Wendichansky, S.S. Chen and J.B. Mander, 10/2/98, (PB99-162927, A15, MF-A03).

MCEER-98-0013 "Design Procedures for Hinge Restrainers and Hinge Sear Width for Multiple-Frame Bridges," by R. Des Roches and G.L. Fenves, 11/3/98, (PB99-140477, A13, MF-A03).

MCEER-98-0014 "Response Modification Factors for Seismically Isolated Bridges," by M.C. Constantinou and J.K. Quarshie, 11/3/98, (PB99-140485, A14, MF-A03).

MCEER-98-0015 "Proceedings of the U.S.-Italy Workshop on Seismic Protective Systems for Bridges," edited by I.M. Friedland and M.C. Constantinou, 11/3/98, (PB2000-101711, A22, MF-A04).

MCEER-98-0016 "Appropriate Seismic Reliability for Critical Equipment Systems: Recommendations Based on Regional Analysis of Financial and Life Loss," by K. Porter, C. Scawthorn, C. Taylor and N. Blais, 11/10/98, (PB99-157265, A08, MF-A02).

MCEER-98-0017 "Proceedings of the U.S. Japan Joint Seminar on Civil Infrastructure Systems Research," edited by M. Shinozuka and A. Rose, 11/12/98, (PB99-156713, A16, MF-A03).

MCEER-98-0018 "Modeling of Pile Footings and Drilled Shafts for Seismic Design," by I. PoLam, M. Kapuskar and D. Chaudhuri, 12/21/98, (PB99-157257, A09, MF-A02).

MCEER-99-0001 "Seismic Evaluation of a Masonry Infilled Reinforced Concrete Frame by Pseudodynamic Testing," by S.G. Buonopane and R.N. White, 2/16/99, (PB99-162851, A09, MF-A02).

MCEER-99-0002 "Response History Analysis of Structures with Seismic Isolation and Energy Dissipation Systems: Verification Examples for Program SAP2000," by J. Scheller and M.C. Constantinou, 2/22/99, (PB99-162869, A08, MF-A02).

MCEER-99-0003 "Experimental Study on the Seismic Design and Retrofit of Bridge Columns Including Axial Load Effects," by A. Dutta, T. Kokorina and J.B. Mander, 2/22/99, (PB99-162877, A09, MF-A02).

MCEER-99-0004 "Experimental Study of Bridge Elastomeric and Other Isolation and Energy Dissipation Systems with Emphasis on Uplift Prevention and High Velocity Near-source Seismic Excitation," by A. Kasalanati and M. C. Constantinou, 2/26/99, (PB99-162885, A12, MF-A03).

MCEER-99-0005 "Truss Modeling of Reinforced Concrete Shear-flexure Behavior," by J.H. Kim and J.B. Mander, 3/8/99, (PB99-163693, A12, MF-A03).

MCEER-99-0006 "Experimental Investigation and Computational Modeling of Seismic Response of a 1:4 Scale Model Steel Structure with a Load Balancing Supplemental Damping System," by G. Pekcan, J.B. Mander and S.S. Chen, 4/2/99, (PB99-162893, A11, MF-A03).

MCEER-99-0007 "Effect of Vertical Ground Motions on the Structural Response of Highway Bridges," by M.R. Button, C.J. Cronin and R.L. Mayes, 4/10/99, (PB2000-101411, A10, MF-A03).

MCEER-99-0008 "Seismic Reliability Assessment of Critical Facilities: A Handbook, Supporting Documentation, and Model Code Provisions," by G.S. Johnson, R.E. Sheppard, M.D. Quilici, S.J. Eder and C.R. Scawthorn, 4/12/99, (PB2000-101701, A18, MF-A04).

MCEER-99-0009 "Impact Assessment of Selected MCEER Highway Project Research on the Seismic Design of Highway Structures," by C. Rojahn, R. Mayes, D.G. Anderson, J.H. Clark, D'Appolonia Engineering, S. Gloyd and R.V. Nutt, 4/14/99, (PB99-162901, A10, MF-A02).

MCEER-99-0010 "Site Factors and Site Categories in Seismic Codes," by R. Dobry, R. Ramos and M.S. Power, 7/19/99, (PB2000-101705, A08, MF-A02).

MCEER-99-0011 "Restrainer Design Procedures for Multi-Span Simply-Supported Bridges," by M.J. Randall, M. Saiidi, E. Maragakis and T. Isakovic, 7/20/99, (PB2000-101702, A10, MF-A02).

MCEER-99-0012 "Property Modification Factors for Seismic Isolation Bearings," by M.C. Constantinou, P. Tsopelas, A. Kasalanati and E. Wolff, 7/20/99, (PB2000-103387, A11, MF-A03).

MCEER-99-0013 "Critical Seismic Issues for Existing Steel Bridges," by P. Ritchie, N. Kauhl and J. Kulicki, 7/20/99, (PB2000-101697, A09, MF-A02).

MCEER-99-0014 "Nonstructural Damage Database," by A. Kao, T.T. Soong and A. Vender, 7/24/99, (PB2000-101407, A06, MF-A01).

MCEER-99-0015 "Guide to Remedial Measures for Liquefaction Mitigation at Existing Highway Bridge Sites," by H.G. Cooke and J. K. Mitchell, 7/26/99, (PB2000-101703, A11, MF-A03).

MCEER-99-0016 "Proceedings of the MCEER Workshop on Ground Motion Methodologies for the Eastern United States," edited by N. Abrahamson and A. Becker, 8/11/99, (PB2000-103385, A07, MF-A02).

MCEER-99-0017 "Quindío, Colombia Earthquake of January 25, 1999: Reconnaissance Report," by A.P. Asfura and P.J. Flores, 10/4/99, (PB2000-106893, A06, MF-A01).

MCEER-99-0018 "Hysteretic Models for Cyclic Behavior of Deteriorating Inelastic Structures," by M.V. Sivaselvan and A.M. Reinhorn, 11/5/99, (PB2000-103386, A08, MF-A02).

MCEER-99-0019 "Proceedings of the 7th U.S.- Japan Workshop on Earthquake Resistant Design of Lifeline Facilities and Countermeasures Against Soil Liquefaction," edited by T.D. O'Rourke, J.P. Bardet and M. Hamada, 11/19/99, (PB2000-103354, A99, MF-A06).

MCEER-99-0020 "Development of Measurement Capability for Micro-Vibration Evaluations with Application to Chip Fabrication Facilities," by G.C. Lee, Z. Liang, J.W. Song, J.D. Shen and W.C. Liu, 12/1/99, (PB2000-105993, A08, MF-A02).

MCEER-99-0021 "Design and Retrofit Methodology for Building Structures with Supplemental Energy Dissipating Systems," by G. Pekcan, J.B. Mander and S.S. Chen, 12/31/99, (PB2000-105994, A11, MF-A03).

MCEER-00-0001 "The Marmara, Turkey Earthquake of August 17, 1999: Reconnaissance Report," edited by C. Scawthorn; with major contributions by M. Bruneau, R. Eguchi, T. Holzer, G. Johnson, J. Mander, J. Mitchell, W. Mitchell, A. Papageorgiou, C. Scaethorn, and G. Webb, 3/23/00, (PB2000-106200, A11, MF-A03).

MCEER-00-0002 "Proceedings of the MCEER Workshop for Seismic Hazard Mitigation of Health Care Facilities," edited by G.C. Lee, M. Ettouney, M. Grigoriu, J. Hauer and J. Nigg, 3/29/00, (PB2000-106892, A08, MF-A02).

MCEER-00-0003 "The Chi-Chi, Taiwan Earthquake of September 21, 1999: Reconnaissance Report," edited by G.C. Lee and C.H. Loh, with major contributions by G.C. Lee, M. Bruneau, I.G. Buckle, S.E. Chang, P.J. Flores, T.D. O'Rourke, M. Shinozuka, T.T. Soong, C-H. Loh, K-C. Chang, Z-J. Chen, J-S. Hwang, M-L. Lin, G-Y. Liu, K-C. Tsai, G.C. Yao and C-L. Yen, 4/30/00, (PB2001-100980, A10, MF-A02).

MCEER-00-0004 "Seismic Retrofit of End-Sway Frames of Steel Deck-Truss Bridges with a Supplemental Tendon System: Experimental and Analytical Investigation," by G. Pekcan, J.B. Mander and S.S. Chen, 7/1/00, (PB2001-100982, A10, MF-A02).

MCEER-00-0005 "Sliding Fragility of Unrestrained Equipment in Critical Facilities," by W.H. Chong and T.T. Soong, 7/5/00, (PB2001-100983, A08, MF-A02).

MCEER-00-0006 "Seismic Response of Reinforced Concrete Bridge Pier Walls in the Weak Direction," by N. Abo-Shadi, M. Saiidi and D. Sanders, 7/17/00, (PB2001-100981, A17, MF-A03).

MCEER-00-0007 "Low-Cycle Fatigue Behavior of Longitudinal Reinforcement in Reinforced Concrete Bridge Columns," by J. Brown and S.K. Kunnath, 7/23/00, (PB2001-104392, A08, MF-A02).

MCEER-00-0008 "Soil Structure Interaction of Bridges for Seismic Analysis," I. PoLam and H. Law, 9/25/00, (PB2001-105397, A08, MF-A02).

MCEER-00-0009 "Proceedings of the First MCEER Workshop on Mitigation of Earthquake Disaster by Advanced Technologies (MEDAT-1), edited by M. Shinozuka, D.J. Inman and T.D. O'Rourke, 11/10/00, (PB2001-105399, A14, MF-A03).

MCEER-00-0010 "Development and Evaluation of Simplified Procedures for Analysis and Design of Buildings with Passive Energy Dissipation Systems, Revision 01," by O.M. Ramirez, M.C. Constantinou, C.A. Kircher, A.S. Whittaker, M.W. Johnson, J.D. Gomez and C. Chrysostomou, 11/16/01, (PB2001-105523, A23, MF-A04).

MCEER-00-0011 "Dynamic Soil-Foundation-Structure Interaction Analyses of Large Caissons," by C-Y. Chang, C-M. Mok, Z-L. Wang, R. Settgast, F. Waggoner, M.A. Ketchum, H.M. Gonnermann and C-C. Chin, 12/30/00, (PB2001-104373, A07, MF-A02).

MCEER-00-0012 "Experimental Evaluation of Seismic Performance of Bridge Restrainers," by A.G. Vlassis, E.M. Maragakis and M. Saiid Saiidi, 12/30/00, (PB2001-104354, A09, MF-A02).

MCEER-00-0013 "Effect of Spatial Variation of Ground Motion on Highway Structures," by M. Shinozuka, V. Saxena and G. Deodatis, 12/31/00, (PB2001-108755, A13, MF-A03).

MCEER-00-0014 "A Risk-Based Methodology for Assessing the Seismic Performance of Highway Systems," by S.D. Werner, C.E. Taylor, J.E. Moore, II, J.S. Walton and S. Cho, 12/31/00, (PB2001-108756, A14, MF-A03).

MCEER-01-0001 "Experimental Investigation of P-Delta Effects to Collapse During Earthquakes," by D. Vian and M. Bruneau, 6/25/01, (PB2002-100534, A17, MF-A03).

MCEER-01-0002 "Proceedings of the Second MCEER Workshop on Mitigation of Earthquake Disaster by Advanced Technologies (MEDAT-2)," edited by M. Bruneau and D.J. Inman, 7/23/01, (PB2002-100434, A16, MF-A03).

MCEER-01-0003 "Sensitivity Analysis of Dynamic Systems Subjected to Seismic Loads," by C. Roth and M. Grigoriu, 9/18/01, (PB2003-100884, A12, MF-A03).

MCEER-01-0004 "Overcoming Obstacles to Implementing Earthquake Hazard Mitigation Policies: Stage 1 Report," by D.J. Alesch and W.J. Petak, 12/17/01, (PB2002-107949, A07, MF-A02).

MCEER-01-0005 "Updating Real-Time Earthquake Loss Estimates: Methods, Problems and Insights," by C.E. Taylor, S.E. Chang and R.T. Eguchi, 12/17/01, (PB2002-107948, A05, MF-A01).

MCEER-01-0006 "Experimental Investigation and Retrofit of Steel Pile Foundations and Pile Bents Under Cyclic Lateral Loadings," by A. Shama, J. Mander, B. Blabac and S. Chen, 12/31/01, (PB2002-107950, A13, MF-A03).

MCEER-02-0001 "Assessment of Performance of Bolu Viaduct in the 1999 Duzce Earthquake in Turkey" by P.C. Roussis, M.C. Constantinou, M. Erdik, E. Durukal and M. Dicleli, 5/8/02, (PB2003-100883, A08, MF-A02).

MCEER-02-0002 "Seismic Behavior of Rail Counterweight Systems of Elevators in Buildings," by M.P. Singh, Rildova and L.E. Suarez, 5/27/02. (PB2003-100882, A11, MF-A03).

MCEER-02-0003 "Development of Analysis and Design Procedures for Spread Footings," by G. Mylonakis, G. Gazetas, S. Nikolaou and A. Chauncey, 10/02/02, (PB2004-101636, A13, MF-A03, CD-A13).

MCEER-02-0004 "Bare-Earth Algorithms for Use with SAR and LIDAR Digital Elevation Models," by C.K. Huyck, R.T. Eguchi and B. Houshmand, 10/16/02, (PB2004-101637, A07, CD-A07).

MCEER-02-0005 "Review of Energy Dissipation of Compression Members in Concentrically Braced Frames," by K.Lee and M. Bruneau, 10/18/02, (PB2004-101638, A10, CD-A10).

MCEER-03-0001 "Experimental Investigation of Light-Gauge Steel Plate Shear Walls for the Seismic Retrofit of Buildings" by J. Berman and M. Bruneau, 5/2/03, (PB2004-101622, A10, MF-A03, CD-A10).

MCEER-03-0002 "Statistical Analysis of Fragility Curves," by M. Shinozuka, M.Q. Feng, H. Kim, T. Uzawa and T. Ueda, 6/16/03, (PB2004-101849, A09, CD-A09).

MCEER-03-0003 "Proceedings of the Eighth U.S.-Japan Workshop on Earthquake Resistant Design f Lifeline Facilities and Countermeasures Against Liquefaction," edited by M. Hamada, J.P. Bardet and T.D. O'Rourke, 6/30/03, (PB2004-104386, A99, CD-A99).

MCEER-03-0004 "Proceedings of the PRC-US Workshop on Seismic Analysis and Design of Special Bridges," edited by L.C. Fan and G.C. Lee, 7/15/03, (PB2004-104387, A14, CD-A14).

MCEER-03-0005 "Urban Disaster Recovery: A Framework and Simulation Model," by S.B. Miles and S.E. Chang, 7/25/03, (PB2004-104388, A07, CD-A07).

MCEER-03-0006 "Behavior of Underground Piping Joints Due to Static and Dynamic Loading," by R.D. Meis, M. Maragakis and R. Siddharthan, 11/17/03, (PB2005-102194, A13, MF-A03, CD-A00).

MCEER-04-0001 "Experimental Study of Seismic Isolation Systems with Emphasis on Secondary System Response and Verification of Accuracy of Dynamic Response History Analysis Methods," by E. Wolff and M. Constantinou, 1/16/04 (PB2005-102195, A99, MF-E08, CD-A00).

MCEER-04-0002 "Tension, Compression and Cyclic Testing of Engineered Cementitious Composite Materials," by K. Kesner and S.L. Billington, 3/1/04, (PB2005-102196, A08, CD-A08).

MCEER-04-0003 "Cyclic Testing of Braces Laterally Restrained by Steel Studs to Enhance Performance During Earthquakes," by O.C. Celik, J.W. Berman and M. Bruneau, 3/16/04, (PB2005-102197, A13, MF-A03, CD-A00).

MCEER-04-0004 "Methodologies for Post Earthquake Building Damage Detection Using SAR and Optical Remote Sensing: Application to the August 17, 1999 Marmara, Turkey Earthquake," by C.K. Huyck, B.J. Adams, S. Cho, R.T. Eguchi, B. Mansouri and B. Houshmand, 6/15/04, (PB2005-104888, A10, CD-A00).

MCEER-04-0005 "Nonlinear Structural Analysis Towards Collapse Simulation: A Dynamical Systems Approach," by M.V. Sivaselvan and A.M. Reinhorn, 6/16/04, (PB2005-104889, A11, MF-A03, CD-A00).

MCEER-04-0006 "Proceedings of the Second PRC-US Workshop on Seismic Analysis and Design of Special Bridges," edited by G.C. Lee and L.C. Fan, 6/25/04, (PB2005-104890, A16, CD-A00).

MCEER-04-0007 "Seismic Vulnerability Evaluation of Axially Loaded Steel Built-up Laced Members," by K. Lee and M. Bruneau, 6/30/04, (PB2005-104891, A16, CD-A00).

MCEER-04-0008 "Evaluation of Accuracy of Simplified Methods of Analysis and Design of Buildings with Damping Systems for Near-Fault and for Soft-Soil Seismic Motions," by E.A. Pavlou and M.C. Constantinou, 8/16/04, (PB2005-104892, A08, MF-A02, CD-A00).

MCEER-04-0009 "Assessment of Geotechnical Issues in Acute Care Facilities in California," by M. Lew, T.D. O'Rourke, R. Dobry and M. Koch, 9/15/04, (PB2005-104893, A08, CD-A00).

MCEER-04-0010 "Scissor-Jack-Damper Energy Dissipation System," by A.N. Sigaher-Boyle and M.C. Constantinou, 12/1/04 (PB2005-108221).

MCEER-04-0011 "Seismic Retrofit of Bridge Steel Truss Piers Using a Controlled Rocking Approach," by M. Pollino and M. Bruneau, 12/20/04 (PB2006-105795).

MCEER-05-0001 "Experimental and Analytical Studies of Structures Seismically Isolated with an Uplift-Restraint Isolation System," by P.C. Roussis and M.C. Constantinou, 1/10/05 (PB2005-108222).

MCEER-05-0002 "A Versatile Experimentation Model for Study of Structures Near Collapse Applied to Seismic Evaluation of Irregular Structures," by D. Kusumastuti, A.M. Reinhorn and A. Rutenberg, 3/31/05 (PB2006-101523).

MCEER-05-0003 "Proceedings of the Third PRC-US Workshop on Seismic Analysis and Design of Special Bridges," edited by L.C. Fan and G.C. Lee, 4/20/05, (PB2006-105796).

MCEER-05-0004 "Approaches for the Seismic Retrofit of Braced Steel Bridge Piers and Proof-of-Concept Testing of an Eccentrically Braced Frame with Tubular Link," by J.W. Berman and M. Bruneau, 4/21/05 (PB2006-101524).

MCEER-05-0005 "Simulation of Strong Ground Motions for Seismic Fragility Evaluation of Nonstructural Components in Hospitals," by A. Wanitkorkul and A. Filiatrault, 5/26/05 (PB2006-500027).

MCEER-05-0006 "Seismic Safety in California Hospitals: Assessing an Attempt to Accelerate the Replacement or Seismic Retrofit of Older Hospital Facilities," by D.J. Alesch, L.A. Arendt and W.J. Petak, 6/6/05 (PB2006-105794).

MCEER-05-0007 "Development of Seismic Strengthening and Retrofit Strategies for Critical Facilities Using Engineered Cementitious Composite Materials," by K. Kesner and S.L. Billington, 8/29/05 (PB2006-111701).

MCEER-05-0008 "Experimental and Analytical Studies of Base Isolation Systems for Seismic Protection of Power Transformers," by N. Murota, M.Q. Feng and G-Y. Liu, 9/30/05 (PB2006-111702).

MCEER-05-0009 "3D-BASIS-ME-MB: Computer Program for Nonlinear Dynamic Analysis of Seismically Isolated Structures," by P.C. Tsopelas, P.C. Roussis, M.C. Constantinou, R. Buchanan and A.M. Reinhorn, 10/3/05 (PB2006-111703).

MCEER-05-0010 "Steel Plate Shear Walls for Seismic Design and Retrofit of Building Structures," by D. Vian and M. Bruneau, 12/15/05 (PB2006-111704).

MCEER-05-0011 "The Performance-Based Design Paradigm," by M.J. Astrella and A. Whittaker, 12/15/05 (PB2006-111705).

MCEER-06-0001 "Seismic Fragility of Suspended Ceiling Systems," H. Badillo-Almaraz, A.S. Whittaker, A.M. Reinhorn and G.P. Cimellaro, 2/4/06 (PB2006-111706).

MCEER-06-0002 "Multi-Dimensional Fragility of Structures," by G.P. Cimellaro, A.M. Reinhorn and M. Bruneau, 3/1/06 (PB2007-106974, A09, MF-A02, CD A00).

MCEER-06-0003 "Built-Up Shear Links as Energy Dissipators for Seismic Protection of Bridges," by P. Dusicka, A.M. Itani and I.G. Buckle, 3/15/06 (PB2006-111708).

MCEER-06-0004 "Analytical Investigation of the Structural Fuse Concept," by R.E. Vargas and M. Bruneau, 3/16/06 (PB2006-111709).

MCEER-06-0005 "Experimental Investigation of the Structural Fuse Concept," by R.E. Vargas and M. Bruneau, 3/17/06 (PB2006-111710).

MCEER-06-0006 "Further Development of Tubular Eccentrically Braced Frame Links for the Seismic Retrofit of Braced Steel Truss Bridge Piers," by J.W. Berman and M. Bruneau, 3/27/06 (PB2007-105147).

MCEER-06-0007 "REDARS Validation Report," by S. Cho, C.K. Huyck, S. Ghosh and R.T. Eguchi, 8/8/06 (PB2007-106983).

MCEER-06-0008 "Review of Current NDE Technologies for Post-Earthquake Assessment of Retrofitted Bridge Columns," by J.W. Song, Z. Liang and G.C. Lee, 8/21/06 (PB2007-106984).

MCEER-06-0009 "Liquefaction Remediation in Silty Soils Using Dynamic Compaction and Stone Columns," by S. Thevanayagam, G.R. Martin, R. Nashed, T. Shenthan, T. Kanagalingam and N. Ecemis, 8/28/06 (PB2007-106985).

MCEER-06-0010 "Conceptual Design and Experimental Investigation of Polymer Matrix Composite Infill Panels for Seismic Retrofitting," by W. Jung, M. Chiewanichakorn and A.J. Aref, 9/21/06 (PB2007-106986).

MCEER-06-0011 "A Study of the Coupled Horizontal-Vertical Behavior of Elastomeric and Lead-Rubber Seismic Isolation Bearings," by G.P. Warn and A.S. Whittaker, 9/22/06 (PB2007-108679).

MCEER-06-0012 "Proceedings of the Fourth PRC-US Workshop on Seismic Analysis and Design of Special Bridges: Advancing Bridge Technologies in Research, Design, Construction and Preservation," Edited by L.C. Fan, G.C. Lee and L. Ziang, 10/12/06 (PB2007-109042).

MCEER-06-0013 "Cyclic Response and Low Cycle Fatigue Characteristics of Plate Steels," by P. Dusicka, A.M. Itani and I.G. Buckle, 11/1/06 06 (PB2007-106987).

MCEER-06-0014 "Proceedings of the Second US-Taiwan Bridge Engineering Workshop," edited by W.P. Yen, J. Shen, J-Y. Chen and M. Wang, 11/15/06 (PB2008-500041).

MCEER-06-0015 "User Manual and Technical Documentation for the REDARS^{TM} Import Wizard," by S. Cho, S. Ghosh, C.K. Huyck and S.D. Werner, 11/30/06 (PB2007-114766).

MCEER-06-0016 "Hazard Mitigation Strategy and Monitoring Technologies for Urban and Infrastructure Public Buildings: Proceedings of the China-US Workshops," edited by X.Y. Zhou, A.L. Zhang, G.C. Lee and M. Tong, 12/12/06 (PB2008-500018).

MCEER-07-0001 "Static and Kinetic Coefficients of Friction for Rigid Blocks," by C. Kafali, S. Fathali, M. Grigoriu and A.S. Whittaker, 3/20/07 (PB2007-114767).

MCEER-07-0002 "Hazard Mitigation Investment Decision Making: Organizational Response to Legislative Mandate," by L.A. Arendt, D.J. Alesch and W.J. Petak, 4/9/07 (PB2007-114768).

MCEER-07-0003 "Seismic Behavior of Bidirectional-Resistant Ductile End Diaphragms with Unbonded Braces in Straight or Skewed Steel Bridges," by O. Celik and M. Bruneau, 4/11/07 (PB2008-105141).

MCEER-07-0004 "Modeling Pile Behavior in Large Pile Groups Under Lateral Loading," by A.M. Dodds and G.R. Martin, 4/16/07(PB2008-105142).

MCEER-07-0005 "Experimental Investigation of Blast Performance of Seismically Resistant Concrete-Filled Steel Tube Bridge Piers," by S. Fujikura, M. Bruneau and D. Lopez-Garcia, 4/20/07 (PB2008-105143).

MCEER-07-0006 "Seismic Analysis of Conventional and Isolated Liquefied Natural Gas Tanks Using Mechanical Analogs," by I.P. Christovasilis and A.S. Whittaker, 5/1/07, not available.

MCEER-07-0007 "Experimental Seismic Performance Evaluation of Isolation/Restraint Systems for Mechanical Equipment – Part 1: Heavy Equipment Study," by S. Fathali and A. Filiatrault, 6/6/07 (PB2008-105144).

MCEER-07-0008 "Seismic Vulnerability of Timber Bridges and Timber Substructures," by A.A. Sharma, J.B. Mander, I.M. Friedland and D.R. Allicock, 6/7/07 (PB2008-105145).

MCEER-07-0009 "Experimental and Analytical Study of the XY-Friction Pendulum (XY-FP) Bearing for Bridge Applications," by C.C. Marin-Artieda, A.S. Whittaker and M.C. Constantinou, 6/7/07 (PB2008-105191).

MCEER-07-0010 "Proceedings of the PRC-US Earthquake Engineering Forum for Young Researchers," Edited by G.C. Lee and X.Z. Qi, 6/8/07 (PB2008-500058).

MCEER-07-0011 "Design Recommendations for Perforated Steel Plate Shear Walls," by R. Purba and M. Bruneau, 6/18/07, (PB2008-105192).

MCEER-07-0012 "Performance of Seismic Isolation Hardware Under Service and Seismic Loading," by M.C. Constantinou, A.S. Whittaker, Y. Kalpakidis, D.M. Fenz and G.P. Warn, 8/27/07, (PB2008-105193).

MCEER-07-0013 "Experimental Evaluation of the Seismic Performance of Hospital Piping Subassemblies," by E.R. Goodwin, E. Maragakis and A.M. Itani, 9/4/07, (PB2008-105194).

MCEER-07-0014 "A Simulation Model of Urban Disaster Recovery and Resilience: Implementation for the 1994 Northridge Earthquake," by S. Miles and S.E. Chang, 9/7/07, (PB2008-106426).

MCEER-07-0015 "Statistical and Mechanistic Fragility Analysis of Concrete Bridges," by M. Shinozuka, S. Banerjee and S-H. Kim, 9/10/07, (PB2008-106427).

MCEER-07-0016 "Three-Dimensional Modeling of Inelastic Buckling in Frame Structures," by M. Schachter and AM. Reinhorn, 9/13/07, (PB2008-108125).

MCEER-07-0017 "Modeling of Seismic Wave Scattering on Pile Groups and Caissons," by I. Po Lam, H. Law and C.T. Yang, 9/17/07 (PB2008-108150).

MCEER-07-0018 "Bridge Foundations: Modeling Large Pile Groups and Caissons for Seismic Design," by I. Po Lam, H. Law and G.R. Martin (Coordinating Author), 12/1/07 (PB2008-111190).

MCEER-07-0019 "Principles and Performance of Roller Seismic Isolation Bearings for Highway Bridges," by G.C. Lee, Y.C. Ou, Z. Liang, T.C. Niu and J. Song, 12/10/07 (PB2009-110466).

MCEER-07-0020 "Centrifuge Modeling of Permeability and Pinning Reinforcement Effects on Pile Response to Lateral Spreading," by L.L Gonzalez-Lagos, T. Abdoun and R. Dobry, 12/10/07 (PB2008-111191).

MCEER-07-0021 "Damage to the Highway System from the Pisco, Perú Earthquake of August 15, 2007," by J.S. O'Connor, L. Mesa and M. Nykamp, 12/10/07, (PB2008-108126).

MCEER-07-0022 "Experimental Seismic Performance Evaluation of Isolation/Restraint Systems for Mechanical Equipment – Part 2: Light Equipment Study," by S. Fathali and A. Filiatrault, 12/13/07 (PB2008-111192).

MCEER-07-0023 "Fragility Considerations in Highway Bridge Design," by M. Shinozuka, S. Banerjee and S.H. Kim, 12/14/07 (PB2008-111193).

MCEER-07-0024 "Performance Estimates for Seismically Isolated Bridges," by G.P. Warn and A.S. Whittaker, 12/30/07 (PB2008-112230).

MCEER-08-0001 "Seismic Performance of Steel Girder Bridge Superstructures with Conventional Cross Frames," by L.P. Carden, A.M. Itani and I.G. Buckle, 1/7/08, (PB2008-112231).

MCEER-08-0002 "Seismic Performance of Steel Girder Bridge Superstructures with Ductile End Cross Frames with Seismic Isolators," by L.P. Carden, A.M. Itani and I.G. Buckle, 1/7/08 (PB2008-112232).

MCEER-08-0003 "Analytical and Experimental Investigation of a Controlled Rocking Approach for Seismic Protection of Bridge Steel Truss Piers," by M. Pollino and M. Bruneau, 1/21/08 (PB2008-112233).

MCEER-08-0004 "Linking Lifeline Infrastructure Performance and Community Disaster Resilience: Models and Multi-Stakeholder Processes," by S.E. Chang, C. Pasion, K. Tatebe and R. Ahmad, 3/3/08 (PB2008-112234).

MCEER-08-0005 "Modal Analysis of Generally Damped Linear Structures Subjected to Seismic Excitations," by J. Song, Y-L. Chu, Z. Liang and G.C. Lee, 3/4/08 (PB2009-102311).

MCEER-08-0006 "System Performance Under Multi-Hazard Environments," by C. Kafali and M. Grigoriu, 3/4/08 (PB2008-112235).

MCEER-08-0007 "Mechanical Behavior of Multi-Spherical Sliding Bearings," by D.M. Fenz and M.C. Constantinou, 3/6/08 (PB2008-112236).

MCEER-08-0008 "Post-Earthquake Restoration of the Los Angeles Water Supply System," by T.H.P. Tabucchi and R.A. Davidson, 3/7/08 (PB2008-112237).

MCEER-08-0009 "Fragility Analysis of Water Supply Systems," by A. Jacobson and M. Grigoriu, 3/10/08 (PB2009-105545).

MCEER-08-0010 "Experimental Investigation of Full-Scale Two-Story Steel Plate Shear Walls with Reduced Beam Section Connections," by B. Qu, M. Bruneau, C-H. Lin and K-C. Tsai, 3/17/08 (PB2009-106368).

MCEER-08-0011 "Seismic Evaluation and Rehabilitation of Critical Components of Electrical Power Systems," S. Ersoy, B. Feizi, A. Ashrafi and M. Ala Saadeghvaziri, 3/17/08 (PB2009-105546).

MCEER-08-0012 "Seismic Behavior and Design of Boundary Frame Members of Steel Plate Shear Walls," by B. Qu and M. Bruneau, 4/26/08 . (PB2009-106744).

MCEER-08-0013 "Development and Appraisal of a Numerical Cyclic Loading Protocol for Quantifying Building System Performance," by A. Filiatrault, A. Wanitkorkul and M. Constantinou, 4/27/08 (PB2009-107906).

MCEER-08-0014 "Structural and Nonstructural Earthquake Design: The Challenge of Integrating Specialty Areas in Designing Complex, Critical Facilities," by W.J. Petak and D.J. Alesch, 4/30/08 (PB2009-107907).

MCEER-08-0015 "Seismic Performance Evaluation of Water Systems," by Y. Wang and T.D. O'Rourke, 5/5/08 (PB2009-107908).

MCEER-08-0016 "Seismic Response Modeling of Water Supply Systems," by P. Shi and T.D. O'Rourke, 5/5/08 (PB2009-107910).

MCEER-08-0017 "Numerical and Experimental Studies of Self-Centering Post-Tensioned Steel Frames," by D. Wang and A. Filiatrault, 5/12/08 (PB2009-110479).

MCEER-08-0018 "Development, Implementation and Verification of Dynamic Analysis Models for Multi-Spherical Sliding Bearings," by D.M. Fenz and M.C. Constantinou, 8/15/08 (PB2009-107911).

MCEER-08-0019 "Performance Assessment of Conventional and Base Isolated Nuclear Power Plants for Earthquake Blast Loadings," by Y.N. Huang, A.S. Whittaker and N. Luco, 10/28/08 (PB2009-107912).

MCEER-08-0020 "Remote Sensing for Resilient Multi-Hazard Disaster Response – Volume I: Introduction to Damage Assessment Methodologies," by B.J. Adams and R.T. Eguchi, 11/17/08 (PB2010-102695).

MCEER-08-0021 "Remote Sensing for Resilient Multi-Hazard Disaster Response – Volume II: Counting the Number of Collapsed Buildings Using an Object-Oriented Analysis: Case Study of the 2003 Bam Earthquake," by L. Gusella, C.K. Huyck and B.J. Adams, 11/17/08 (PB2010-100925).

MCEER-08-0022 "Remote Sensing for Resilient Multi-Hazard Disaster Response – Volume III: Multi-Sensor Image Fusion Techniques for Robust Neighborhood-Scale Urban Damage Assessment," by B.J. Adams and A. McMillan, 11/17/08 (PB2010-100926).

MCEER-08-0023 "Remote Sensing for Resilient Multi-Hazard Disaster Response – Volume IV: A Study of Multi-Temporal and Multi-Resolution SAR Imagery for Post-Katrina Flood Monitoring in New Orleans," by A. McMillan, J.G. Morley, B.J. Adams and S. Chesworth, 11/17/08 (PB2010-100927).

MCEER-08-0024 "Remote Sensing for Resilient Multi-Hazard Disaster Response – Volume V: Integration of Remote Sensing Imagery and VIEWS^{TM} Field Data for Post-Hurricane Charley Building Damage Assessment," by J.A. Womble, K. Mehta and B.J. Adams, 11/17/08 (PB2009-115532).

MCEER-08-0025 "Building Inventory Compilation for Disaster Management: Application of Remote Sensing and Statistical Modeling," by P. Sarabandi, A.S. Kiremidjian, R.T. Eguchi and B. J. Adams, 11/20/08 (PB2009-110484).

MCEER-08-0026 "New Experimental Capabilities and Loading Protocols for Seismic Qualification and Fragility Assessment of Nonstructural Systems," by R. Retamales, G. Mosqueda, A. Filiatrault and A. Reinhorn, 11/24/08 (PB2009-110485).

MCEER-08-0027 "Effects of Heating and Load History on the Behavior of Lead-Rubber Bearings," by I.V. Kalpakidis and M.C. Constantinou, 12/1/08 (PB2009-115533).

MCEER-08-0028 "Experimental and Analytical Investigation of Blast Performance of Seismically Resistant Bridge Piers," by S.Fujikura and M. Bruneau, 12/8/08 (PB2009-115534).

MCEER-08-0029 "Evolutionary Methodology for Aseismic Decision Support," by Y. Hu and G. Dargush, 12/15/08.

MCEER-08-0030 "Development of a Steel Plate Shear Wall Bridge Pier System Conceived from a Multi-Hazard Perspective," by D. Keller and M. Bruneau, 12/19/08 (PB2010-102696).

MCEER-09-0001 "Modal Analysis of Arbitrarily Damped Three-Dimensional Linear Structures Subjected to Seismic Excitations," by Y.L. Chu, J. Song and G.C. Lee, 1/31/09 (PB2010-100922).

MCEER-09-0002 "Air-Blast Effects on Structural Shapes," by G. Ballantyne, A.S. Whittaker, A.J. Aref and G.F. Dargush, 2/2/09 (PB2010-102697).

MCEER-09-0003 "Water Supply Performance During Earthquakes and Extreme Events," by A.L. Bonneau and T.D. O'Rourke, 2/16/09 (PB2010-100923).

MCEER-09-0004 "Generalized Linear (Mixed) Models of Post-Earthquake Ignitions," by R.A. Davidson, 7/20/09 (PB2010-102698).

MCEER-09-0005 "Seismic Testing of a Full-Scale Two-Story Light-Frame Wood Building: NEESWood Benchmark Test," by I.P. Christovasilis, A. Filiatrault and A. Wanitkorkul, 7/22/09 (PB2012-102401).

MCEER-09-0006 "IDARC2D Version 7.0: A Program for the Inelastic Damage Analysis of Structures," by A.M. Reinhorn, H. Roh, M. Sivaselvan, S.K. Kunnath, R.E. Valles, A. Madan, C. Li, R. Lobo and Y.J. Park, 7/28/09 (PB2010-103199).

MCEER-09-0007 "Enhancements to Hospital Resiliency: Improving Emergency Planning for and Response to Hurricanes," by D.B. Hess and L.A. Arendt, 7/30/09 (PB2010-100924).

MCEER-09-0008 "Assessment of Base-Isolated Nuclear Structures for Design and Beyond-Design Basis Earthquake Shaking," by Y.N. Huang, A.S. Whittaker, R.P. Kennedy and R.L. Mayes, 8/20/09 (PB2010-102699).

MCEER-09-0009 "Quantification of Disaster Resilience of Health Care Facilities," by G.P. Cimellaro, C. Fumo, A.M Reinhorn and M. Bruneau, 9/14/09 (PB2010-105384).

MCEER-09-0010 "Performance-Based Assessment and Design of Squat Reinforced Concrete Shear Walls," by C.K. Gulec and A.S. Whittaker, 9/15/09 (PB2010-102700).

MCEER-09-0011 "Proceedings of the Fourth US-Taiwan Bridge Engineering Workshop," edited by W.P. Yen, J.J. Shen, T.M. Lee and R.B. Zheng, 10/27/09 (PB2010-500009).

MCEER-09-0012 "Proceedings of the Special International Workshop on Seismic Connection Details for Segmental Bridge Construction," edited by W. Phillip Yen and George C. Lee, 12/21/09 (PB2012-102402).

MCEER-10-0001 "Direct Displacement Procedure for Performance-Based Seismic Design of Multistory Woodframe Structures," by W. Pang and D. Rosowsky, 4/26/10 (PB2012-102403).

MCEER-10-0002 "Simplified Direct Displacement Design of Six-Story NEESWood Capstone Building and Pre-Test Seismic Performance Assessment," by W. Pang, D. Rosowsky, J. van de Lindt and S. Pei, 5/28/10 (PB2012-102404).

MCEER-10-0003 "Integration of Seismic Protection Systems in Performance-Based Seismic Design of Woodframed Structures," by J.K. Shinde and M.D. Symans, 6/18/10 (PB2012-102405).

MCEER-10-0004 "Modeling and Seismic Evaluation of Nonstructural Components: Testing Frame for Experimental Evaluation of Suspended Ceiling Systems," by A.M. Reinhorn, K.P. Ryu and G. Maddaloni, 6/30/10 (PB2012-102406).

MCEER-10-0005 "Analytical Development and Experimental Validation of a Structural-Fuse Bridge Pier Concept," by S. El-Bahey and M. Bruneau, 10/1/10 (PB2012-102407).

MCEER-10-0006 "A Framework for Defining and Measuring Resilience at the Community Scale: The PEOPLES Resilience Framework," by C.S. Renschler, A.E. Frazier, L.A. Arendt, G.P. Cimellaro, A.M. Reinhorn and M. Bruneau, 10/8/10 (PB2012-102408).

MCEER-10-0007 "Impact of Horizontal Boundary Elements Design on Seismic Behavior of Steel Plate Shear Walls," by R. Purba and M. Bruneau, 11/14/10 (PB2012-102409).

MCEER-10-0008 "Seismic Testing of a Full-Scale Mid-Rise Building: The NEESWood Capstone Test," by S. Pei, J.W. van de Lindt, S.E. Pryor, H. Shimizu, H. Isoda and D.R. Rammer, 12/1/10 (PB2012-102410).

MCEER-10-0009 "Modeling the Effects of Detonations of High Explosives to Inform Blast-Resistant Design," by P. Sherkar, A.S. Whittaker and A.J. Aref, 12/1/10 (PB2012-102411).

MCEER-10-0010 "L'Aquila Earthquake of April 6, 2009 in Italy: Rebuilding a Resilient City to Withstand Multiple Hazards," by G.P. Cimellaro, I.P. Christovasilis, A.M. Reinhorn, A. De Stefano and T. Kirova, 12/29/10.

MCEER-11-0001 "Numerical and Experimental Investigation of the Seismic Response of Light-Frame Wood Structures," by I.P. Christovasilis and A. Filiatrault, 8/8/11 (PB2012-102412).

MCEER-11-0002 "Seismic Design and Analysis of a Precast Segmental Concrete Bridge Model," by M. Anagnostopoulou, A. Filiatrault and A. Aref, 9/15/11.

MCEER-11-0003 'Proceedings of the Workshop on Improving Earthquake Response of Substation Equipment," Edited by A.M. Reinhorn, 9/19/11 (PB2012-102413).

MCEER-11-0004 "LRFD-Based Analysis and Design Procedures for Bridge Bearings and Seismic Isolators," by M.C. Constantinou, I. Kalpakidis, A. Filiatrault and R.A. Ecker Lay, 9/26/11.

MCEER-11-0005 "Experimental Seismic Evaluation, Model Parameterization, and Effects of Cold-Formed Steel-Framed Gypsum Partition Walls on the Seismic Performance of an Essential Facility," by R. Davies, R. Retamales, G. Mosqueda and A. Filiatrault, 10/12/11.

MCEER-11-0006 "Modeling and Seismic Performance Evaluation of High Voltage Transformers and Bushings," by A.M. Reinhorn, K. Oikonomou, H. Roh, A. Schiff and L. Kempner, Jr., 10/3/11.

MCEER-11-0007 "Extreme Load Combinations: A Survey of State Bridge Engineers," by G.C. Lee, Z. Liang, J.J. Shen and J.S. O'Connor, 10/14/11.

MCEER-12-0001 "Simplified Analysis Procedures in Support of Performance Based Seismic Design," by Y.N. Huang and A.S. Whittaker.

MCEER-12-0002 "Seismic Protection of Electrical Transformer Bushing Systems by Stiffening Techniques," by M. Koliou, A. Filiatrault, A.M. Reinhorn and N. Oliveto, 6/1/12.

MCEER-12-0003 "Post-Earthquake Bridge Inspection Guidelines," by J.S. O'Connor and S. Alampalli, 6/8/12.

MCEER-12-0004 "Integrated Design Methodology for Isolated Floor Systems in Single-Degree-of-Freedom Structural Fuse Systems," by S. Cui, M. Bruneau and M.C. Constantinou, 6/13/12.

MCEER-12-0005 "Characterizing the Rotational Components of Earthquake Ground Motion," by D. Basu, A.S. Whittaker and M.C. Constantinou, 6/15/12.

MCEER-12-0006 "Bayesian Fragility for Nonstructural Systems," by C.H. Lee and M.D. Grigoriu, 9/12/12.

MCEER-12-0007 "A Numerical Model for Capturing the In-Plane Seismic Response of Interior Metal Stud Partition Walls," by R.L. Wood and T.C. Hutchinson, 9/12/12.

MCEER-12-0008 "Assessment of Floor Accelerations in Yielding Buildings," by J.D. Wieser, G. Pekcan, A.E. Zaghi, A.M. Itani and E. Maragakis, 10/5/12.

MCEER-13-0001 "Experimental Seismic Study of Pressurized Fire Sprinkler Piping Systems," by Y. Tian, A. Filiatrault and G. Mosqueda, 4/8/13.

MCEER-13-0002 "Enhancing Resource Coordination for Multi-Modal Evacuation Planning," by D.B. Hess, B.W. Conley and C.M. Farrell, 2/8/13.

MCEER-13-0003 "Seismic Response of Base Isolated Buildings Considering Pounding to Moat Walls," by A. Masroor and G. Mosqueda, 2/26/13.

MCEER-13-0004 "Seismic Response Control of Structures Using a Novel Adaptive Passive Negative Stiffness Device," by D.T.R. Pasala, A.A. Sarlis, S. Nagarajaiah, A.M. Reinhorn, M.C. Constantinou and D.P. Taylor, 6/10/13.

MCEER-13-0005 "Negative Stiffness Device for Seismic Protection of Structures," by A.A. Sarlis, D.T.R. Pasala, M.C. Constantinou, A.M. Reinhorn, S. Nagarajaiah and D.P. Taylor, 6/12/13.

MCEER-13-0006 "Emilia Earthquake of May 20, 2012 in Northern Italy: Rebuilding a Resilient Community to Withstand Multiple Hazards," by G.P. Cimellaro, M. Chiriatti, A.M. Reinhorn and L. Tirca, June 30, 2013.

MCEER-13-0007 "Precast Concrete Segmental Components and Systems for Accelerated Bridge Construction in Seismic Regions," by A.J. Aref, G.C. Lee, Y.C. Ou and P. Sideris, with contributions from K.C. Chang, S. Chen, A. Filiatrault and Y. Zhou, June 13, 2013.

MCEER-13-0008 "A Study of U.S. Bridge Failures (1980-2012)," by G.C. Lee, S.B. Mohan, C. Huang and B.N. Fard, June 15, 2013.

MCEER-13-0009 "Development of a Database Framework for Modeling Damaged Bridges," by G.C. Lee, J.C. Qi and C. Huang, June 16, 2013.

MCEER-13-0010 "Model of Triple Friction Pendulum Bearing for General Geometric and Frictional Parameters and for Uplift Conditions," by A.A. Sarlis and M.C. Constantinou, July 1, 2013.

MCEER-13-0011 "Shake Table Testing of Triple Friction Pendulum Isolators under Extreme Conditions," by A.A. Sarlis, M.C. Constantinou and A.M. Reinhorn, July 2, 2013.

MCEER-13-0012 "Theoretical Framework for the Development of MH-LRFD," by G.C. Lee (coordinating author), H.A Capers, Jr., C. Huang, J.M. Kulicki, Z. Liang, T. Murphy, J.J.D. Shen, M. Shinozuka and P.W.H. Yen, July 31, 2013.

MCEER-13-0013 "Seismic Protection of Highway Bridges with Negative Stiffness Devices," by N.K.A. Attary, M.D. Symans, S. Nagarajaiah, A.M. Reinhorn, M.C. Constantinou, A.A. Sarlis, D.T.R. Pasala, and D.P. Taylor, September 3, 2014.

MCEER-14-0001 "Simplified Seismic Collapse Capacity-Based Evaluation and Design of Frame Buildings with and without Supplemental Damping Systems," by M. Hamidia, A. Filiatrault, and A. Aref, May 19, 2014.

MCEER-14-0002 "Comprehensive Analytical Seismic Fragility of Fire Sprinkler Piping Systems," by Siavash Soroushian, Emmanuel "Manos" Maragakis, Arash E. Zaghi, Alicia Echevarria, Yuan Tian and Andre Filiatrault, August 26, 2014.

MCEER-14-0003 "Hybrid Simulation of the Seismic Response of a Steel Moment Frame Building Structure through Collapse," by M. Del Carpio Ramos, G. Mosqueda and D.G. Lignos, October 30, 2014.

MCEER-14-0004 "Blast and Seismic Resistant Concrete-Filled Double Skin Tubes and Modified Steel Jacketed Bridge Columns," by P.P. Fouche and M. Bruneau, June 30, 2015.

MCEER-14-0005 "Seismic Performance of Steel Plate Shear Walls Considering Various Design Approaches," by R. Purba and M. Bruneau, October 31, 2014.

MCEER-14-0006 "Air-Blast Effects on Civil Structures," by Jinwon Shin, Andrew S. Whittaker, Amjad J. Aref and David Cormie, October 30, 2014.

MCEER-14-0007 "Seismic Performance Evaluation of Precast Girders with Field-Cast Ultra High Performance Concrete (UHPC) Connections," by G.C. Lee, C. Huang, J. Song, and J. S. O'Connor, July 31, 2014.

MCEER-14-0008 "Post-Earthquake Fire Resistance of Ductile Concrete-Filled Double-Skin Tube Columns," by Reza Imani, Gilberto Mosqueda and Michel Bruneau, December 1, 2014.

MCEER-14-0009 "Cyclic Inelastic Behavior of Concrete Filled Sandwich Panel Walls Subjected to In-Plane Flexure," by Y. Alzeni and M. Bruneau, December 19, 2014.

MCEER-14-0010 "Analytical and Experimental Investigation of Self-Centering Steel Plate Shear Walls," by D.M. Dowden and M. Bruneau, December 19, 2014.

MCEER-15-0001 "Seismic Analysis of Multi-story Unreinforced Masonry Buildings with Flexible Diaphragms," by J. Aleman, G. Mosqueda and A.S. Whittaker, June 12, 2015.

MCEER-15-0002 "Site Response, Soil-Structure Interaction and Structure-Soil-Structure Interaction for Performance Assessment of Buildings and Nuclear Structures," by C. Bolisetti and A.S. Whittaker, June 15, 2015.

MCEER-15-0003 "Stress Wave Attenuation in Solids for Mitigating Impulsive Loadings," by R. Rafiee-Dehkharghani, A.J. Aref and G. Dargush, August 15, 2015.

MCEER-15-0004 "Computational, Analytical, and Experimental Modeling of Masonry Structures," by K.M. Dolatshahi and A.J. Aref, November 16, 2015.

MCEER-15-0005 "Property Modification Factors for Seismic Isolators: Design Guidance for Buildings," by W.J. McVitty and M.C. Constantinou, June 30, 2015.

MCEER-15-0006 "Seismic Isolation of Nuclear Power Plants using Sliding Bearings," by Manish Kumar, Andrew S. Whittaker and Michael C. Constantinou, December 27, 2015.

MCEER-15-0007 "Quintuple Friction Pendulum Isolator Behavior, Modeling and Validation," by Donghun Lee and Michael C. Constantinou, December 28, 2015.

MCEER-15-0008 "Seismic Isolation of Nuclear Power Plants using Elastomeric Bearings," by Manish Kumar, Andrew S. Whittaker and Michael C. Constantinou, December 29, 2015.

MCEER-16-0001 "Experimental, Numerical and Analytical Studies on the Seismic Response of Steel-Plate Concrete (SC) Composite Shear Walls," by Siamak Epackachi and Andrew S. Whittaker, June 15, 2016.

MCEER-16-0002 "Seismic Demand in Columns of Steel Frames," by Lisa Shrestha and Michel Bruneau, June 17, 2016.

MCEER-16-0003 "Development and Evaluation of Procedures for Analysis and Design of Buildings with Fluidic Self-Centering Systems" by Shoma Kitayama and Michael C. Constantinou, July 21, 2016.

MCEER-16-0004 "Real Time Control of Shake Tables for Nonlinear Hysteretic Systems," by Ki Pung Ryu and Andrei M. Reinhorn, October 22, 2016.

MCEER-16-0006 "Seismic Isolation of High Voltage Electrical Power Transformers," by Kostis Oikonomou, Michael C. Constantinou, Andrei M. Reinhorn and Leon Kemper, Jr., November 2, 2016.

MCEER-16-0007 "Open Space Damping System Theory and Experimental Validation," by Erkan Polat and Michael C. Constantinou, December 13, 2016.

MCEER
EARTHQUAKE ENGINEERING TO EXTREME EVENTS
University at Buffalo, The State University of New York
133A Ketter Hall ▪ Buffalo, New York 14260-4300
Phone: (716) 645-3391 ▪ Fax: (716) 645-3399
Email: *mceer@buffalo.edu* ▪ Web: *http://mceer.buffalo.edu*
University at Buffalo *The State University of New York*

ISSN 1520-295X